Molecular clouds and star formation

Jan Brand
INAF – Istituto di Radioastronomia
Bologna

Scuola Nazionale di Astrofisica
20-26 May 2007

Overview of these lectures:

The galactic interstellar medium (ISM):

constituents and their co-existence; large-scale distribution

Molecular clouds

properties; chemistry; mass and temperature

Kinematics

rotation curve, kinematic distances

Star formation

young stellar objects (YSOs); IMF

manifestations (interaction with surroundings)

Star formation: high-mass

IMF: a universal function?

THE PHASES OF THE INTERSTELLAR MEDIUM

Not just stars…

ISM: 90% H, 9% He, 1% “rest”

Dust mixed with gas

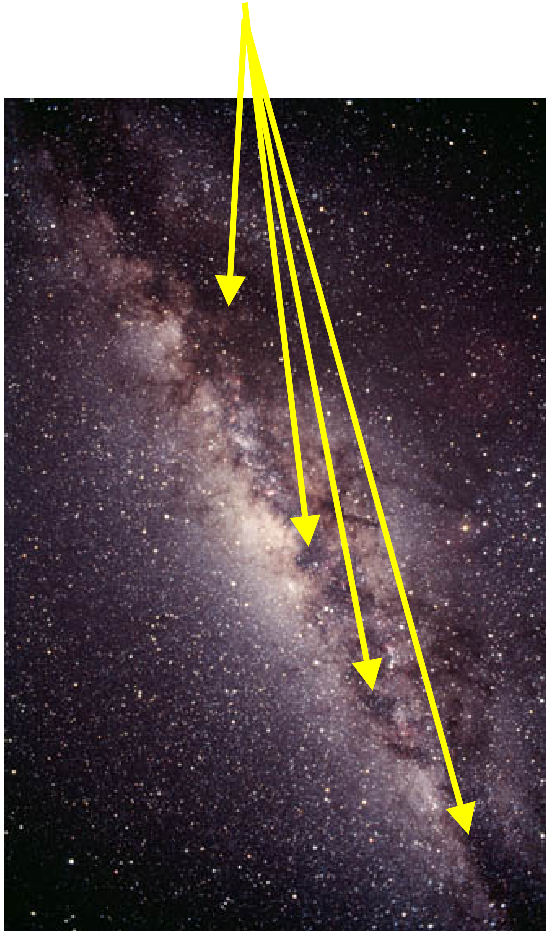

Abundances: for every 10^6 H atoms, there are 250 C, 500 O, 80 N atoms ~solar (≡ cosmic). Other elements: IS abundance <<cosmic: depletion (material locked up in dust grains)

Characterize ISM acc. to condition of H:

HI: M ~ 2 x 10^9 $M_\odot$
H_2: M ~ M(HI)
HII: M ~ 1 x 10^8 $M_\odot$

M(ISM) ~ 4% M(visible matter in Galaxy)
M(dust) ~ 1-2% M(ISM)

Energy in the ISM:
Radiation field, magnetic fields, cosmic rays

High density? Not really… (only in some locations):

High-density molecular cloud core: $\geq 10^6$ particles cm^{-3}

Earth's atmosphere at sea level: ~ $3x10^{19}$ particles cm^{-3}

Best terrestrial vacuum: $3x10^{12-13}$ particles cm^{-3} !!

Average density ISM: ~ 1 particle cm^{-3}


H_2 , HII, dust
© Anglo-Australian Obs/Royal Obs. Edinburgh

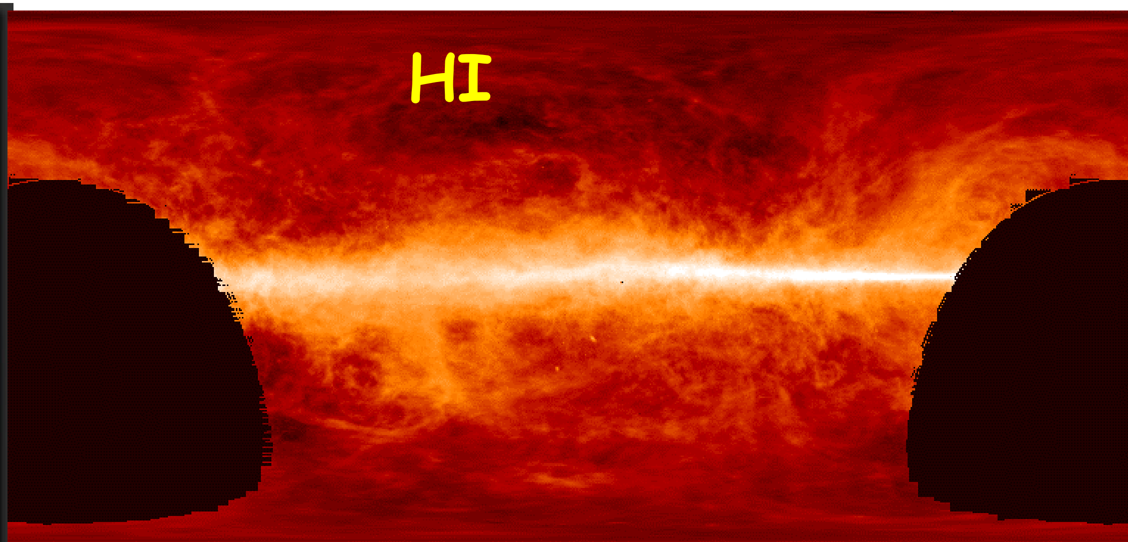
HI


H_2 , dust


© Anglo-Australian Obs./Royal Obs. Edinburgh


© Anglo-Australian Obs./Royal Obs. Edinburgh

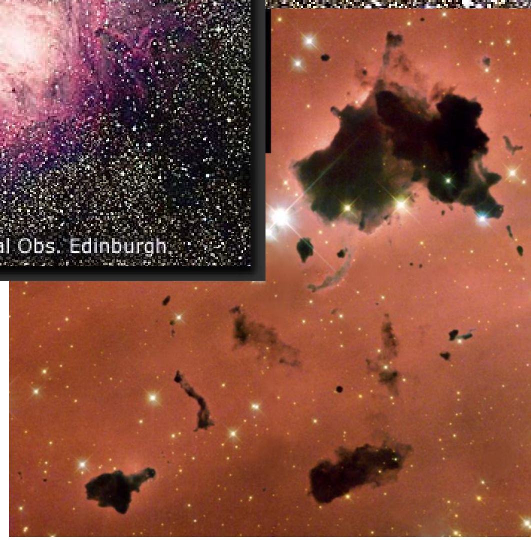

What you see depends on frequency

Orion: optical, IR, and mm

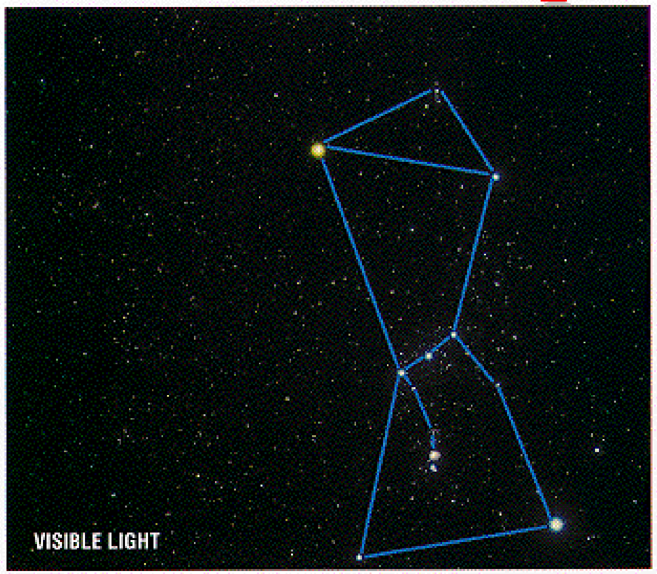

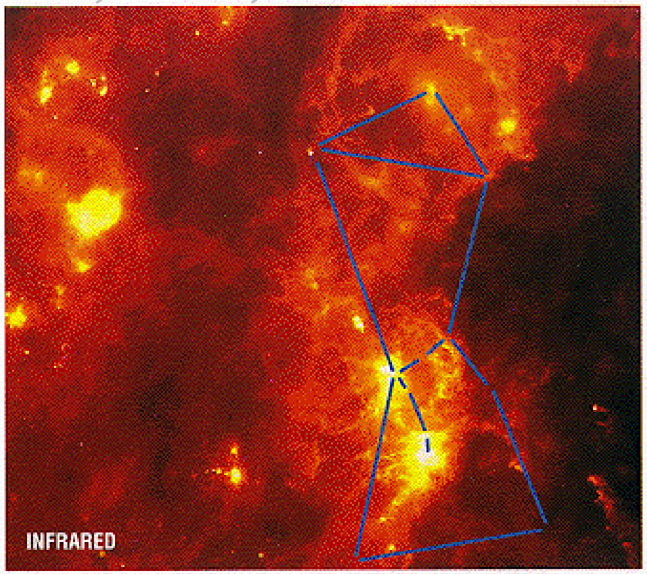

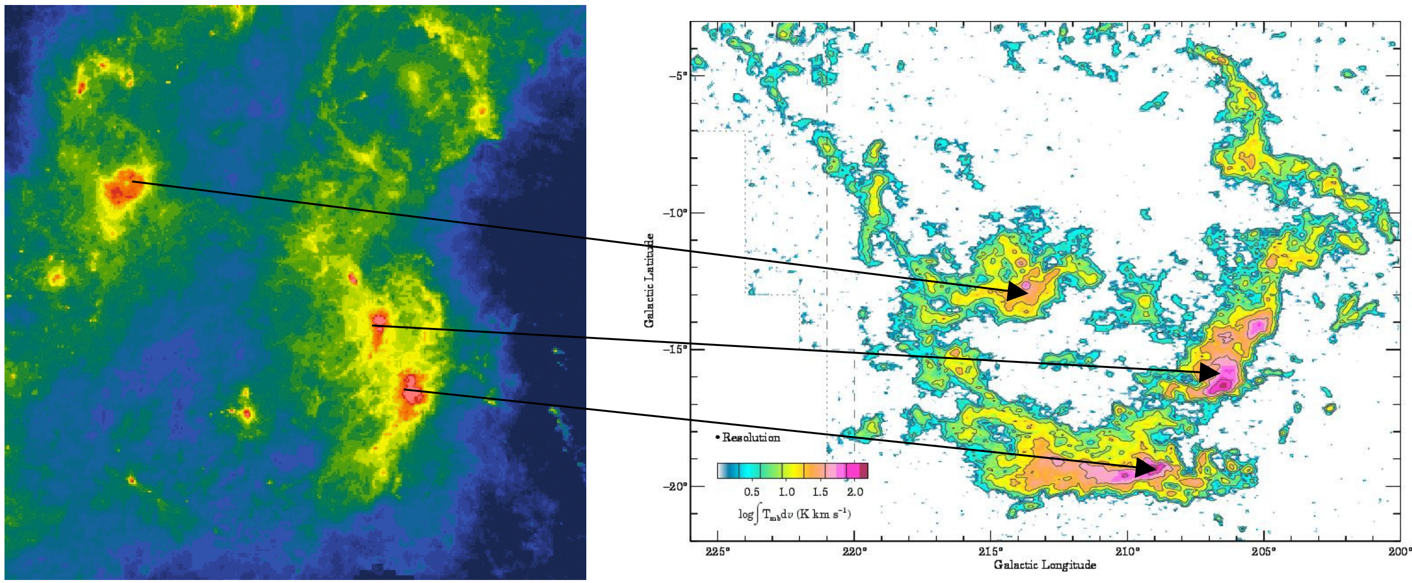

CO

HH46 – Visual → NIR → MIR

The Spitzer-view

Inner, outer, & (far-) outer Galaxy

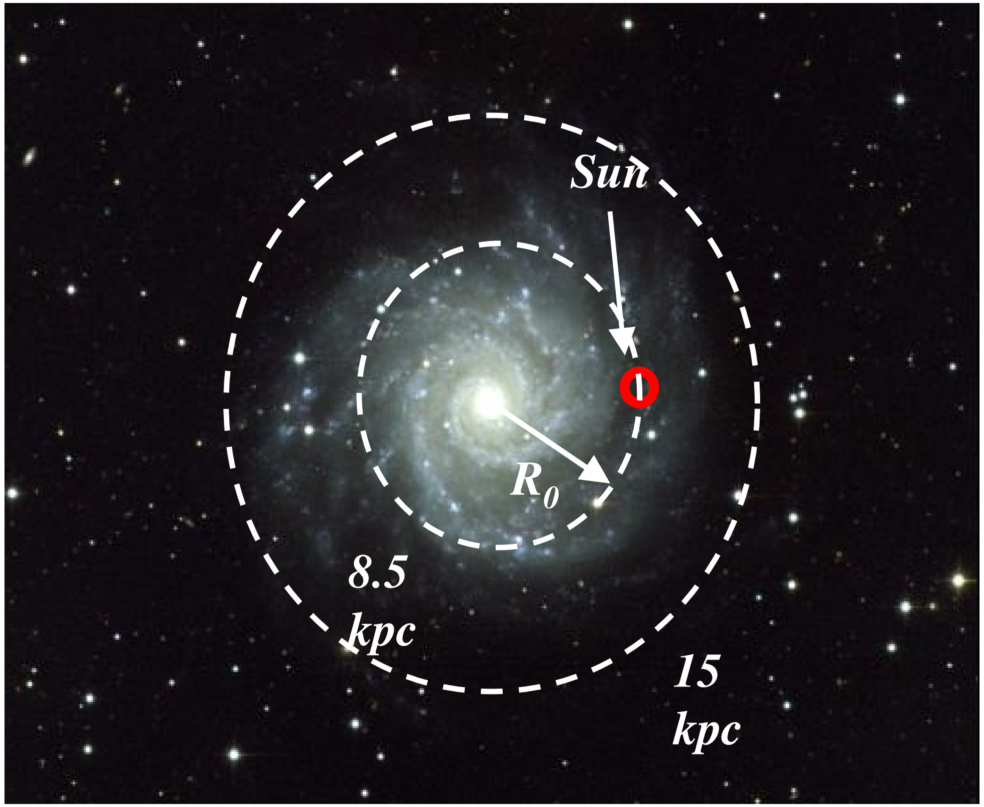

Solar circle: $R = R_0 = 8.5$ kpc

Inner Galaxy: $R < R_0$

Outer Galaxy: $R > R_0$

Far-Outer Galaxy: $R > 15$ kpc

Distribution ISM

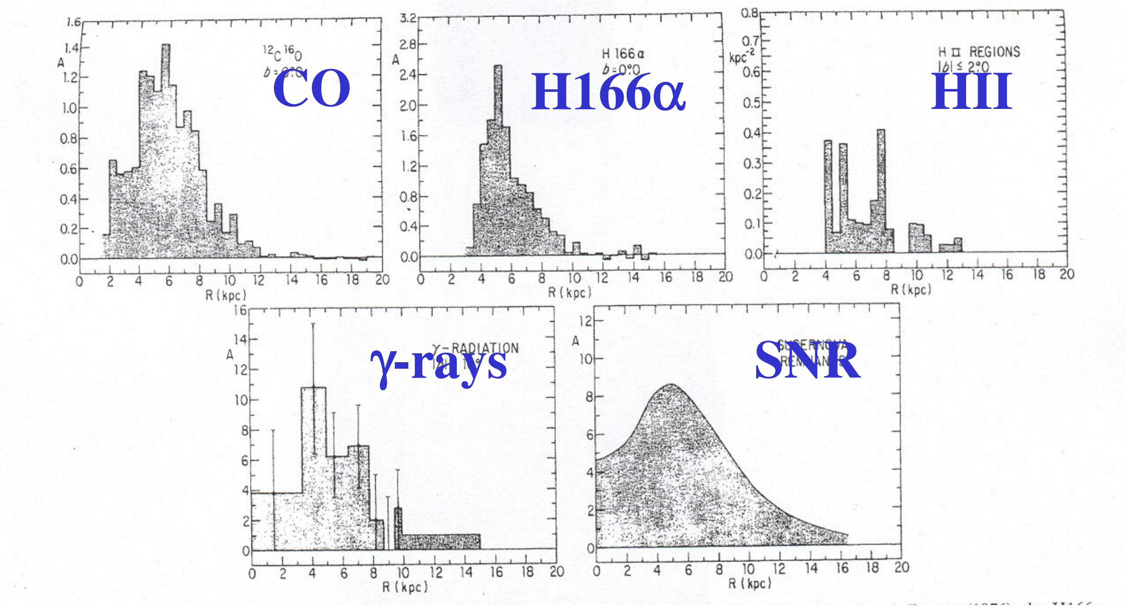

R(kpc): 0 10 20

Galactic ring
4 < R < 6 kpc

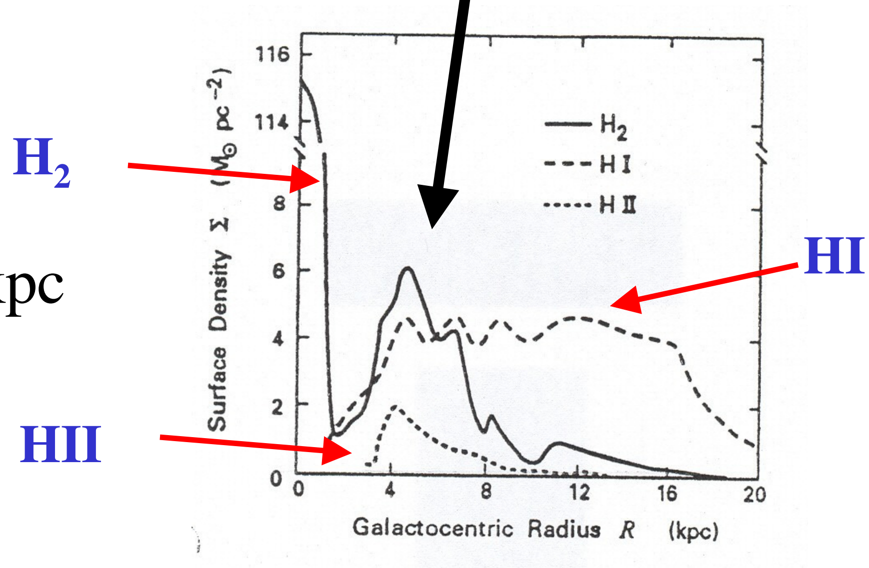

Distributions peak at $R < R_0 = 8.5$kpc
Max. extent ~ 2 R_0

Radiation mechanism of HI

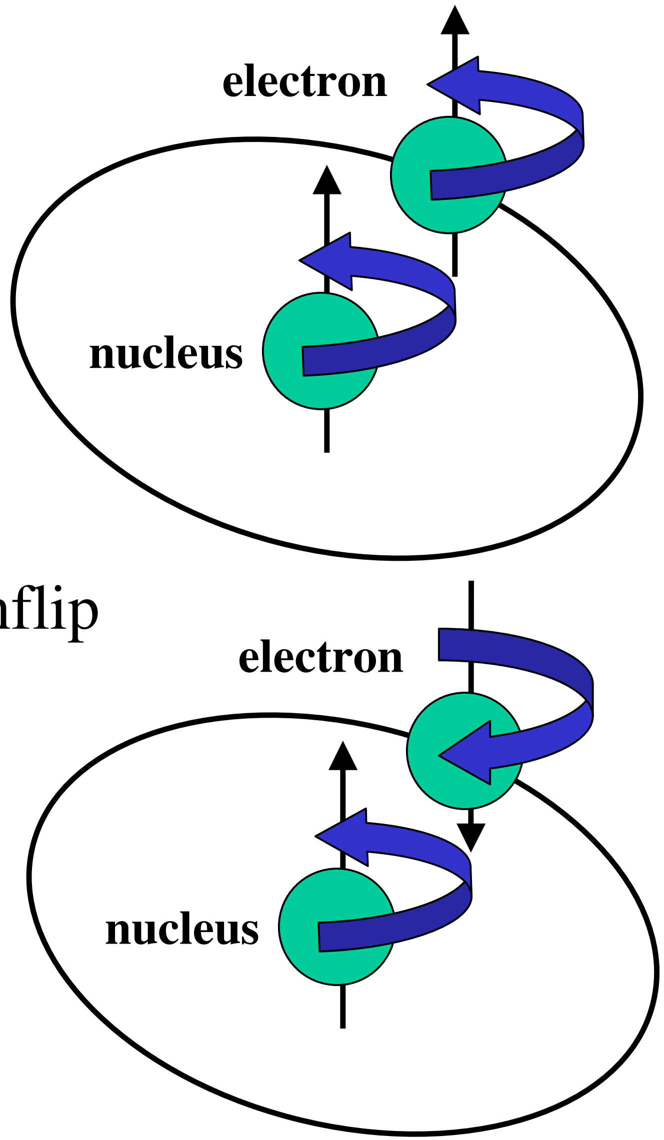

E_2: high

spinflip

$\Delta E = E_2 - E_1 = h\nu$
at 1.4 GHz (21.2 cm)

E_1: low

Spontaneous trans. prob. $A=2.85\ 10^{-15}\ s^{-1}$,
i.e. once every 12 Myr!
De-excitation governed by collisions.

Galactic distribution HI

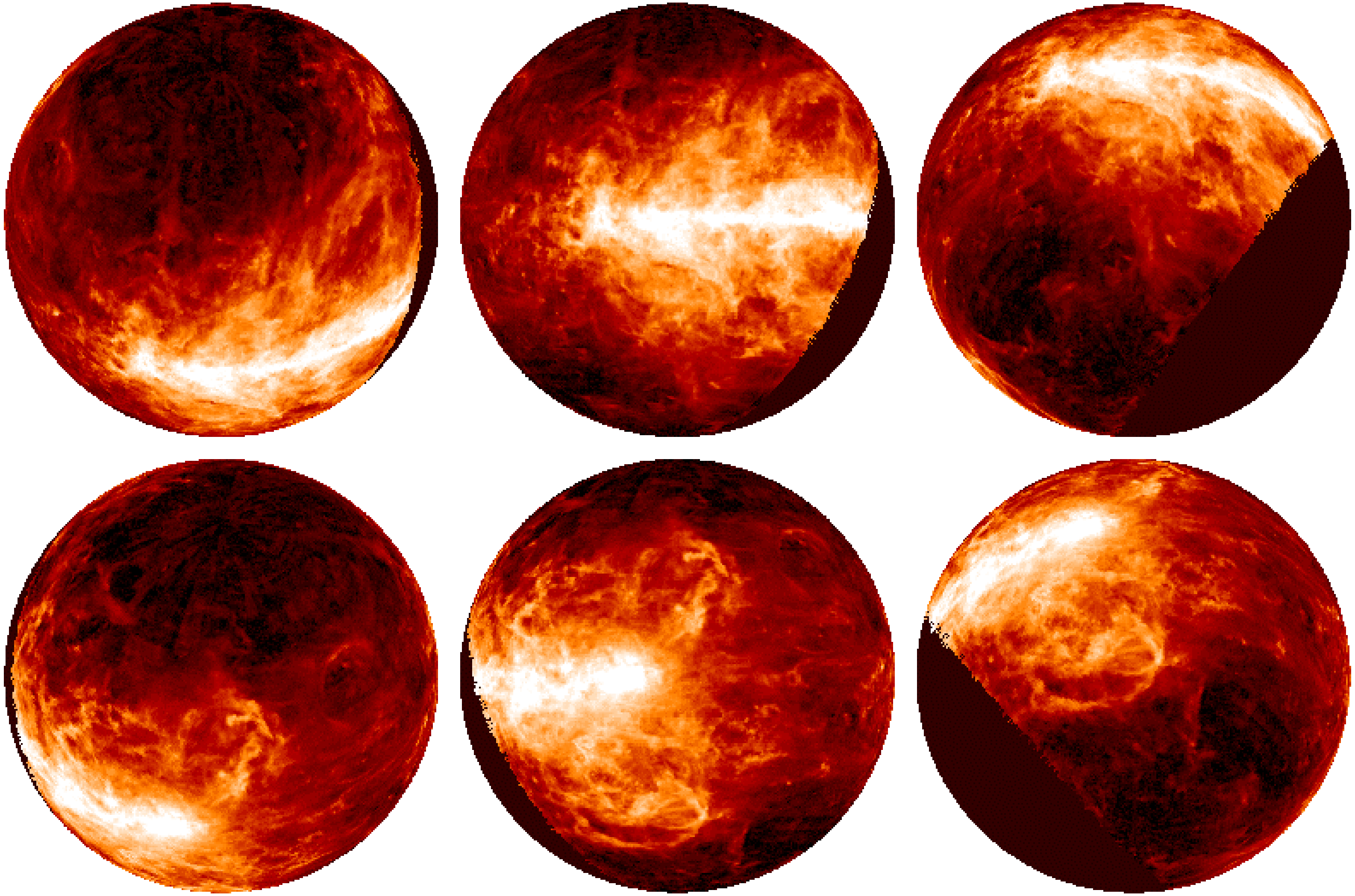

Hartmann & Burton 1994

CO, not H_2

ISM composed essentially of hydrogen:

HI: 21-cm line

H_2: symmetric molecule $\Rightarrow$ no radio emission

- **UV absorption lines**
- **IR emission lines**

CO: most abundant after H_2 : $[H_2]/[CO] \sim 1 \times 10^{-4}$.

- **excited by collisions with H_2**
- **easily observed rotational transitions at (sub-)mm wavelengths**
- **$n(H_2) \geq$ a few $\times 10^3$ cm^{-3}**

Galactic distribution CO

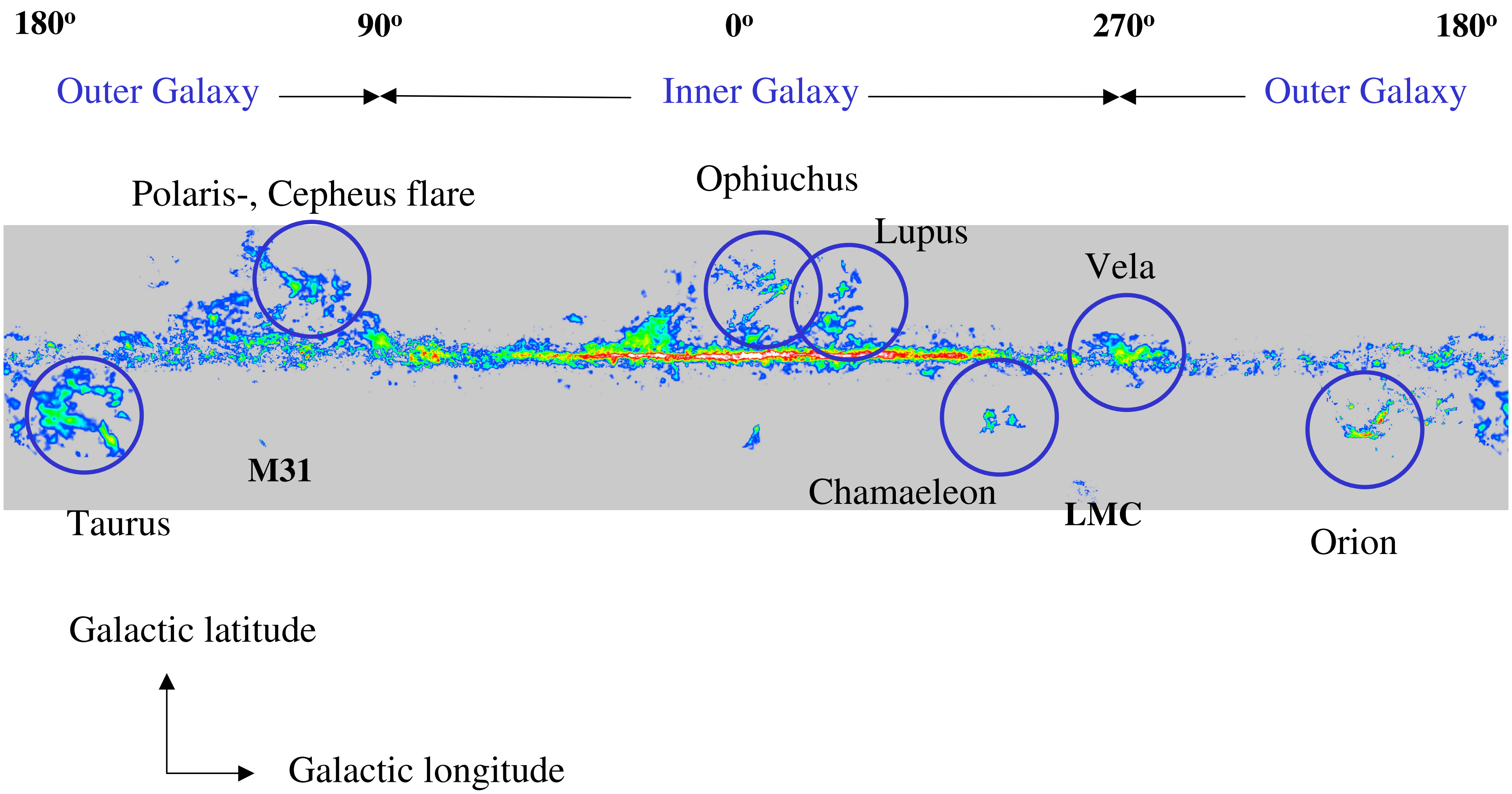

Dame, Hartmann & Thaddeus 2001

HI: tilted disk

HI: warped & flared disk

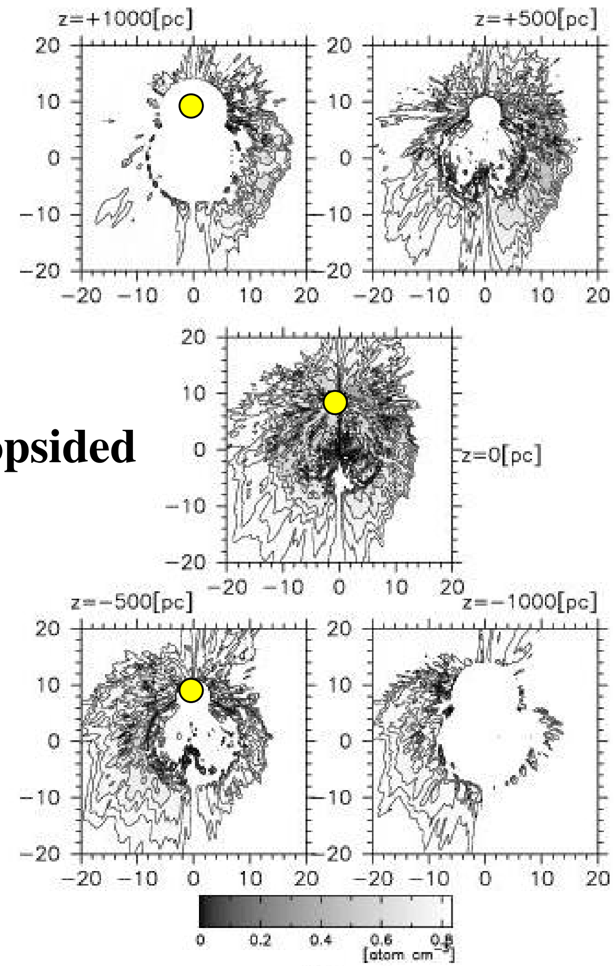

lopsided

Fig 6

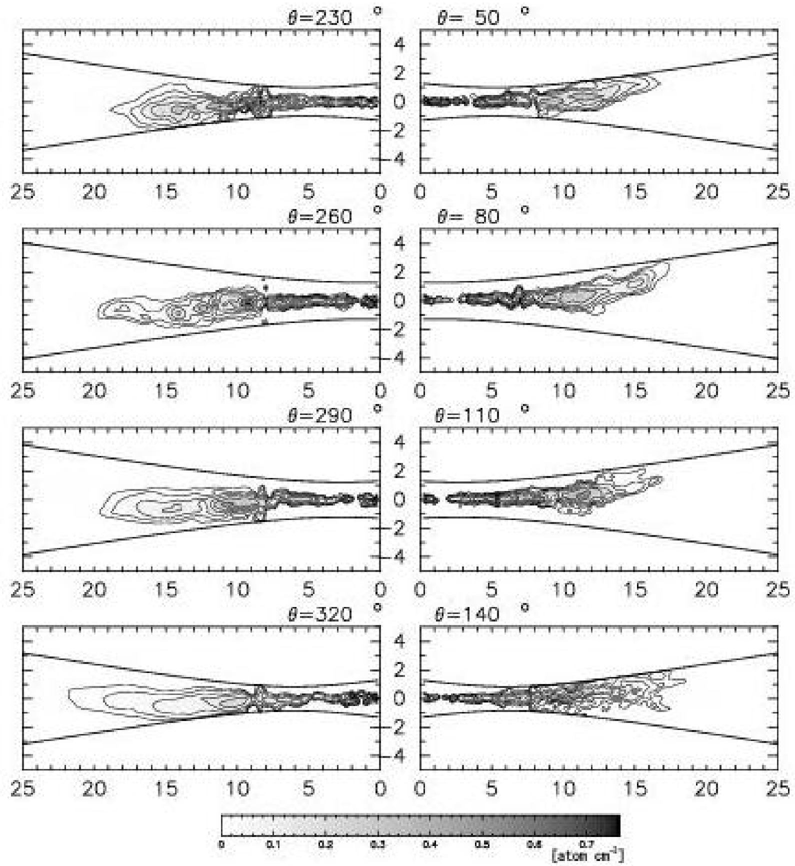

Fig 7

Nakanishi & Sofue 2003 PASJ

Same seen in H_2/CO

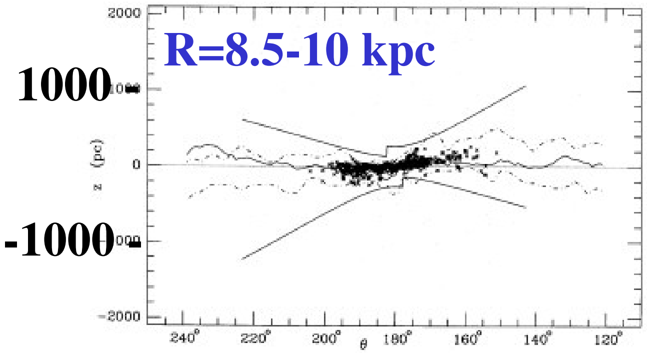

Fig. 8a. Distribution with galactocentric azimuth of the z heights of molecular clouds with kinematic distances in the range R = 8.5 to 10.0 kpc

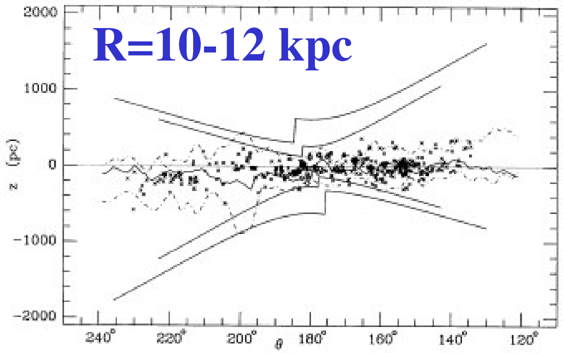

Fig. 8b. Shape of the molecular cloud layer at 10 < R < 12 kpc

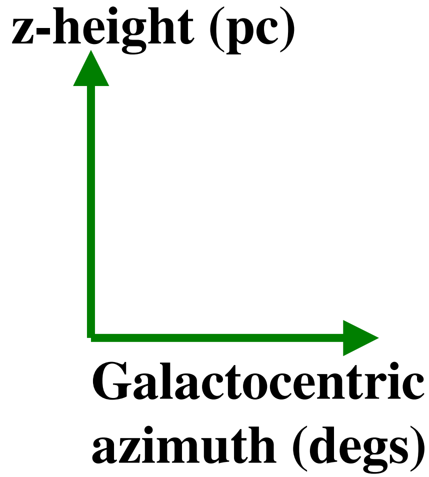

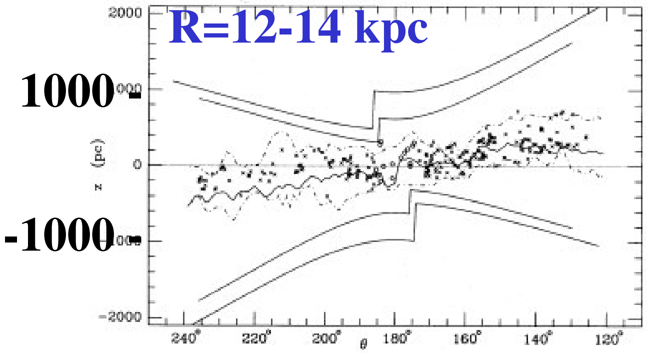

Fig. 8c. Shape of the molecular cloud layer at 12 < R < 14 kpc

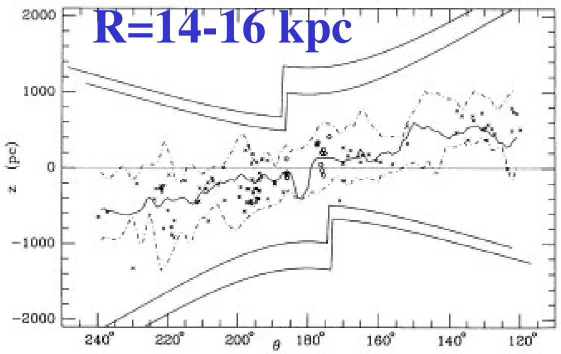

Fig. 8d. Shape of the molecular cloud layer at 14 < R < 16 kpc

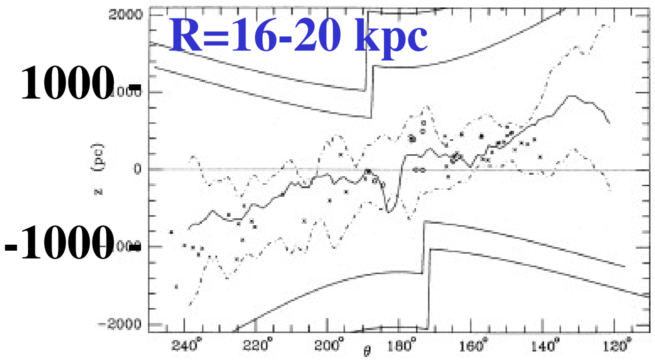

Fig. 8e. Shape of the molecular cloud layer at 16 < R < 20 kpc

Warping & flaring in CO

Wouterloot, Brand, Burton, & Kwee 1990, A&A 120, 21

Surface density

Scale height

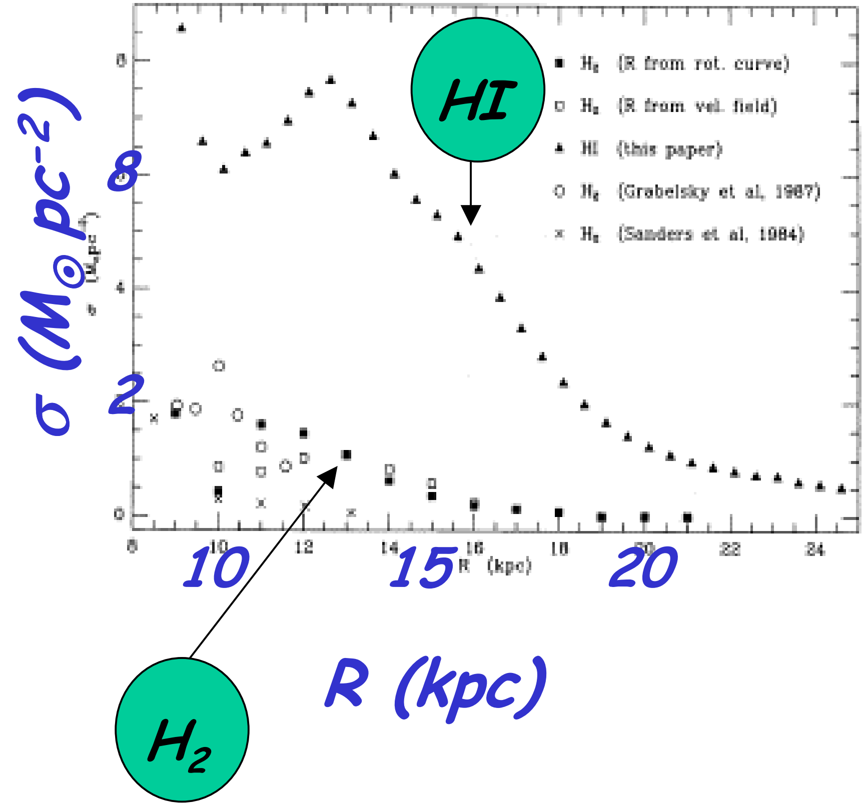

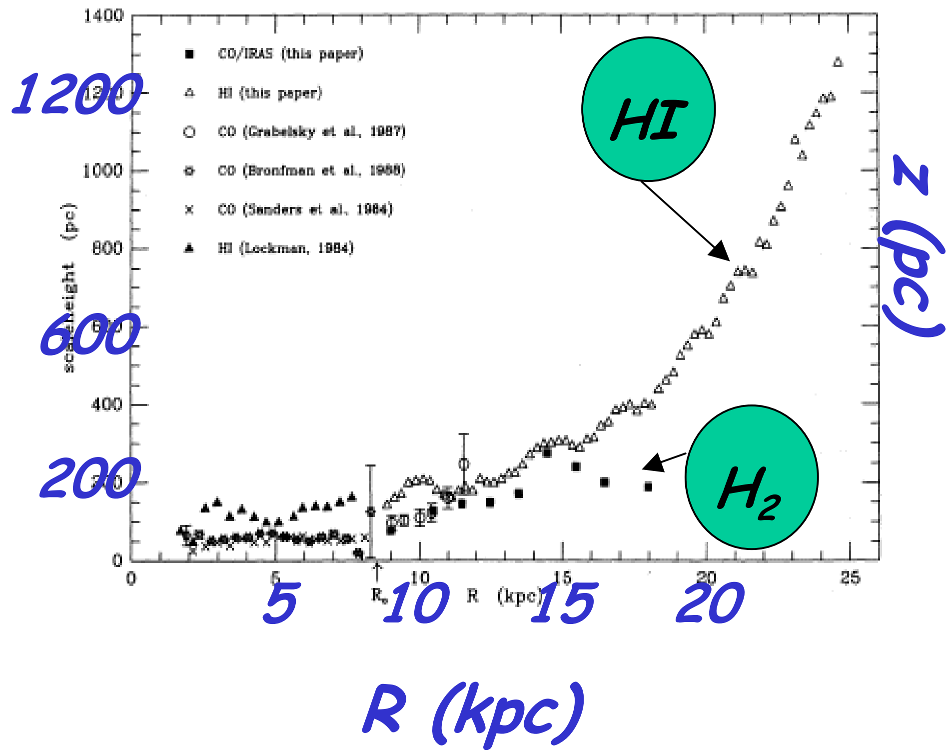

"flared disk" ('a svasato')

In OG: Surface density down, scale height up ⇒ volume density even lower

Wouterloot, Brand, Burton, & Kwee 1990

A thick disk in CO

(Dame & Thaddeus 1994)

CO (29.5-30.5 degs) HI

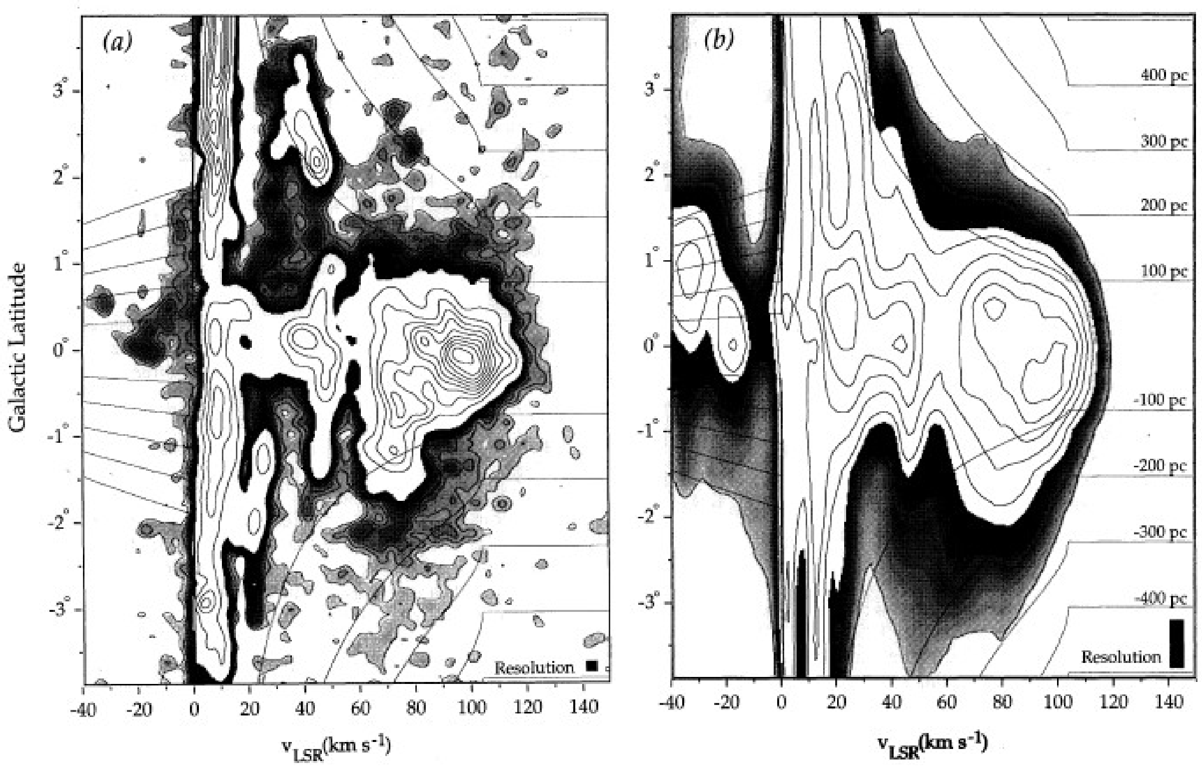

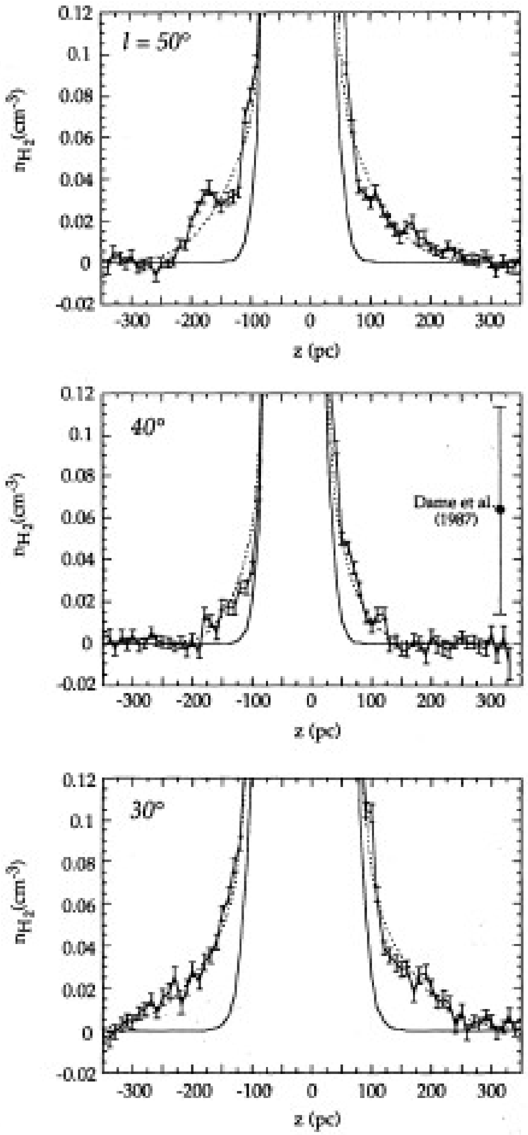

$n(H_2)$ vs. z-height

Is there a spiral arm pattern?

Distribution of HII regions (young stars)

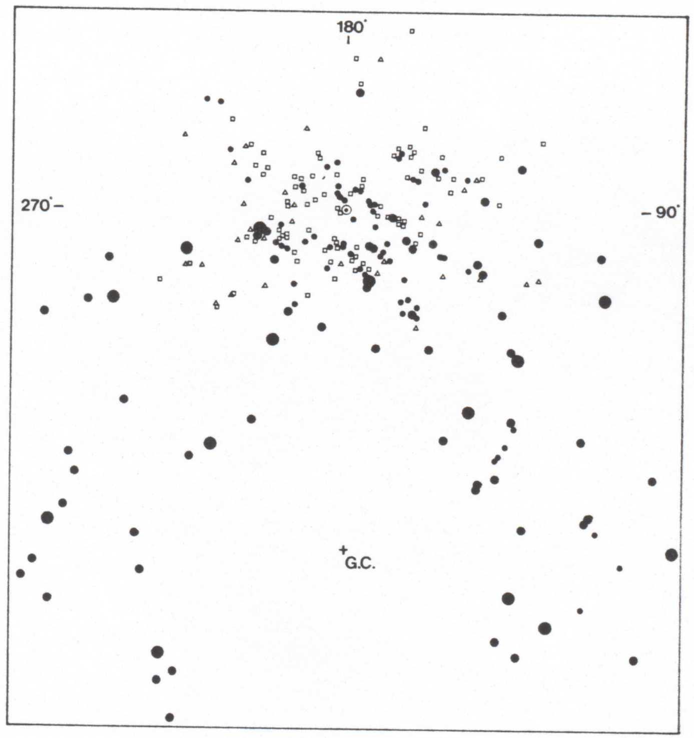

Same, but with spiral pattern drawn in

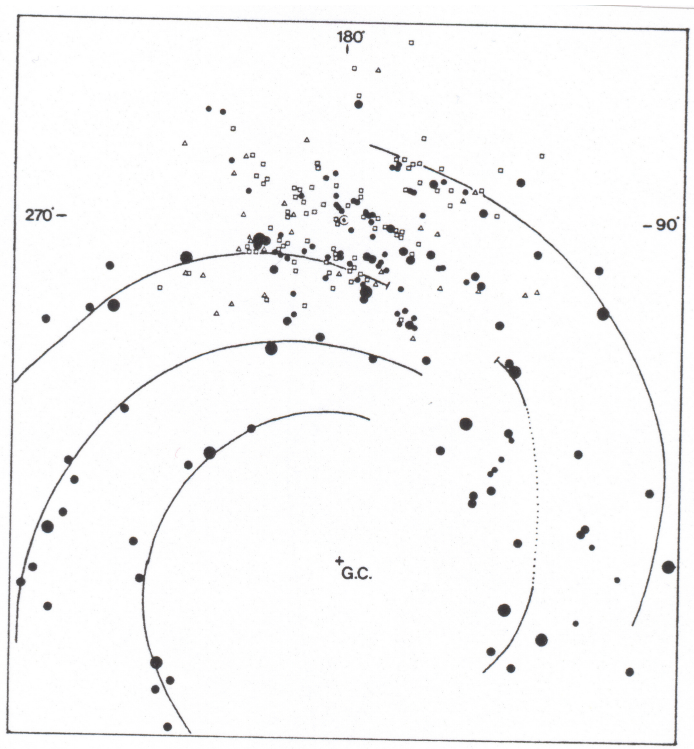

Georgelin 1975

Spiral structure

From Hα (Russeil, A&A 2003)

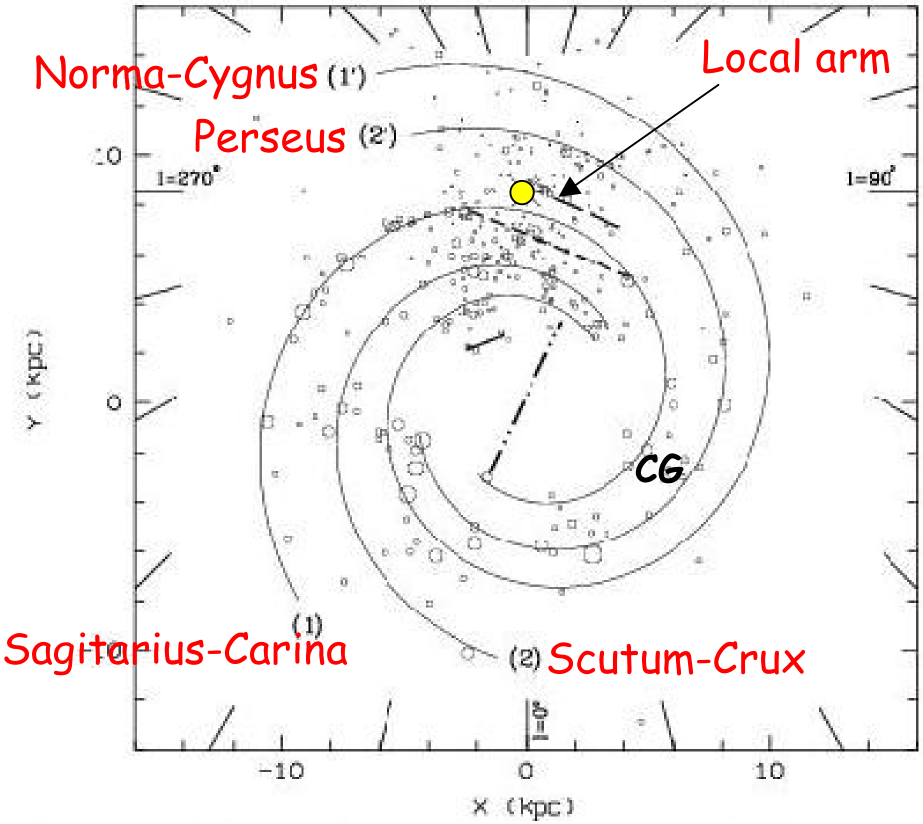

From HI (Nakanishi & Sofue 2003 PASJ)

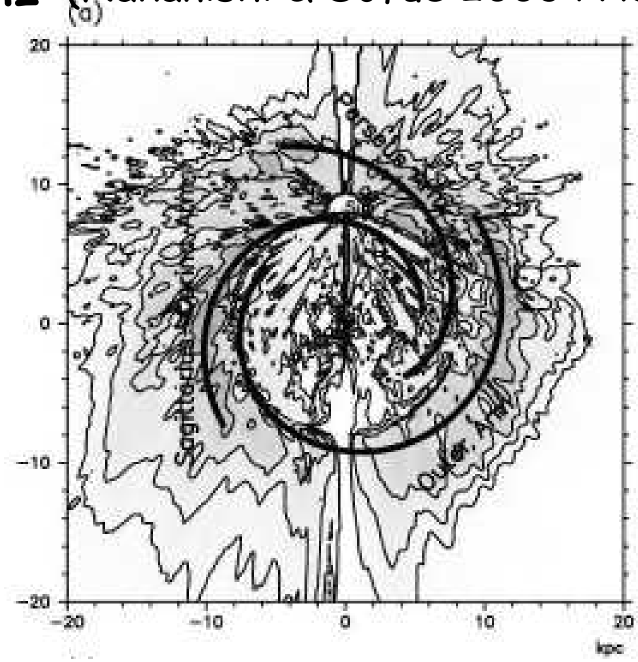

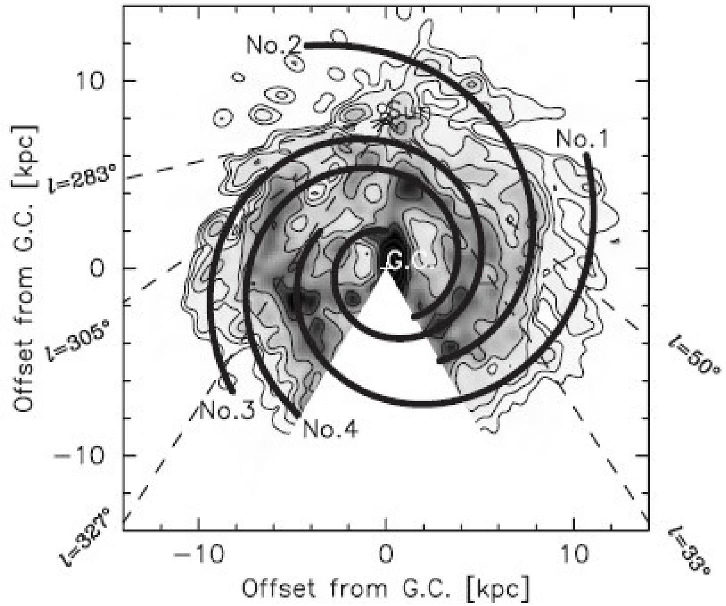

From CO(1-0)

(Nakanishi & Sofue 2006 PASJ)

NEW Outer arm in HI

McClure-Griffiths et al. 2004

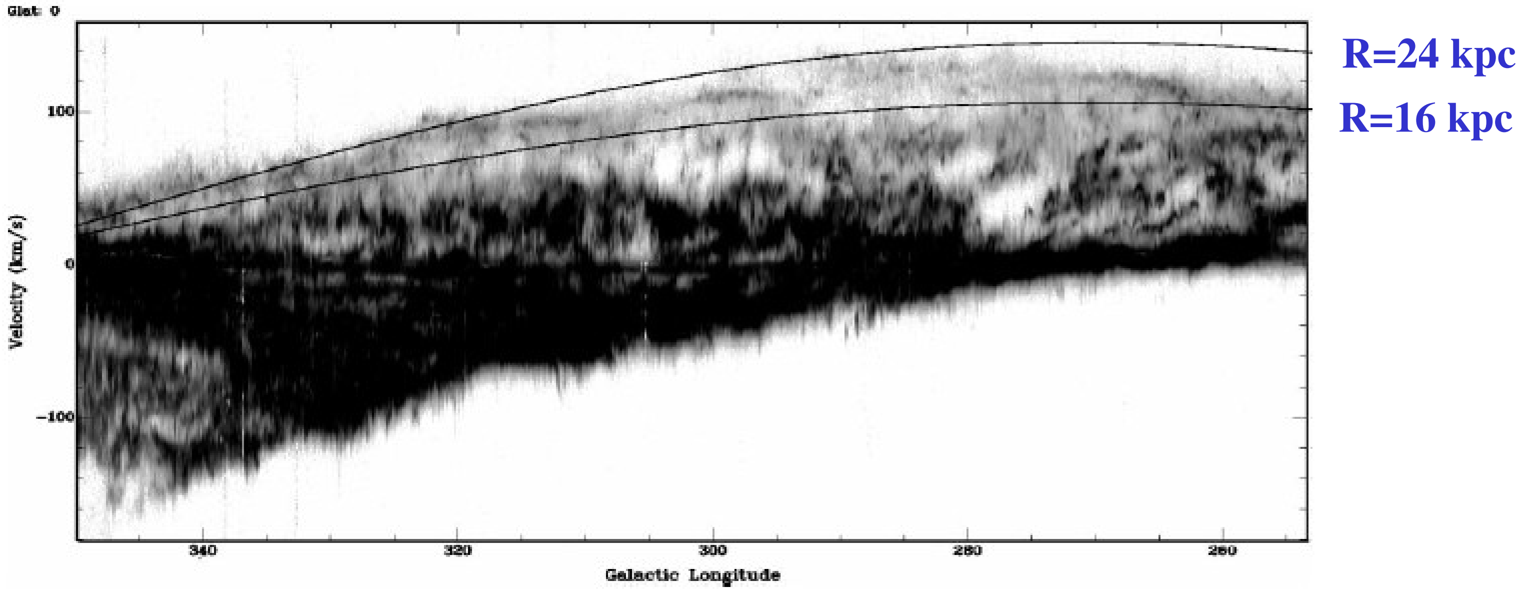

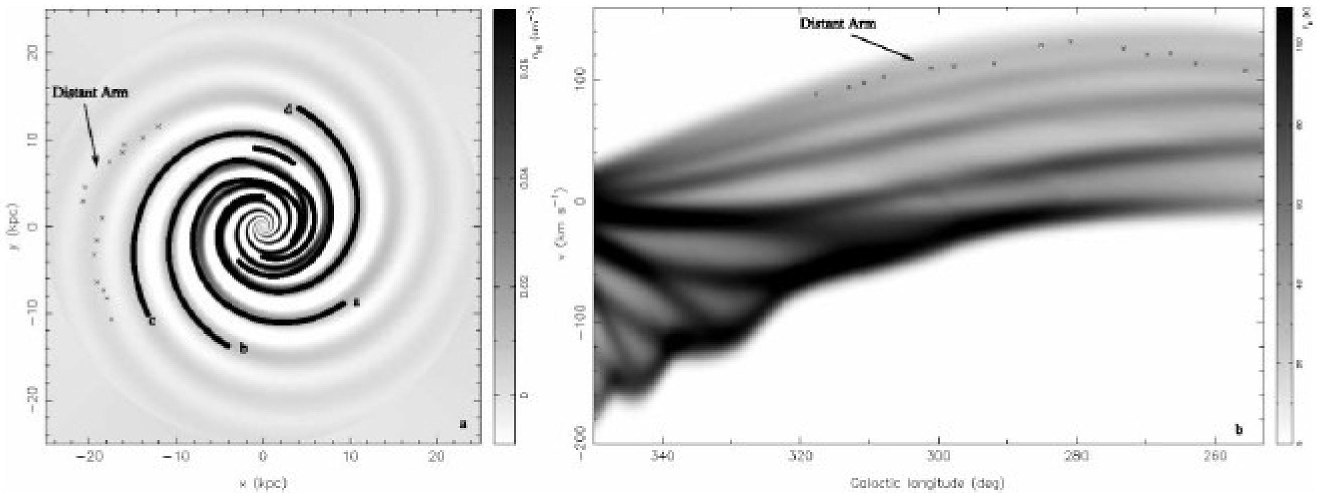

FIG. 1.—(a) Differential H I density (spiral perturbation minus the underlying Toomre disk) for the simple four-arm Milky Way spiral model described in § 4.

The multi-phase ISM

		T(K)	n_H(cm^{-3})	f_V	f_M	Probes
HII						
traditional		10^4	0.1-10^4	0.001	0.02	Hα, recomb. lines
coronal	HIM	≥3x10^5	0.003	0.6?	0.001	[OVI], X-rays
warm	WIM	8000	0.25	0.2	0.1?	HI,Hα, H166α
HI						
clouds	CNM	80	40	0.025	0.4	HI
warm	WNM	8000	0.4	0.1-0.5?		HI
H_2						
diffuse	Transl	30-80	10^2-10^3	≤0.01		HI,CO,100μm
dense	Dark	10-100	10^3-10^6	0.005	0.5	mm molec.lines FIR dust

Models of the ISM (2-phase)

Early model: Field, Goldsmith & Habing 1969

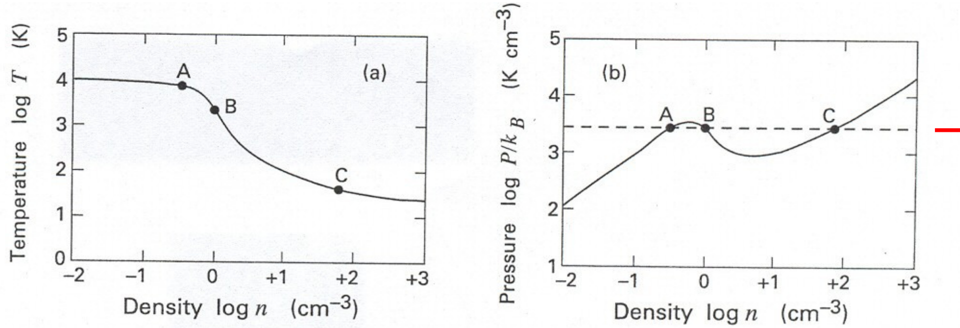

Figure 2.5 (a) Theoretical prediction for the equilibrium temperature of interstellar gas, displayed as a function of the number density n. (b) Equilibrium pressure nT as a function of number density. The horizontal dashed line indicates the empirical nT-value for the interstellar medium.

→ Log(P/k) = 3.5 cm^{-3} K

Assume pressure equilibrium (P/k ∝ nT = constant)

Stable points: A and C, corresponding to:

WNM (n=0.4, T=7000) and CNM (n=60, T=50)

Explained most of the then-known observations.

Models of the ISM (3-phase)

Ostriker & McKee 1977: 3-phase model

Gas distributed among 4(!) forms: HIM, WIM, WNM, CNM
that are in P-equil. at $P/k \approx 3000\ \mathrm{K cm^{-3}}$.

SNe, OB-winds create system of hot tunnels in ISM

Recent assesment: Cox, 2005 Ann. Rev. A&A 43

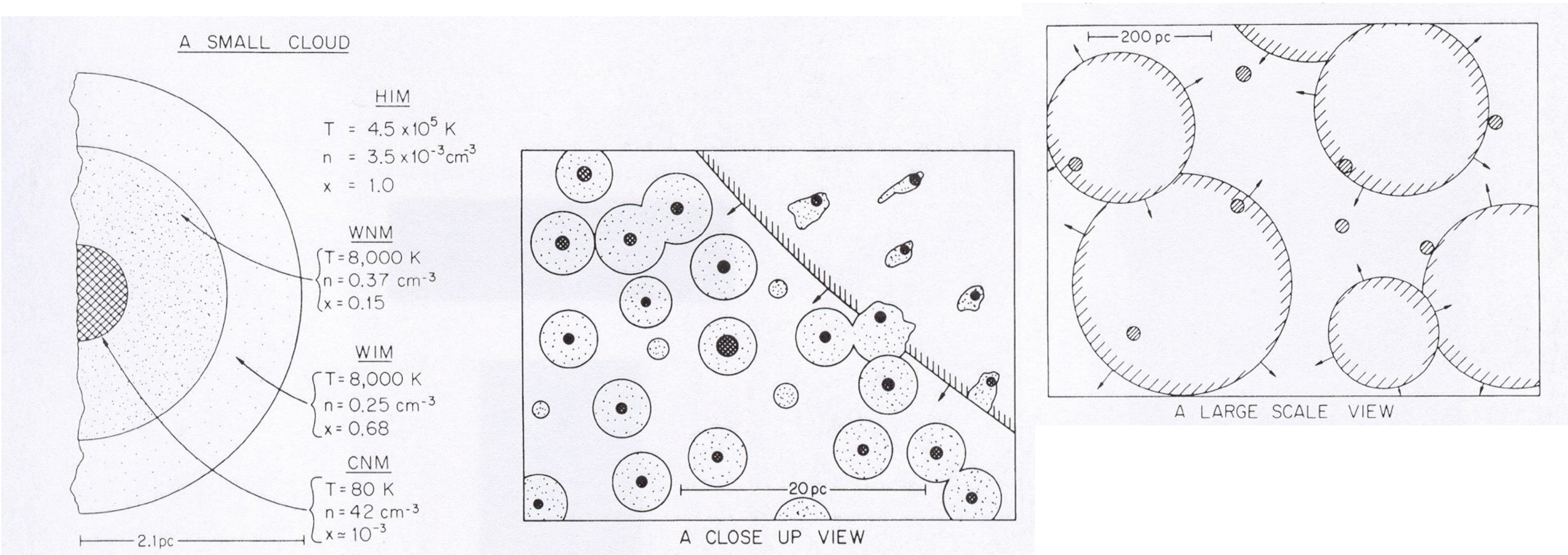

Models of the ISM (Cox upgrade)

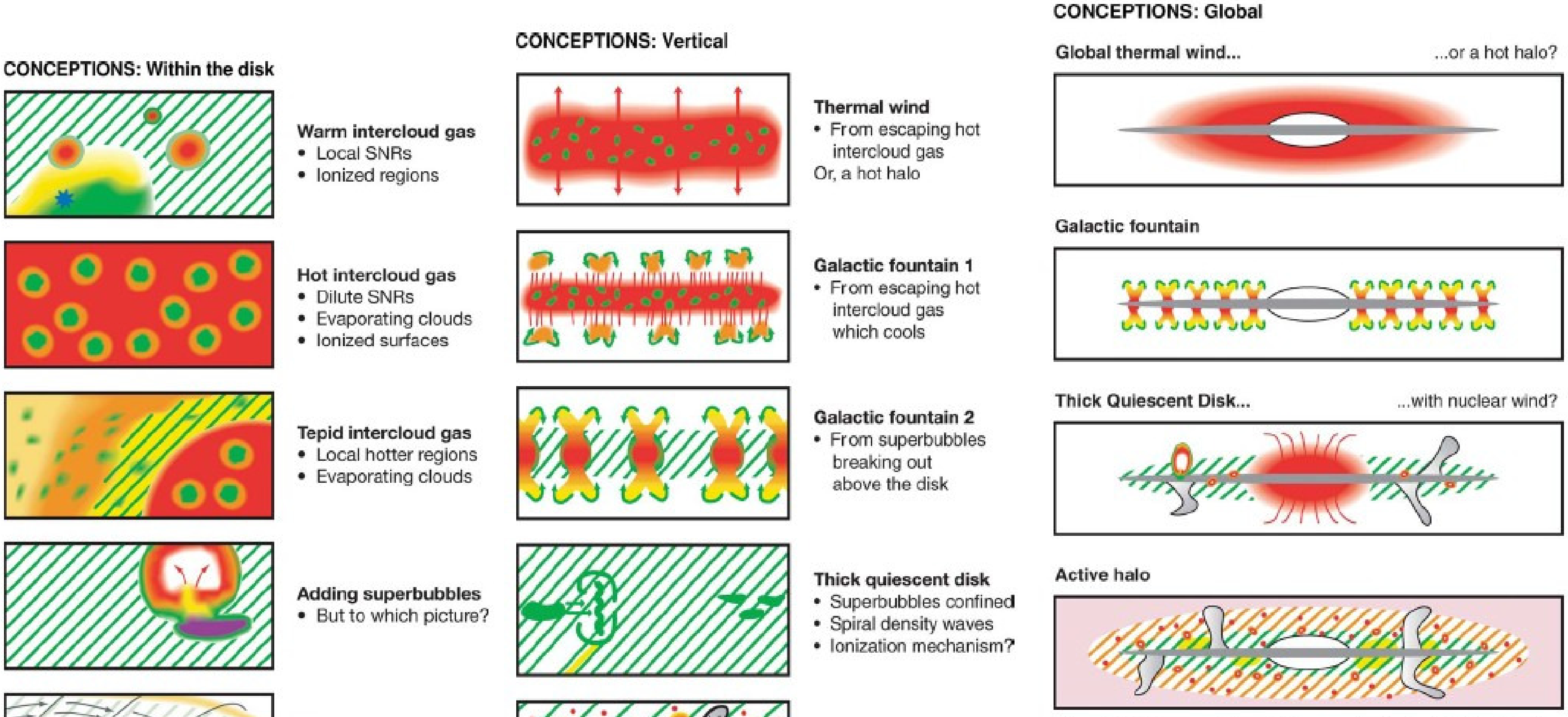

Firure 10 Various conceptions of the larger scale structure of the Galactic atmosphere. In this figure, *hatched green* indicates warm HI; *hatched green on yellow background*—diffuse warm HII; *orange*—hotter gas bearing OVI; *red*—material hot enough to emit X rays; *gray*—plumes of escaping cosmic rays; and *red dots*—microflares. Problems with the *top two panels* are discussed in the text. The *lower two panels* contain some elements of potentially greater realism.

Cox 2005 ARAA

Molecular clouds – transition interface

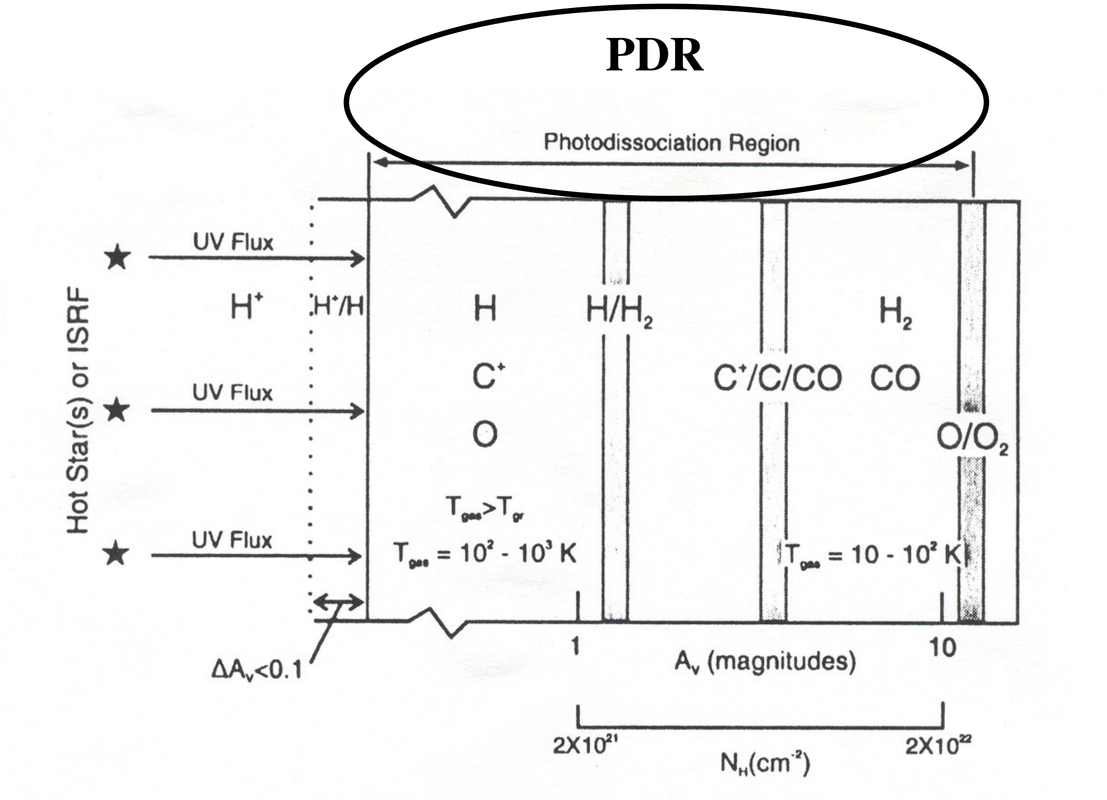

Figure 3 A schematic diagram of a photodissociation region. The PDR is illuminated from the left and extends from the predominantly atomic surface region to the point where O_2 is not appreciably photodissociated ($\simeq$10 visual magnitude). Hence, the PDR includes gas whose hydrogen is mainly H_2 and whose carbon is mostly CO. Large columns of warm O, C, C^+, and CO and vibrationally excited H_2 are produced in the PDR. The gas temperature T_{gas} generally exceeds the dust temperature T_{gr} in the surface layer.

Molecular clouds are self-shielding against UV radiation.

Clouds are surrounded by envelope of HI.

Inside: molecules. Most abundant after H_2 is CO (10^{-4}).

Molecular clouds: atomic envelope

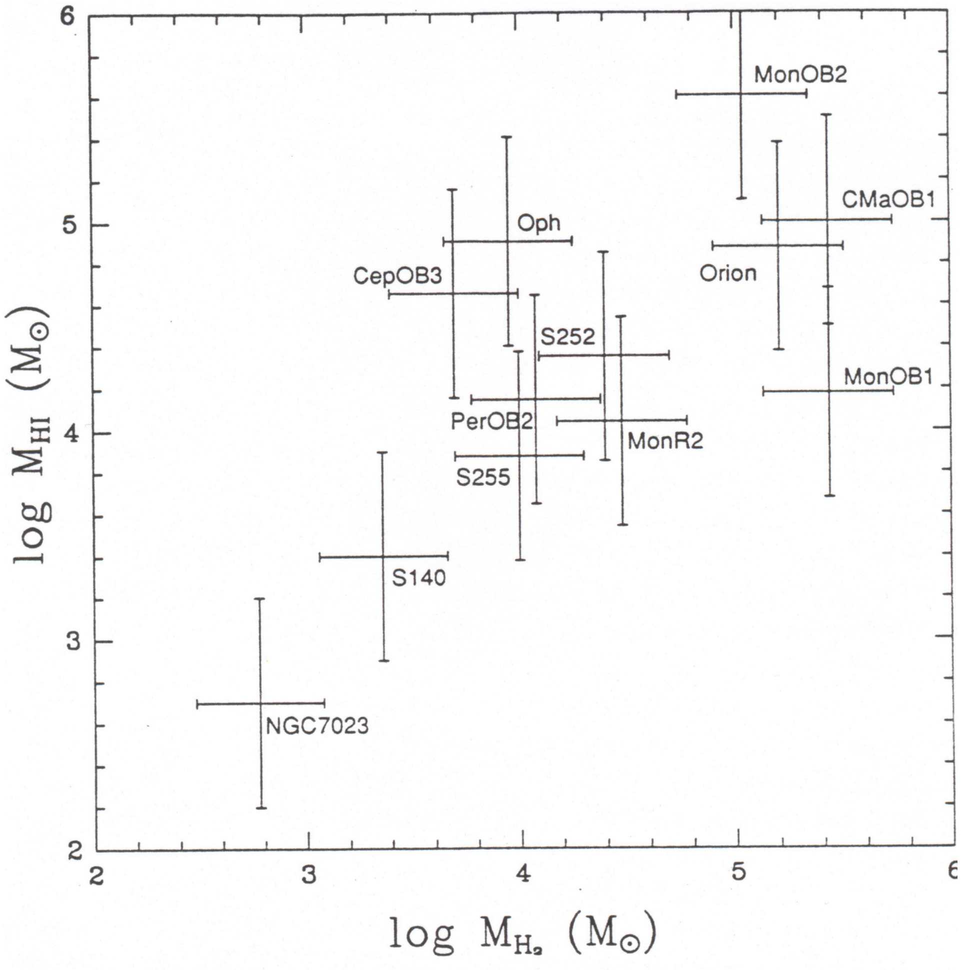

Blitz, 1993 PPIII

Interstellar Molecules

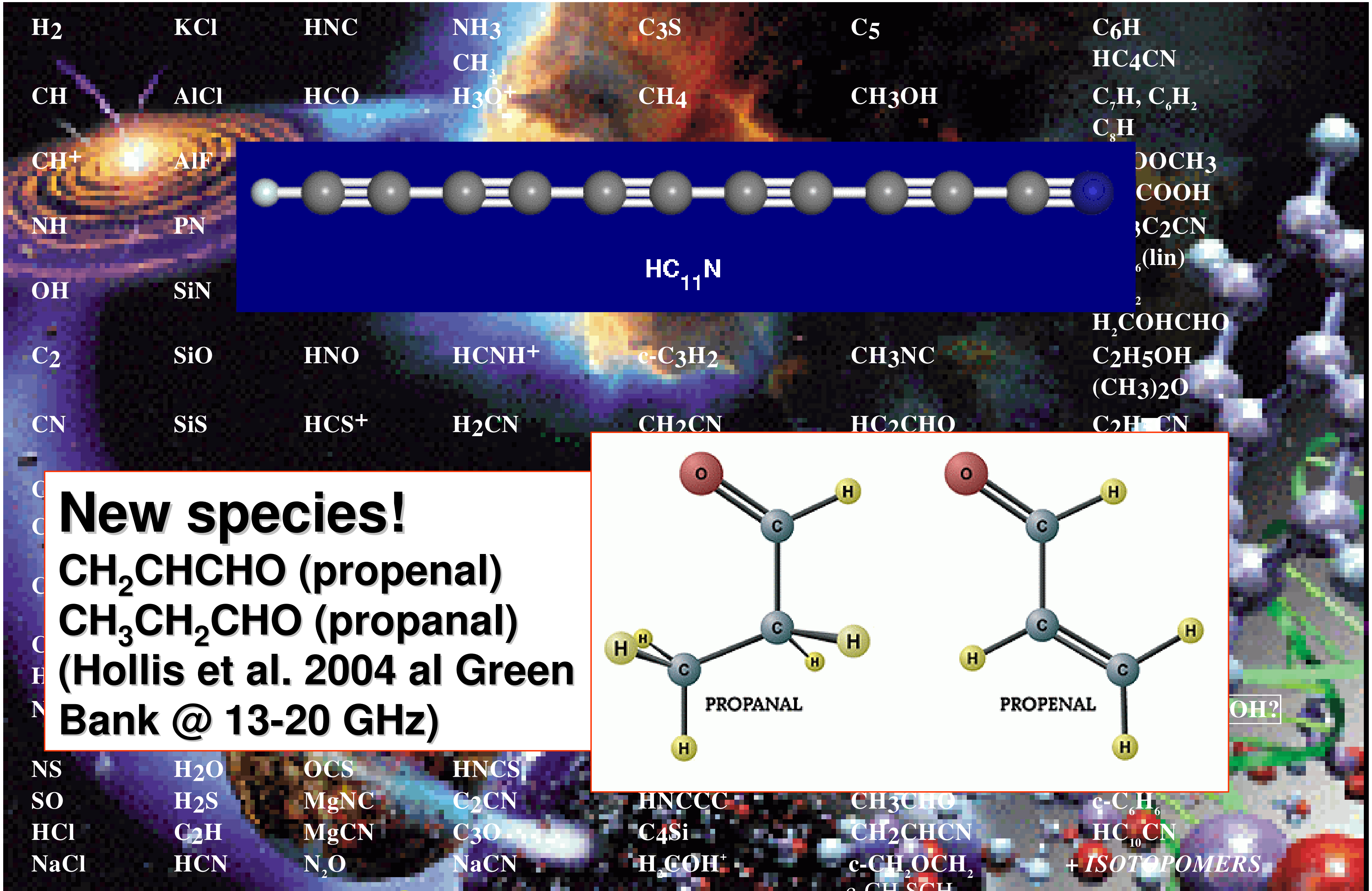

137 molecules have been detected in space (205 including isotopomers, 50 in comets)

Astrochemistry. I.

- **Formation of H_2** (Gould & Salpeter 1963; Hollenbach & Salpeter 1970; Pirronello et al. 1999; Katz et al. 1999; Cazaux & Tielens 2002; Habart et al. 2003)

$R \sim 10^{-17}\ cm^3\ s^{-1}$

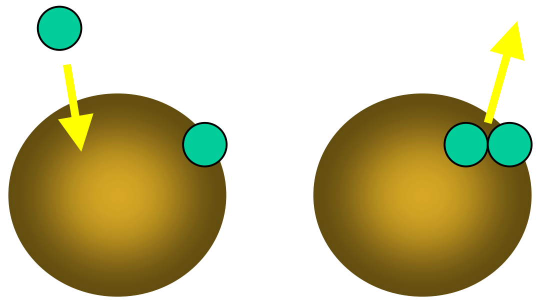

In gas phase:

$H^- + H \Rightarrow H_2 + e \quad R \sim 10^{-21} - 10^{-20}\ cm^3\ s^{-1}$

$H + H \Rightarrow H_2 + h\nu \quad R \sim 10^{-29} - 10^{-31}\ cm^3\ s^{-1}$

In molecular clouds: ion-neutral reactions

$C^+ + H_2 \Rightarrow CH_2^+ +$

$CH_2^+ + e^- \Rightarrow CH + H$

$CH + O \Rightarrow CO + H$

Astrochemistry. II.

- **Complex organic molecules** are easily observed near young stellar objects (e.g. Charnley et al. 1992; Caselli et al. 1993)

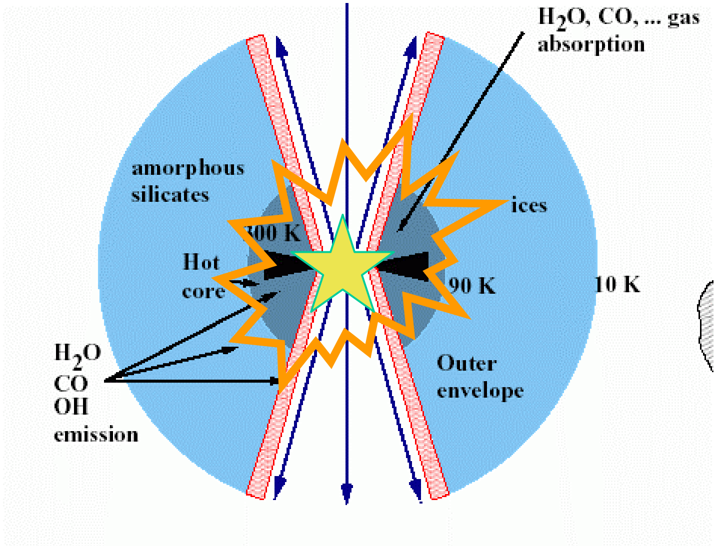

H-rich complex N-bearing and O-bearing molecules: CH_3CN, CH_2CHCN, CH_3CH_2CN, CH_3OCH_3, $HCOOCH_3$, C_2H_5OH.. (e.g. Blake et al. 1987)

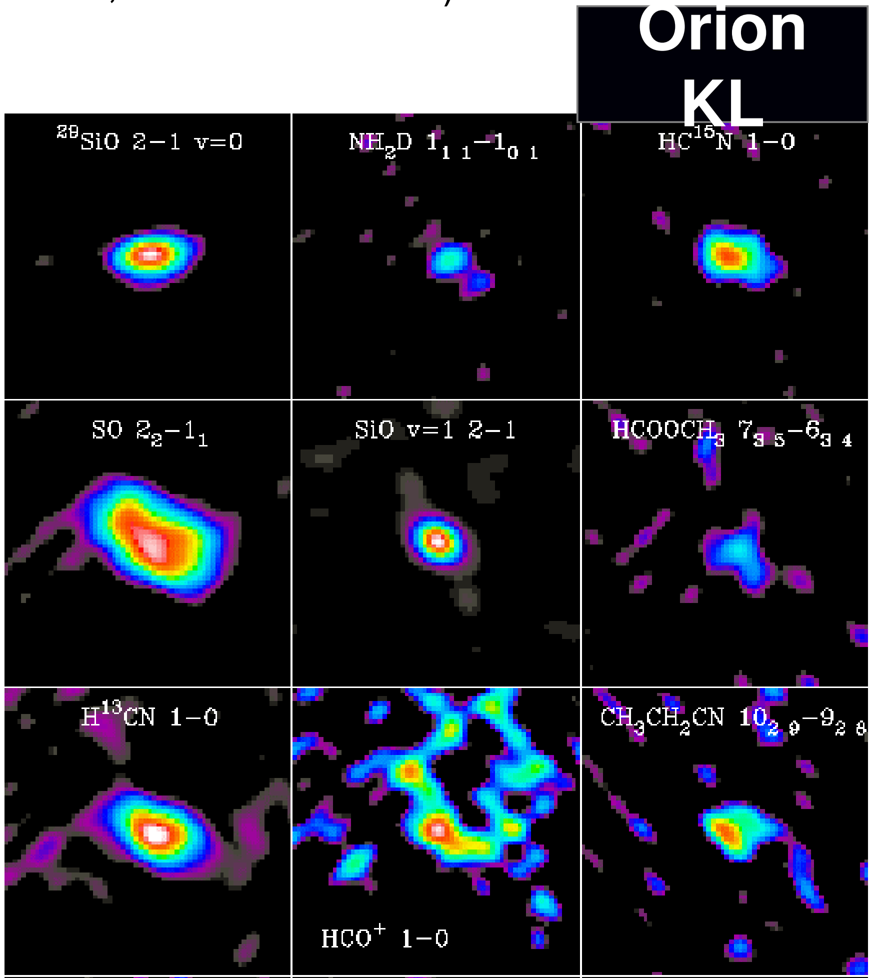

Astrochemistry. III.

- **To understand the distribution of the various molecular species to study the physical and kinematical properties of molecular clouds and of star formation.**
- Example: CO, typically used to determine the mass of molecular clouds, disappears from the gas phase at densities n(H2) > 10^4 cm^{-3} and T < 20 K.

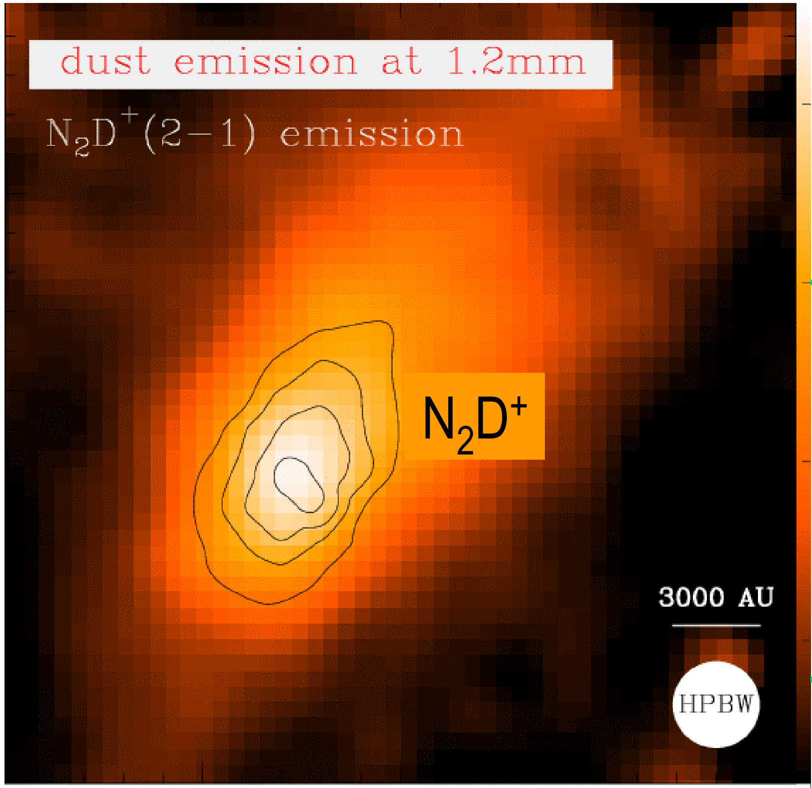

CO disappears from gas phase at R < 7000 AU

N_2 remains in the gas phase: more volatile than CO ?

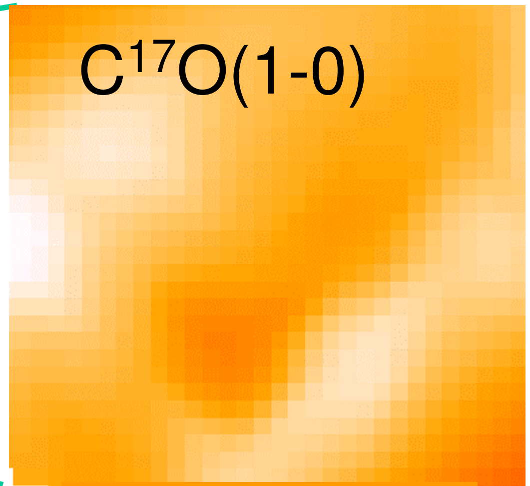

Caselli et al. 1999

L1517B: a low-mass pre-stellar core with depletion

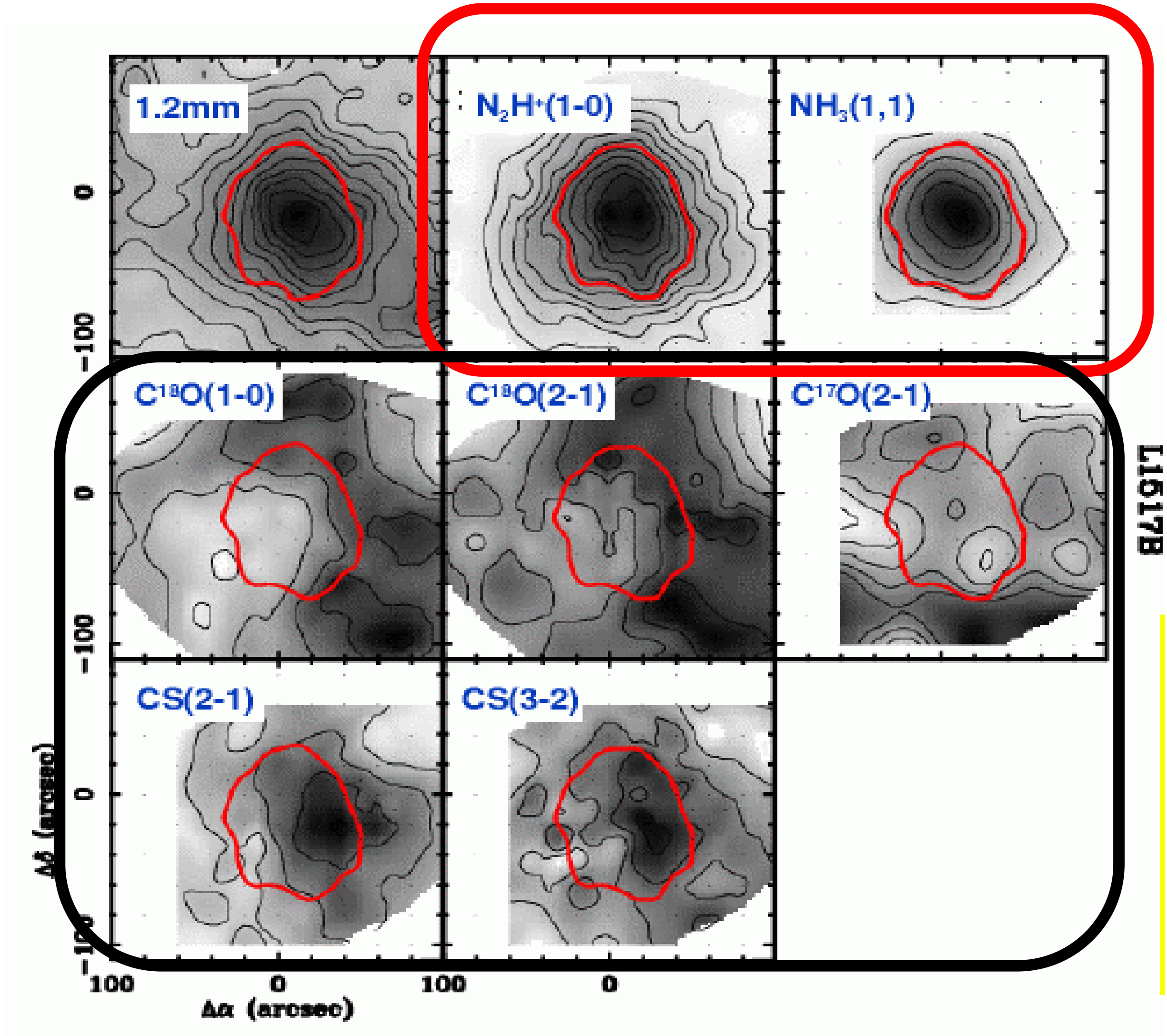

On the other hand, N-bearing species well trace the density profile seen in the dust continuum emission

C-bearing species completely miss the central density peak

Tafalla et al. 2004

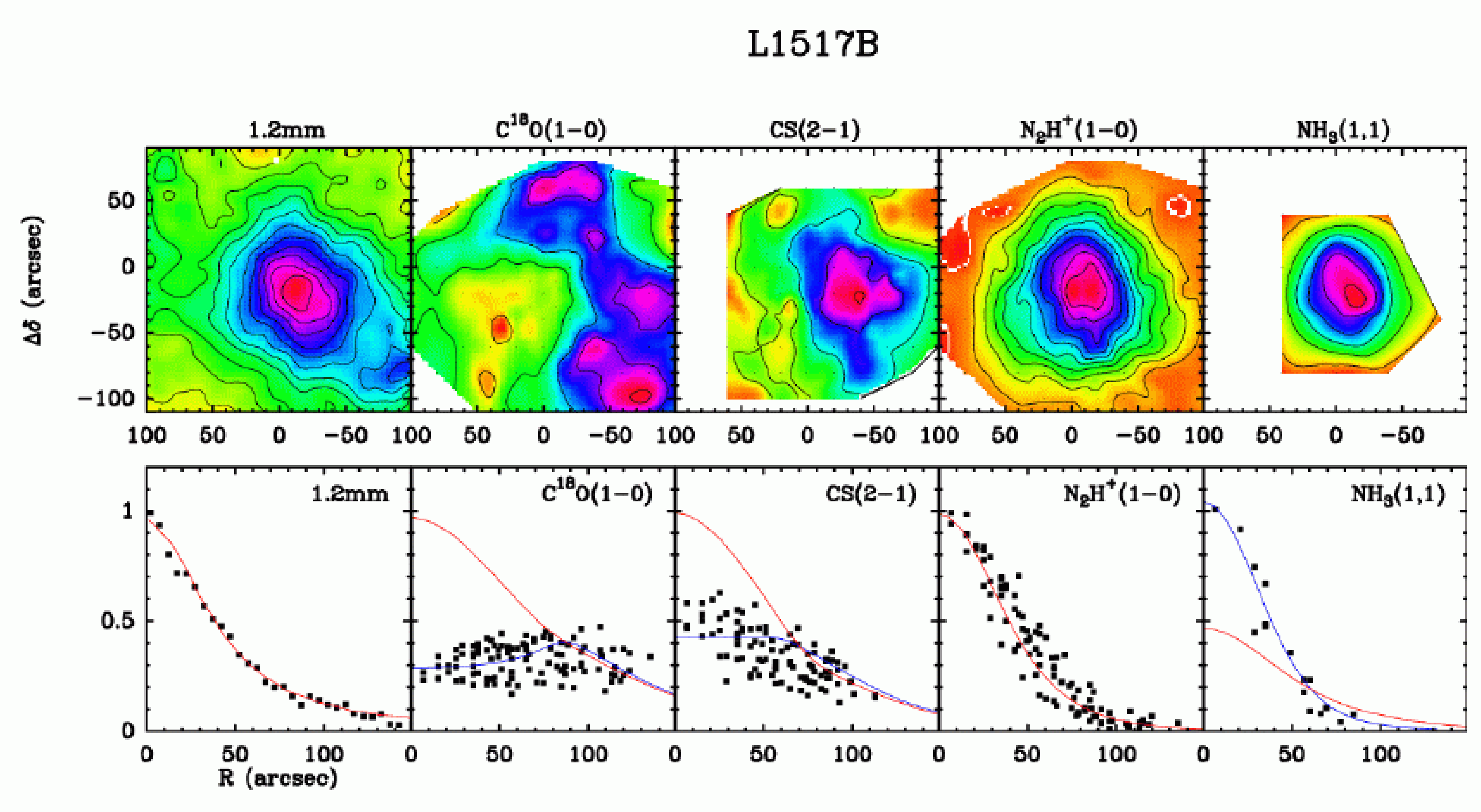

Cores have order-of-magnitude radial CS and CO abundance gradients

Shock-chemistry!

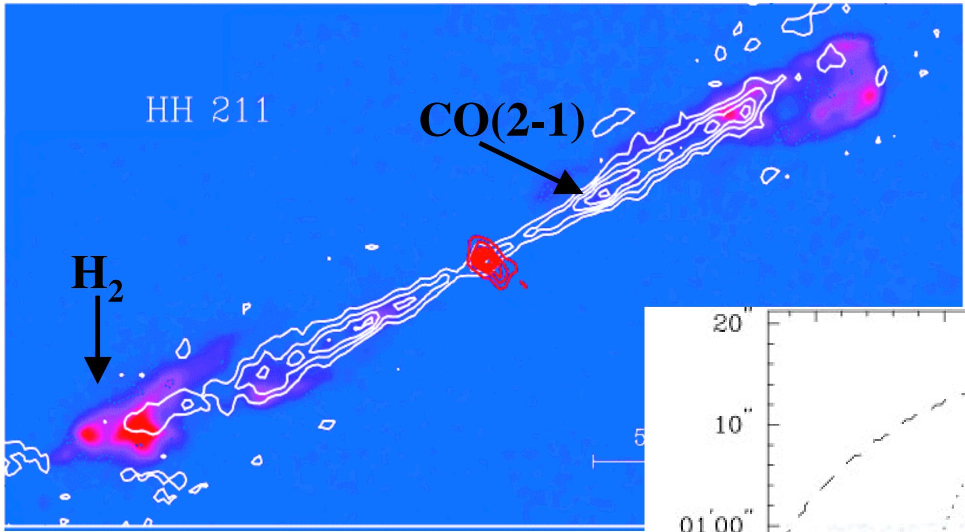

Gueth & Guilloteau (1999)

The heating and compression caused by shocks gives rise to dramatic effects in the chemical composition of the surrounding cloud. Dissociation, endothermic reactions, sublimation of ices and disruption of grains lead to a shock-chemistry.

HH211

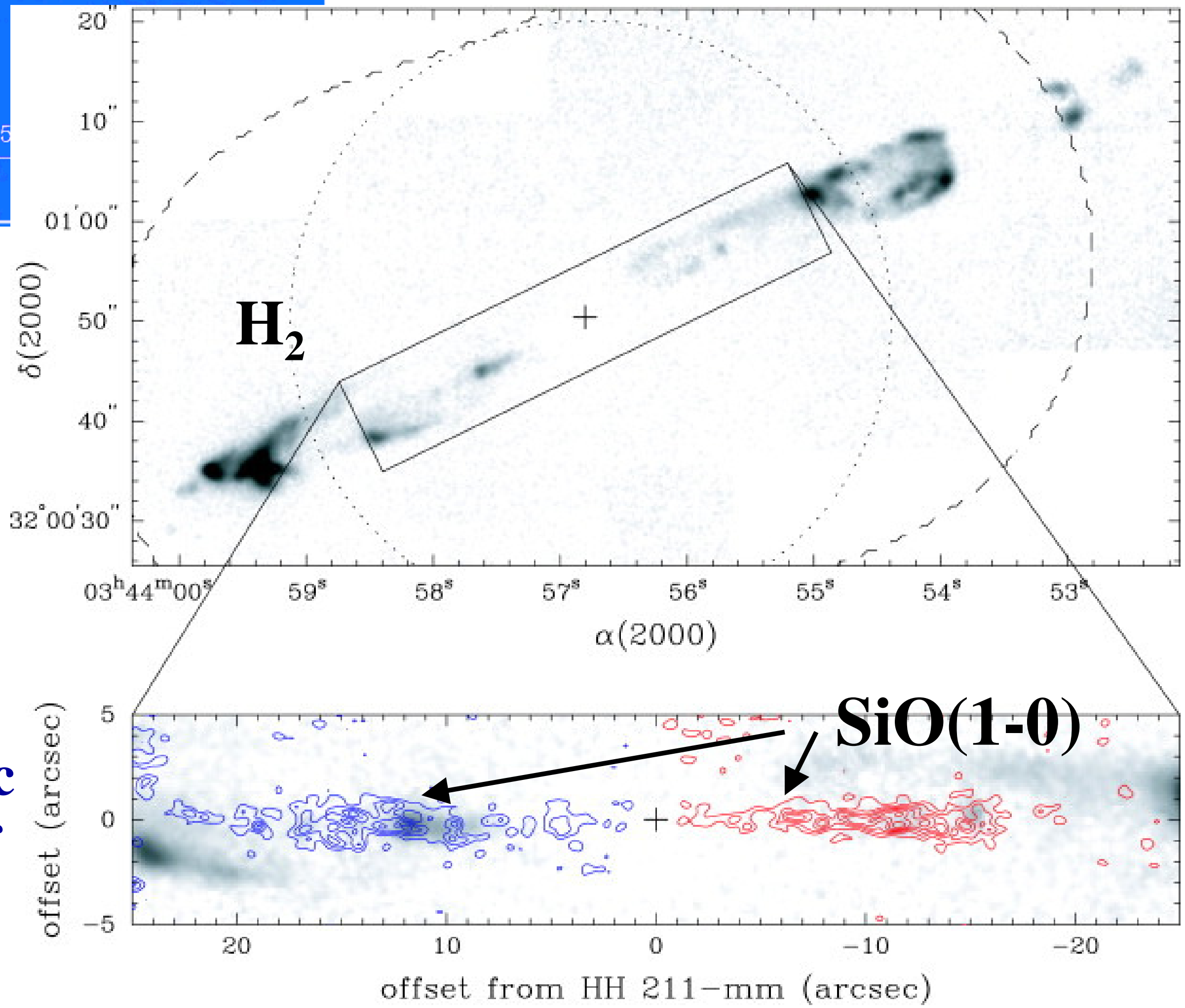

Chandler & Richer (2001)

Chemically rich outflows

Shock tracers:
CH_3OH, SiO, H_2O,
S-bearing species,
H_2CO……

Bachiller & Tafalla (2000): an empirical time sequence of low-mass outflows?

1st stage (Class 0): jet-like, HV bullets;
2nd stage (Class 0): no bullets, rich chemistry;
3rd stage (Class I): shell structure, evacuated cavity.

L1157

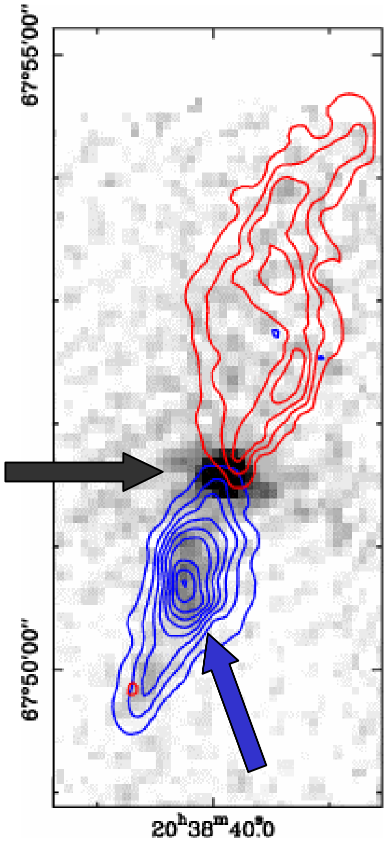

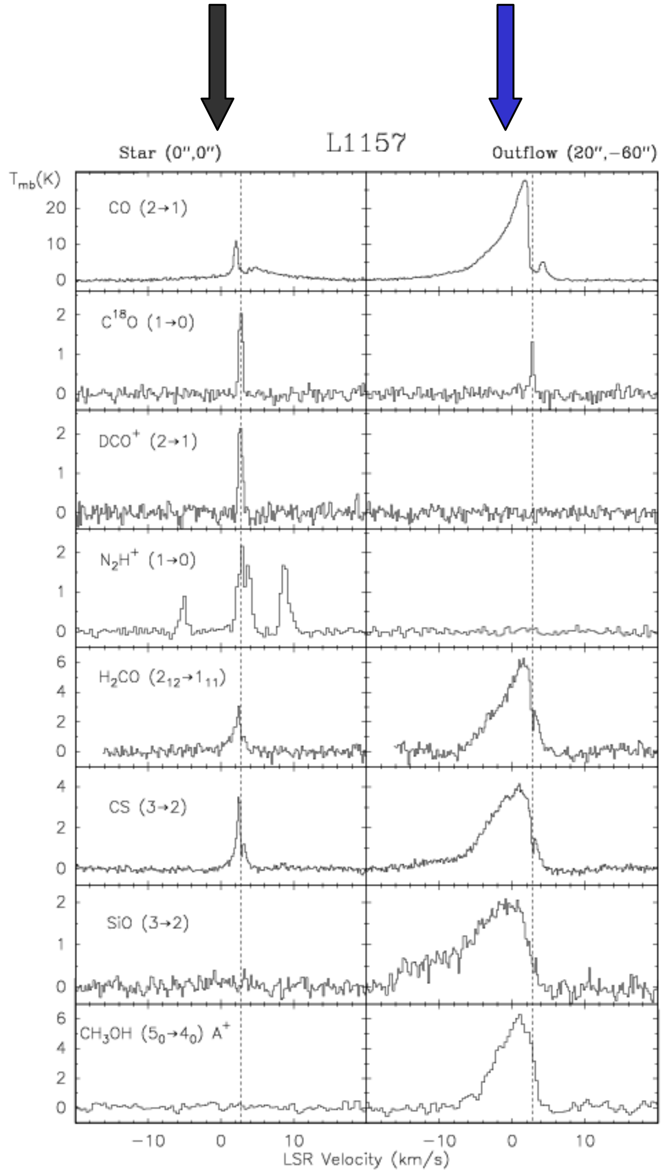

Bachiller et al. (2001)

Shock-enhanced abundances in outflows

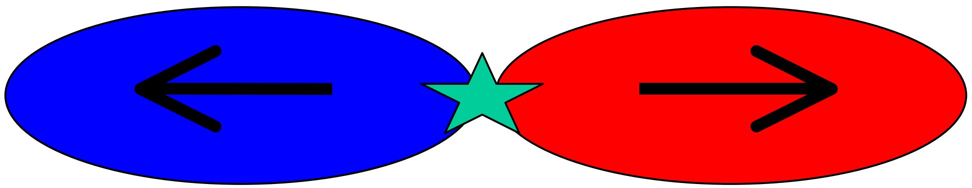

SiO	$10^{-10} - 10^{-6}$	$< 10^{-12}$
CH_3OH	$10^{-7} - 10^{-5}$	$\sim 10^{-9}$
NH_3	$\sim 10^{-6}$	$\sim 10^{-8}$
H_2CO	$\sim 10^{-7}$	$\sim 10^{-8}$
HCN	$\sim 10^{-7}$	$\sim 10^{-8}$
SO	$\sim 10^{-7}$	$\sim 5x10^{-9}$

(with respect to H_2)

PROPERTIES
OF
MOLECULAR CLOUDS

Typical properties GMCs

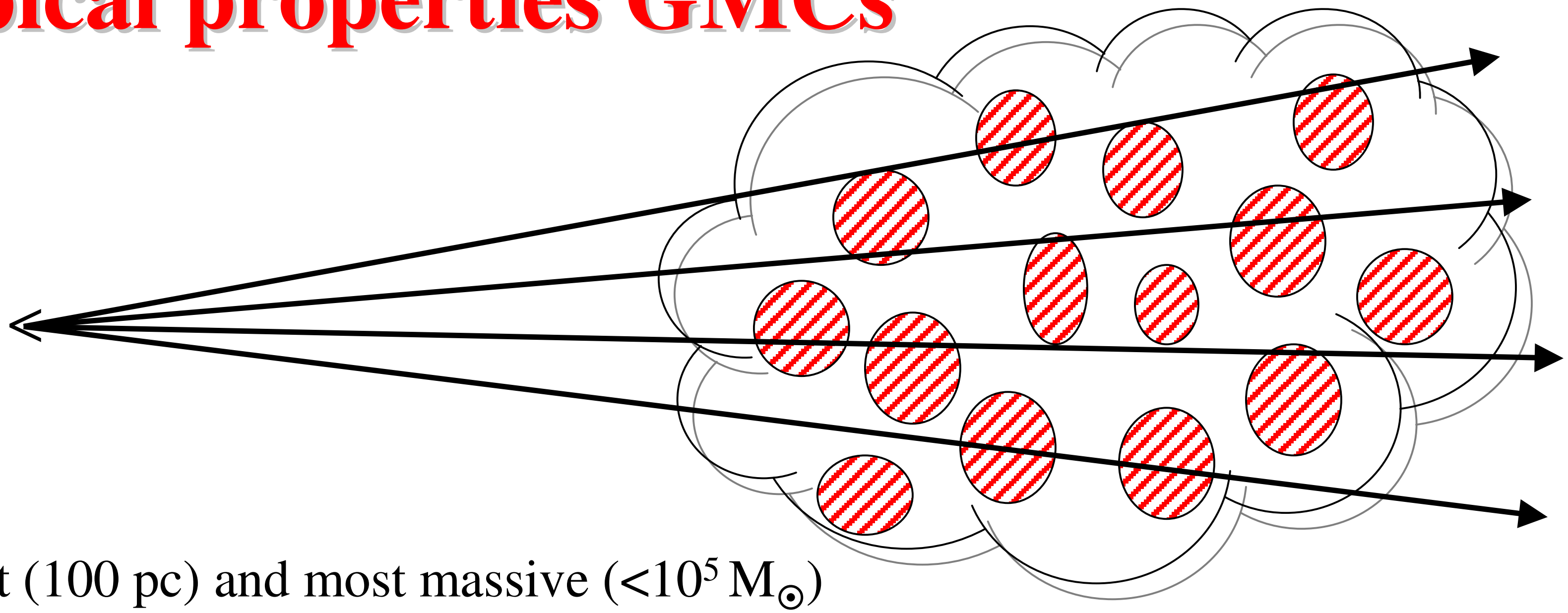

- Largest (100 pc) and most massive ($<10^5\, M_\odot$) objects in Galaxy
- Not uniform: volume f.f.<<1
  surface f.f. ≈ 1
  (≥ 1 clump along the l.o.s.)
- $\Delta V_{obs} >> \Delta V_{therm} \approx (8\ln 2\, kT/\mu m_H)^{0.5}$
  line profile determined by velocity field of clumps: bulk motions.
- Gravitationally bound
  $P_{int}/k \sim 10^5\, Kcm^{-3} >>$
  $< P_{ism}/k > \sim 10^4\, Kcm^{-3}$

- All OB stars form in GMCs
- Strong confinement to spiral arms
  (contrast arm-interarm > 28:1)
- ΔV(cloud-cloud) ≈ 3-9 km/s (median 4.2)
  ≠ f(M) ≠ f(R)
- GMCs are young (< few 10^7 yr)
- Material stays locked up in stars: replenishment needed
  (SFR ~ 2-4 $M_\odot$/yr, return ~ 0.8 $M_\odot$/yr

Orion A **^{13}CO 220 GHz = 1.3 mm**

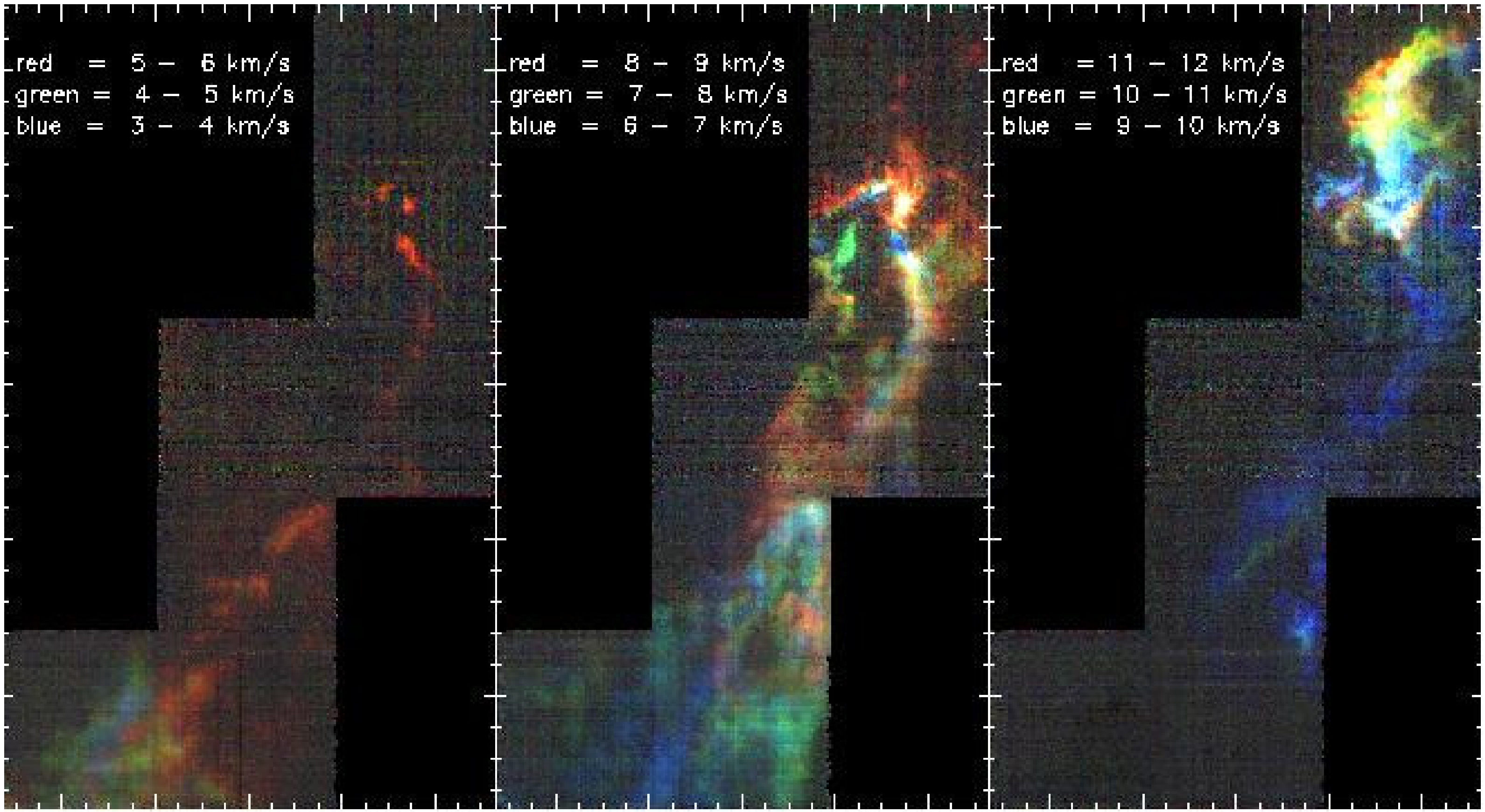

Sheets and filaments

J. Bally (IAU227)

Molecular clouds: elongated

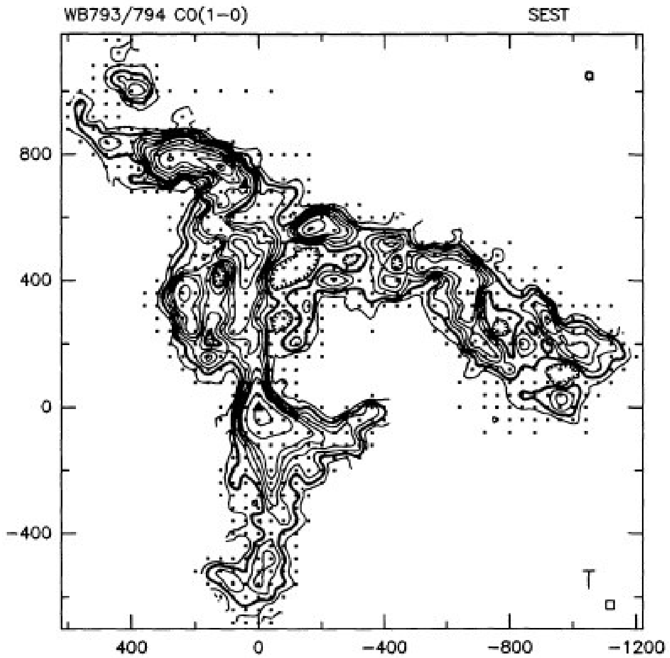

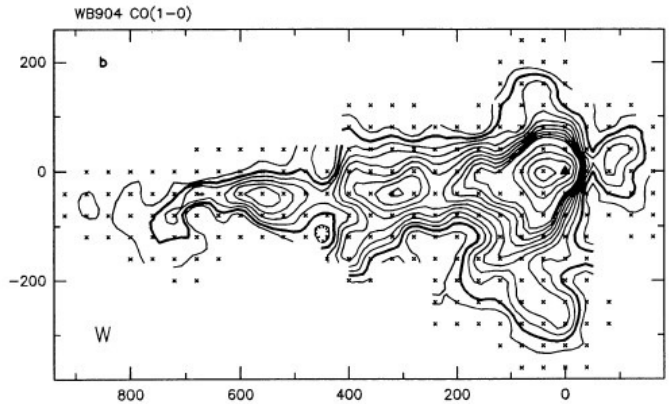

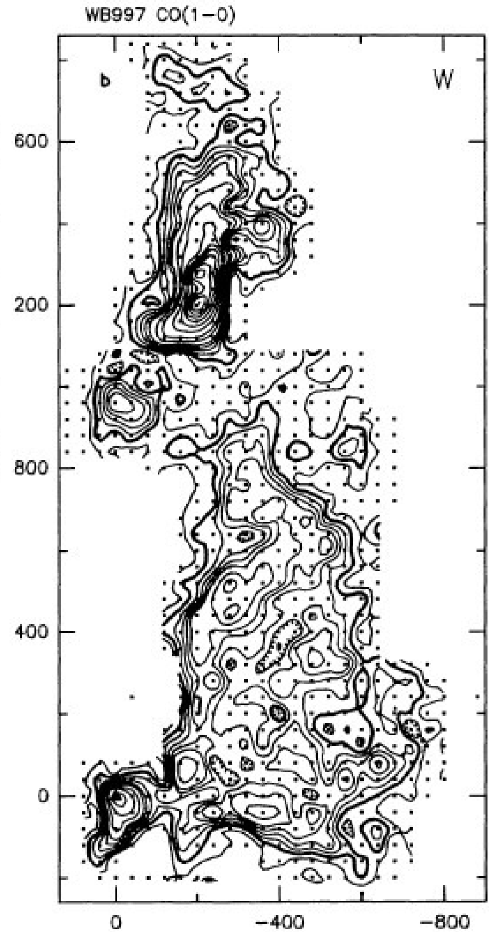

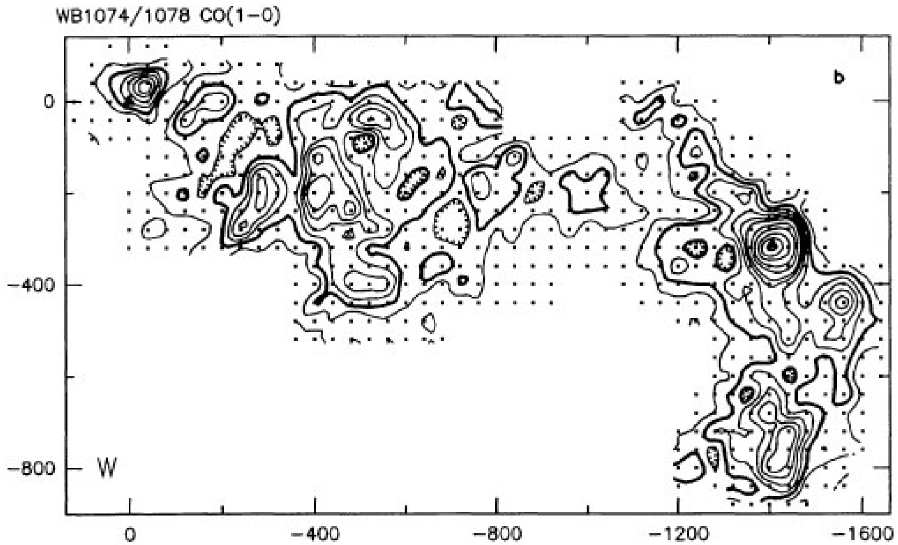

Brand & Wouterloot 1994

Masses and mass-ratios

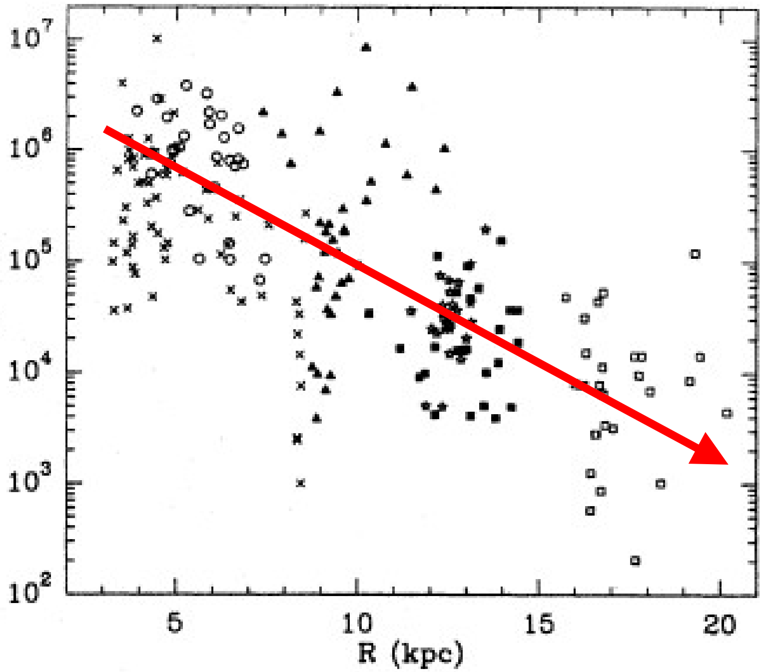

M(CO) ($M_\odot$)

R (kpc)

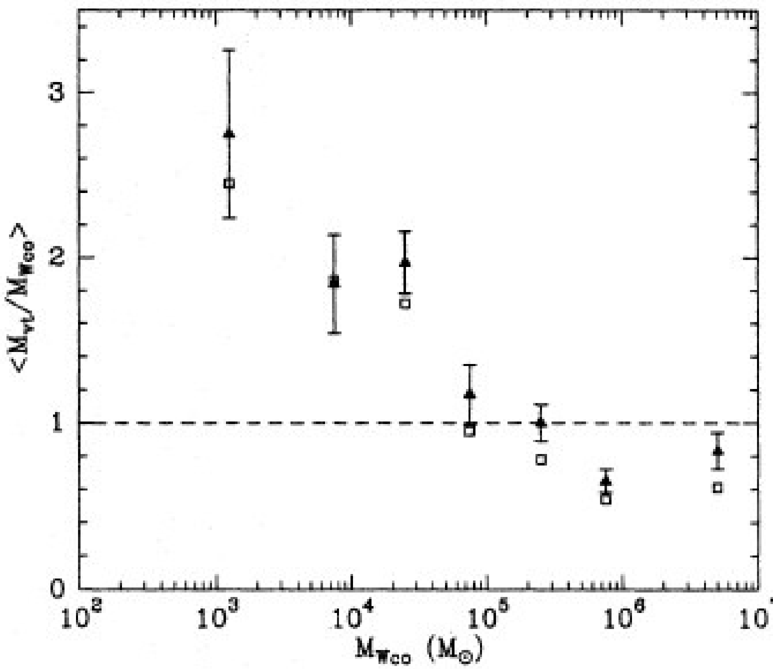

M(vir)/M(CO)

M(CO) ($M_\odot$)

Brand & Wouterloot 1995

Molecular clouds – virial- and pressure equilibrium

$$4\pi r^3 P_{ext} = M(\sigma_{3D})^2 - \frac{3}{5}\frac{GM^2}{r} \qquad \Rightarrow \frac{\Delta v^2}{r} = \frac{[fac1 * P_{ext}/k + fac2 * N(H_2)^2]}{[fac3 * N(H_2)]}$$

P_{ext} dominates: $$\frac{\Delta v^2}{r} \propto N(H_2)^{-1}$$

Self-grav. dominates: $$\frac{\Delta v^2}{r} \propto N(H_2)$$

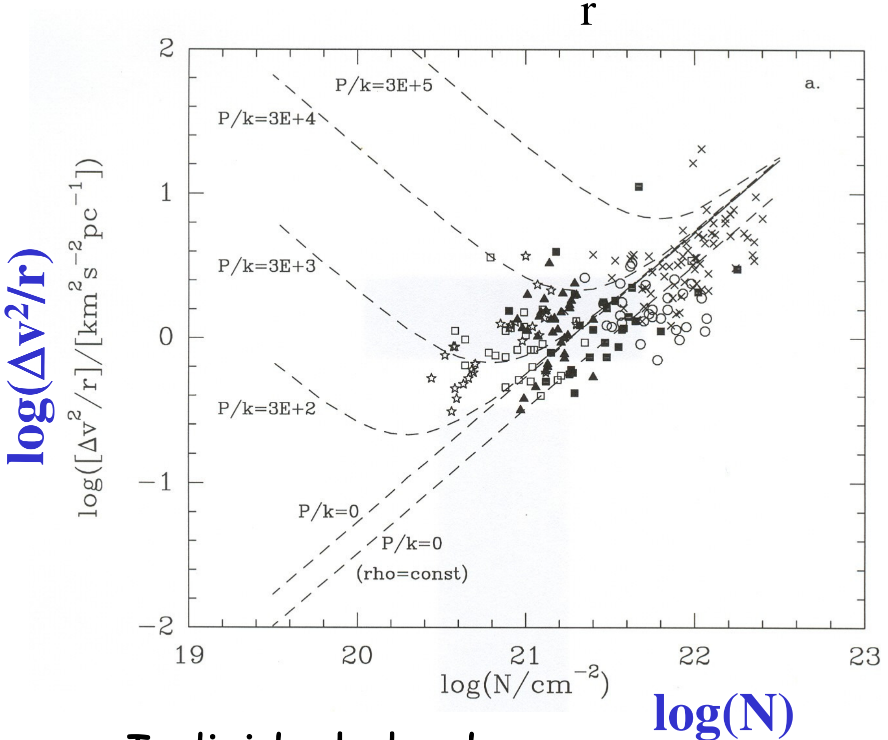

Individual clouds

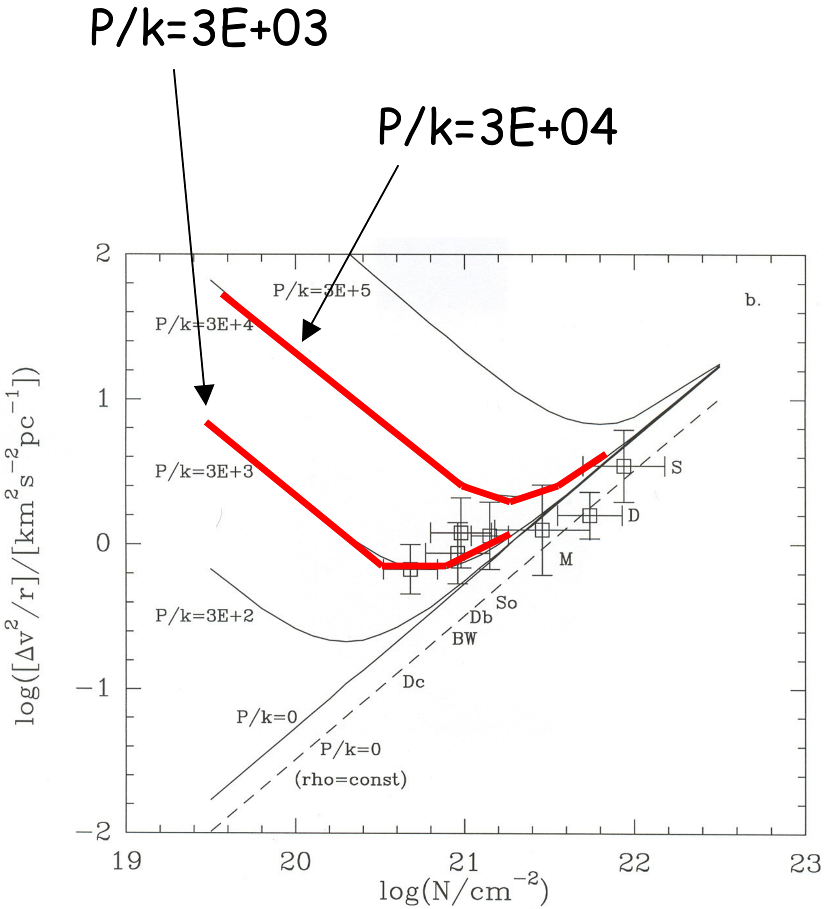

Sample averages

Brand & Wouterloot 1995

Molecular clouds & star formation

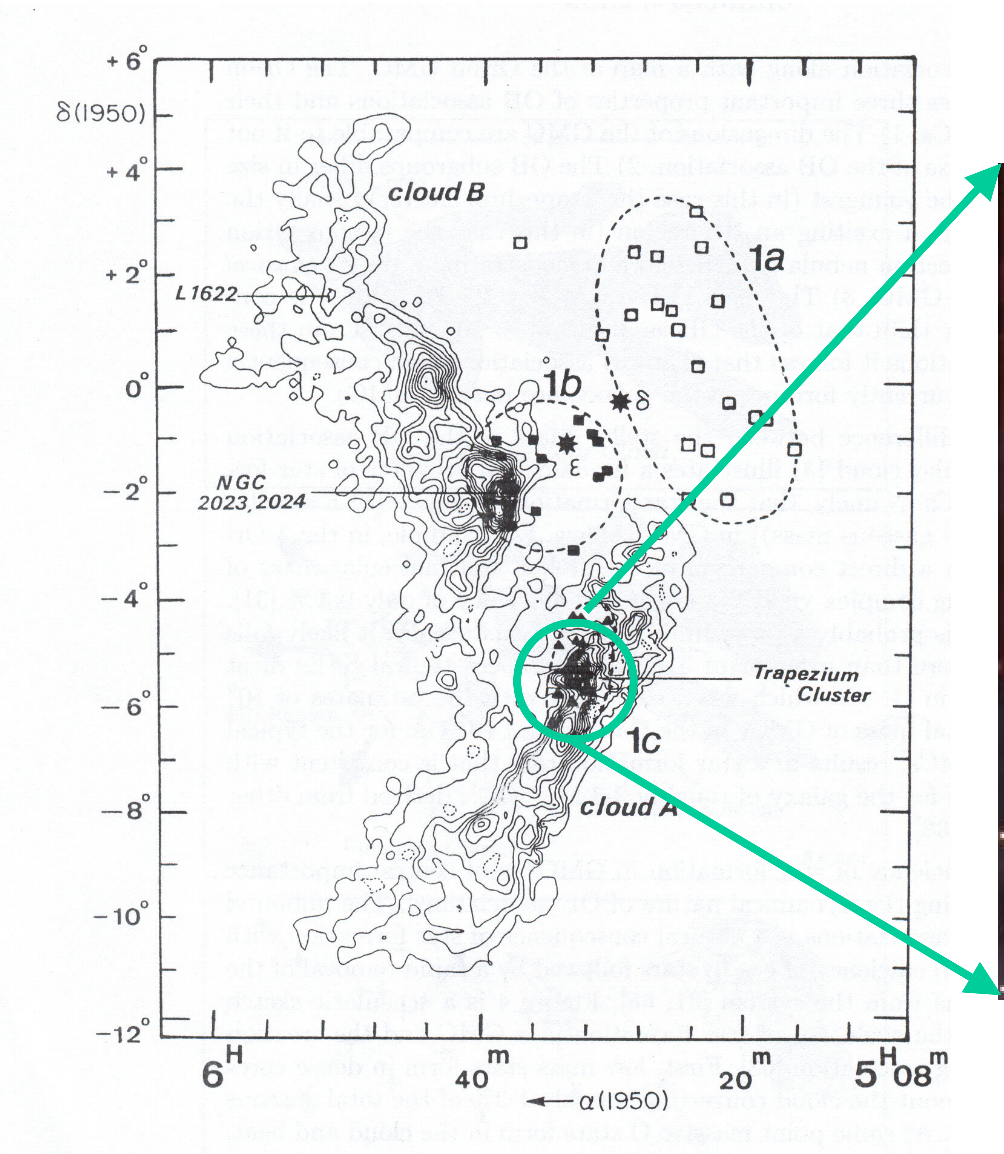

Molecular clouds & star formation

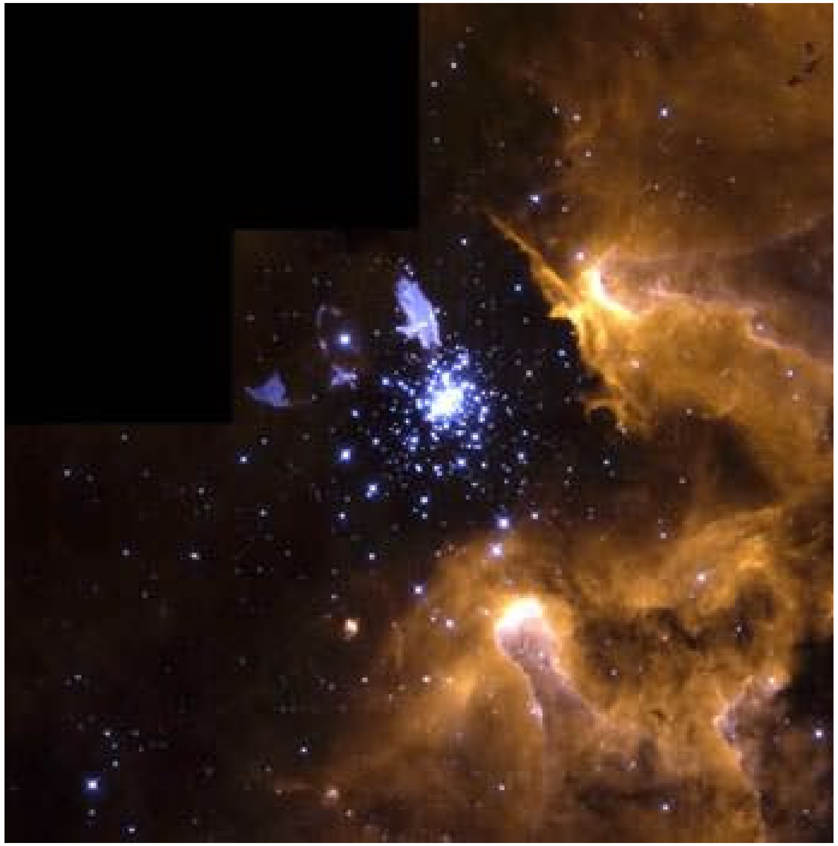

HST: NGC3603

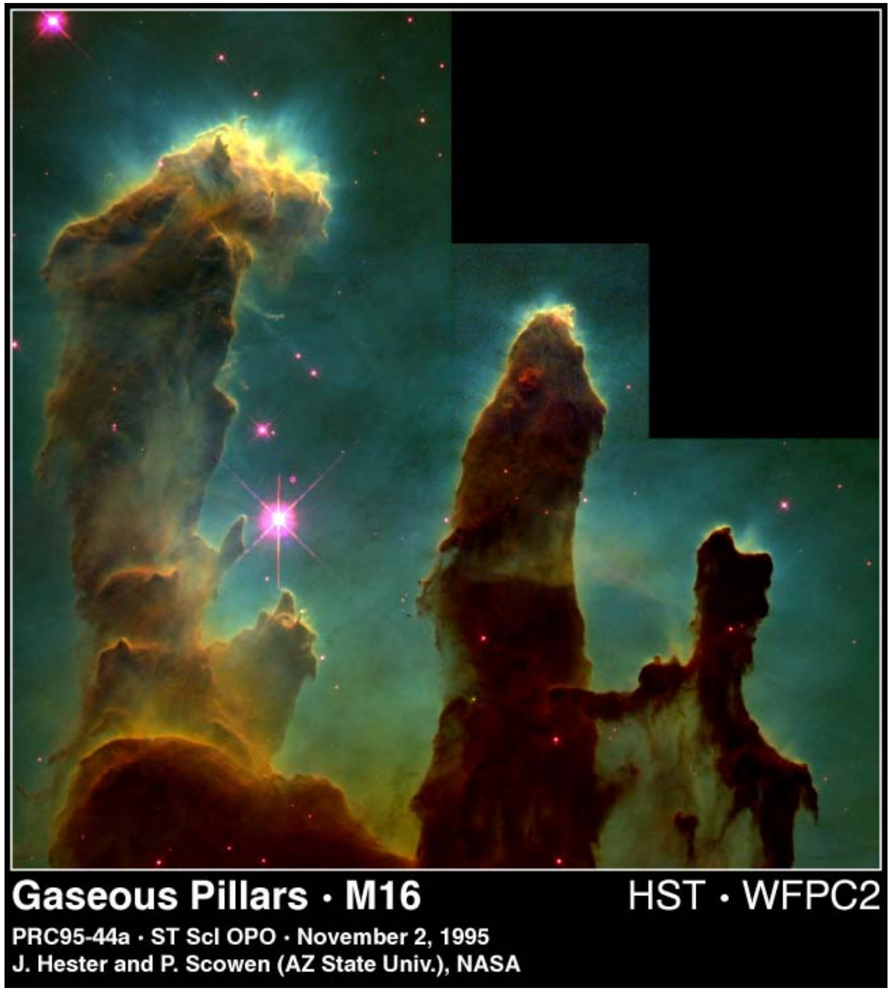

Star formation sites in outer Galaxy

Projected distribution
WB89-clouds
Wouterloot & Brand
1989 A&AS 80, 149
(WB89)

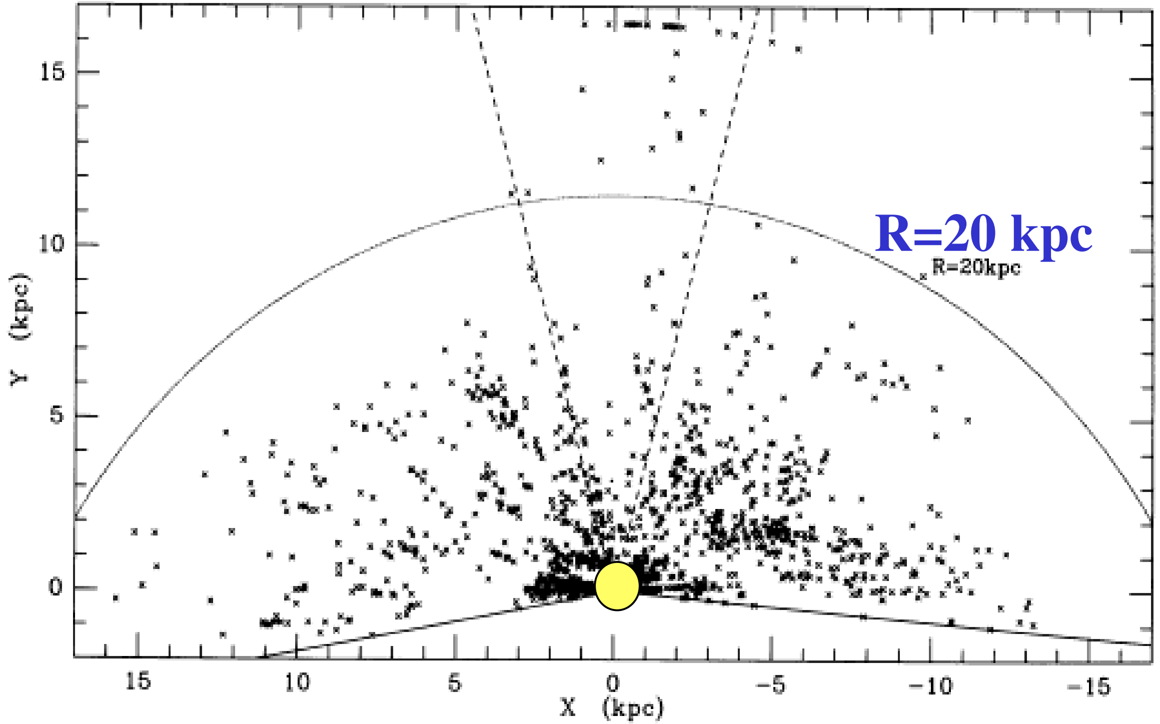

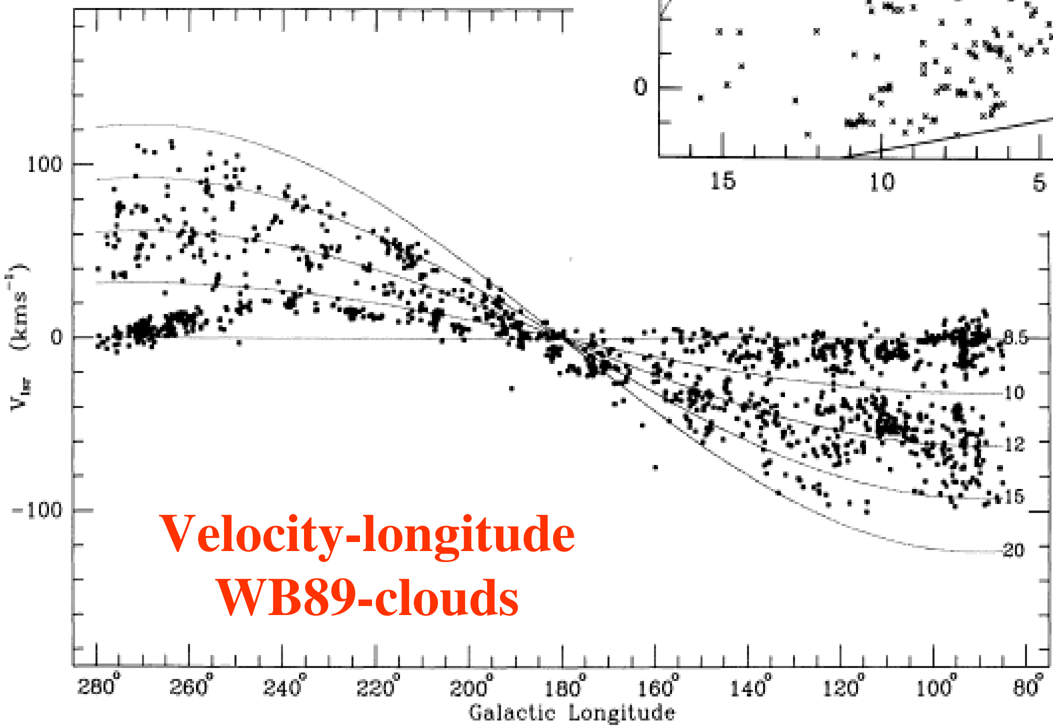

Fig. Distribution of IRAS sources with colours of star-forming regions; shows there IS star formation out to the edge of the galactic molecular disk.

Embedded clusters I

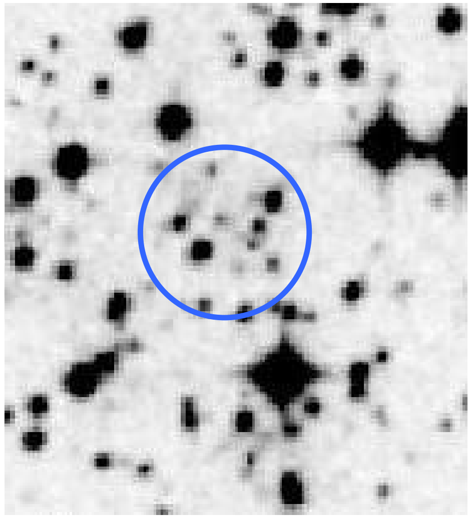

DSS-optical

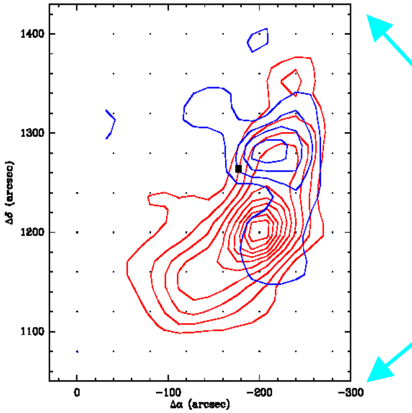

Outflow in $^{12}CO(1-0)$ (SEST)

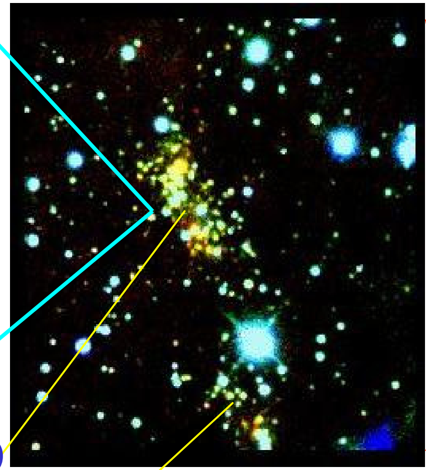

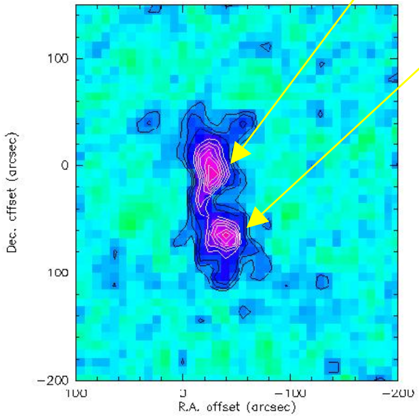

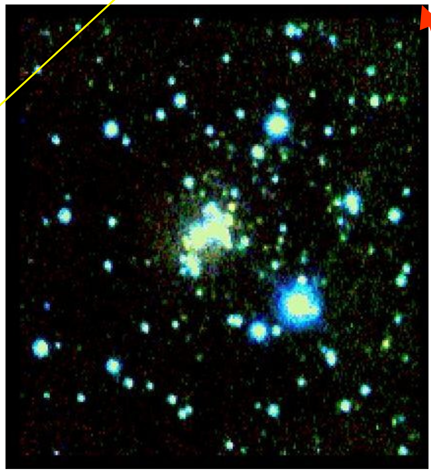

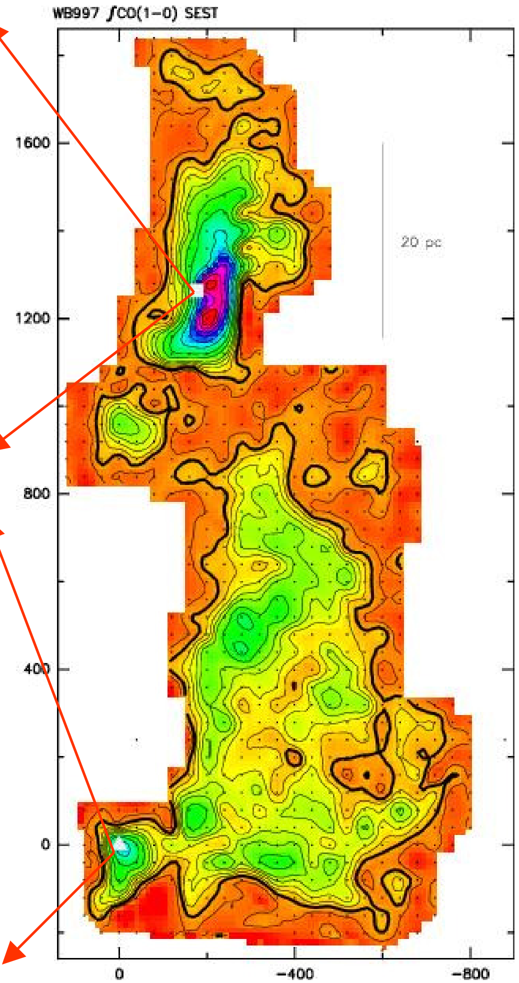

IRAS07255-2012
IRAS07257-2033

Brand & Wouterloot 1994, 2003 & in prep.

1.2 mm continuum (SEST/SIMBA)

JHK-composite
~ 1'.7x1'.7

Cloud: $M=6.0 \times 10^4 M_\odot$
d, R = 9.3, 15.7 kpc

Embedded clusters II

Brand & Wouterloot, A&A 2007

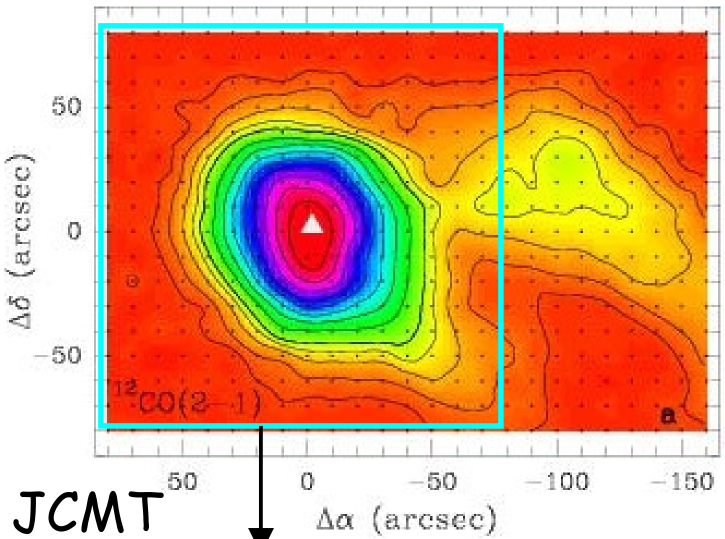

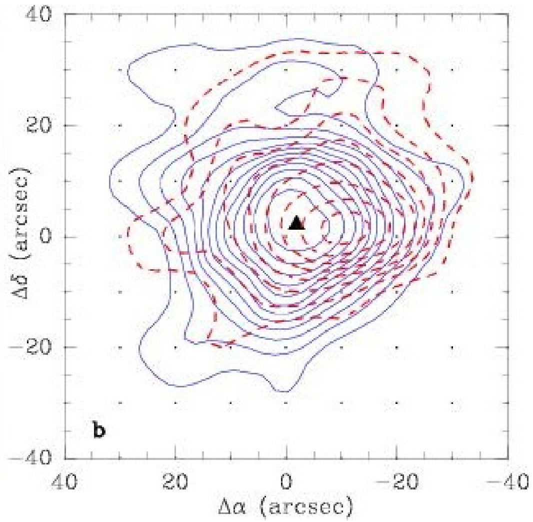

△: dust core

White contour: half of the peak value

JCMT

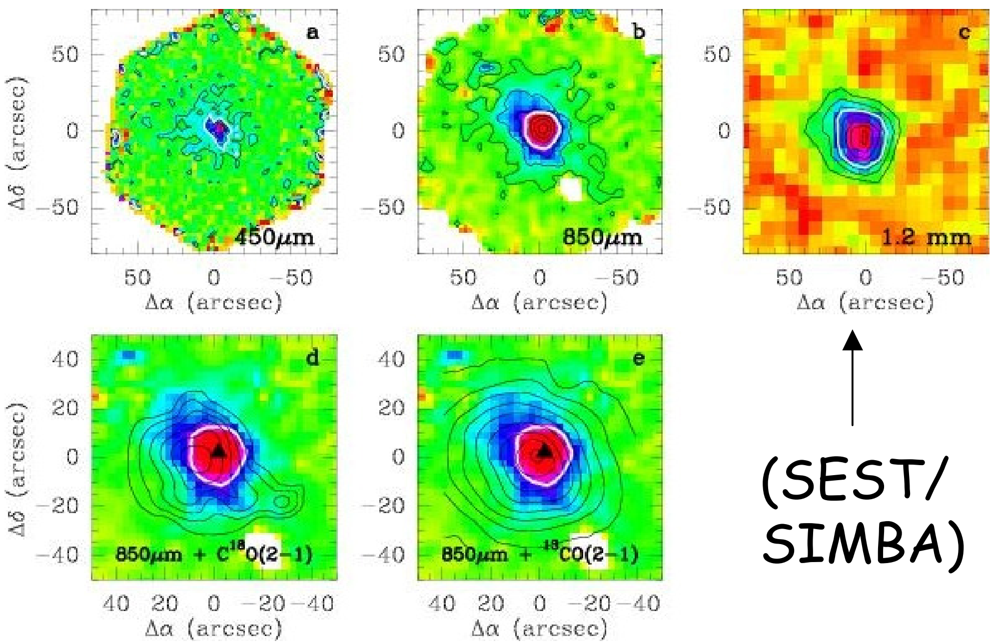

(SEST/ SIMBA)

WB89-789. JCMT data.
$M_{cloud} \approx 5 \times 10^3\ M_\odot$ (CO);
$M_{vir}(core) \approx 400\ M_\odot$ (CS);
$M_{dust} \approx 10\ M_\odot$ (SED-fit; $T_{dust} \approx 22$ K).
$M_{outflow} \approx 12\ M_\odot$ (CO);
$t_{dyn} \approx 4 \times 10^4$ yrs.

Brand & Wouterloot, A&A 2007

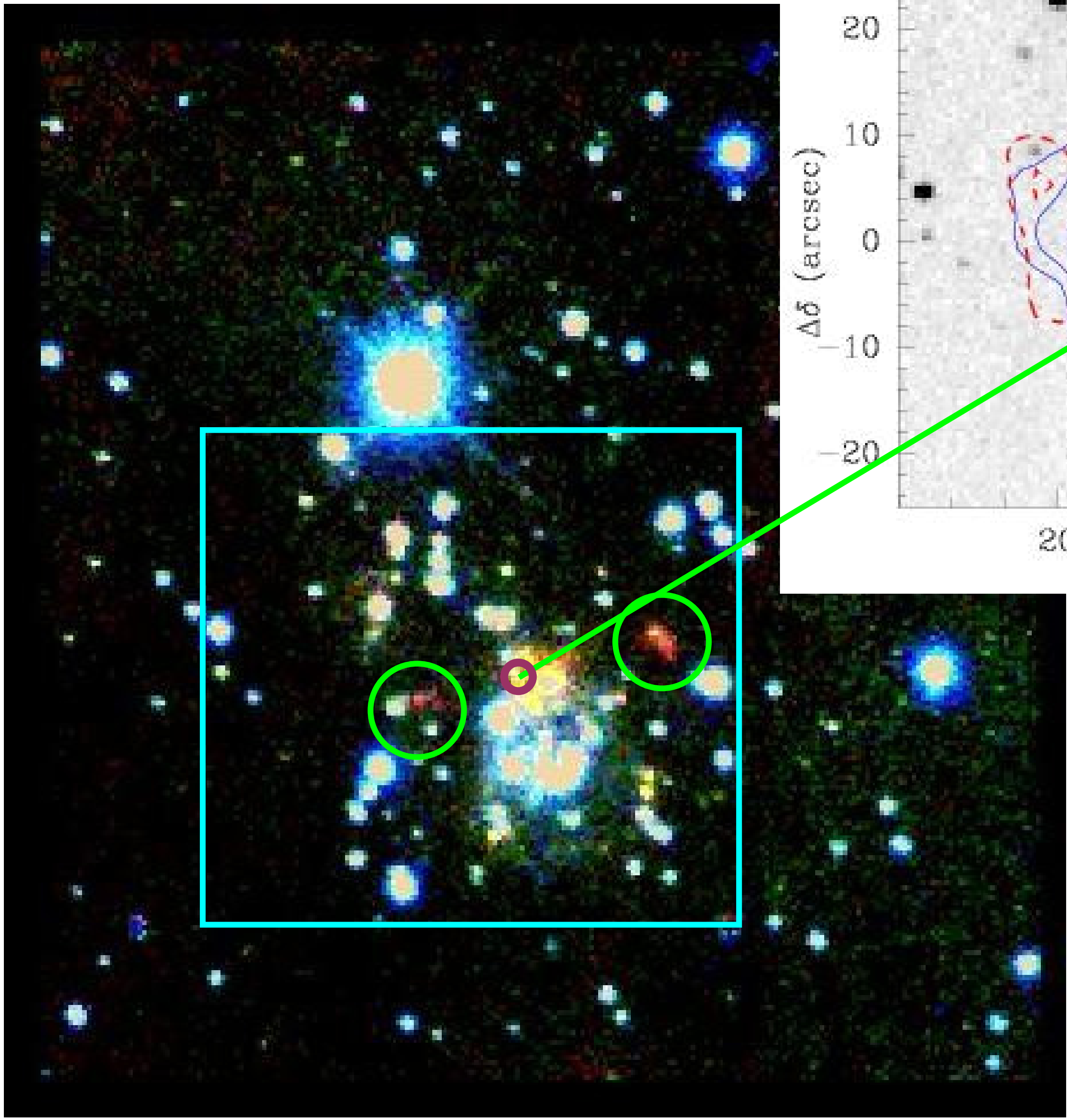

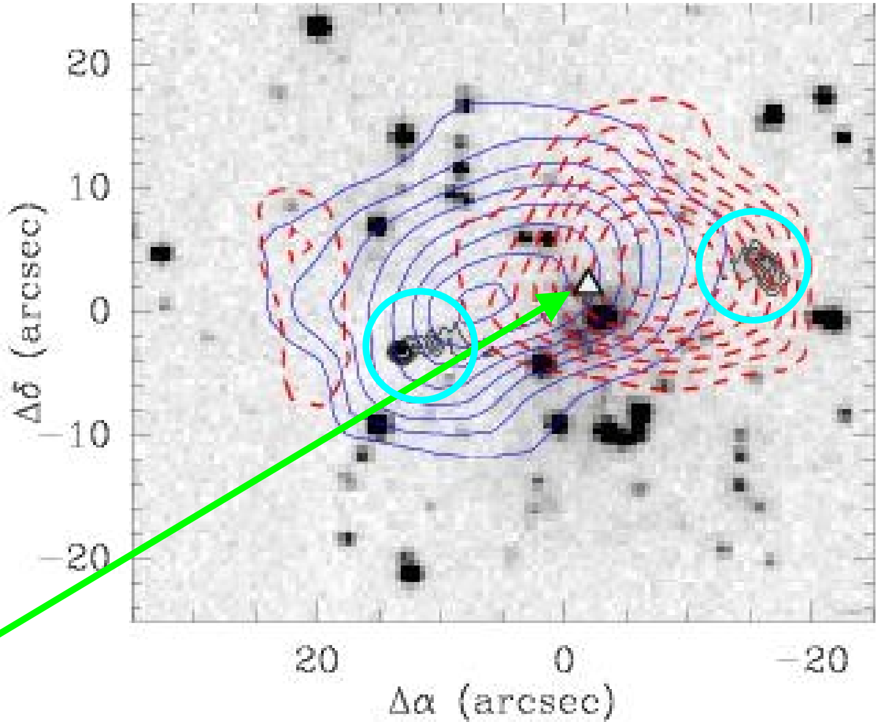

JCMT data.
∫T[CO(3-2)]dV
+
K-frame (ESO)

ESO-data

JHK-combined

A cloud without star formation

G216-2.5: "Maddalena's Cloud"

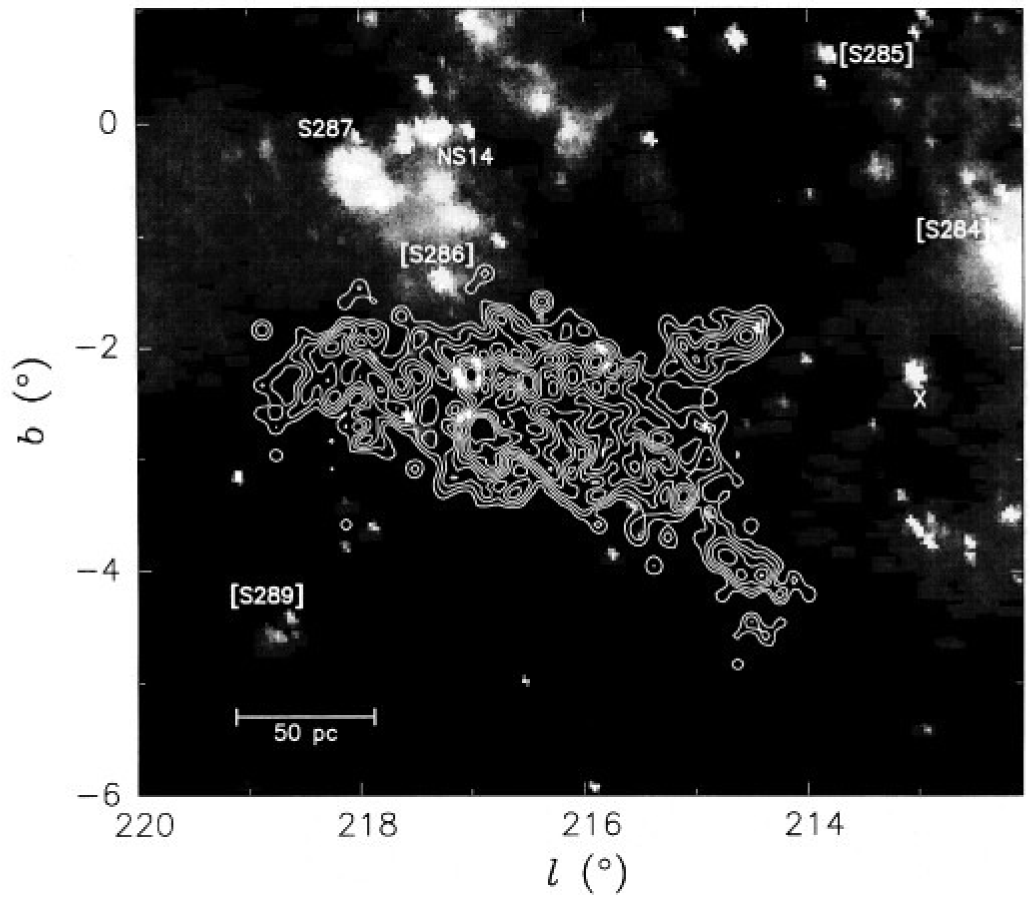

$L_{IR}/M_{cloud} < 0.07\ L_\odot/M_\odot$

while typically

$L_{IR}/M_{cloud} \sim 1\ L_\odot/M_\odot$

DERIVING
FUNDAMENTAL PROPERTIES

Observing molecular clouds at large

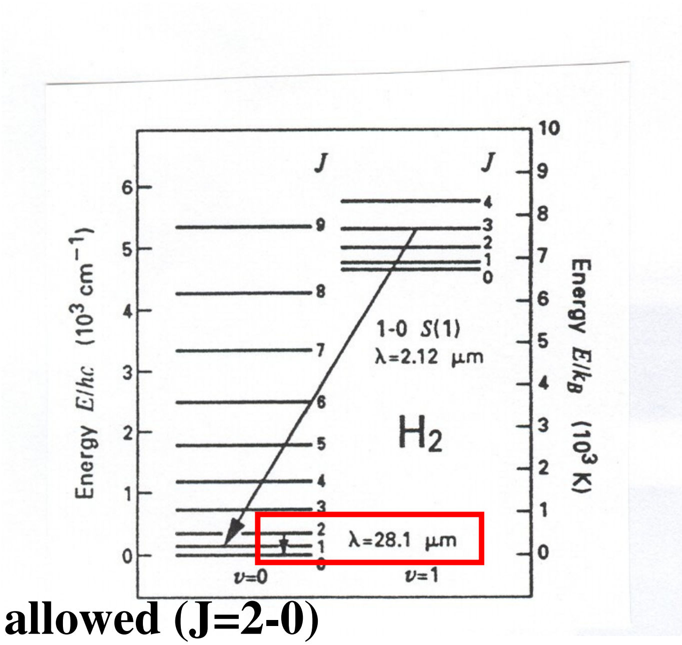

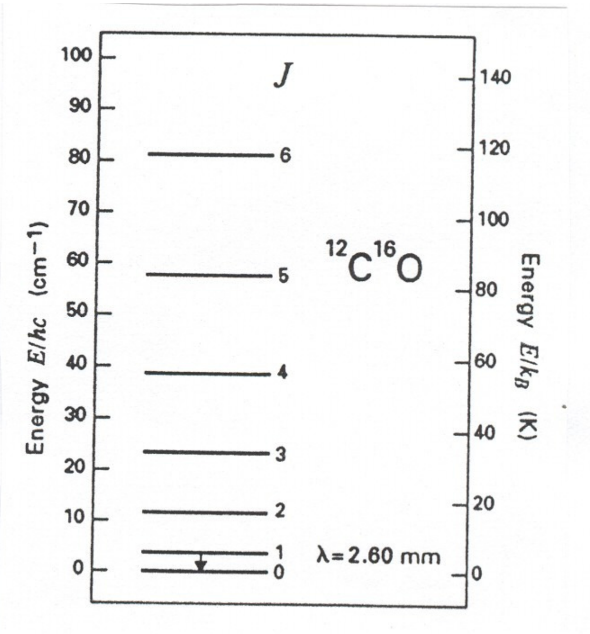

Lowest allowed (J=2-0)
ΔE = 510 K

H_2 smallest diatomic molecule: widely-spaced energy levels
Even lowest excited rot. levels too far above ground state to be easily populated at normal molecular cloud T.
no dipole moment, hence quadrupole radiation (slow)

CO: more closely-spaced energy levels; easily populated also at low T

Two-level system

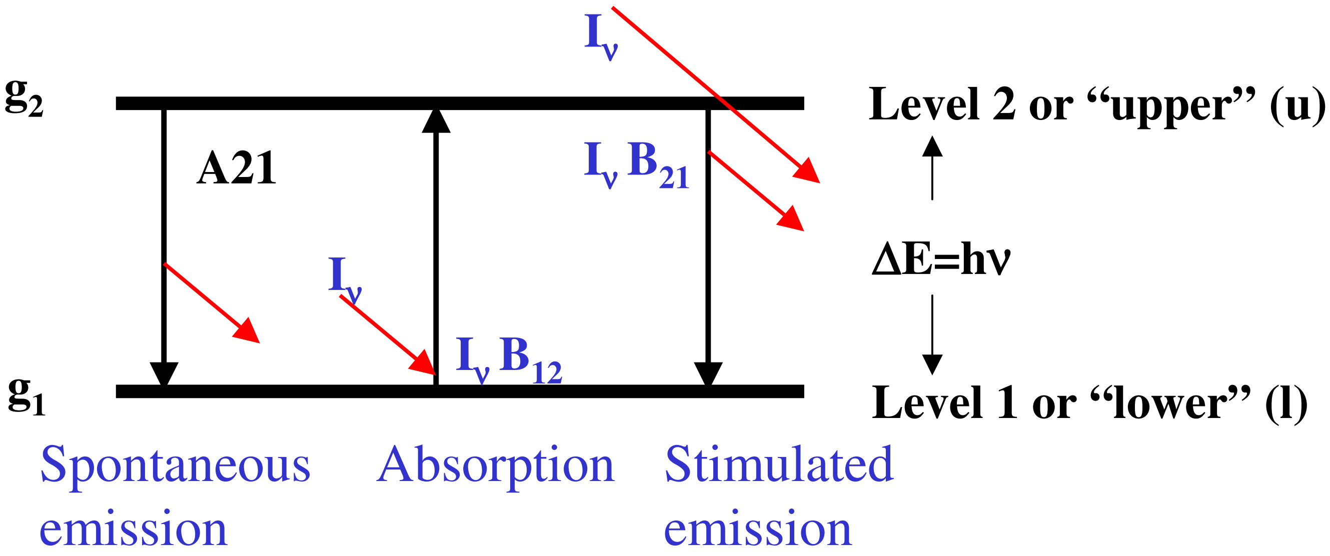

$$g_1 B_{12} = g_2 B_{21} \; ; \; A_{21} = (2h\nu^3/c^2)\, B_{21}$$

$$n_2/n_1 = (g_2/g_1)\exp(-\Delta E/kT_{ex})$$

Boltzmann equation

Statistical equilibrium: in=out, regardless of process:

$$dn_1/dt = (A_{21} + IB_{21} + C_{21})n_2 - (IB_{12} + C_{12})n_1 = 0 \text{ for each level}$$

Example: CO. In molecular cloud, excitation J=1 level through collisions with H_2.

If n_{tot} low, each upward transition followed by spontaneous emission of photon (rate = $n_1 A_{10}$).

If n_{tot} high, excited CO loses energy in collisions with H_2, without emission photon. Two regimes are separated at critical density $A_{10}/\gamma_{10} = 3 \times 10^3$ cm^{-3}.

$$n_1 / n_0 = (g_1 / g_0) \exp(- \Delta E / kT_{ex})$$

$n_{tot} << n_{crit}$: n_1 / n_0 small and $\propto n_{tot}$, $T_{ex} < T_{kin}$

$n_{tot} >> n_{crit}$: CO in LTE and $T_{ex} = T_{kin}$

NH_3(1,1)	$n_{crit} = 1.9 \times 10^4$ cm^{-3}.
CS	$n_{crit} = 4.2 \times 10^5$ cm^{-3}.
H_2O (thermal emission)	$n_{crit} = 1.7 \times 10^7$ cm^{-3}.

Radiation transport I

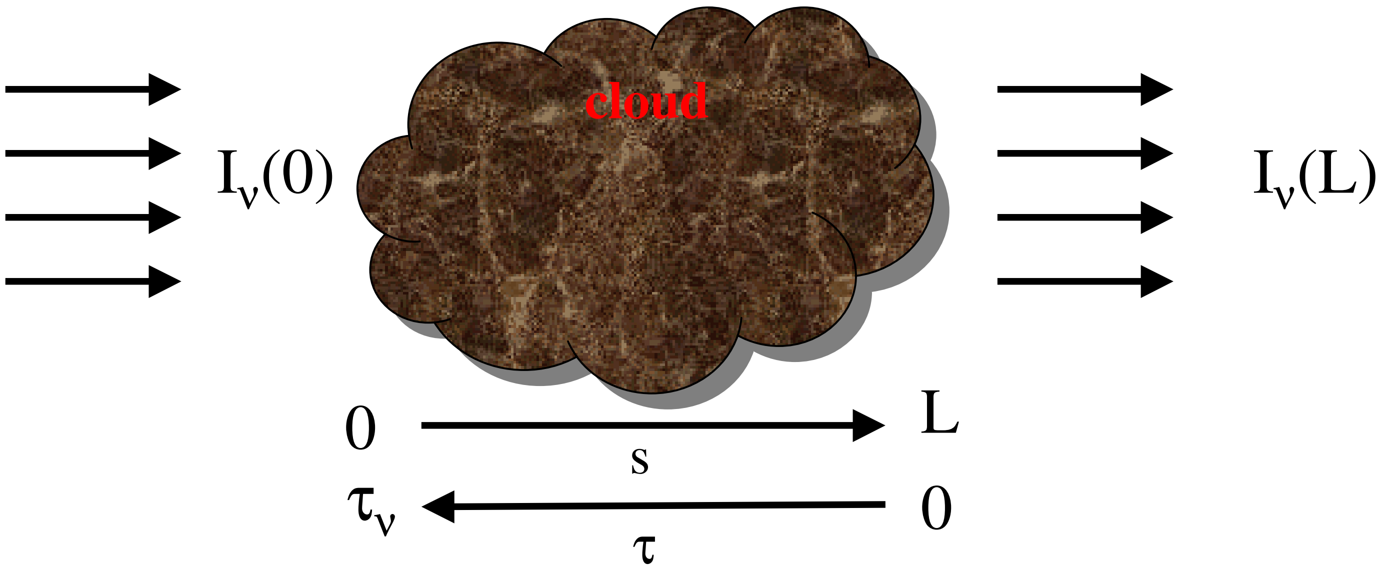

$dI_\nu = -k_\nu I_\nu\, ds + j_\nu ds$ $\qquad$ $d\tau_\nu \equiv -k_\nu ds$

$dI_\nu = I_\nu\, d\tau_\nu + (j_\nu / k_\nu)\, d\tau_\nu$ $\qquad$ (j_ν / k_ν) = source function S_ν

$j_\nu = (h\nu/4\pi) n_u A_{ul} \phi(\nu)$

$k_\nu = (h\nu/4\pi)(n_l B_{lu} - n_u B_{ul})\phi(\nu)$

TE at temperature T: $S_\nu = B_\nu(T_{ex})$: Planck function. Then:

$$I_\nu = I_\nu(0) e^{-\tau_\nu} + B_\nu(T_{ex})(1 - e^{-\tau_\nu})$$

Radiation transport II

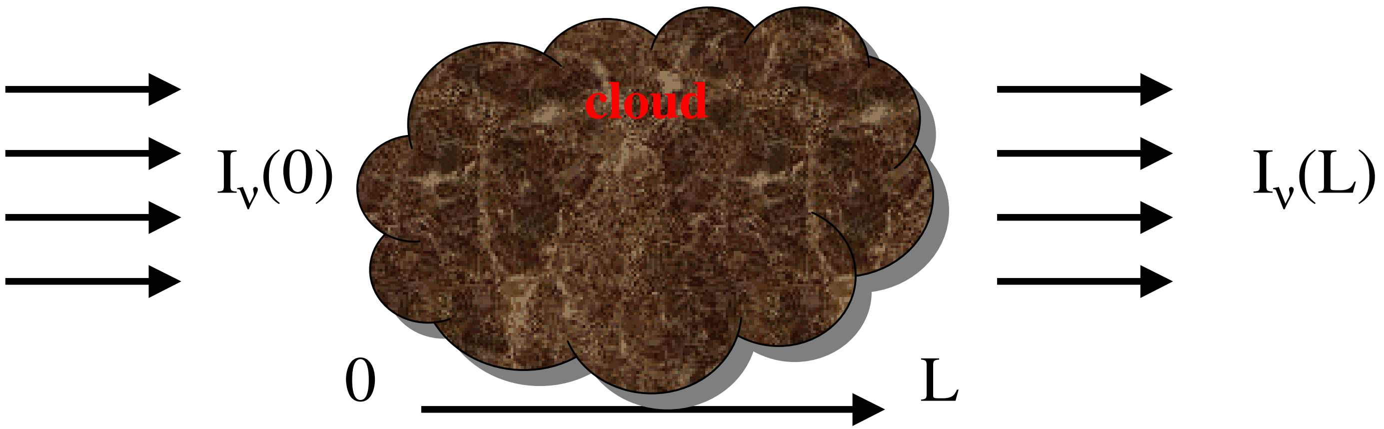

So we have: $I_\nu = I_\nu(0)e^{-\tau_\nu} + B_\nu(T_{ex})(1-e^{-\tau_\nu})$

Define $T_A(\nu) \equiv I_\nu / [2k\nu^2 c^{-2}]$, $T_A(0) = T_{bg}$, and define $J_\nu(T) = (h\nu/k)(e^{h\nu/kT} - 1)^{-1}$
(Note: in Rayleigh-Jeans limit $h\nu/kT << 1$ and $J_\nu(T) = T$)

Then: $T_A = J(T_{ex})(1-e^{-\tau_\nu}) + J(T_{bg})e^{-\tau_\nu}$ → **Detection equation**

in Rayleigh-Jeans limit: $T_A = T_{ex}(1-e^{-\tau_\nu}) + T_{bg}e^{-\tau_\nu}$
In practice one measures $\Delta T_A = T_A - T_{bg}$ (ON-OFF) $= (T_{ex} - T_{bg})(1-e^{-\tau_\nu})$

1) $\tau_\nu \ll 1$: $\Delta T_A \approx T\,\tau_\nu$ measure column density. All photons escape.
2) $\tau_\nu \gg 1$: $\Delta T_A \approx T$ measure kinetic temperature, but independent of col. dens.
Only photons at cloud surface ($\tau_\nu \leq 1$) escape.

T_{ex}, τ, and column density in LTE

For an optically thick line, e.g. CO(1-0): $\tau_\nu \gg 1$; the detection equation yields:

$$T_{ex} = (h\nu/k)\ \ln^{-1}(h\nu/k\ [T_A + J(T_{bg})\ ]^{-1} + 1)$$
$$= 5.532\ \ln^{-1}(5.532[T_A + 0.818\ ]^{-1} + 1)$$

For an optically thin line, e.g. $^{13}CO(1\text{-}0)$: $\tau_\nu \ll 1$; it follows that:

$$\tau_\nu = -\ln[1 - T_A\,/(J(T_{ex})\ - J(T_{bg})\ )]^{-1}$$

Column density – derived from transition between levels J and J-1.
Detection equation: $T_A = J(T_{ex})\ (1- e^{-\tau\nu}\ ) + J(T_{bg})\ e^{-\tau\nu}$ and $\tau_\nu \ll 1$, solve for τ_ν.
From definition of T_{ex}, the definitions of theEinstein-coefficients, the equation for the absorption coefficient, and the definition of τ

$$N_{tot} = (3h/8\pi^3\mu^2)(Z/J)\exp(h\nu/k\ T_{ex})[1-\exp(-h\nu/k\ T_{ex})]^{-1}\ [/(J(T_{ex})\ - J(T_{bg})\ ]^{-1} \int T_A\, dv$$

with Z the partition function (linking N_l to N_{tot}).

or: $N_{tot} = f(T_{ex}) \int T_A\, dv$

Total column density

$$N_{tot} = f(T_{ex}) \int T_A \, dv$$

For $^{13}CO(1\text{-}0)$ and $C^{18}O(1\text{-}0)$ and $T_{ex} \approx 5 - 20$ K:

$$f(T_{ex}) \approx (1.1 \pm 0.2) \times 10^{15} \text{ cm}^{-2}/(\text{Kkm/s})$$

Hence:

$N_{tot} = (1.1 \pm 0.2) \times 10^{15} \int T_A \, dv \text{ cm}^{-2} \Rightarrow$ Mass!

If $\tau_\nu \leq 1$ then correction factor $\tau_0 / [1 - \exp(-\tau_0)]$, with τ_0 the opt. depth at line center $\tau_0 = -\ln(1-1/R)$ and $R = T_A(^{12}CO)/T_A(^{13}CO)$.

Therefore:

$$N_{tot} = (1.1 \pm 0.2) \times 10^{15} \times \tau_0 / [1 - \exp(-\tau_0)] \times \int T_A \, dv \text{ cm}^{-2}$$

Mass follows via abundances: $N(^{12}CO)/N(^{13}CO) \sim 90$ and $N(^{12}CO)/N(H_2) \sim 1 \times 10^{-4}$

Deriving $N(H_2)$, total mass

1. Lines (Planck & Boltzmann)

Detection eqn., LTE, $\tau(^{12}CO) \gg 1$ ($\Rightarrow T_{ex}$), $\tau(^{13}CO) \ll 1$

$N(^{13}CO) = f(\tau_{13}, T_{ex}, \Delta v_{13}) + [H_2]/[^{13}CO] = \ldots. \Rightarrow N(H_2)_{LTE}$

$^{12}C/H$, $^{12}C/^{13}C$ gradients $\Rightarrow [H_2]/[^{13}CO] = f(R)$

Non-LTE transitions: LVG model (full radiation transport eqns.)

2. Lines (empirical)

$N(H_2)/\int T_{12}\, dv \equiv X \Rightarrow N(H_2)_{Wco}$

X = constant or $f(R)$?

3. Virial theorem

Cloud radius (r), linewidth (Δv), assumptions about density distribution. For spherical cloud, $n \propto r^{-2} \Rightarrow M_{vir} = 126\, r\, \Delta v^2$

Exclude non-bound motions (e.g. outflows); actual density distribution?

4. Dust continuum

$M = (gS_\nu d^2)/\kappa_\nu B(T_{dust})$

κ_ν, T-structure, gas-to-dust ratio (g) uncertain

Results of molecular cloud mapping

Type	**R (pc)**	**n (cm^{-3})**	**M ($M_{\odot}$)**	**ΔV (km/s)**	**T (K)**	**Cores & stars**
Diffuse	0.3-3	30-500	$0.5\text{-}10^{2}$	0.7-1.5	10?	Low-mass
Dark	3-10	$10^{2\text{-}3}$	$10^{3\text{-}4}$	1-3	10	Low-mass
Giant	20-100	10-300	$10^{5\text{-}6}$	5-15	10-20	High-mass (+Low-mass)

Total molecular mass in Galaxy ~ 2-4 x $10^9\ M_{\odot} \approx M(HI)$

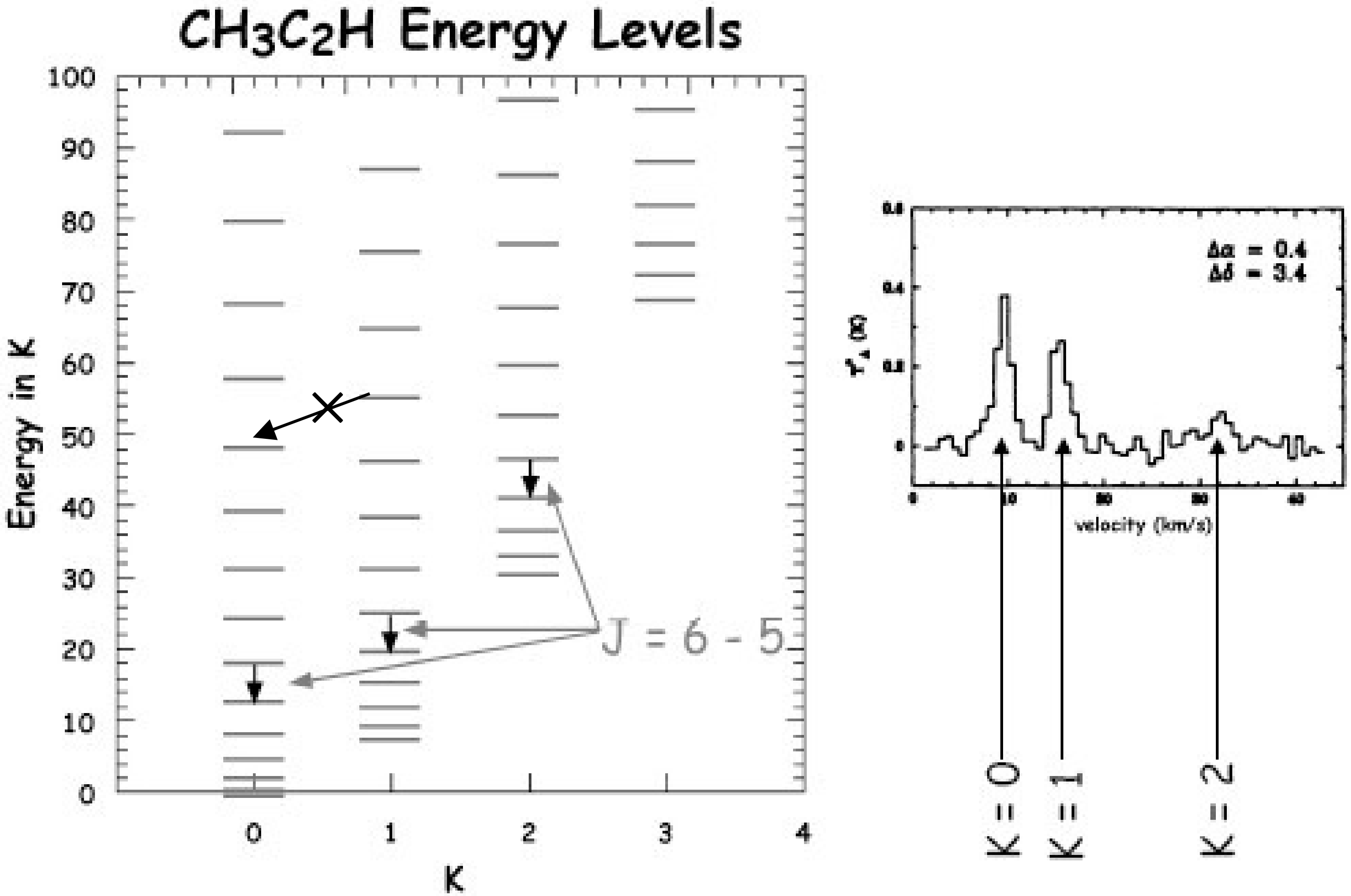

K-ladders connected through collisions. Relative population of K-ladders reflects a thermal distribution at T_{kin} .

Application: Boltzmann plot

$$N_i / g_i = [N_{tot}/Q(T)] \exp(-E_i/kT)$$

Plot $\ln(N_i / g_i)$ vs. E_i:

line with slope ∝ 1/T,
intercept ∝ N_{tot}

$$\ln[(3k\int T dV)/(8\pi^3 \nu \mu^2 S)]$$

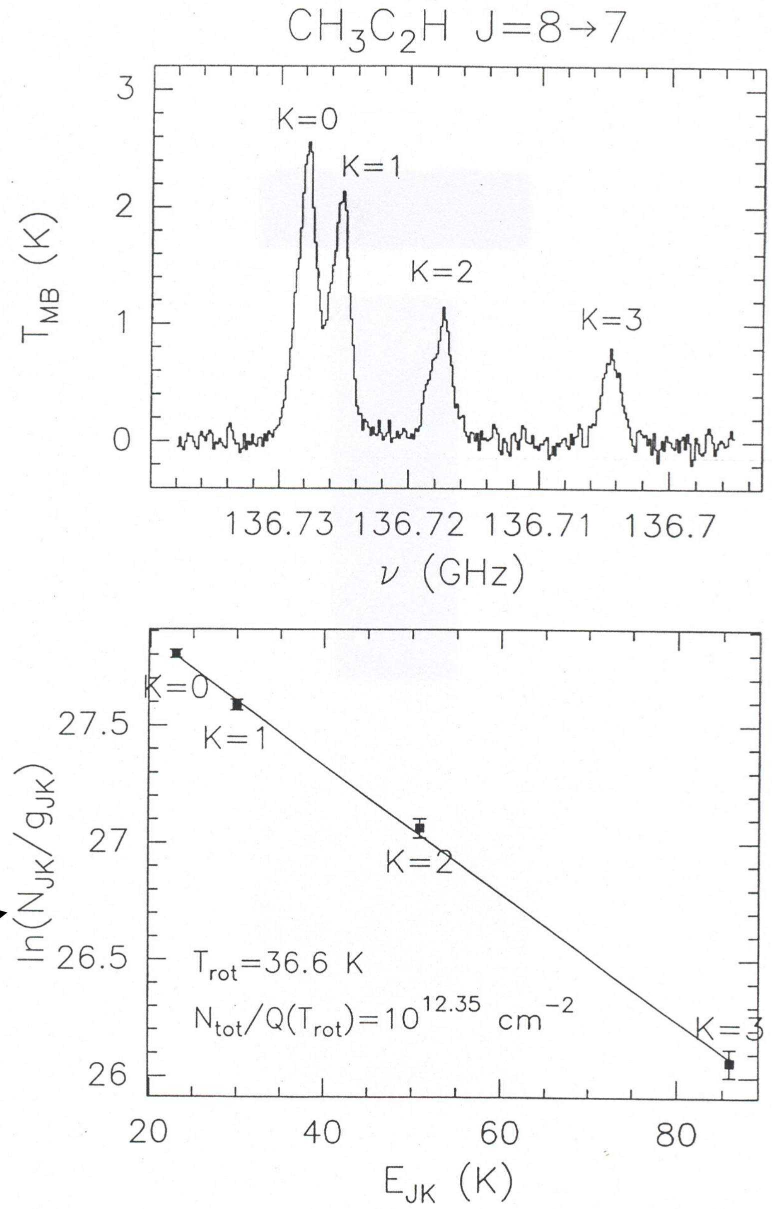

Changing Critical Densities with J

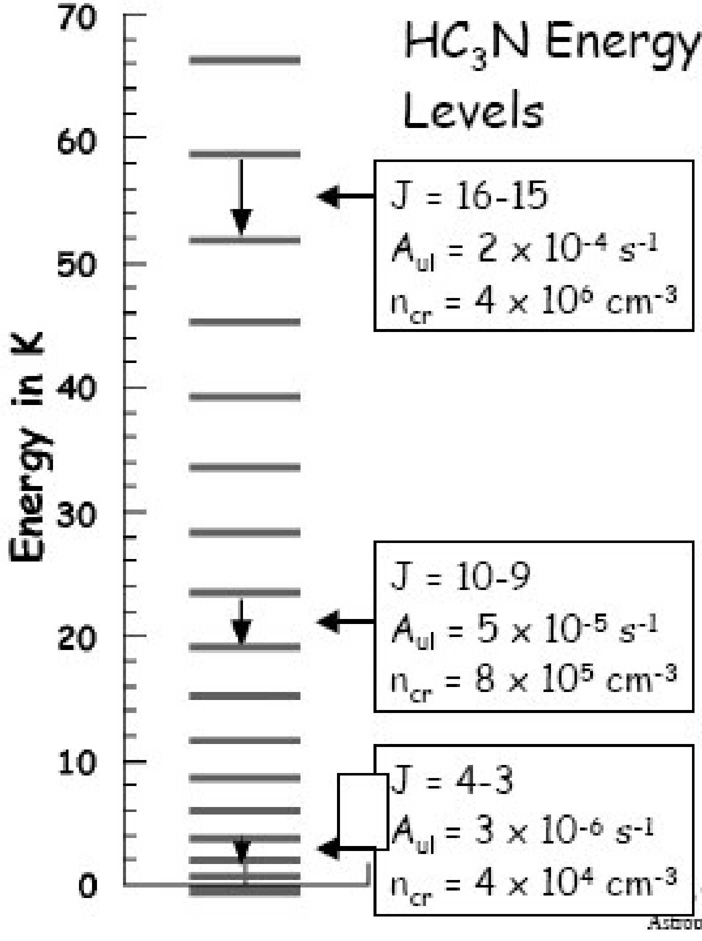

- Critical density (n_{cr}): density required to excite transition or populate level.
- $n_{cr} = A_{ul}/\gamma_{ul}$
- Higher transitions are sensitive to higher densities and temperatures.

Column density vs. extinction

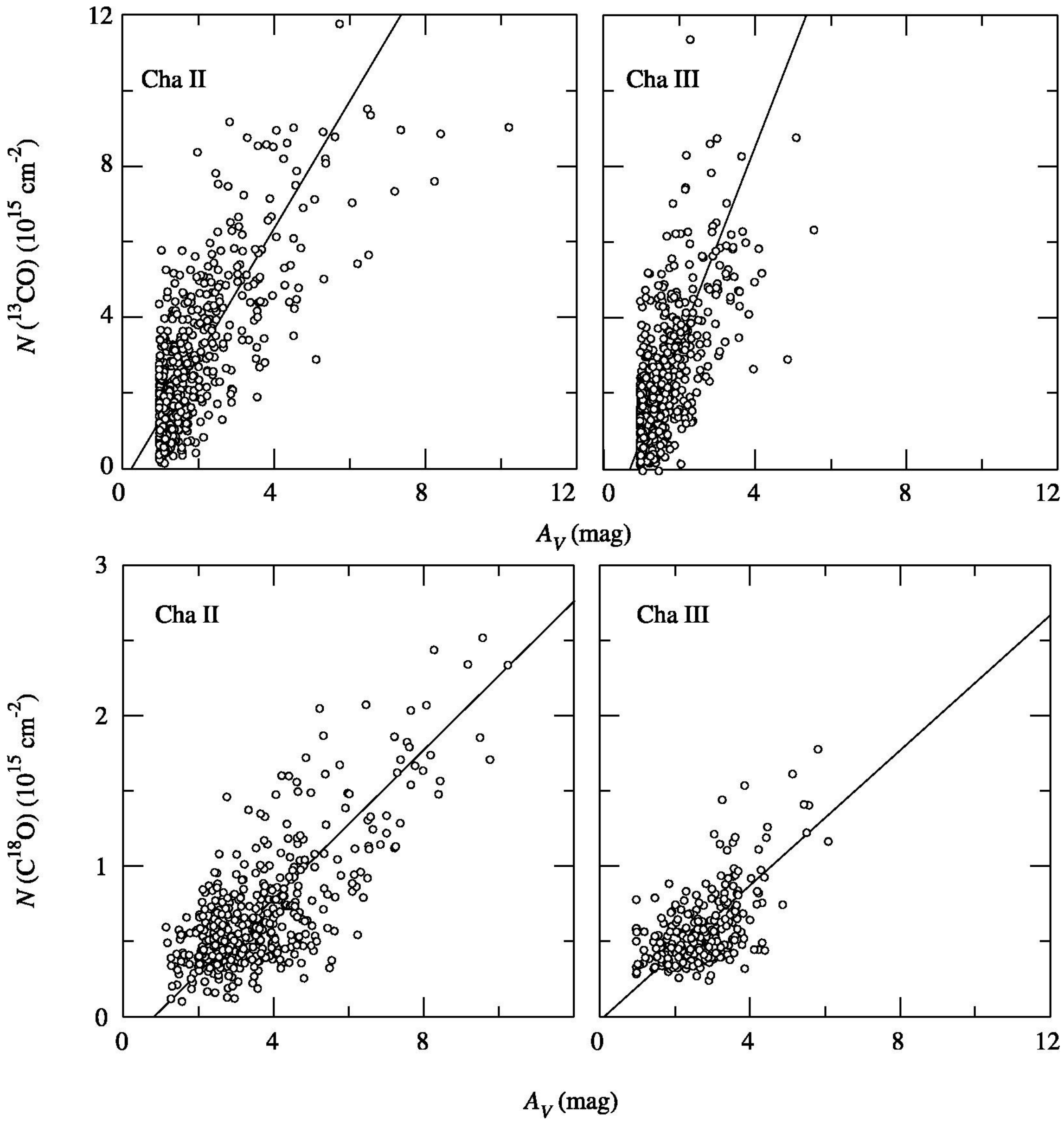

Hayakawa et al. 2001

Column density vs. extinction

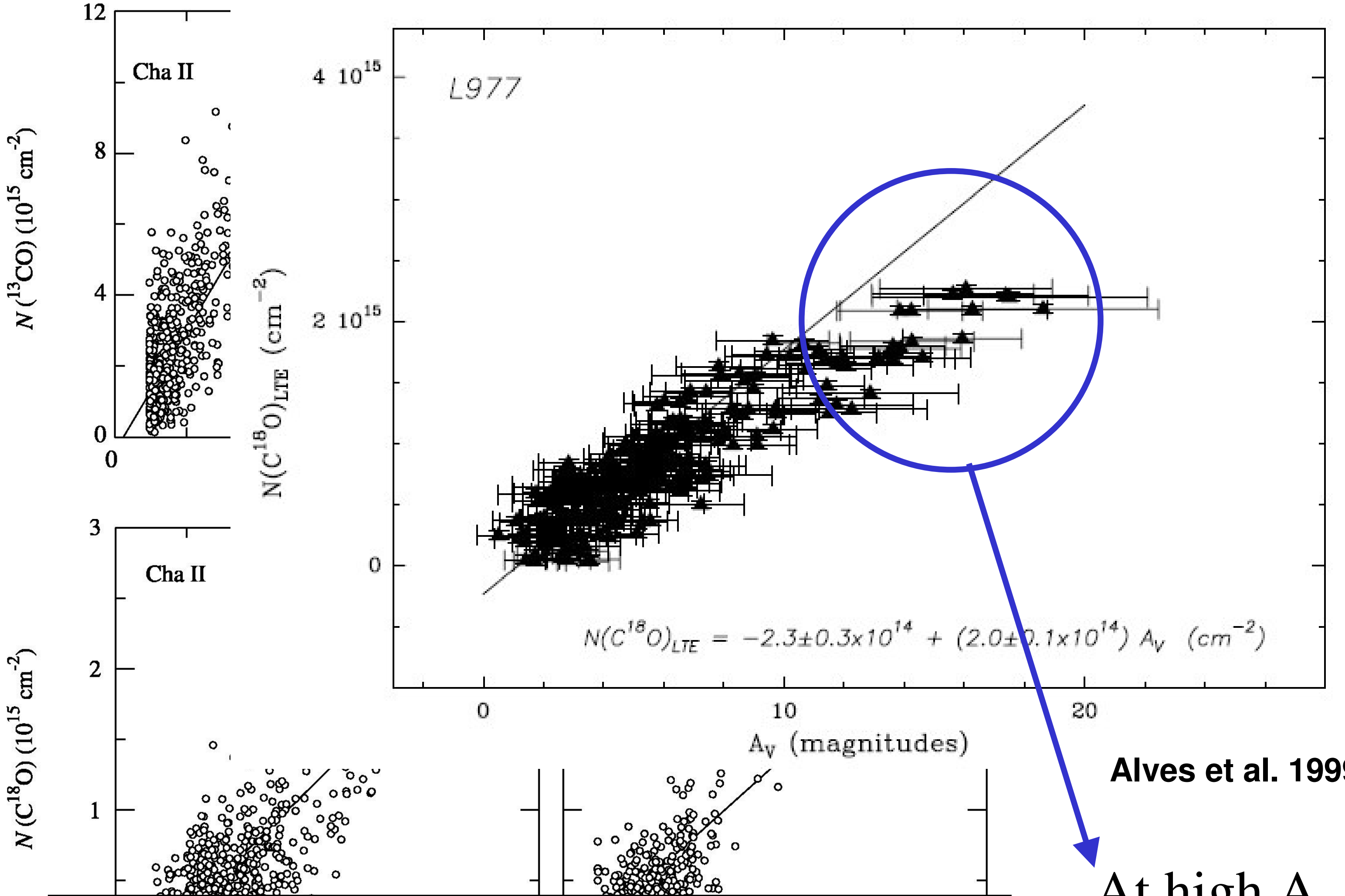

Alves et al. 1999

At high A_V: $C^{18}O$ depletion (or becomes opt. thick)

From HI: $N(HI+H_2) = 1.9\ 10^{21}\ A_V$ cm^{-2} mag^{-1}
(Bohlin et al. 1978)

CLUMPY STRUCTURE
AND
MASS DISTRIBUTIONS

Our Galaxy at 115 GHz

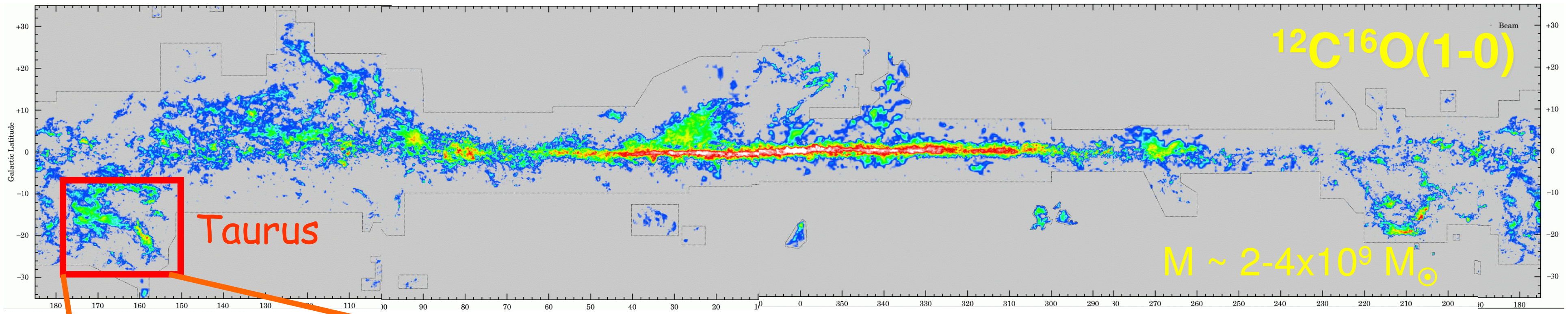

Dame, Hartmann and Thaddeus 2001

Onishi et al. 1998

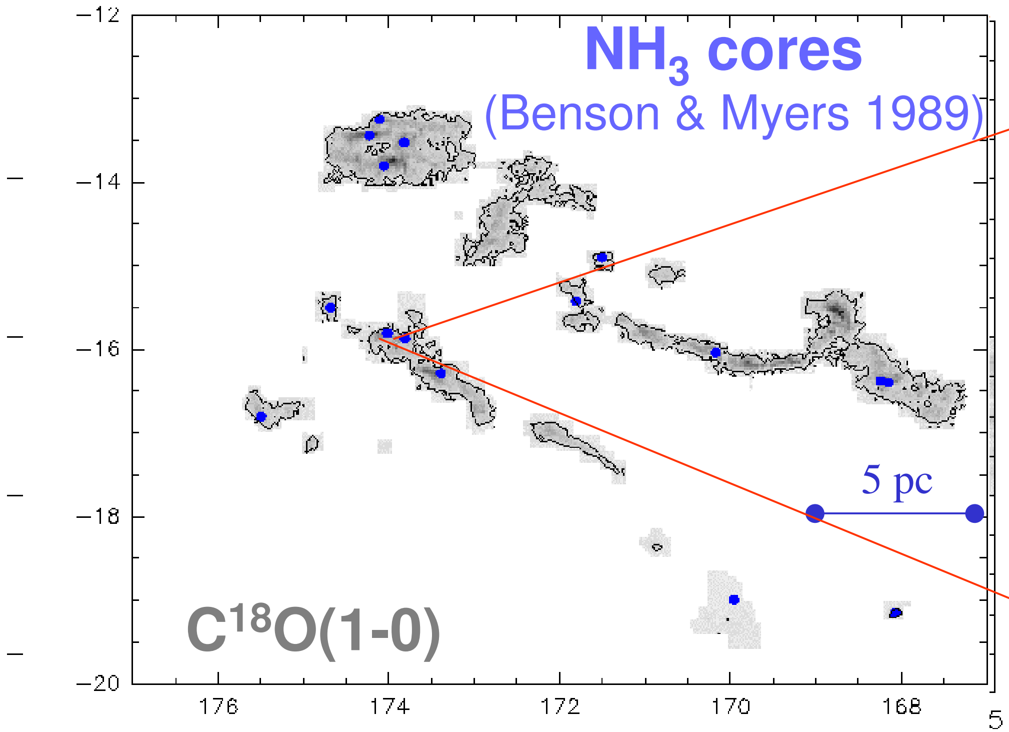

Caselli et al. 2002a

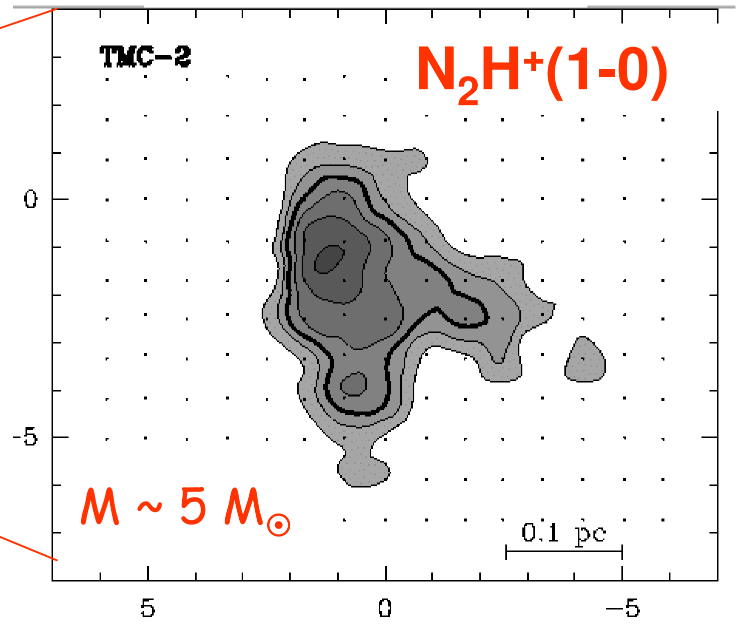

Cloud structure

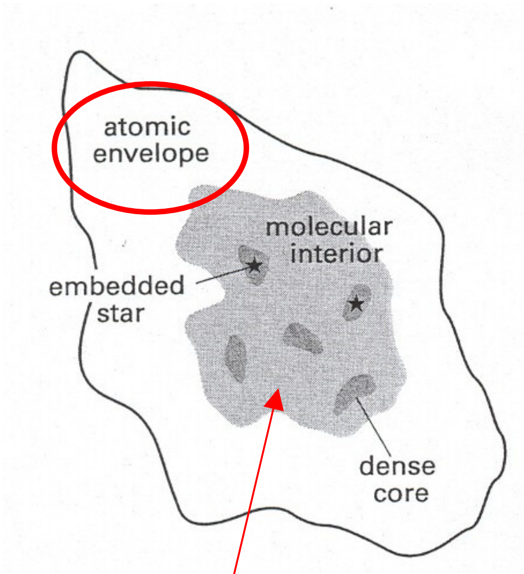

Interclump gas:
predominantly
atomic

Self-similar, fractal structure

Cloud , clump, core

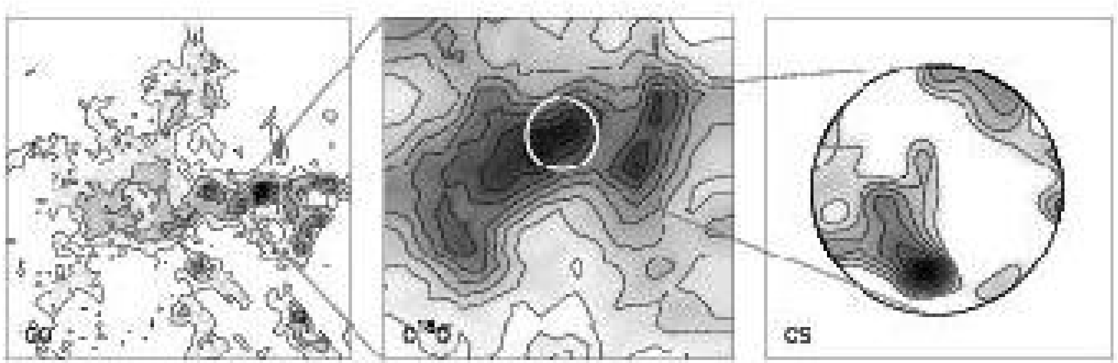

Figure 4. Hierarchical cloud structure. The three panels show a representative view from cloud to clump to core. The bulk of the molecular gas (cloud; left panel) is best seen in CO which, although optically thick, faithfully outlines the location of the H_2. Internal structure (clumps; middle panel) is observed at higher resolution in an optically thin line such as $C^{18}O$. With a higher density tracer such as CS, cores (right panel) stand out. The observations here are of the Rosette molecular cloud and are respectively, Bell Labs (90″), FCRAO data (50″), and BIMA data (10″).

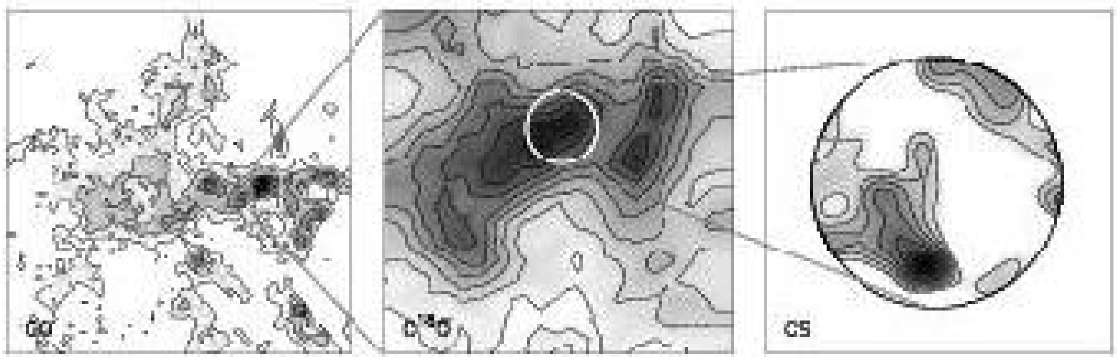

Clouds

$D \geq 10$ pc

$n(H_2) \approx 10^2\text{-}10^3$ cm^{-3}

$M \geq 10^4\ M_\odot$

$T \approx 10$ K

CO, ^{13}CO

$N(CO)/N(H_2) \approx 10^{-4}$

clumps

$D \approx 1$ pc

$n(H_2) \approx 10^5$ cm^{-3}

$M \approx 10^3\ M_\odot$

$T \approx 50$ K

CS, $C^{34}S$

$N(CS)/N(H_2) \approx 10^{-8}$

cores

$D \approx 0.1$ pc

$n(H_2) \approx 10^7$ cm^{-3}

$M \approx 10\text{-}10^3\ M_\odot$

$T \approx 100$ K

NH_3, CH_3CN

$N(CH_3CN)/N(H_2) \approx 10^{-10}$

Clumpy structure - Self-similarity

CO [∅ ≈8'≈1 pc]

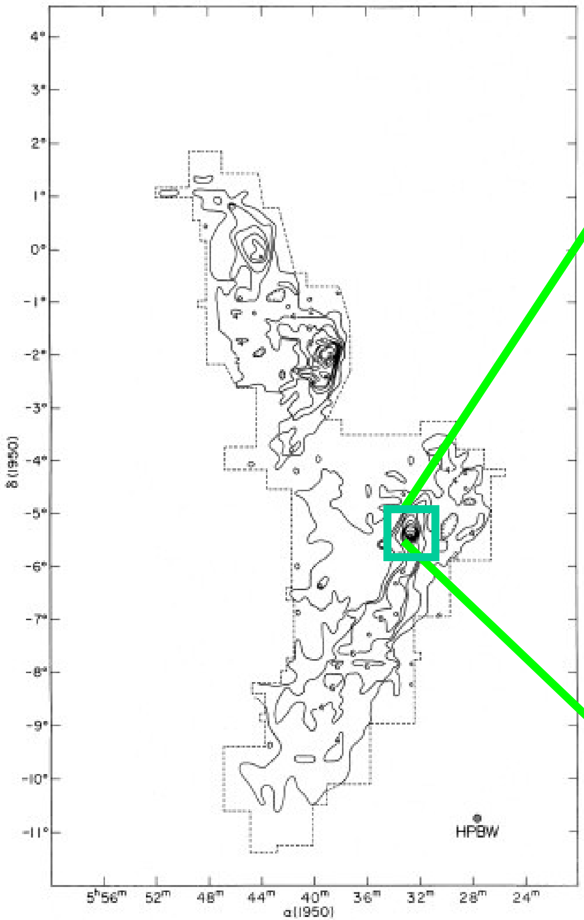

Kutner et al. 1977

NH_3 [∅ ≈43"≈0.1 pc]

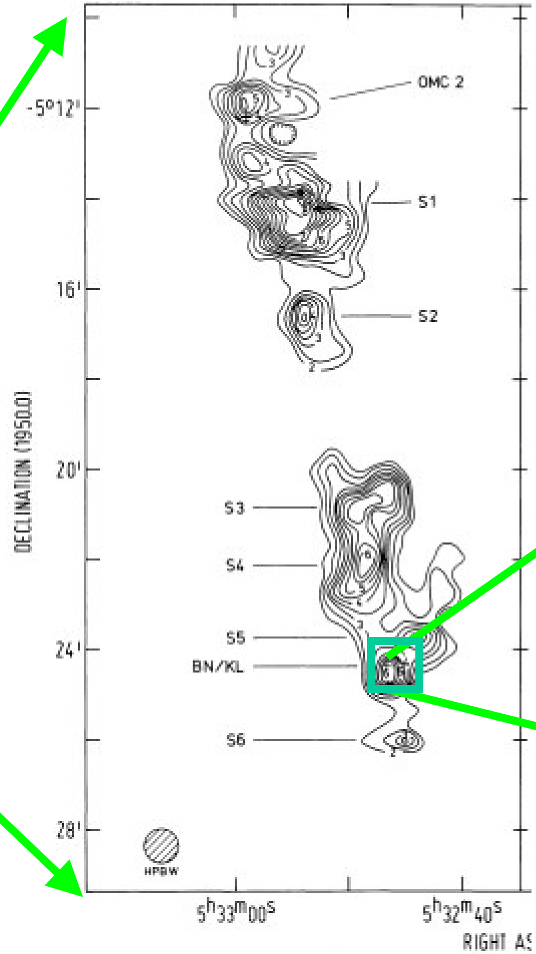

Batrla et al. 1983

NH_3 [∅ ≈1".5x2".2 ≈ 4 10^{-3} pc]

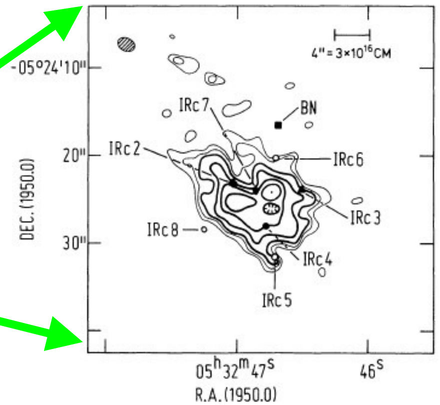

Pauls et al. 1983

Typical clump properties

(based on a study of the RMC – Rosette Molecular Cloud)

- 60 –90% of H_2 in clumps

- $<n>$ ~10^3 cm^{-3}; $<n_{vol}>$ ~25 cm^{-3} . Thus: volume filling factor ~ 2.5%
  Hence: n(interclump) ~ 2.5-12.5 cm^{-3}

- $\Sigma(r) \propto r^{-1}$, i.e. $\rho(r) \propto r^{-2}$

- Mass spectrum $dN/dM \propto M^{\alpha}$, $\alpha = -1.4$ to -1.7 for M = 1-3000 $M_{\odot}$.
  Idem for clouds as a whole

Self-similarity – Clump mass distribution

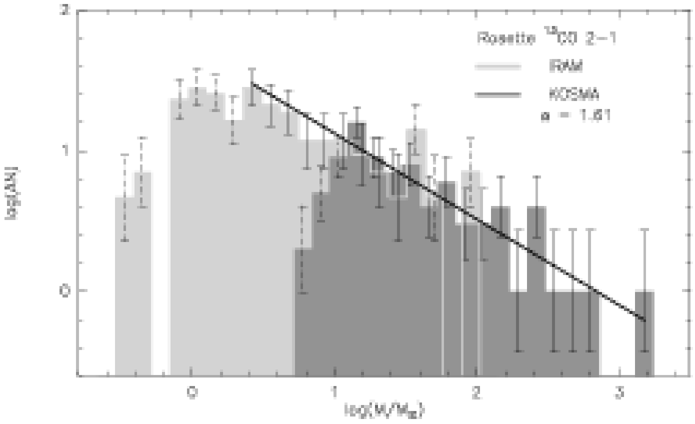

Fig. 16. Clump mass spectrum derived from ^{13}CO J=2→1 data obtained with KOSMA (85 clumps) and IRAM. The continous line delineates a fit to the power law function $dN/dM \propto M^{-\alpha}$. The resulting index is α=1.61. The dashed lines of the error bars mark the mass range beyond the turnover points and the IRAM high-mass end which are not included in the fit.

Rosette Molecular Cloud
Schneider et al. 1998

Kramer et al. 1998

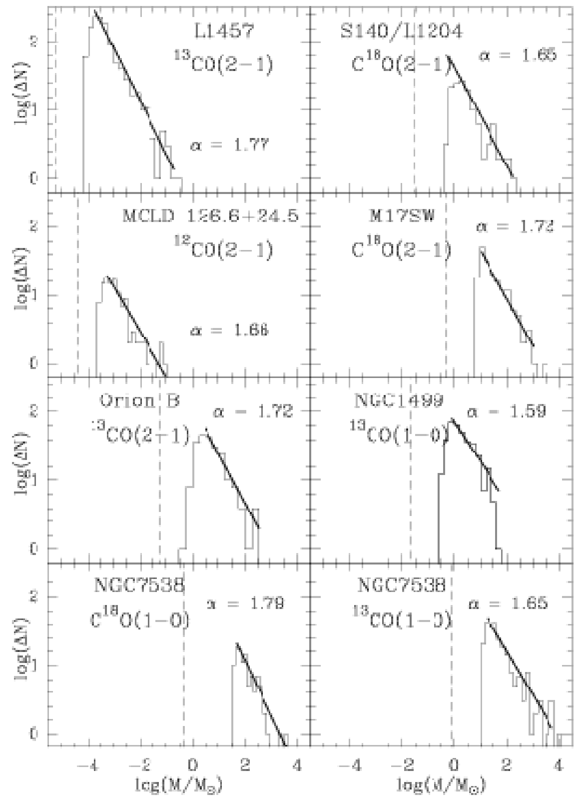

Power-law mass distribution $10^{-4} \leq M \leq 10^{4}\ M_\odot$: $dN/dM \propto M^{-1.7 \pm 0.1}$

Most clumps at low-mass end, but most of mass in the few high-mass clumps

Self-similarity – Clump mass distribution

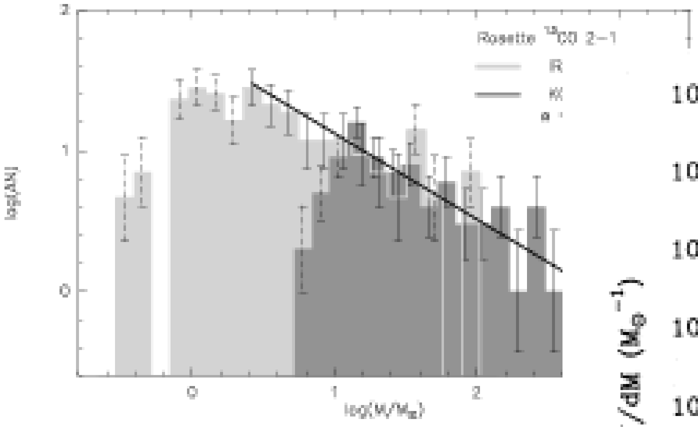

Fig. 16. Clump mass spectrum derived from ^{13}CO J=2→1 with KOSMA (85 clumps) and IRAM. The continuous li… a fit to the power law function $dN/dM \propto M^{-\alpha}$. The re… is α=1.61. The dashed lines of the error bars mark the… beyond the turnover points and the IRAM high-mass e… not included in the fit.

Rosette Molecular Cloud
Schneider et al. 1998

Kramer et al. 1998

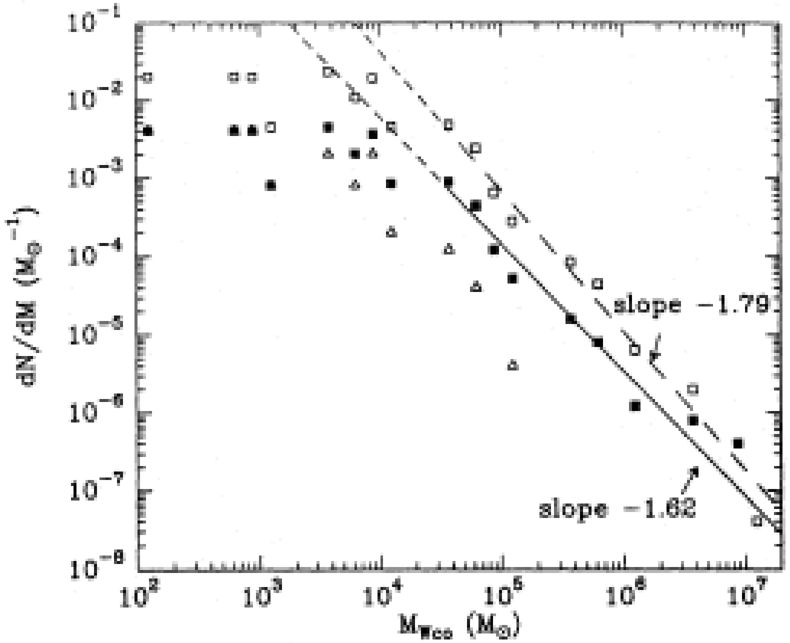

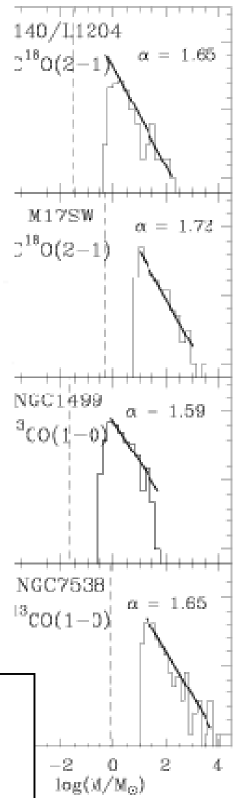

Power-law mass distribution 10

Most clumps at low-mass end, … ss clumps

204 clouds between
R=2-25kpc: same slope!

Mass distribution of sample of GMCs has **same slope**

Brand & Wouterloot 1995

Simba results 1

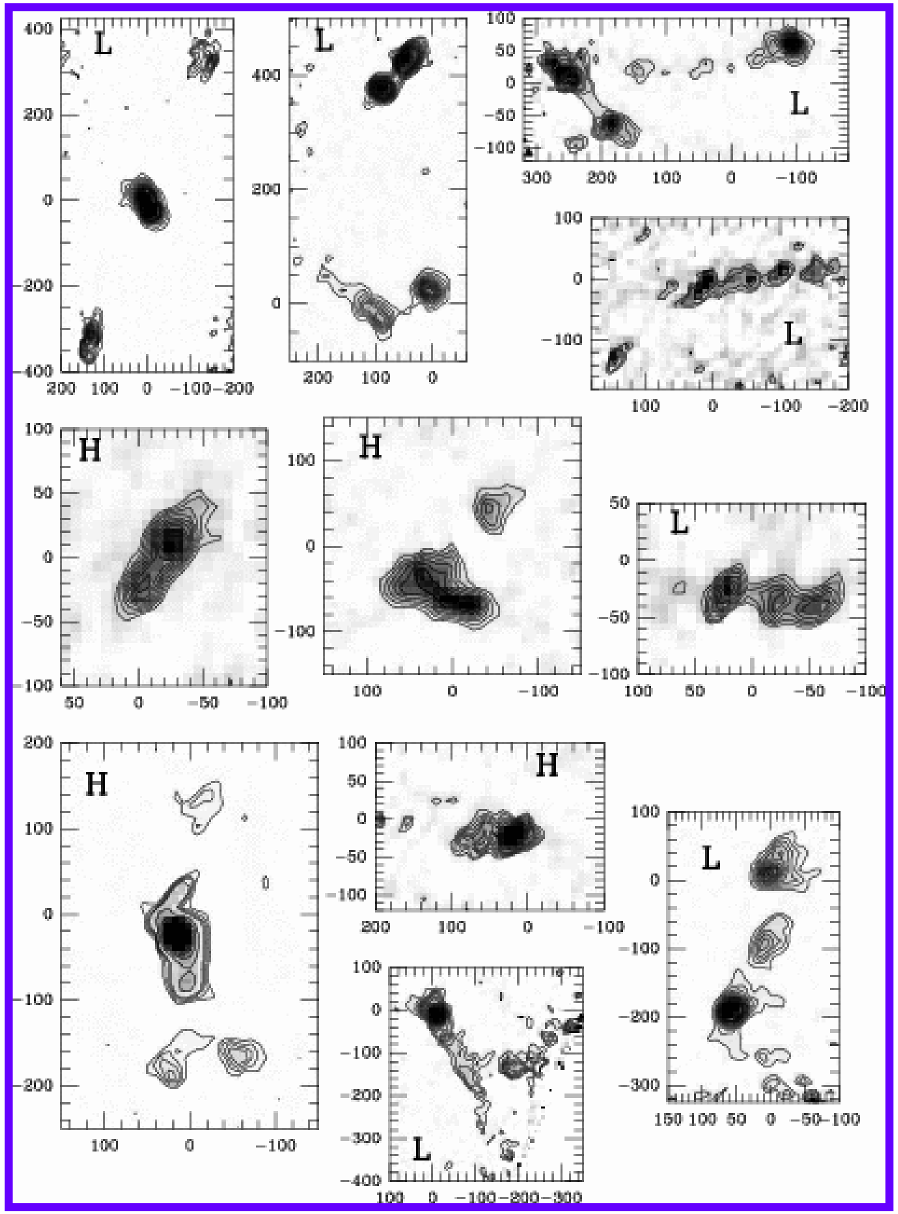

Multiple cores & chains

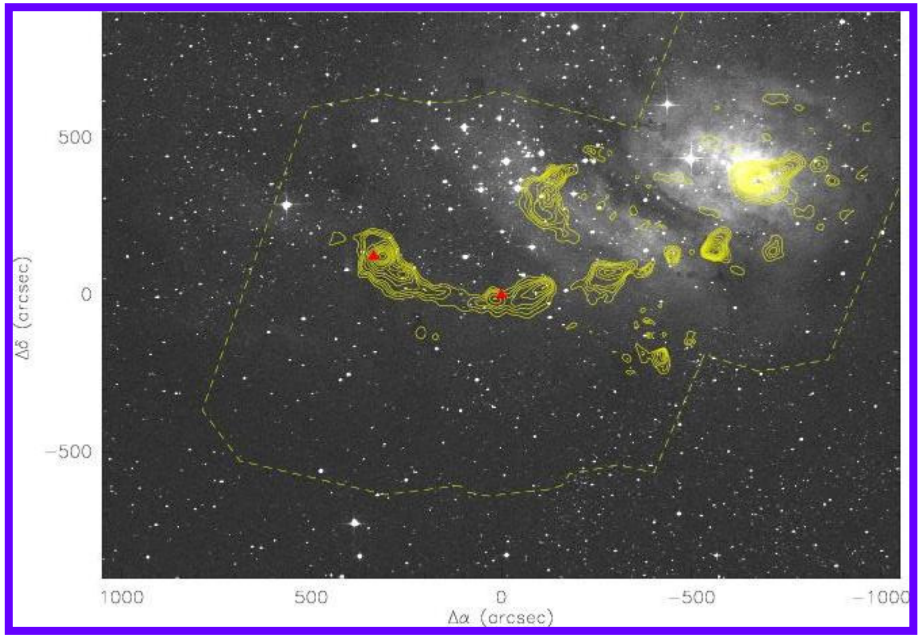

DSS + SIMBA (1.2-mm cont.)

AND: 95 pre-stellar or pre-cluster cores!

Beltran, Brand, Cesaroni et al. 2006

Simba results 2: clump mass function

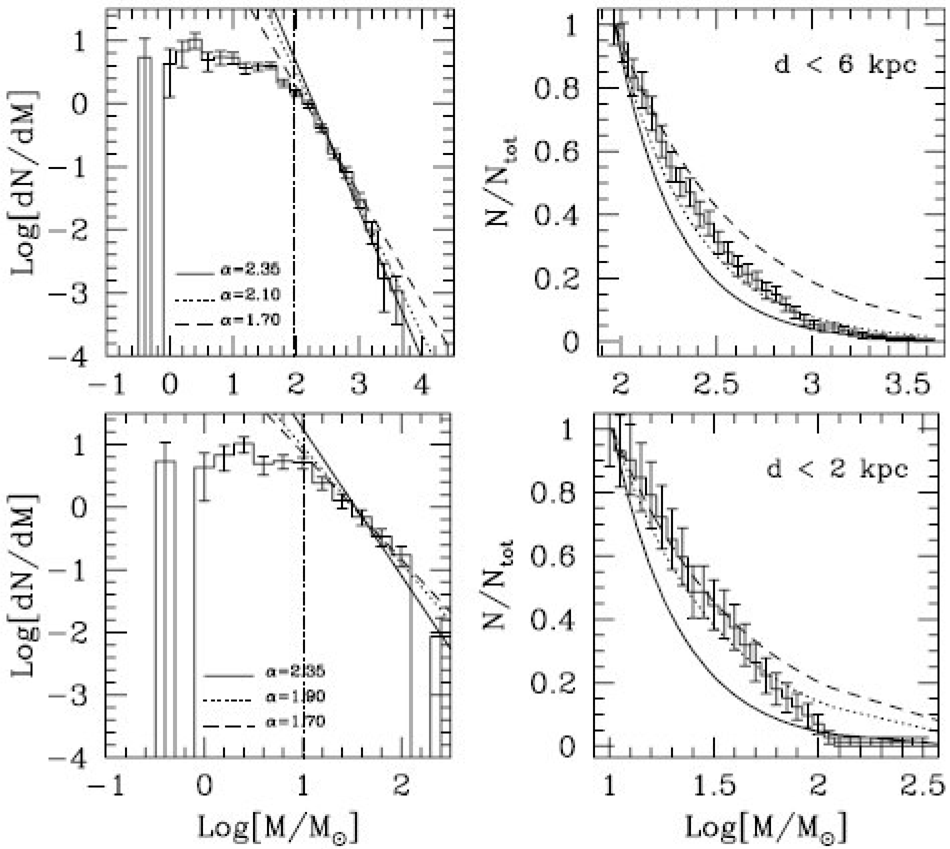

Fig. 10. *Left top panel*: the mass spectrum of the 1.2 mm clumps detected at a distance <6 kpc. The solid line represents the Salpeter IMF, $dN/dM \propto M^{-2.35}$; the dotted line is a −2.1 power law, obtained from the least square fit to the data, and the dashed line is a −1.7 power law. The vertical dot-dashed line indicates the completeness limit at 6 kpc. *Right top panel*: the normalized cumulative mass distribution of clumps with masses above the completeness limit at 6 kpc. The solid, and dashed lines are the same as in the left panel, and the dotted line is a −1.9 power law, obtained from the least square fit to the data. *Left bottom panel*: same as above for clumps detected at a distance <2 kpc. The vertical dot-dashed line indicates the completeness limit at 2 kpc. *Right bottom panel*: same as above for clumps with masses above the completeness limit at 2 kpc.

Slope 10-100 $M_\odot$: -(1.5-1.9); >100 $M_\odot$: -2.1

Beltran, Brand, Cesaroni et al. 2006

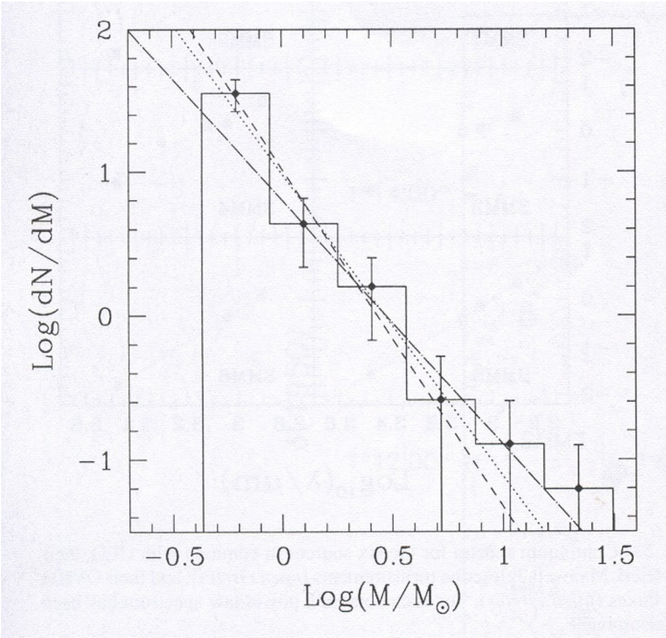

Serpens: Testi & Sargent 1998

26 pre-stellar clumps
Slope -2.1

IMF:
Salpeter: -2.5 for M= 1-10 M$_\odot$.
Miller-Scalo: -1.5 for M < 1 M$_\odot$.

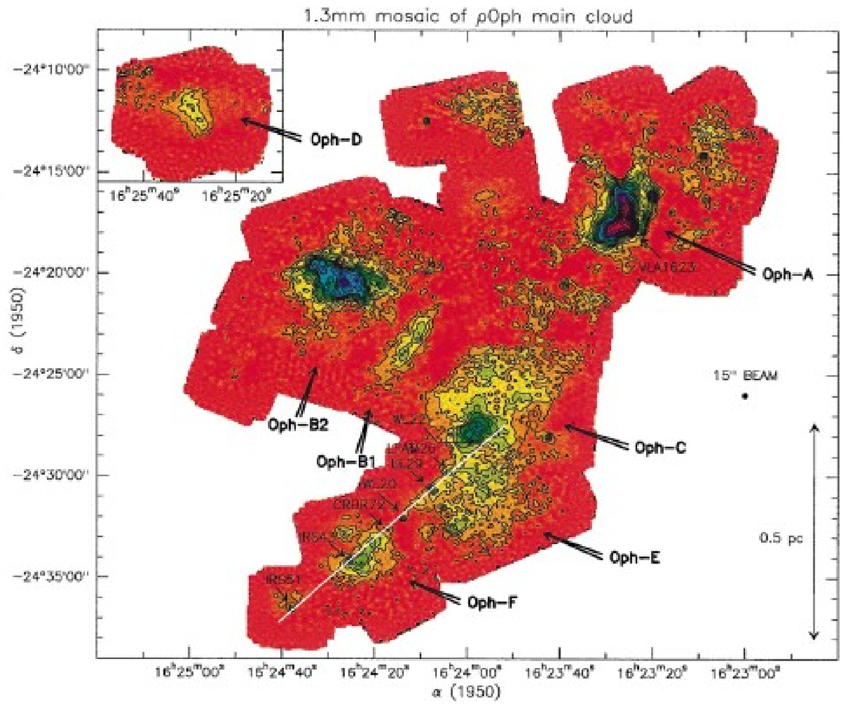

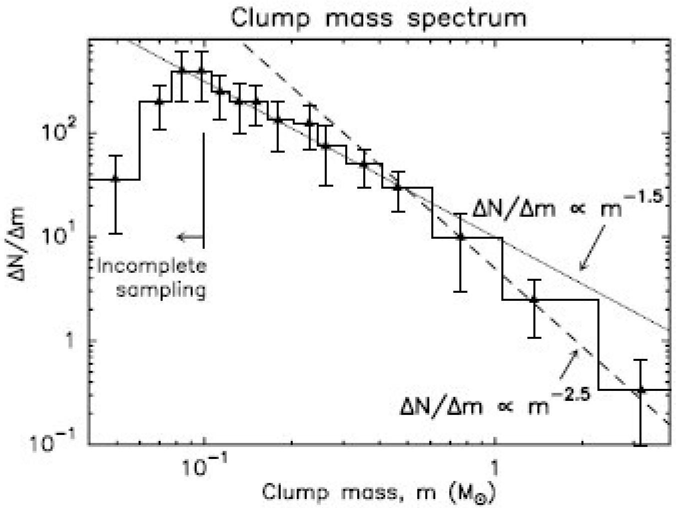

60 pre-stellar clumps in ρ Oph
Slope -1.5 for M= 0.1-0.5 M$_\odot$.
-2.5 0.5-3 M$_\odot$.

Ophiuchus: Motte et al. 1998

Typical clump properties

(based on a study of the RMC – Rosette Molecular Cloud; Blitz et al.)

- 60 –90% of H_2 in clumps

- $\langle n \rangle \sim 10^3$ cm^{-3}; $\langle n_{vol} \rangle \sim 25$ cm^{-3} . Thus: volume filling factor ~ 2.5%
  Hence: n(interclump) ~ 2.5-12.5 cm^{-3}

-$\Sigma(r) \propto r^{-1}$, i.e. $\rho(r) \propto r^{-2}$

- Mass spectrum $dN/dM \propto M^{\alpha}$, $\alpha = -1.4$ to -1.7 for M = 1-3000 $M_{\odot}$.
  Idem for clouds as a whole

- Most clumps not gravitationally bound, but most mass is in clumps that are.
  Yet clumps are not expanding: pressure-confinement

- Inside clump: $P_{int}/k \sim 6\text{-}12 \times 10^4$ Kcm^{-3} (bulk gas motions)
  Inside GMC, due to gravity: $P_{grav}/k \sim 8 \times 10^4$ Kcm^{-3}
  $P_{HI}/k \sim 10 \times 10^4$ Kcm^{-3}
  $\Rightarrow$ clumps confined by interclumps gas (which is HI)

MOLECULAR GAS KINEMATICS
rotation curve and kinematic distances

The observed velocity field

(Brand & Blitz 1993)

Radial velocity as a function of distance

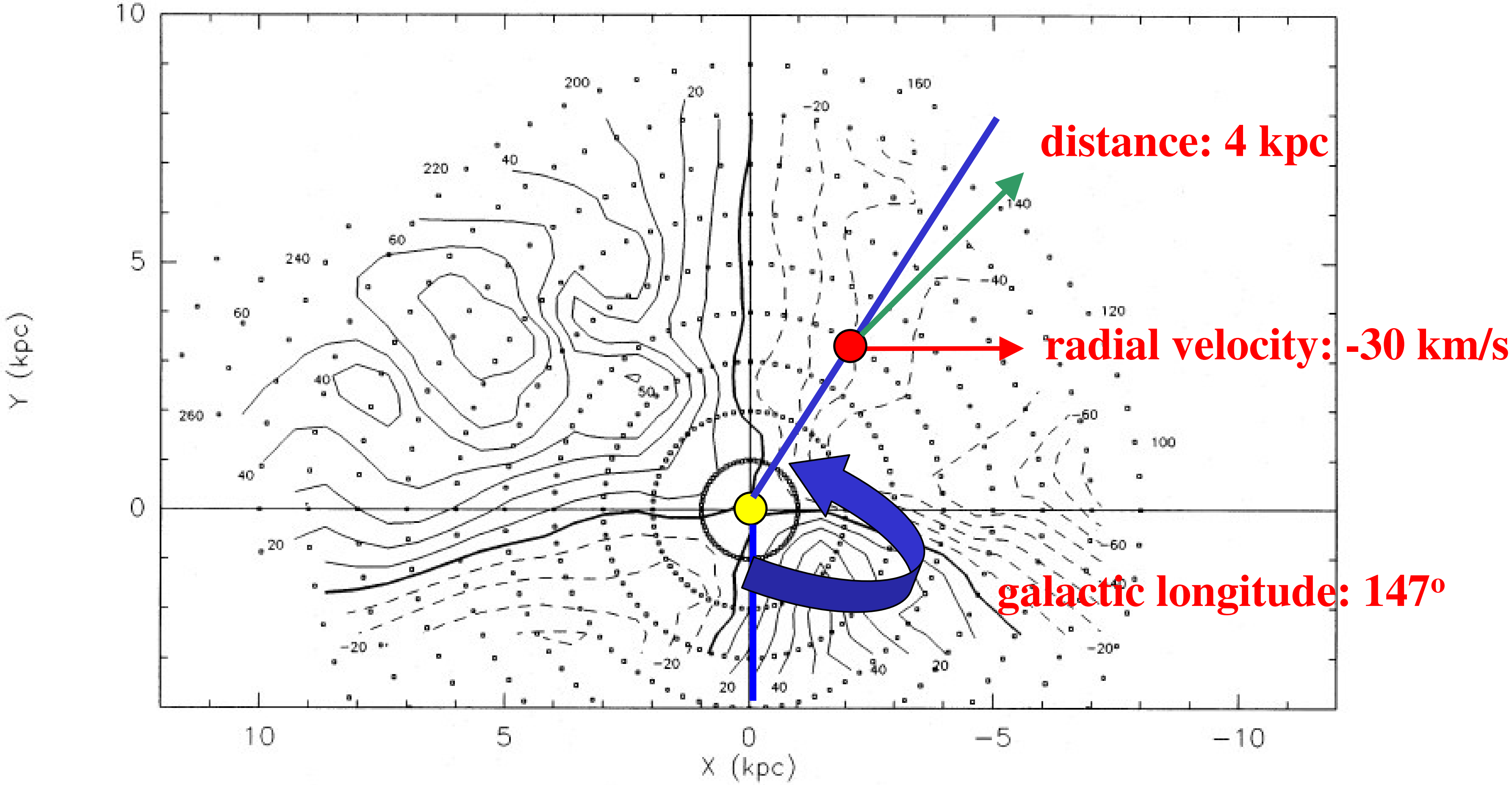

Kinematic distances I

Observed velocity field is useful to determine kinematic distances, but its range of use is limited (e.g., <2 kpc from Sun in inner Galaxy)

Therefore: construct the rotation curve (Θ versus R)

Transform observed radial velocities and spectro-photometric distances into galactic rotation velocity Θ and galactocentric distance R:

$V_{lsr} = (\Theta R_0/R - \Theta_0) \sin l \cos b$ for circular rotation.

$\omega = \Theta / R$: angular rotation velocity $\Rightarrow V_{lsr} = R_0(\omega - \omega_0) \sin l \cos b \Rightarrow$

$\omega = V_{lsr}/(R_0 \sin l \cos b) + \omega_0$

$R = (d^2\cos^2 b + R_0^2 - 2 R_0 d \cos b \cos l)^{1/2}$

Advantage: get distances everywhere.

Disadvantage: in some regions erroneous because streaming motions are not included.

Rotation curve from HI and CO

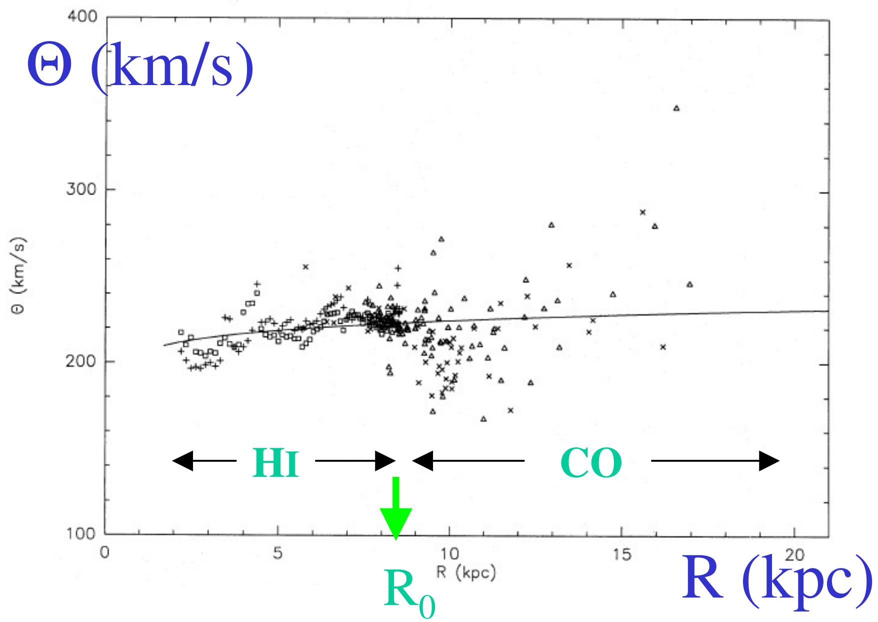

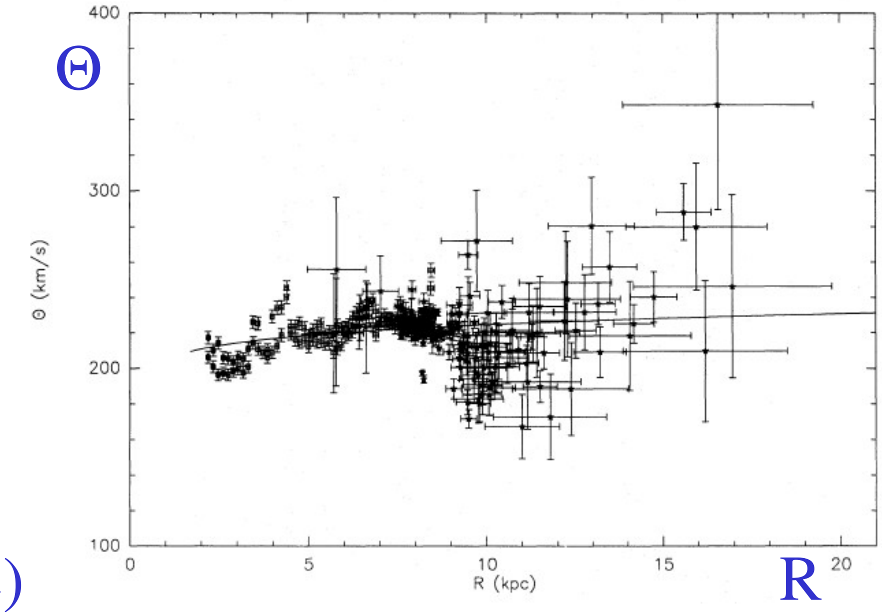

Fit a function of type:

$\omega/\omega_0 = a_1(R/R_0)^{a2-1} + a_3(R/R_0)$

Implying

$\Theta/\Theta_0 = a_1(R/R_0)^{a2} + a_3$

$a_1 = 1.0077,\ a_2 = 0.0394,\ a_3 = 0.00712$

(Brand & Blitz 1993)

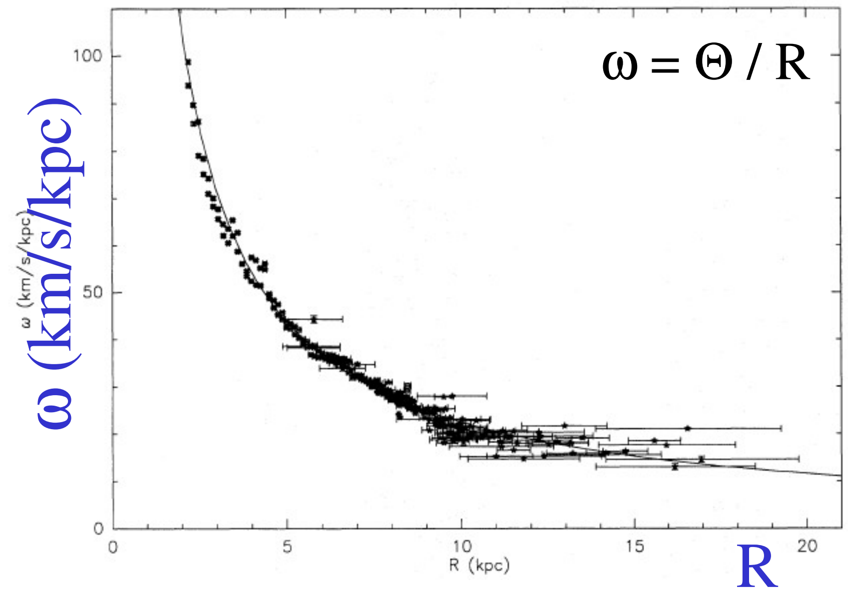

Kinematic distances II

Rotation curve: $\Theta = \Theta_0 \, (R/R_0)^a$ with $\Theta_0 = 220$ km/s, $R_0 = 8.5$ kpc

In general: $V_{lsr} = R_0(\omega - \omega_0) \sin l \cos b$, and $\omega = \Theta/R$.

It follows that:

$$R = \left(\left[(V_{lsr} / \sin l \cos b) + \Theta_0 \right] / \Theta_0 \, R_0^{\,1-a} \right)^{1/(a-1)} \text{ and}$$

$$d = [R_0 \cos l \pm (R^2 - R_0^2 \sin^2 l)]^{0.5} / \cos b$$

For outer Galaxy: choose '+'
For inner Galaxy, there are 2 solutions: distance ambiguity!

Distance ambiguity in inner Galaxy

Velocity field from rotation curve

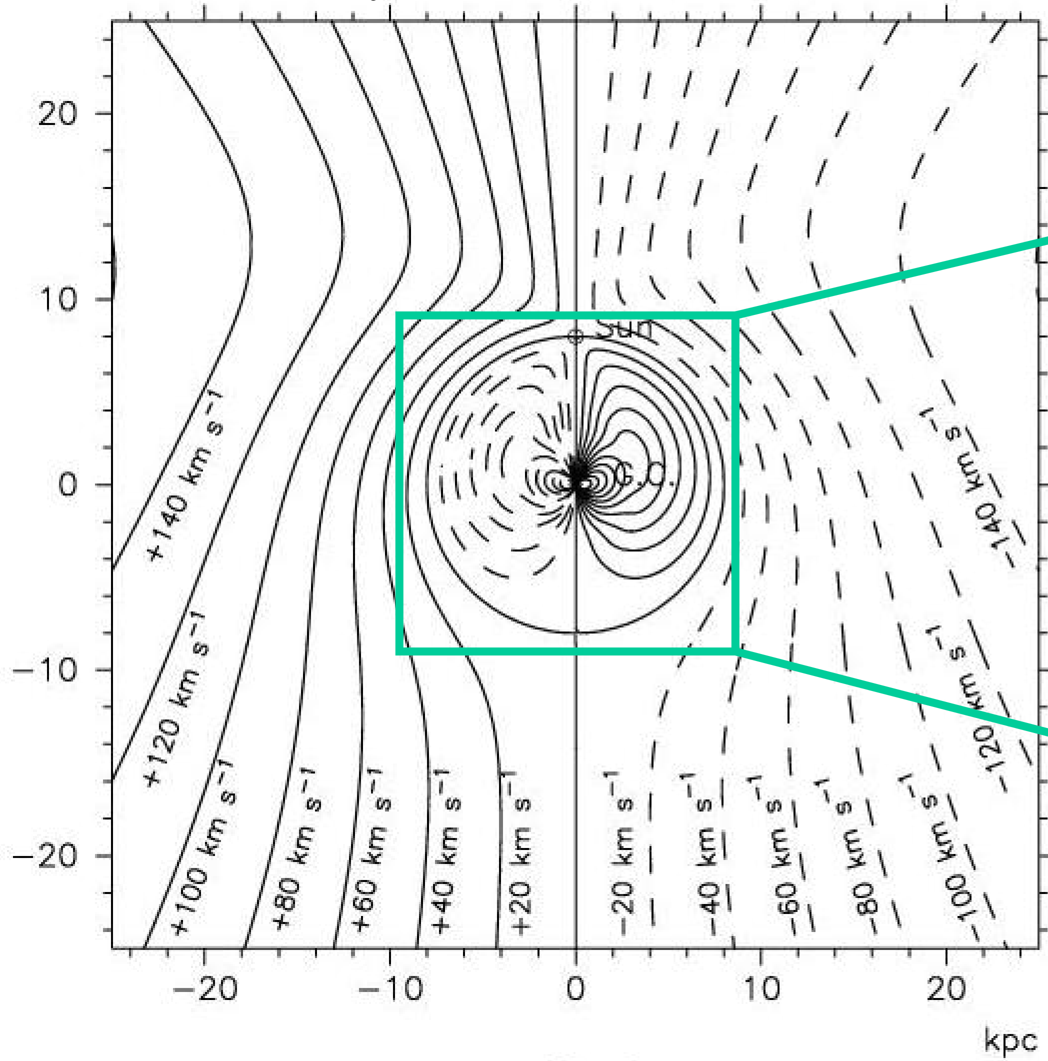

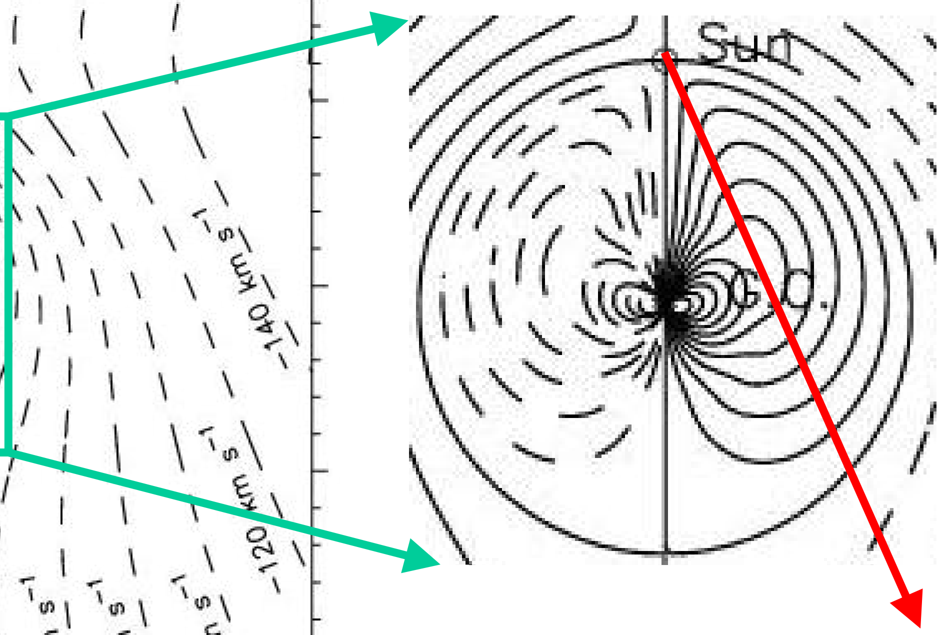

Two values for d at the same V_{lsr} : ambiguity

Nakanishi & Sofue 2003 PASJ

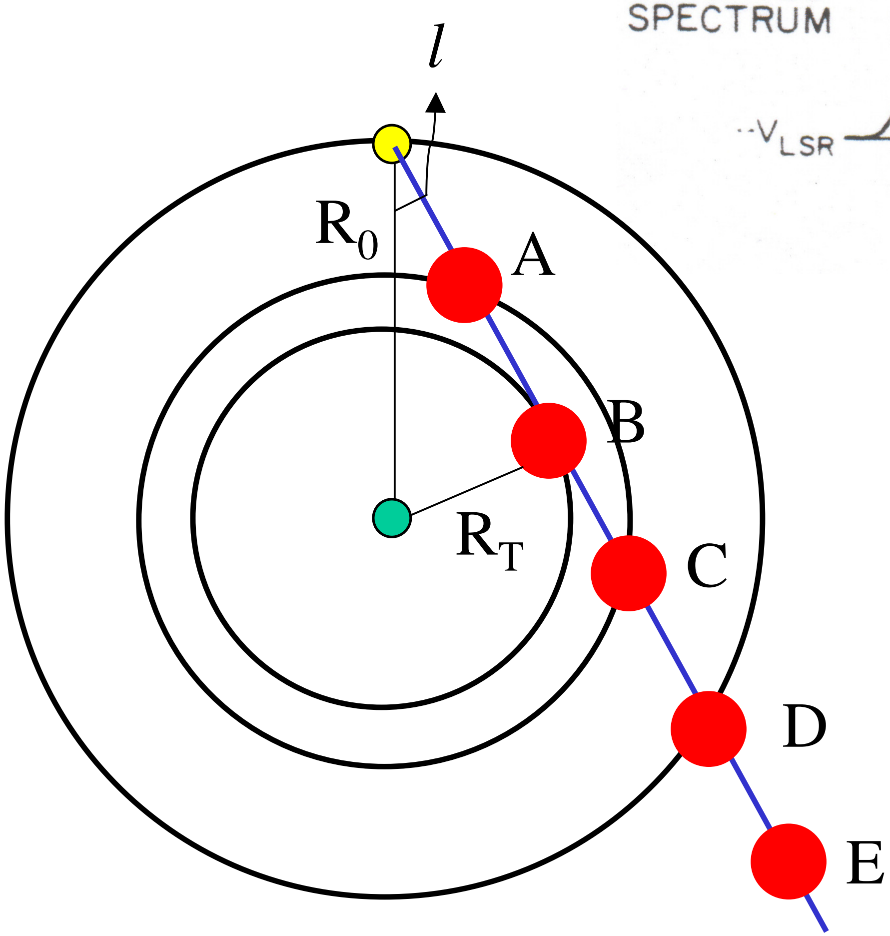

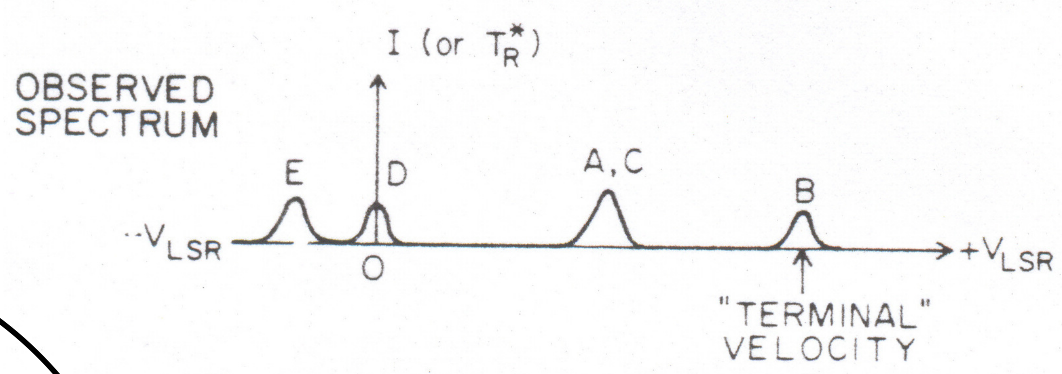

$R_T = R_0 \sin l$: subcentral (tangent) point. Maximum V_{lsr} long l.o.s.

Velocity crowding

Arched in green:
dV/dr ≤ 6 km/s/kpc

Artificial density structures

Contours of dV/dr

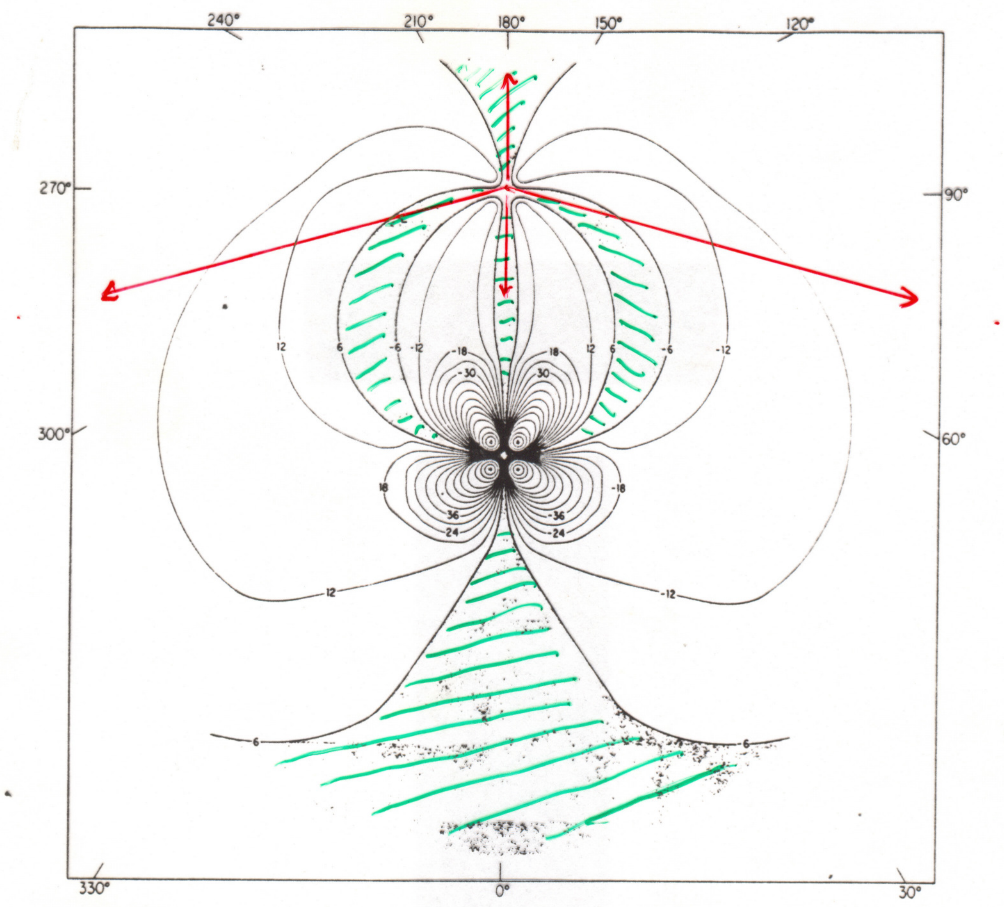

(Burton 1988)

Streaming motions

V_{lsr} - residuals: observed – expected from rotation curve

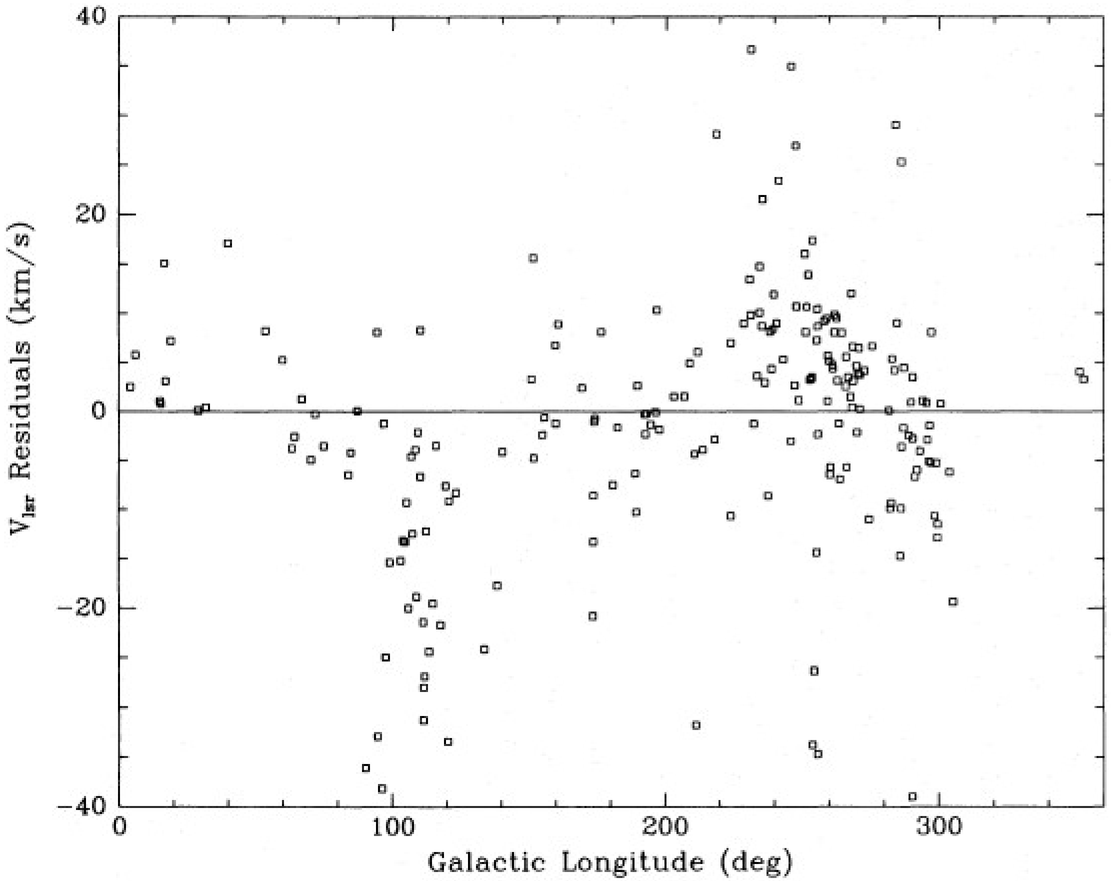

(Brand & Blitz 1993)

HI: V-residuals

(Burton & Bania 1974)

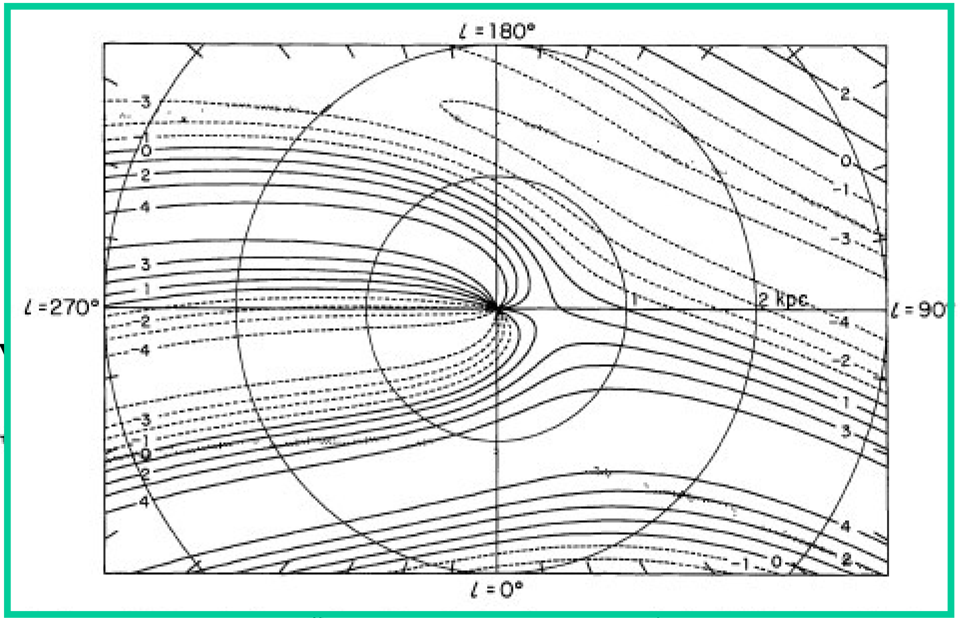

V_{lsr} - residuals: obser

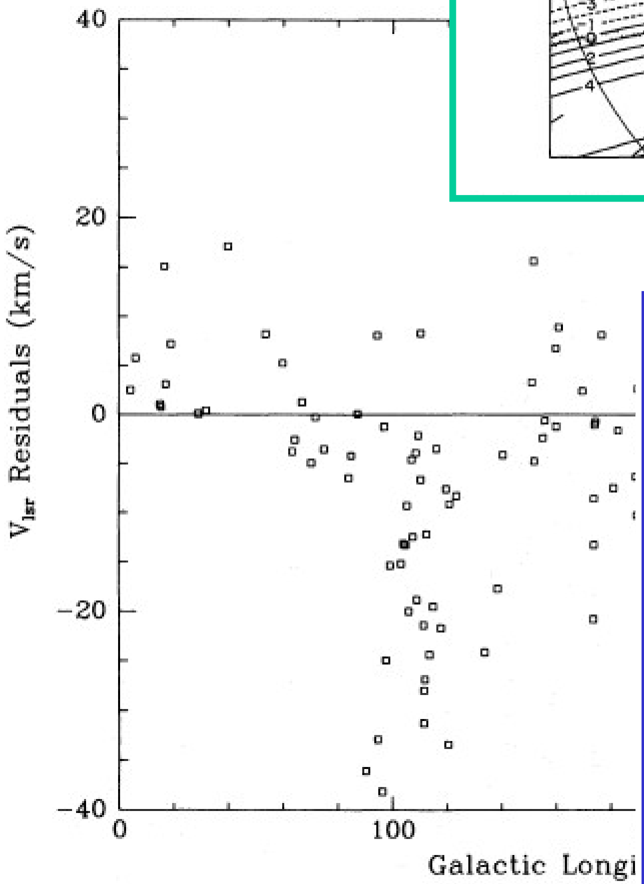

(Brand & Blitz 1993)

CO: Streaming motions pattern

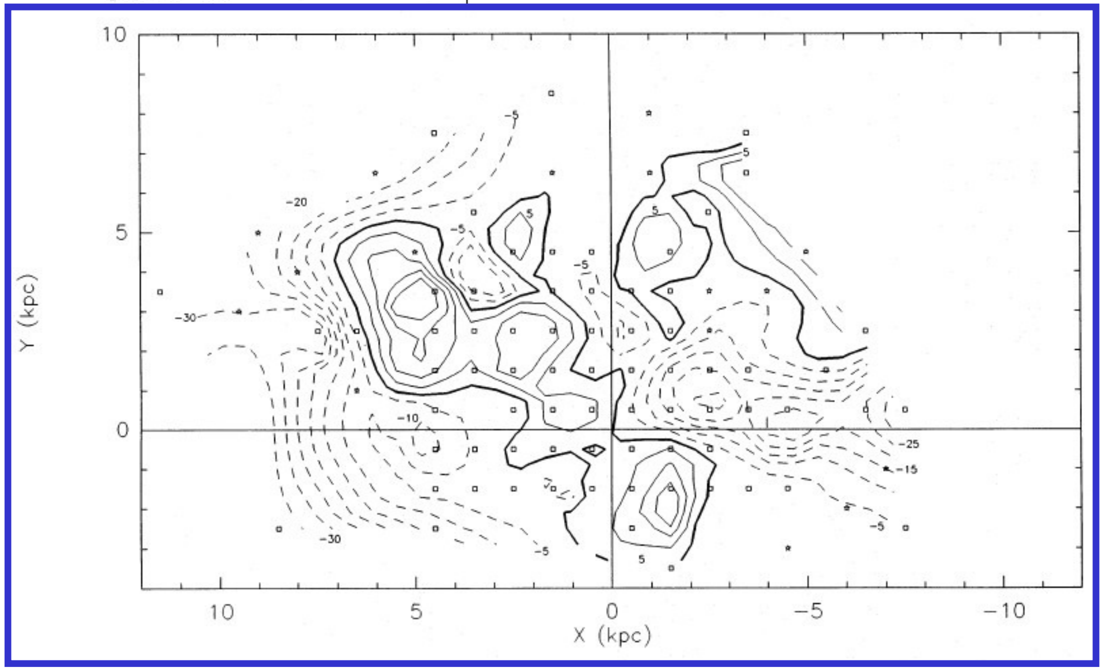

Trigonometric parallax

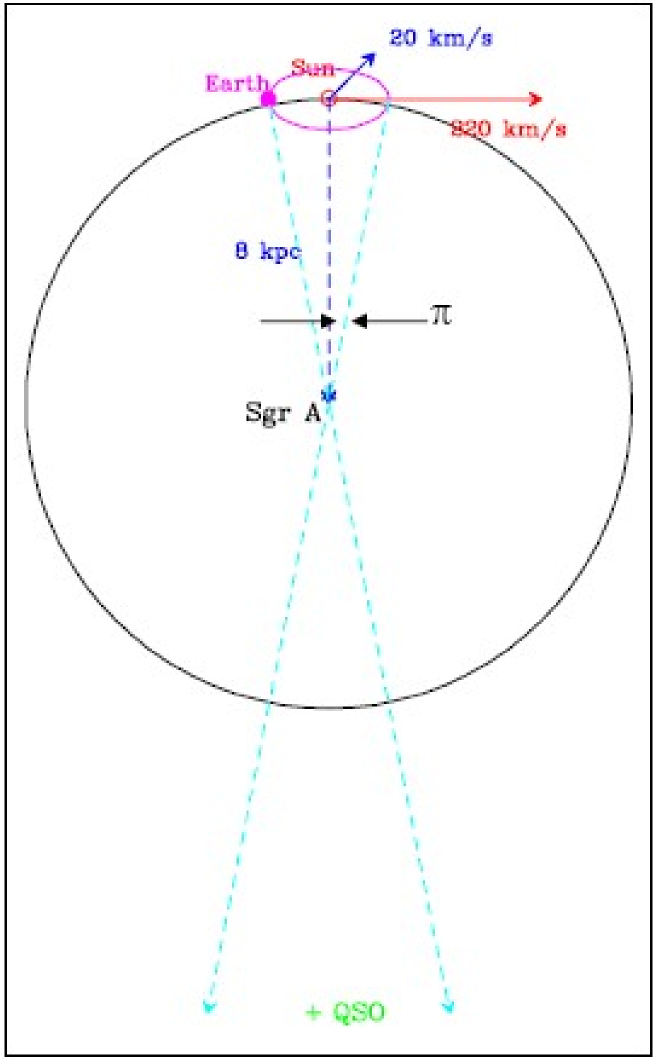

(Reid – IAU242, 2007)

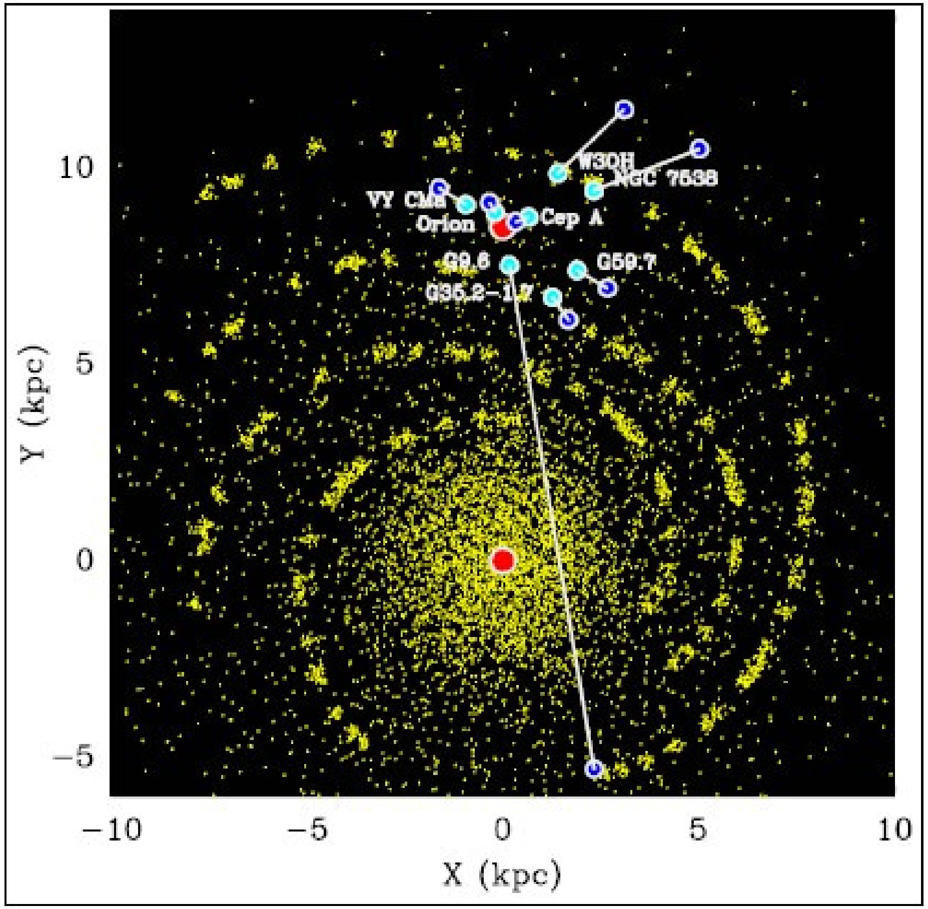

The new Galaxy

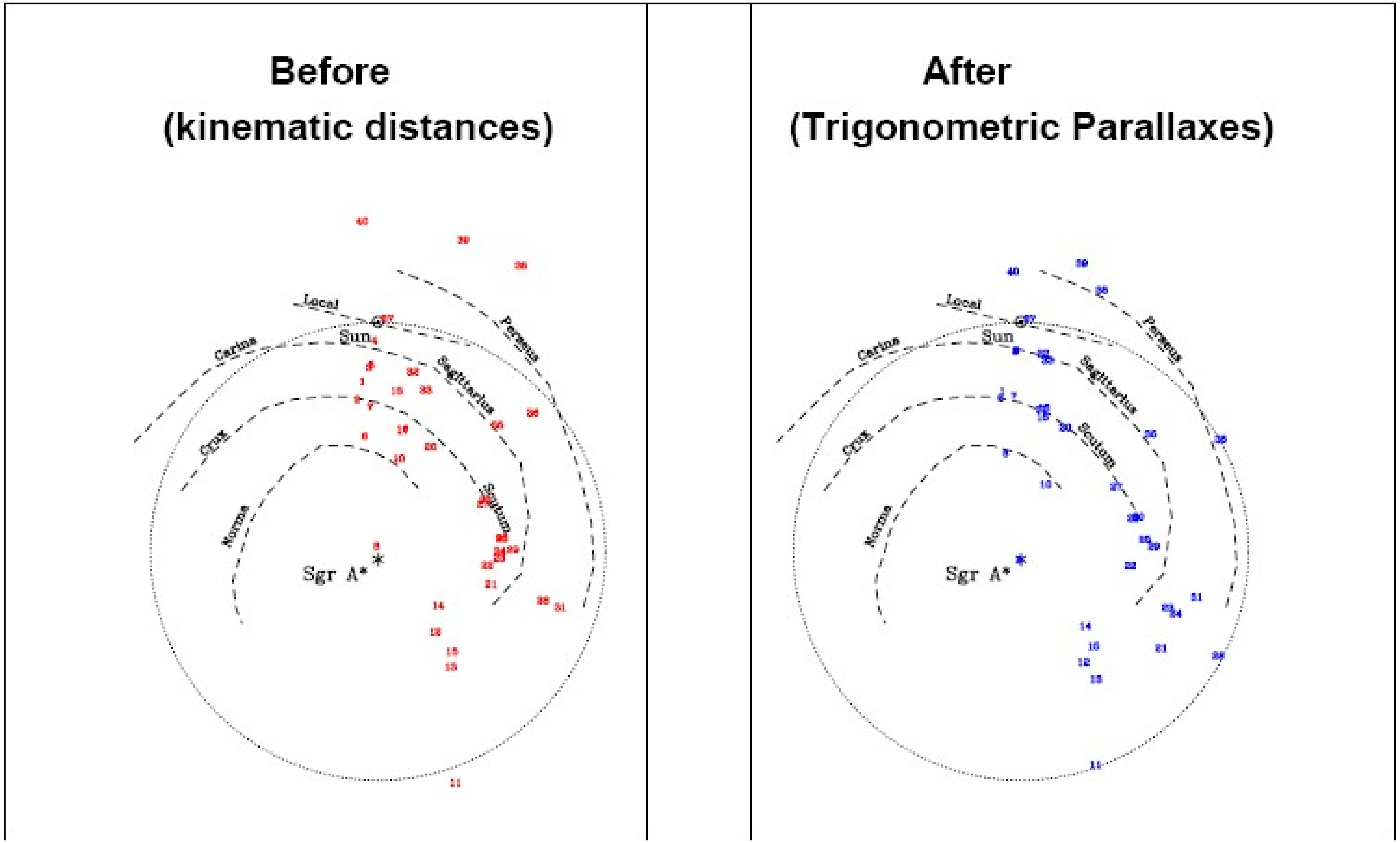

(Reid - IAU242, 2007)

STAR FORMATION

Star formation: in molecular clouds

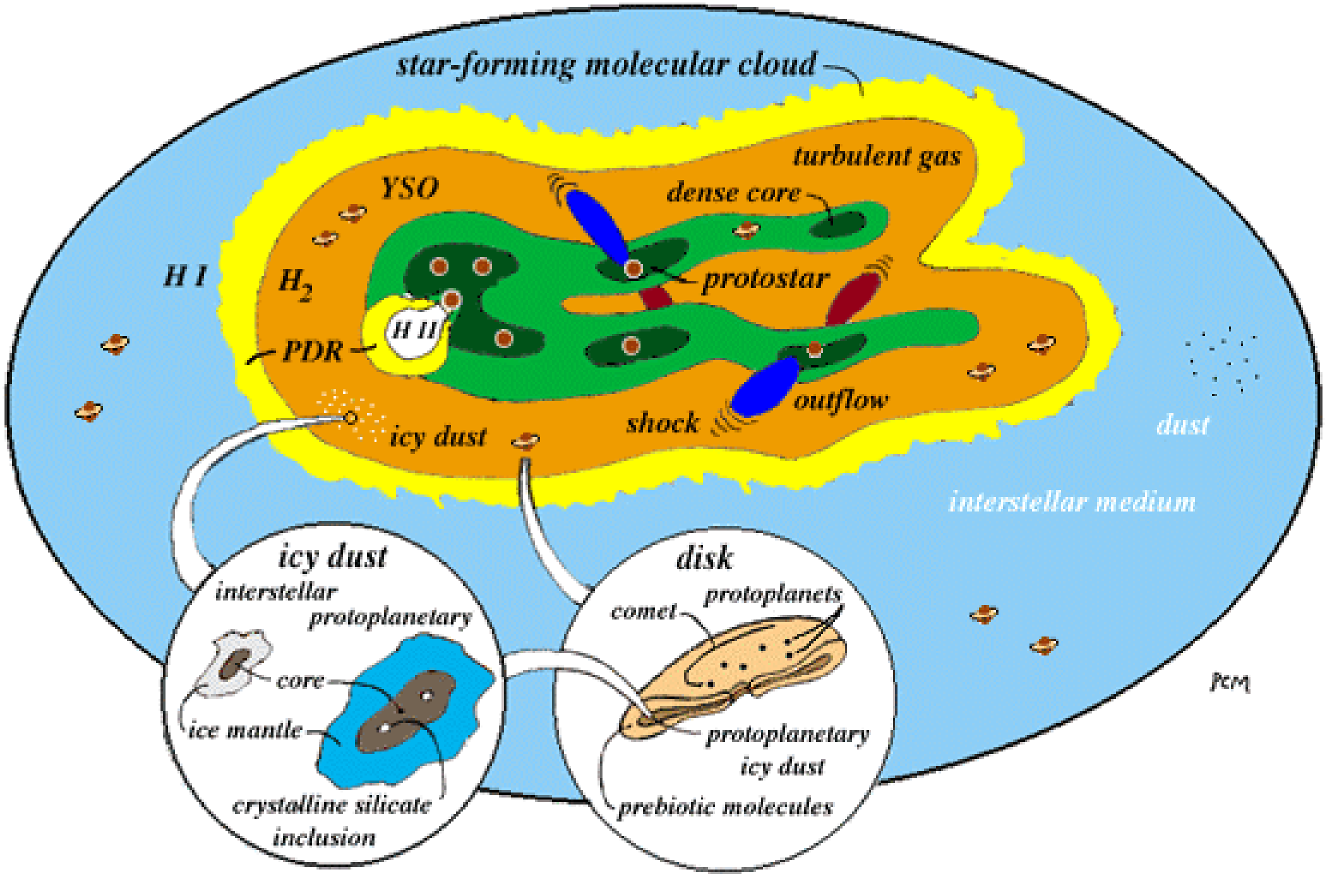

Star formation catastrophe?

$M_{cloud} \approx 10^{4\text{-}5}\, M_\odot \gg M_{Jeans} \approx 10^2\, M_\odot \Rightarrow$ collapse on

free-fall timescale $t_{ff} \approx \sqrt{(3\pi/32G\rho)} \approx 10^6$ yrs.

On galactic scale:

$SFR = M_{GMC}/t_{ff} \approx 10^9\, M_\odot/\, 10^6\, \text{yrs} \approx 10^3\, M_\odot\ /\text{yr}$

$\gg SFR_{obs} \approx 3\, M_\odot\ /\text{yr}$

Clouds are prevented from total collapse!

SFE: Star formation efficiency

TABLE 2 Star-formation efficiencies for nearby embedded clusters

Cluster name	Core mass ($M_\odot$)	Stellar mass ($M_\odot$)	SFE	References
Serpens	300	27	0.08	Olmi & Testi 2002
Rho Oph	550	53	0.09	Wilking & Lada 1983
NGC 1333	950	79	0.08	Warin et al. 1996
Mon R2	1000	341	0.25	Wolf et al. 1990
NGC 2024	430	182	0.33	E.A. Lada et al. 1991a,b
NGC 2068	266	113	0.30	E.A. Lada et al. 1991a,b
NGC 2071	456	62	0.12	E.A. Lada et al. 1991a,b

Lada & Lada 2003 ARAA

Cloud support

Virial theorem: $2T+2U+W+M=0$

Gravitational energy

Thermal energy (random motions): $U/W \approx 3 \times 10^{-3} \rightarrow$ irrelevant

Magnetic field term: $M/W = 0.3$

Kinetic energy (bulk motions, mostly from clumps): $T/W \approx 0.5$

Clouds are supported by turbulence and magnetic fields

B-field: Zeeman splitting

In presence of B-field, hyperfine splitting of levels is modified: spectral line splits in 2, centered on primary component, with opposing polarisations.

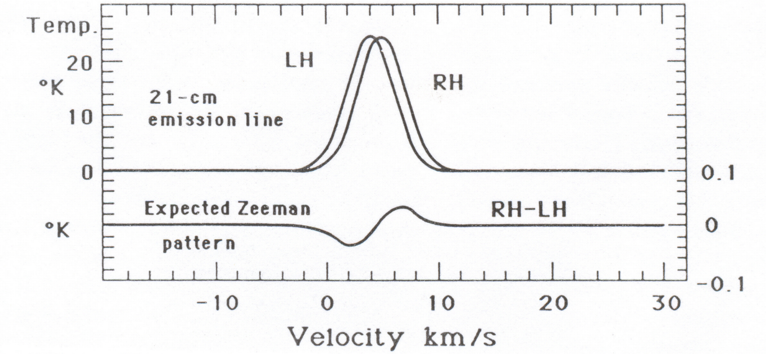

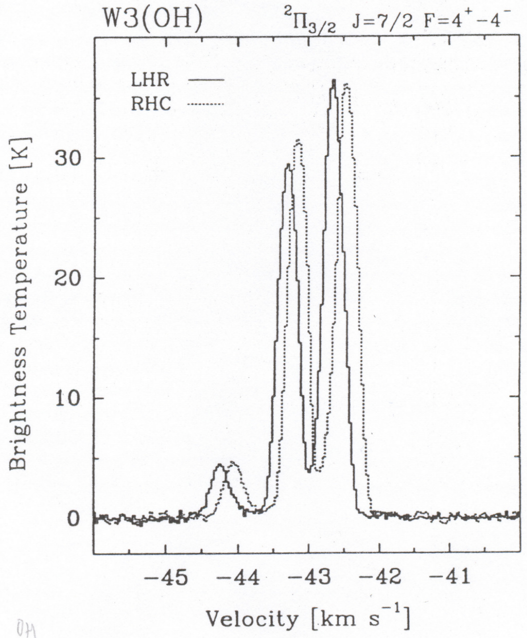

$$\frac{\Delta\nu_{\rm mag}}{\Delta\nu_{\rm therm}} \approx 10^{-3}\left(\frac{B}{\mu{\rm G}}\right)\left(\frac{T_k}{10{\rm K}}\right)^{-1/2}$$

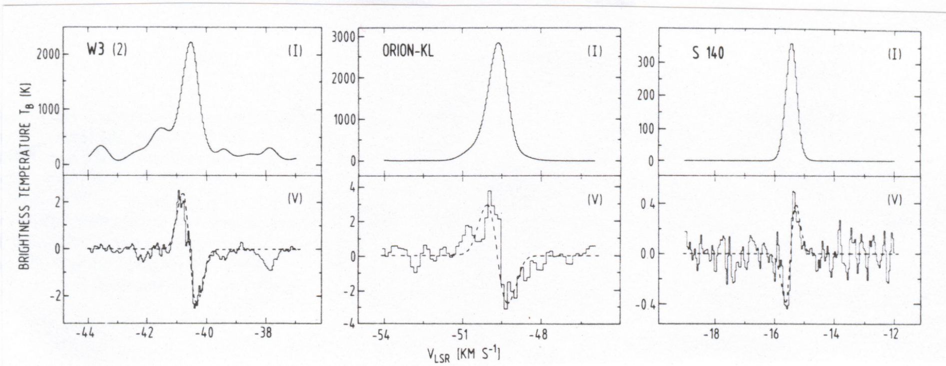

3.27 Hz/µG OH @ 1665 MHz

1.96 Hz/µG OH @ 1665 MHz

$7.2\ 10^{-4}$ Hz/µG NH_3 @ 22 GHz

$2.3\ 10^{-3}$ Hz/µG H_2O @ 22 GHz

Güsten et al. 1994

B-field: Zeeman splitting

In presence of B-field, hyperfine splitting of levels is modified: spectral line splits in 2, centered on primary component, with opposing pol

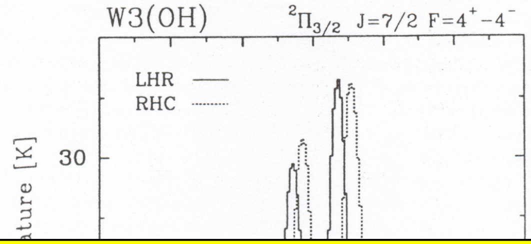

Measured values:

HI 21cm, OH 18cm: few μG (diffuse ISM; $n<100\ cm^{-3}$)

few μG (dark cloud envelopes; $n\sim10^3\ cm^{-3}$)

few μG (OH masing layers; $n\sim10^{7-8}\ cm^{-3}$)

H_2O 22GHz: 50mG (maser spots; $n\sim10^{10}\ cm^{-3}$)

$$\frac{\Delta\nu_{mag}}{\Delta\nu_{therm}} \approx 10^{-3}\left(\frac{B}{\mu G}\right)\left(\frac{T_k}{10K}\right)$$

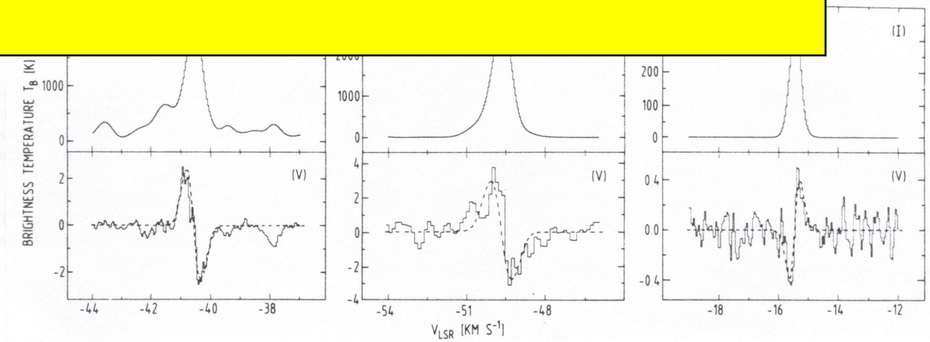

3.27 Hz/μG OH @ 1665 MHz

1.96 Hz/μG OH @ 1665 MHz

$7.2\ 10^{-4}$ Hz/μG NH_3 @ 22 GHz

$2.3\ 10^{-3}$ Hz/μG H_2O @ 22 GHz

Güsten et al. 1994

Results for Field Strength

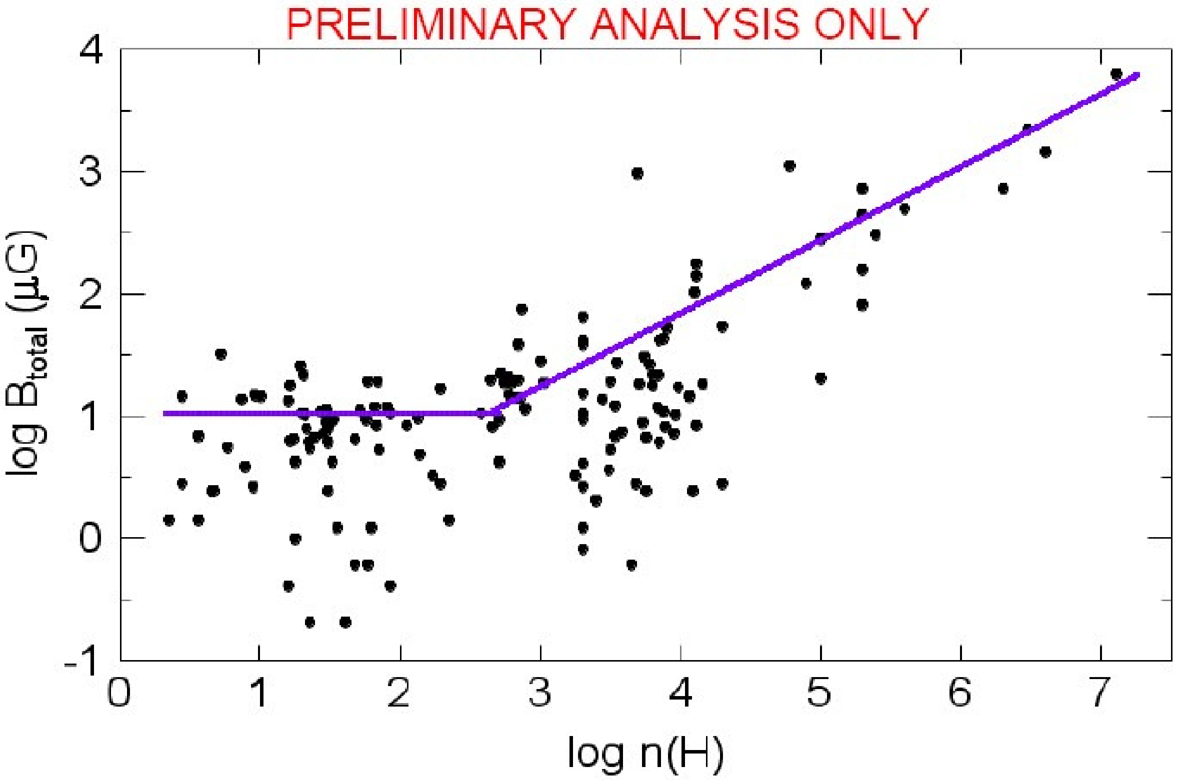

(Crutcher – IAU242, 2007)

Clump stability

Forces working on clumps:

- Clump (self-) gravity
- Clump turbulence (and thermal pressure)
- Interclump pressure
- Magnetic fields

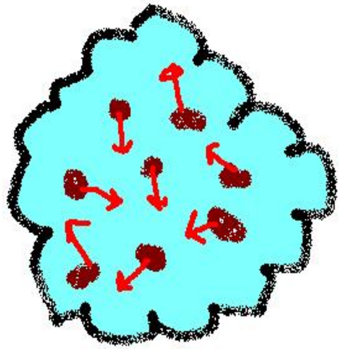

Clump virial theorem (e.g. Fleck 1988)**:**

$4\pi r^3 P = 3M_{CO}\sigma^2 - GM_{CO}{}^2/r + B^2/8\pi$

Expressed in pressures:

$P/k = \rho\sigma^2/k - GM_{CO}\rho/3rk + B^2/8\pi k$

$\mathbf{P_{ext}/k = P_{turb}/k + P_{grav}/k + P_{magn}/k}$

$P_{turb}/P_{grav} = \alpha = 126\ r[pc]\ \Delta v[kms^{-1}]^2/M_{CO} = M_{vir}/M_{CO}$: virial parameter

$P_{magn}/k = 2.9 \times 10^4$ Kcm^{-3} for 10μG

Interclump pressure (self-gravity GMC): $P_{ext}/k = 1.7 \times 10^4 - 5.9 \times 10^4$ Kcm^{-3}

Clump pressure ratios

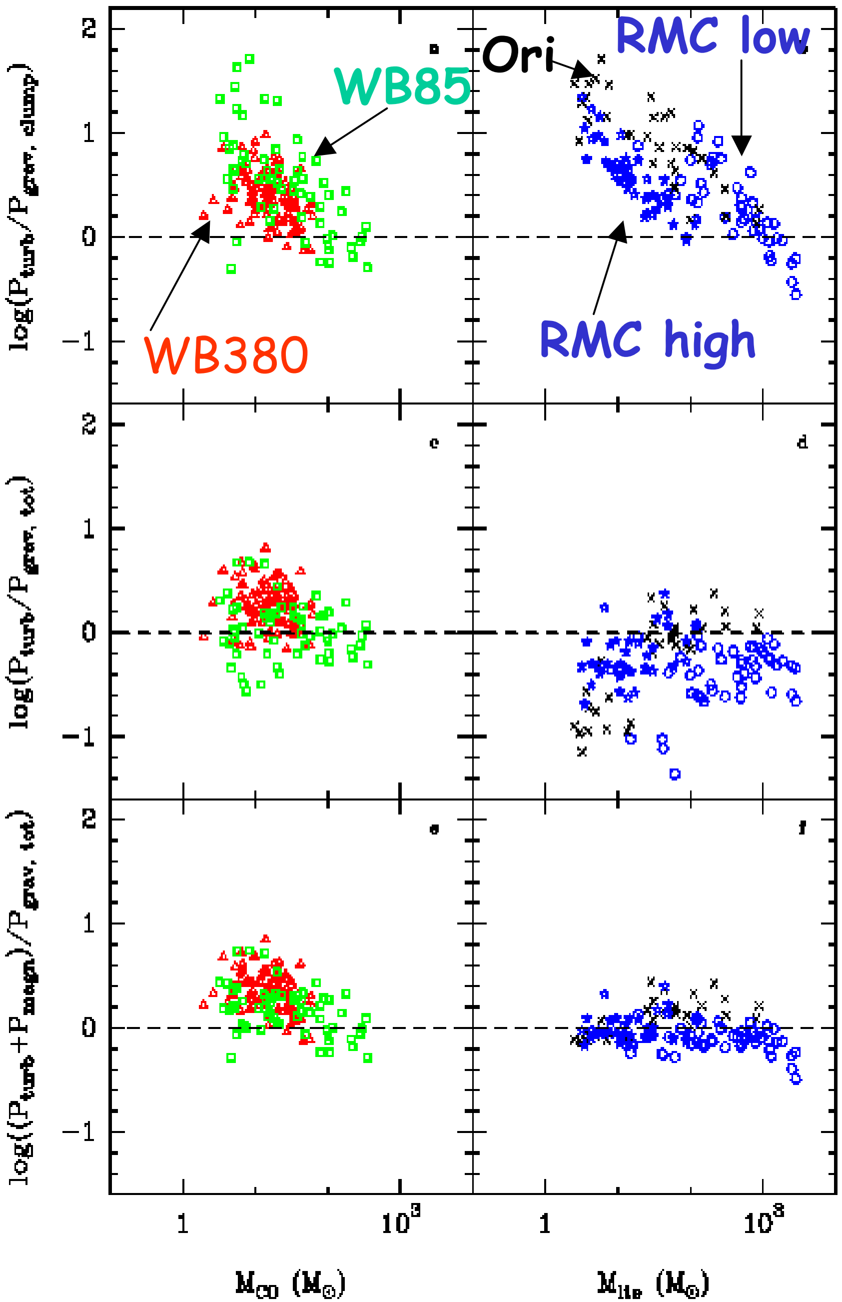

Turbulence
&
gravity

Turbulence
&
total gravity

Turbulence,
total gravity
&
magnetic field
pressure

Brand et al. 2001

Formation of stars of high and low mass

Two mechanisms:

Accretion onto the protostar:

Static envelope: $n \propto R^{-2}$

Infall zone: $n \propto R^{-3/2}$

$\mathbf{t_{acc}} = M_* /(dM_{acc}/dt)$

Contraction of the protostar:

$\mathbf{t_{KH}} = GM^2/R_* L_*$

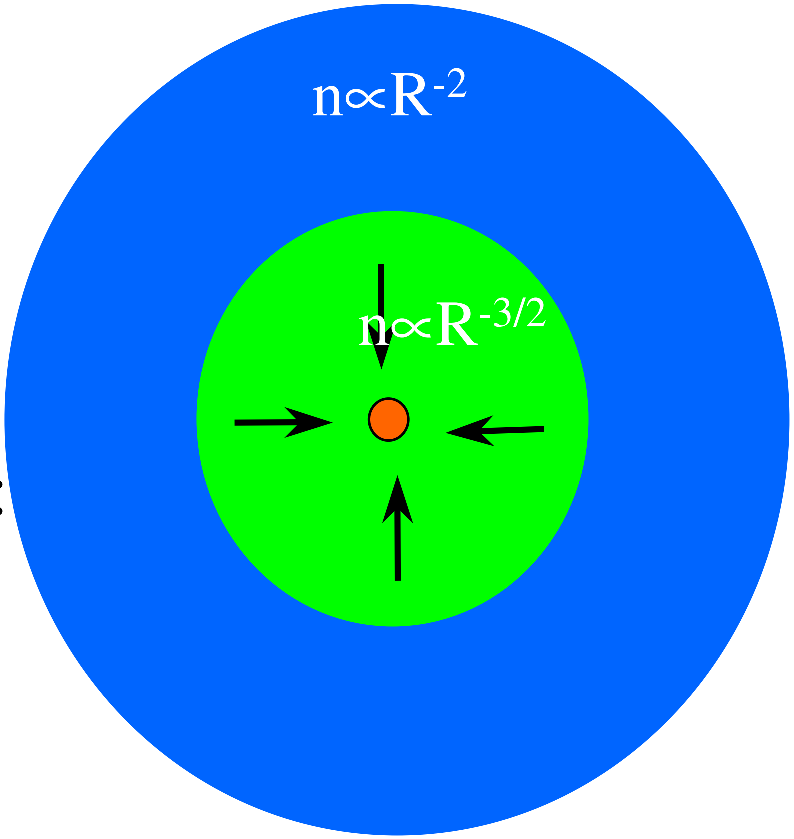

- Stars > 8 M_{sun}: $t_{KH} > t_{acc}$
- Stars < 8 M_{sun}: $t_{KH} < t_{acc}$

➔ The high-mass stars form while still accreting

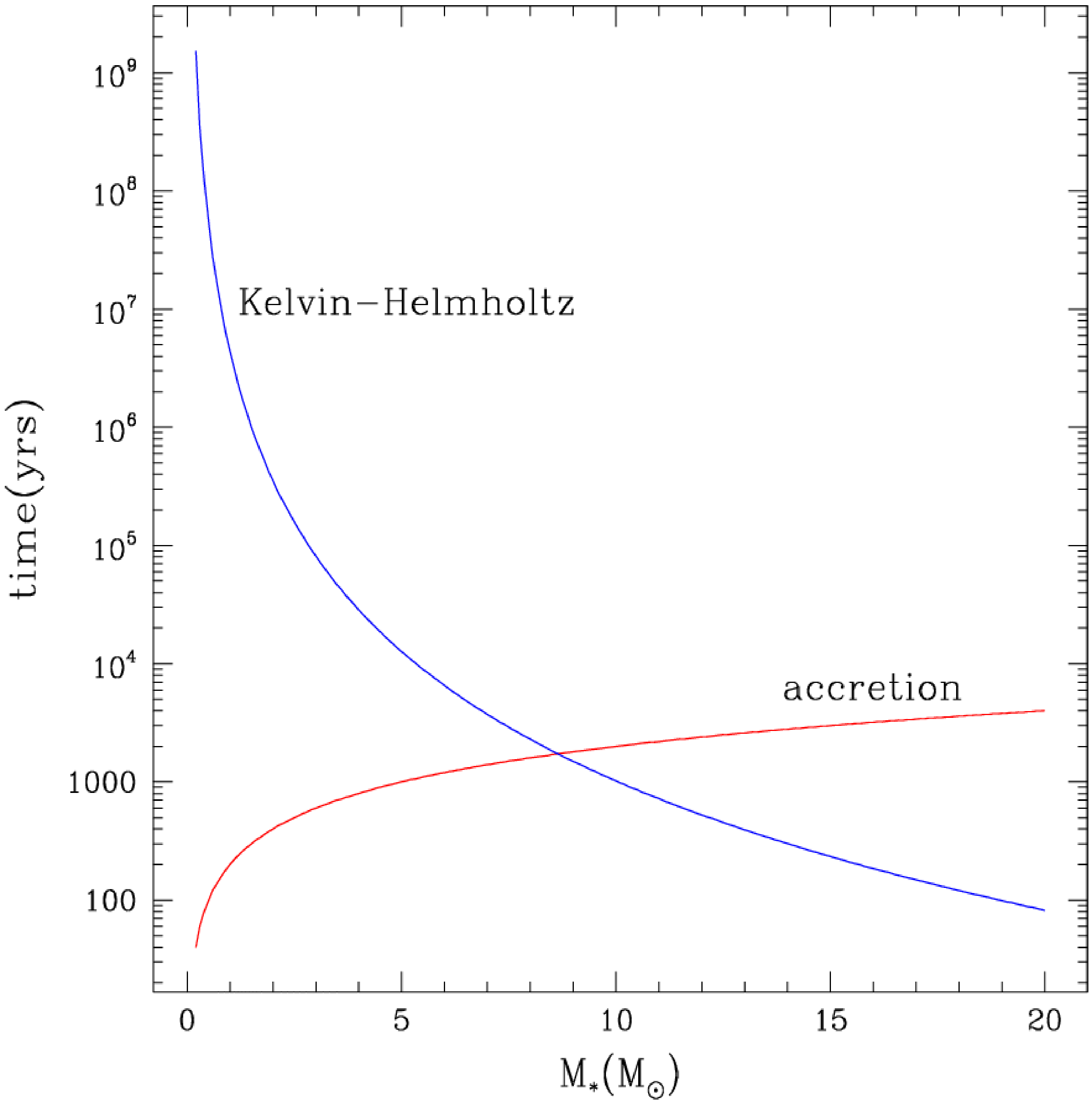

Kelvin−Helmholtz
accretion
time(yrs)
10^9
10^8
10^7
10^6
10^5
10^4
1000
100
0
5
10
15
20
M*(M⊙)

Formation of stars of high and low mass

Two mechanisms:

Accretion onto the protostar:

Static envelope: $n \propto R^{-2}$

Infall zone: $n \propto R^{-3/2}$

$\mathbf{t_{acc}} = M_* / (dM_{acc}/dt)$

Contraction of the protostar:

$\mathbf{t_{KH}} = GM^2/R_* L_*$

- Stars $> 8\ M_{sun}$: $t_{KH} > t_{acc}$
- Stars $< 8\ M_{sun}$: $t_{KH} < t_{acc}$

➔ The high-mass stars form while still accreting

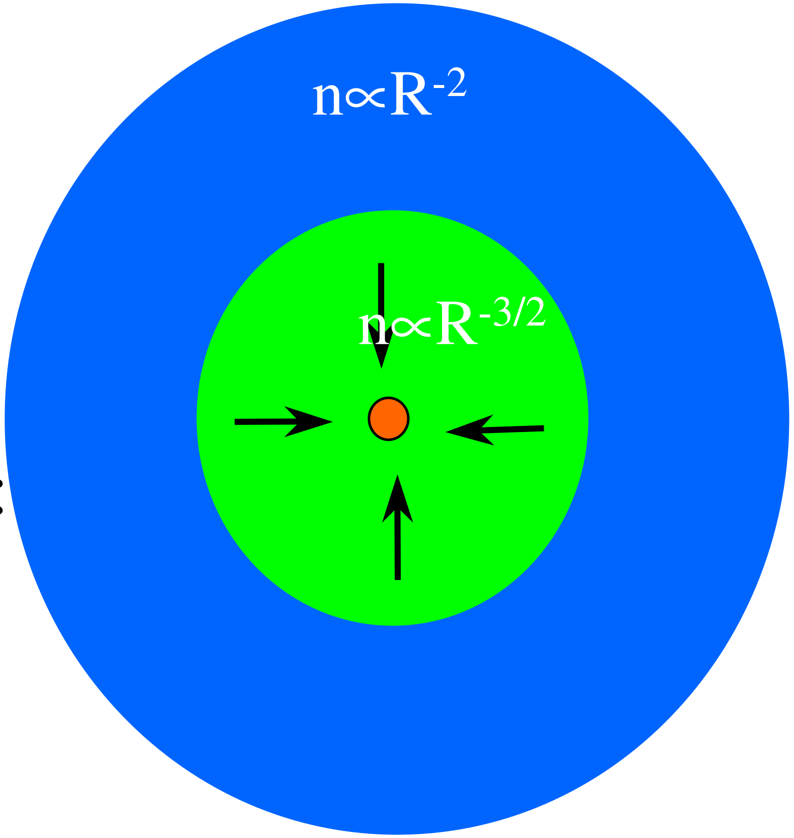

Palla & Stahler (1990)

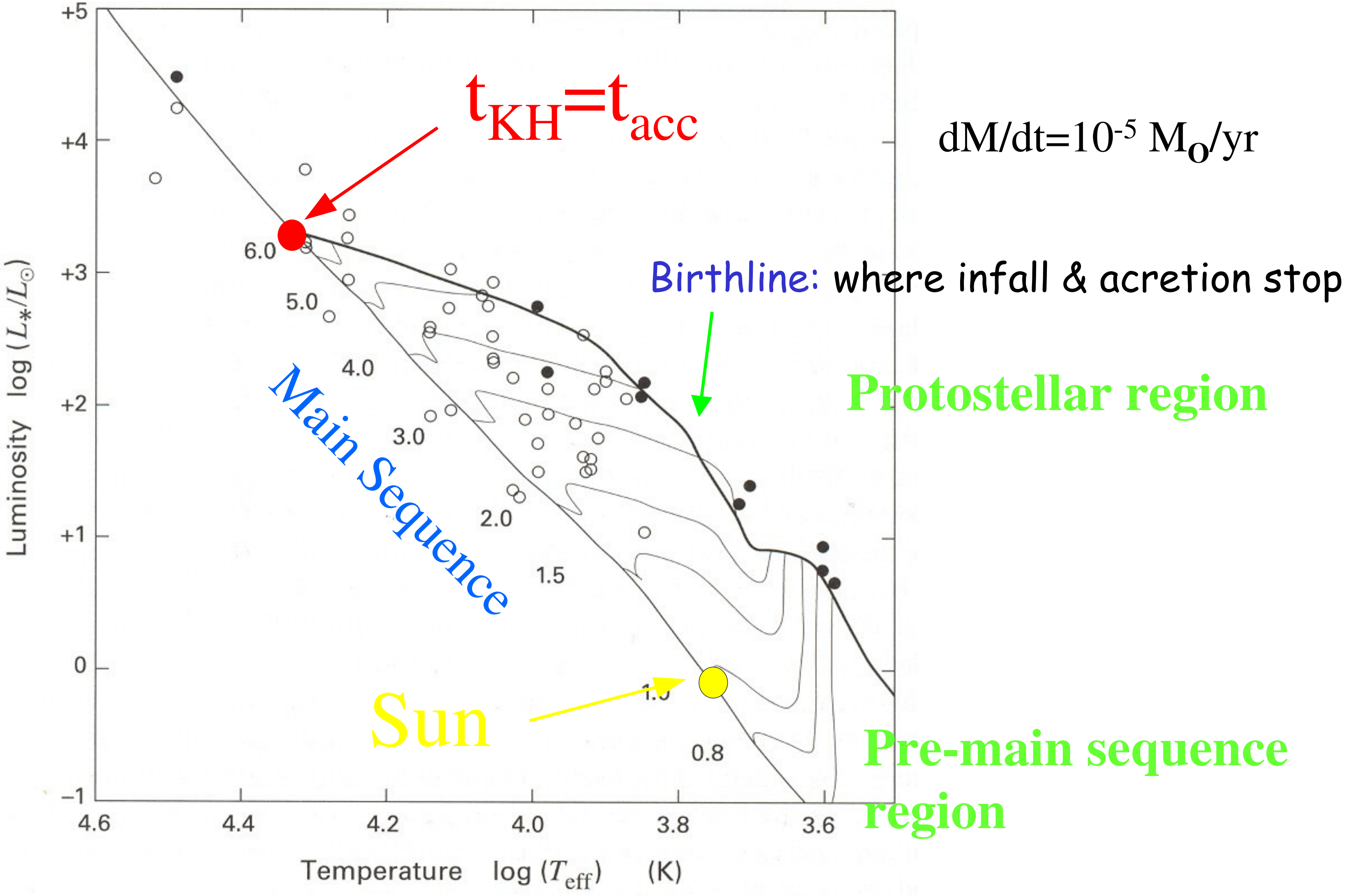

Normal star: evolutionary status determined by location HRD:
L, T_{eff}

Embedded YSOs: associated with natal gas & dust
Cannot be placed in HRD

Protostellar stage: circumstellar gas & dust:
absorbs and reprocesses radiation embedded object
Has extent >> stellar photosphere → dust has wide range of T
SED wider than single-T BB;
shape SED depends on nature & distribution of circumstellar material

More evolved object (pre-ms, ms): envelope, disk almost gone
Shape of SED is f(evolutionary state)

Observationally:
YSOs fall into 4 classes, based on shape of SED

Stars < $8M_O$

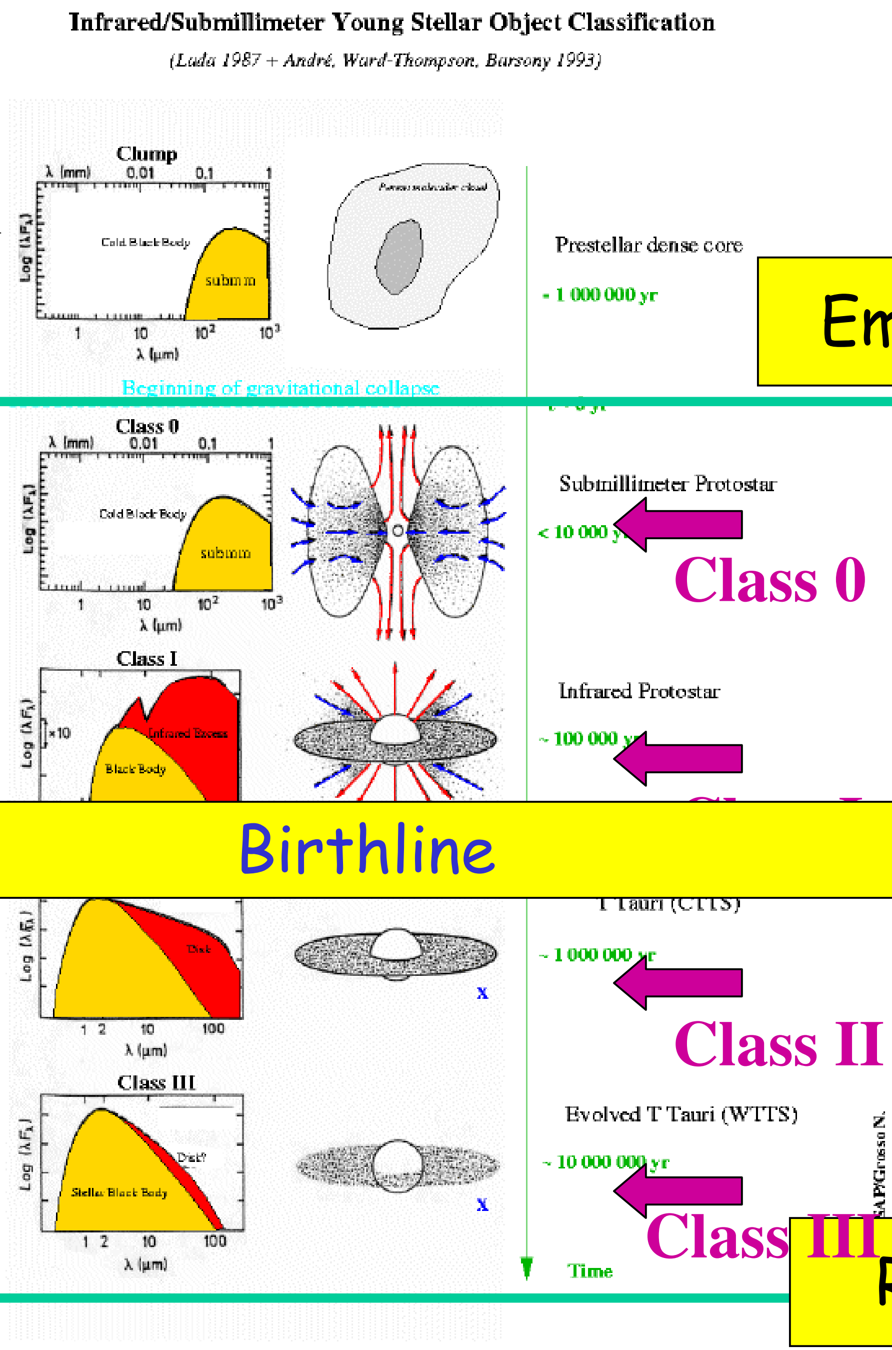

sub-mm

far-IR

near-IR

optical +NIR

optical

unstable isothermal clump

Embedded phase

accretion onto protostar

Class 0

formation of disk & outflow

Birthline

disk without accretion

Class II

protoplanetary disk

Class III

Revealed phase

Embedded phase: protostars

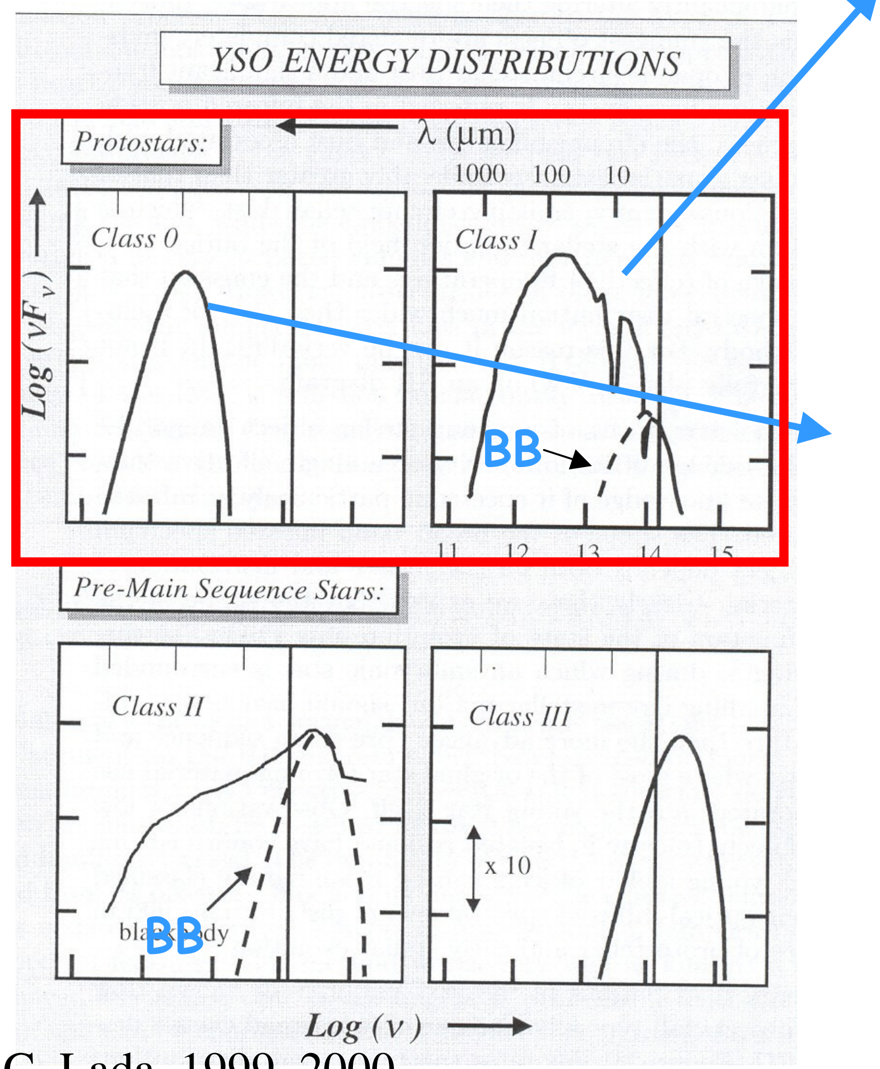

C. Lada, 1999, 2000

Class I:

- -SED broader than single-T BB
- -At λ>2μm SED rises with λ:
  huge IR-excess
- -Deeply embedded; detected in NIR (freq. assoc'd with RNe)
- -Often associated with outflows
- -$M_{circumst}$(r<1000AU) << M_*
- -Age ca. 1-5 x 10^5 yrs

Class 0:

- -Much more extincted & embedded;
- -SED peak in submm;
  not detected at λ<20μm
- -SED similar to BB at T=20-30K
- -All have energetic, v. highly collimated outflows.
- -$M_{circumst}$(r<1000AU) $\approx$ M_*
- -Constitute 10% of embedded sources
- -Age ca. 10^4 yrs

Protostellar nature embedded YSOs: evidence

Protostar: objects in process of accumulating into star-like configuration the bulk of the material they will contain as ms stars

1) SED can be modeled as embryonic stellar core + circumstellar disk + massive gas & dust envelope with density structure as predicted by theory for ellar cloud cores.

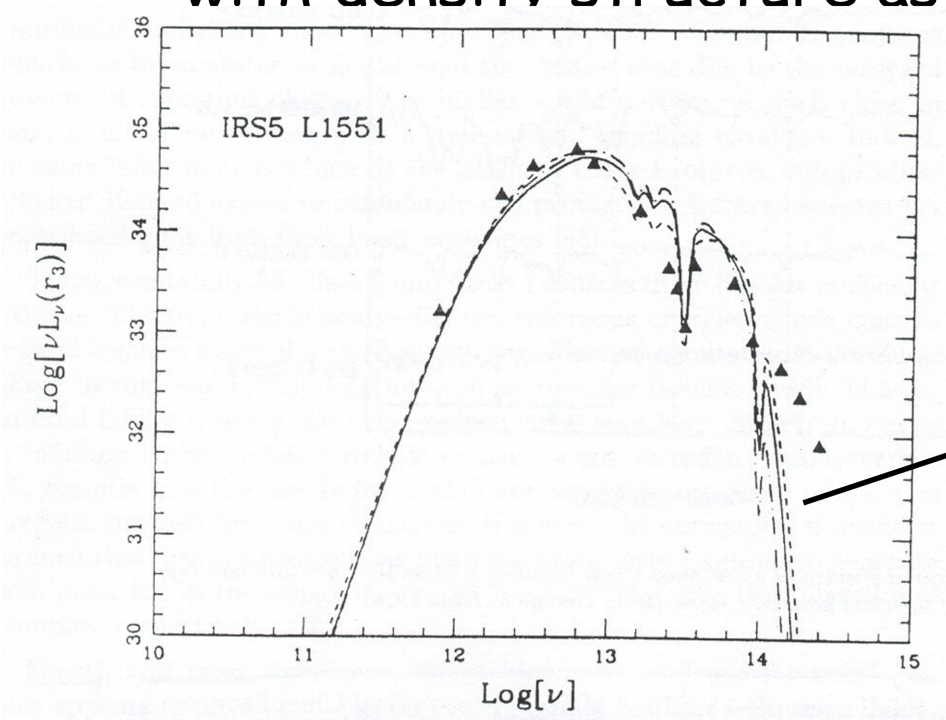

fits: rotating-collapsing isothermal protostellar models

Mass infall rate ~ 5 x 10^{-6} $M_\odot$ /yr

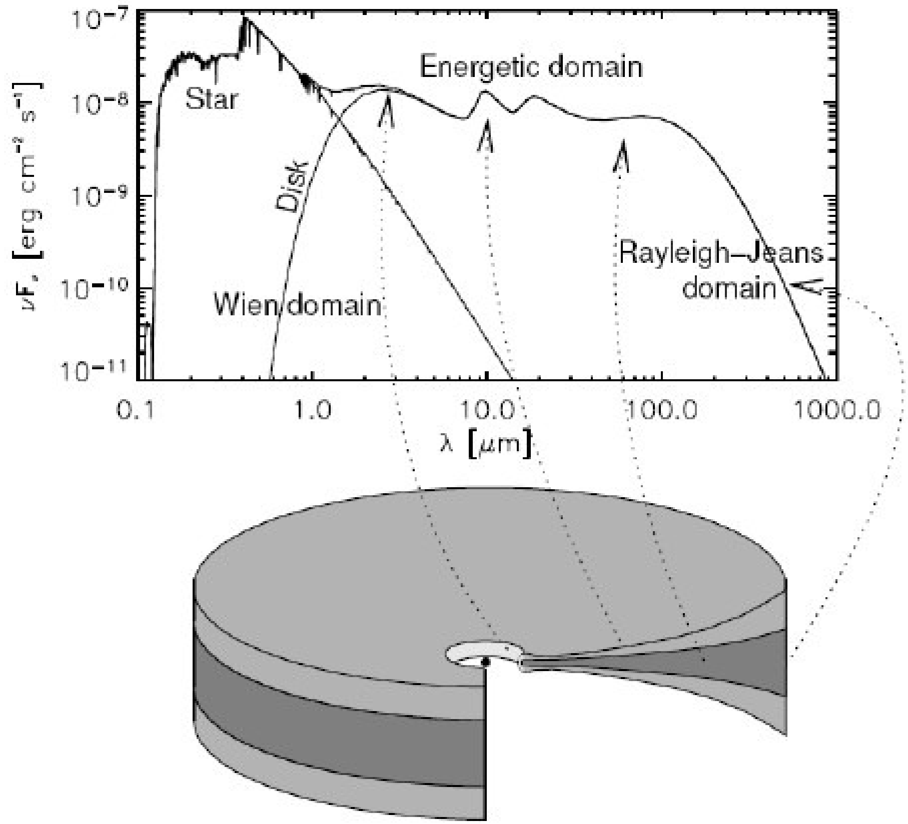

Figure 1.2: From Dullemond et al. (2006). Build-up of the SED of a flaring circumstellar disk and the origin of various components: the near infrared bump is supposed to originate in the puffed-up inner rim, the infrared dust features (as the silicate ones between 10μm and 20μm) from the warm surface layer, and the underlying continuum from the deeper and cooler disk regions. Typically the near and mid-infrared emission comes from small radii, while the far-infrared and the millimeter emission come from the outer disk regions.

Isella 2006: Dullemond et al. 2006

Protostellar nature embedded YSOs: evidence

1) SED can be modeled as embryonic stellar core + circumstellar disk + massive gas & dust envelope with density structure as predicted by theory for rotating, infalling protostellar cloud cores.

2) Featureless spectrum, requires hot dust at << 1 AU to provide additional cont. flux to 'veil' absorption lines. Infall models acount for that.

Protostellar nature embedded YSOs: evidence

1) SED can be modeled as embryonic stellar core + circumstellar disk + massive gas & dust envelope with density structure as predicted by theory for rotating, infalling protostellar cloud cores.

2

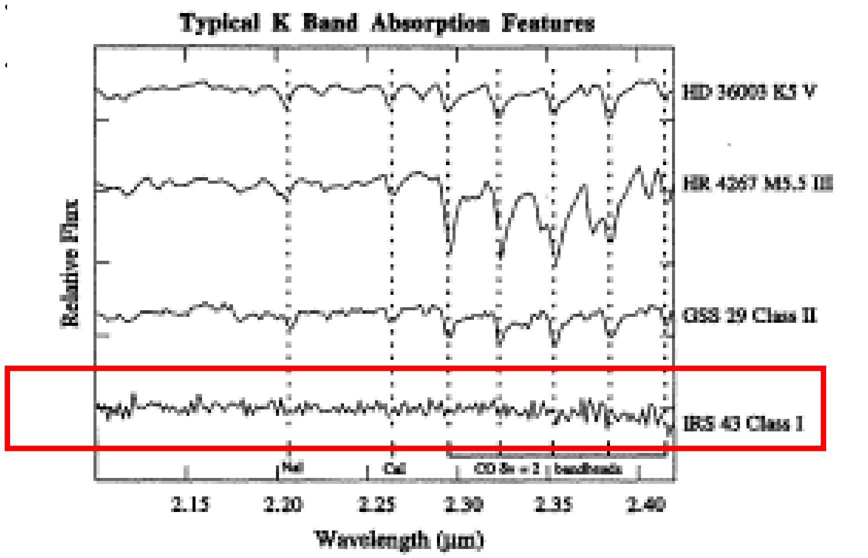

es hot dust at $\ll$ 1 AU
ıx to 'veil' absorption
· that.

FIG. 1. *K*-band absorption features. The indicated Na I, Ca I, and CO features are commonly seen in the spectra of late-type stars such as the typical MK standards HD 36003 and HR 4267. Class II (and III) YSOs (such as GSS 29 shown) usually show similar features, but Class I YSOs (such as IRS 43 shown) usually do not show any early- or late-type features. The data shown are enlarged subregions of spectra presented in Appendix, but baseline continuum slopes have been removed.

Greene & Lada, AJ 1996

Protostellar nature embedded YSOs: evidence

1) SED can be modeled as embryonic stellar core + circumstellar disk + massive gas & dust envelope with density structure as predicted by theory for rotating, infalling protostellar cloud cores.

2) Featureless spectrum, requires hot dust at << 1 AU to provide additional cont. flux to 'veil' absorption lines. Infall models acount for that.

3) Only viable source for outflow energy is gravity (from infall).

4) Direct kinematic evidence for infall motions found in Class 0 sources!

Protostellar infall

Detecting infall from opt. thick line

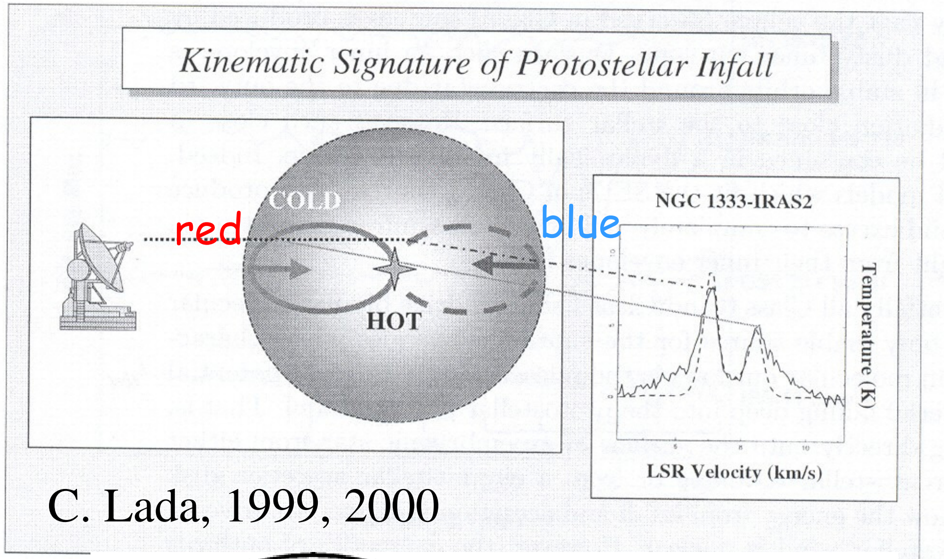

C. Lada, 1999, 2000

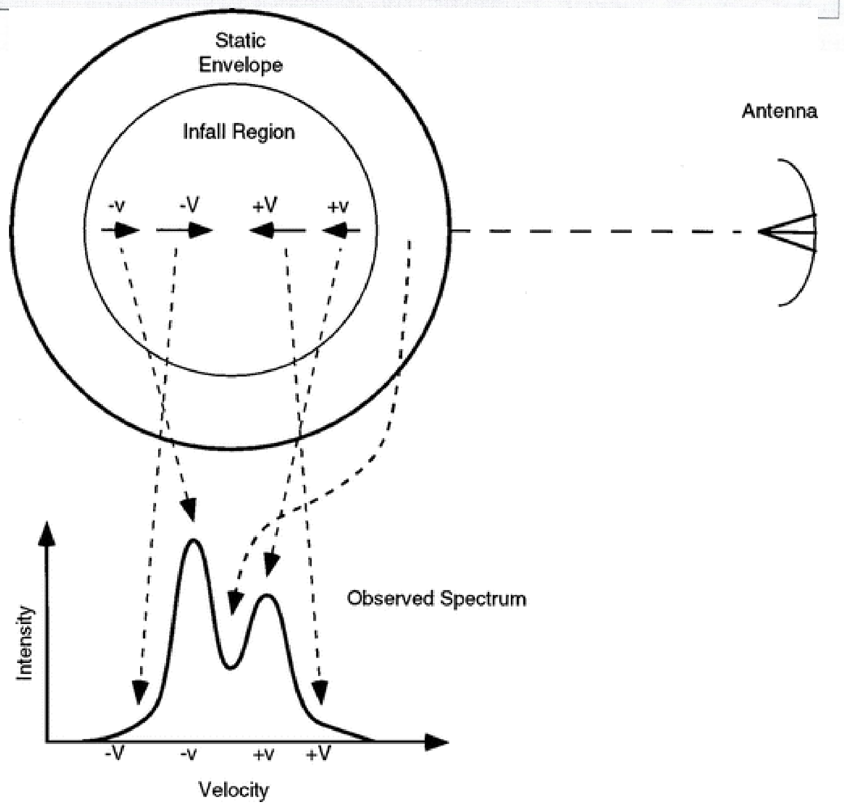

B335; Zhou et al. 1993

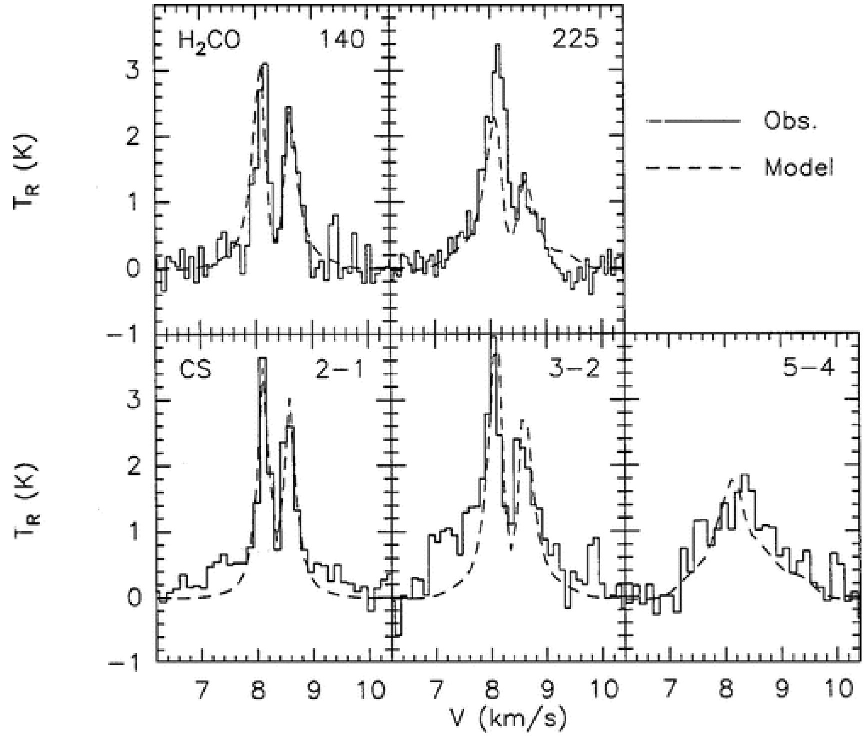

Revealed phase: Pre-ms stars

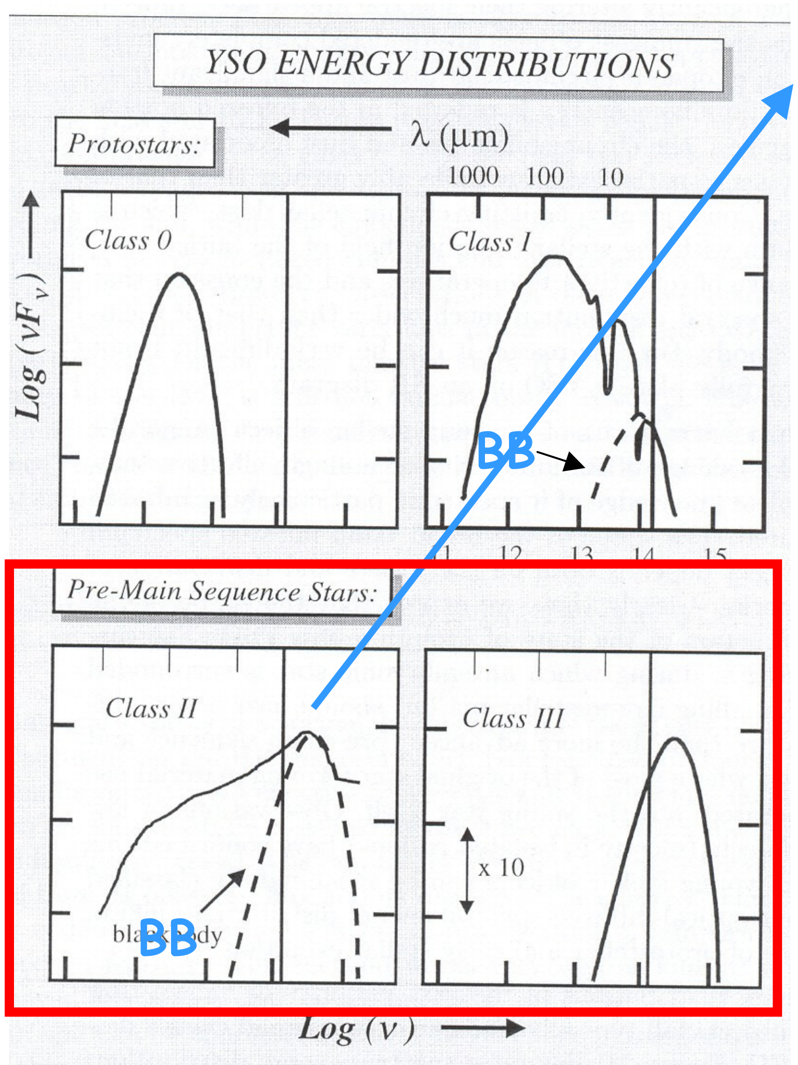

Class II:

- -SED peaks in visible or NIR
- -SED broader than single-T BB
- -At λ>2μm SED falls with λ (power-law): IR-excess, but smaller than Class I
- -Disk, but no massive envelope
- -$M_{disk} \approx 0.01\text{-}0.1\ M_\odot$
- -Accretion rate ~ $10^{-8}\ M_\odot$/yr
- -in SFRs: 10x more than ClassI
- -in optical, ClassII are CTTS

SED can be fitted with model of disk with T-gradient, reprocessing and reradiating light from central star

C. Lada, 1999, 2000

ClassII model fit

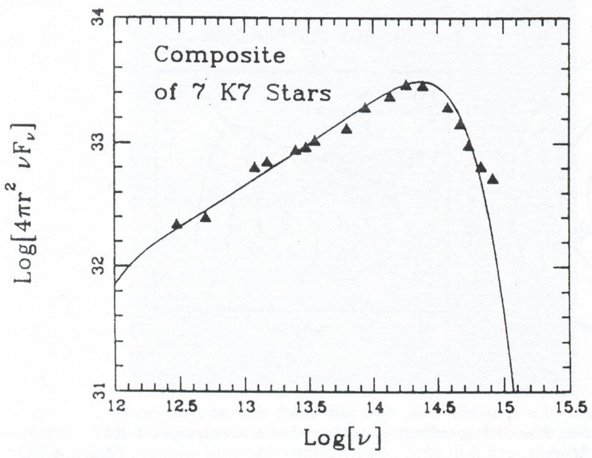

Figure 15. The composite SED of seven Class II stars along with that (solid line) of a model circumstellar disk. (From Adams, Lada and Shu 1988).

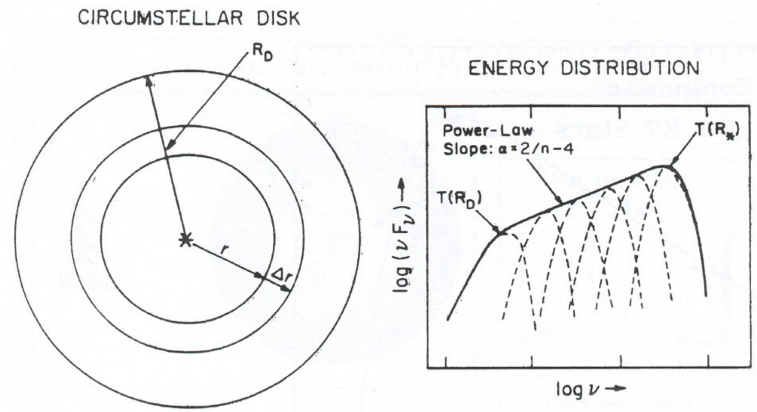

Figure 16. Schematic diagram of a spatially thin, optically thick disk and its emergent spectral energy distribution. The disk spectrum is composed of a superposition of blackbodies of varying temperature.

Disk: each annulus has area $2\pi R\Delta R$ and radiates as BB with $T(R)$
SED is superposition of series of BB-curves
If $T(R) \sim R^{-n}$, then (Wien's law) max. emission at $\nu \sim T(R) \sim R^{-n}$.
Luminosity each annulus: $L_\nu d\nu = 2\pi R\Delta R\sigma T(R)^4 \sim R^{2-3n} d\nu \sim \nu^{3-2/n}$.

For a SED, $\nu L_\nu \sim \nu^{4-2/n}$.

C. Lada, 1999, 2000

Revealed phase: Pre-ms stars

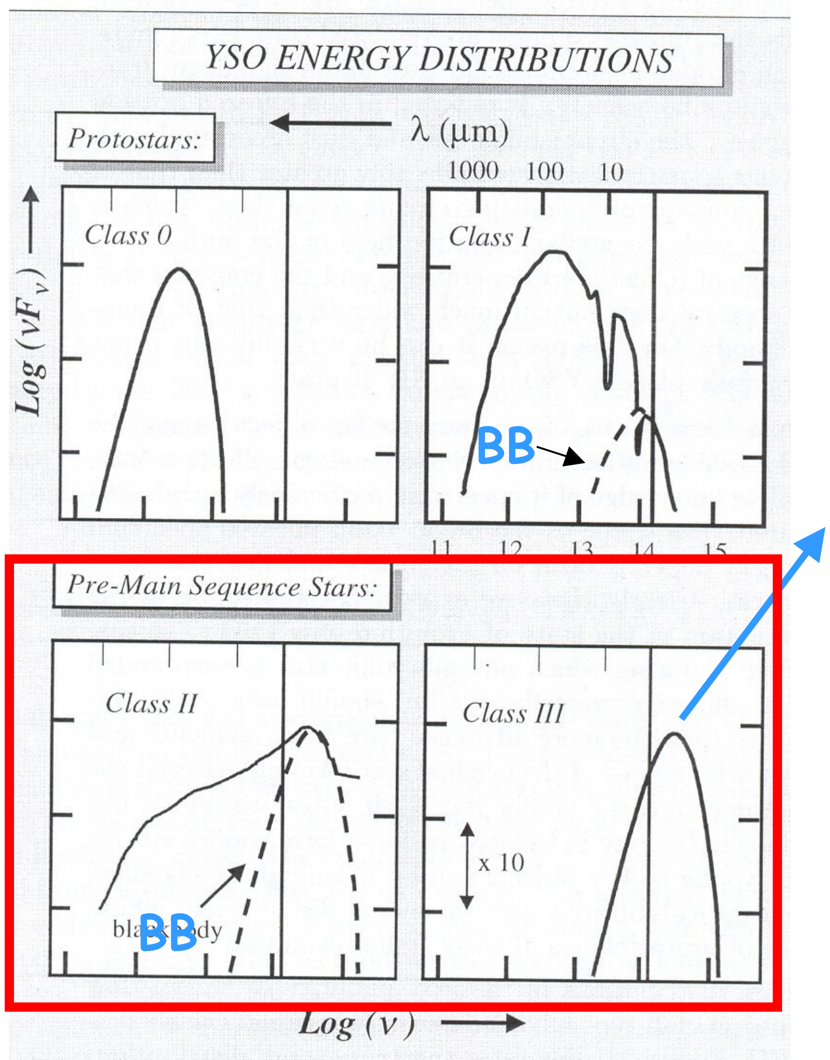

Class III:

-SED peak in visible/NIR

-SED similar to single-T BB; interpreted as photospheres of young stars with extinction.

-No significant amounts circumstellar gas, dust

-ClassIII are WTTS

-Age ca. 10^6 - 10^7 yrs

No IR excess, confused with fore- & background stars in SFRs. But are X-ray sources.

C. Lada, 1999, 2000

Evolutionary sequence low-mass YSOs

Evolution Class 0 $\Rightarrow$ I $\Rightarrow$ II:
requires removal circumstellar material in infalling envelope

Evolution Class II $\Rightarrow$ III:
Requires clearing of circumstellar disk

Total accretion: NO – because SFE is very low ($M_* \ll M_{core}$)

Therefore: very early on cloudy material physically removed
Most likely by bipolar outflows, originating from stellar wind
(virtually all Class 0,I drive molecular outflows).

A protostar can only gain mass if it loses mass at same time

Disk lifetimes

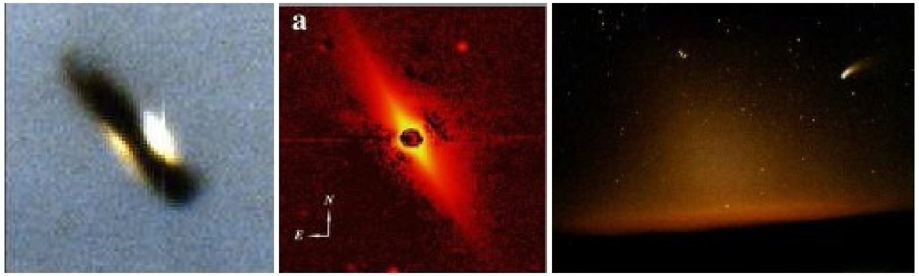

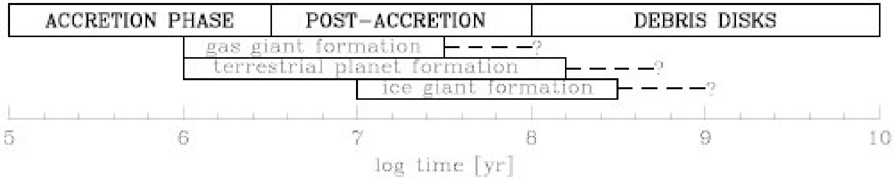

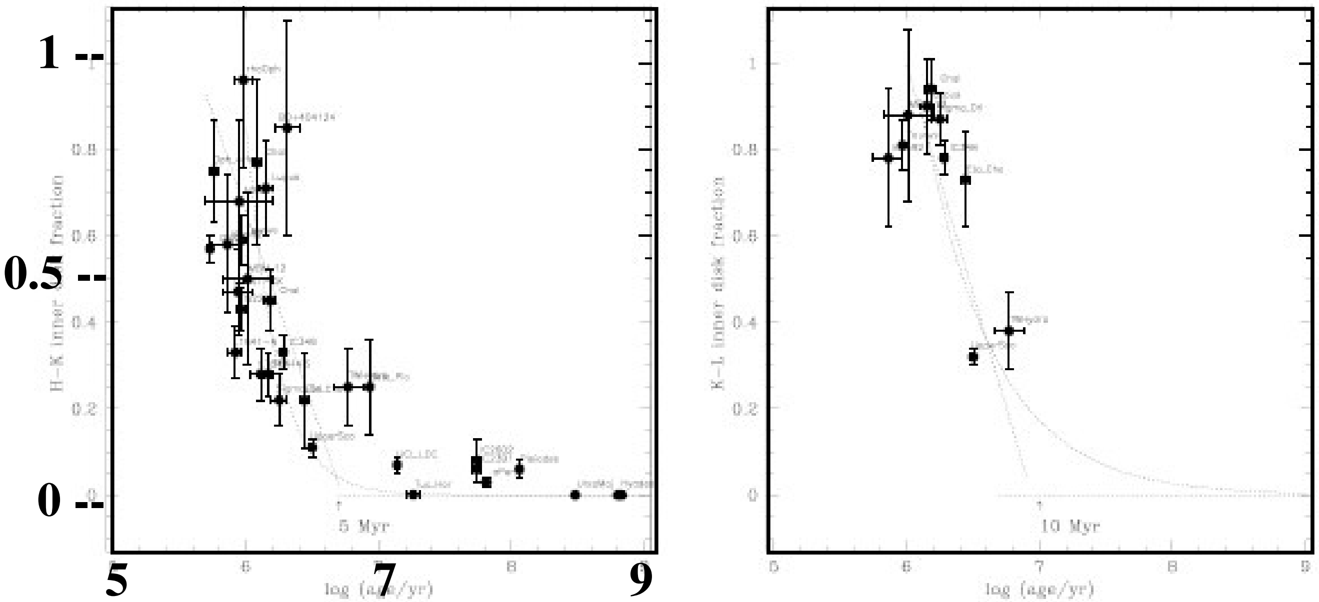

Disk fraction vs. log(cluster age) for ca. 3500 stars, 0.3-1 $M_\odot$

Hillenbrand 2006

YSOs: IR colour-colour diagram

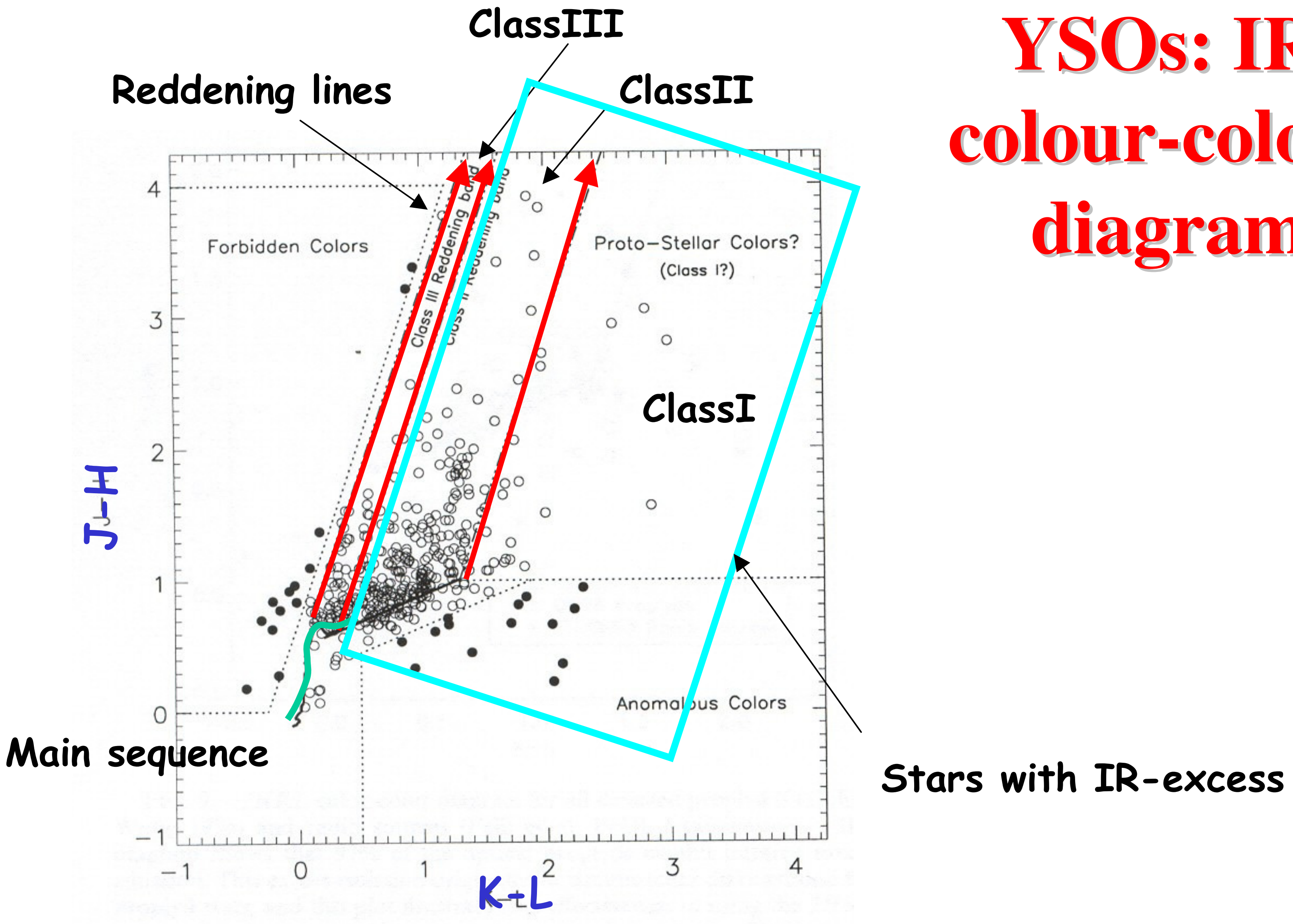

Disks… with HST (IR)

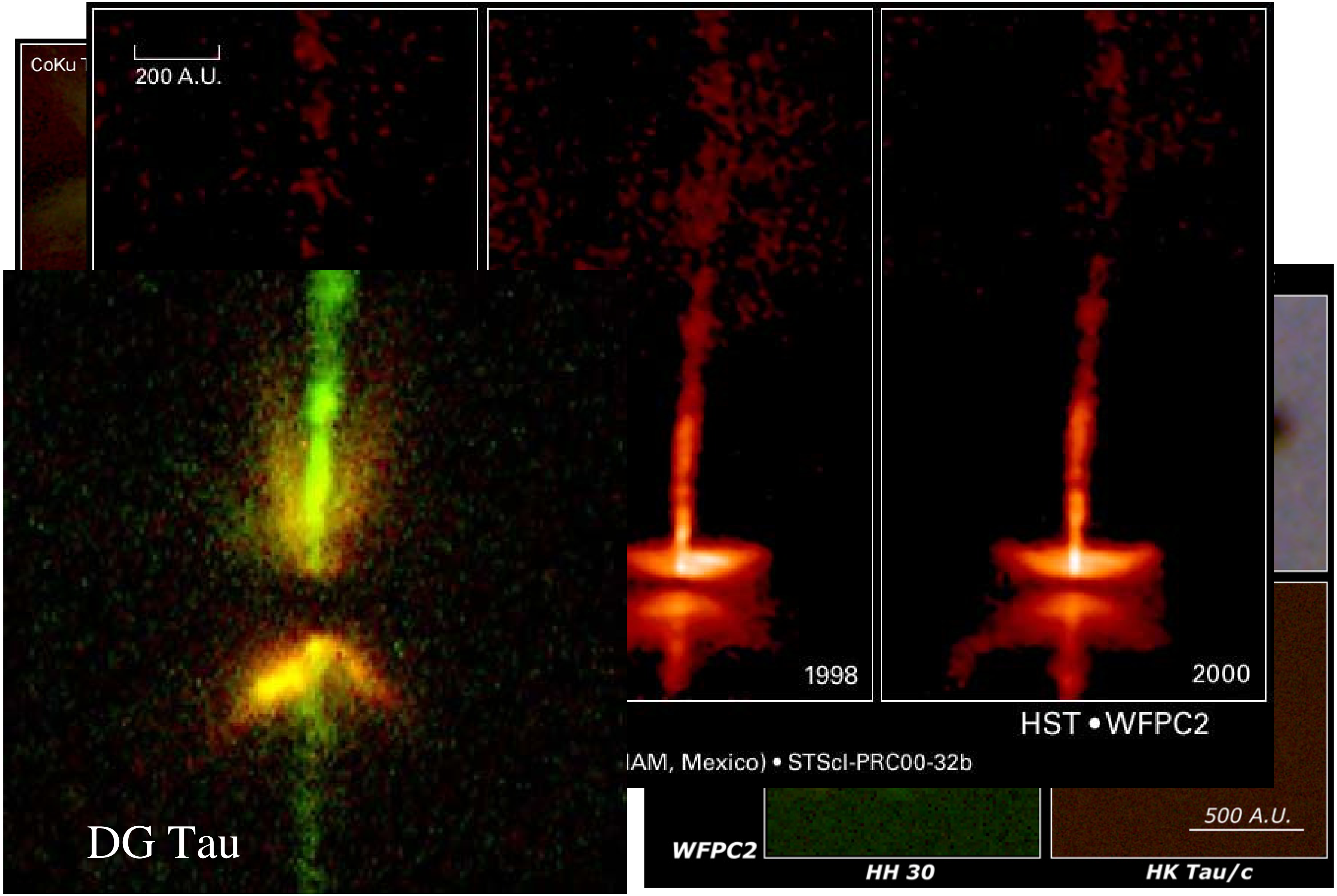

Disks… in mm-continuum

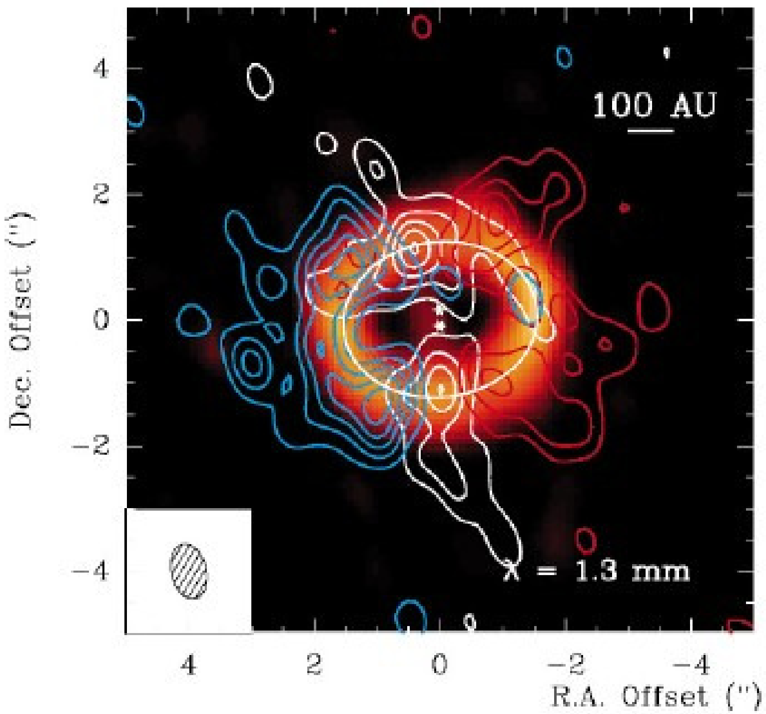

GG Tau; Guilloteau et al., 1999

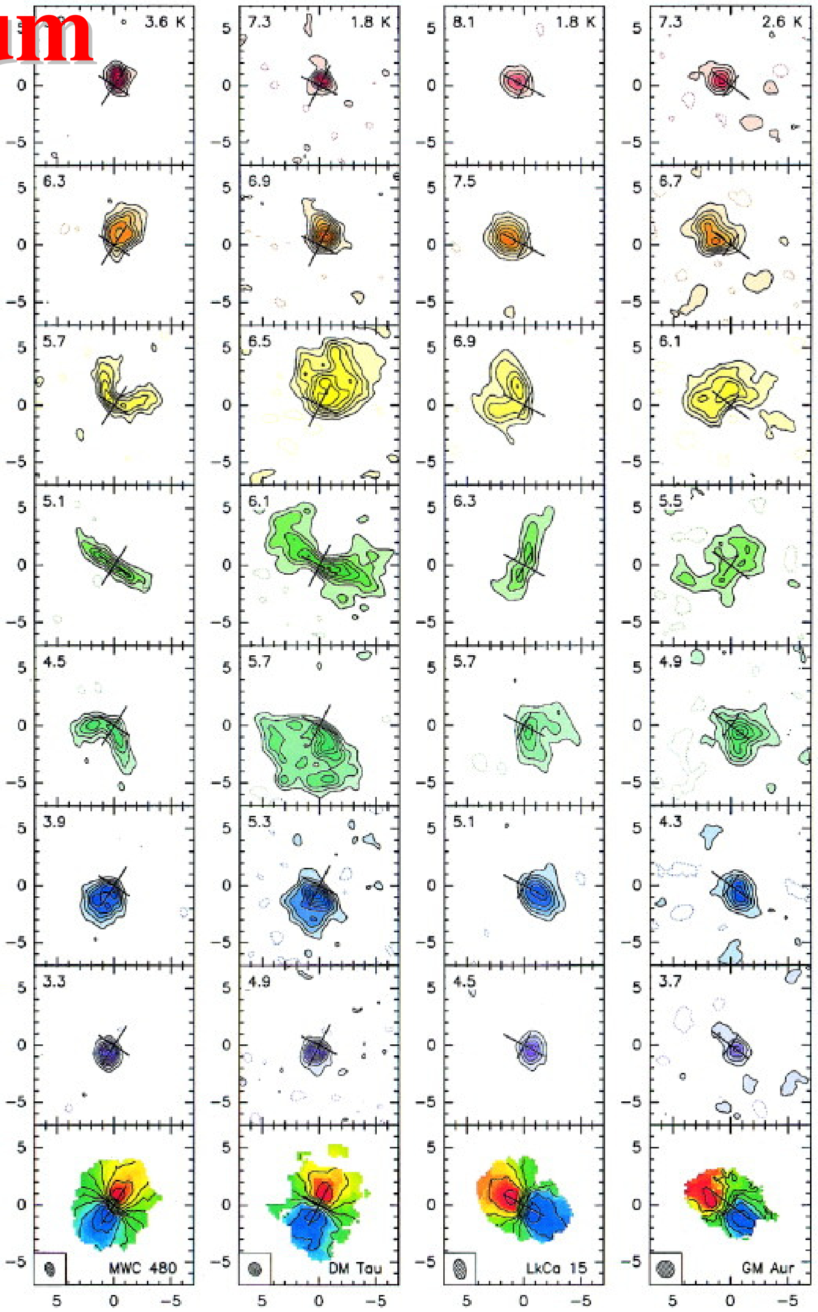

Simon et al., 2000

Embedded Outflow in HH 46/47

Spitzer Space Telescope • IRAC

Inset: visible light (DSS)

NASA / JPL-Caltech / A. Noriega-Crespo (SSC/Caltech)

ssc2003-06f

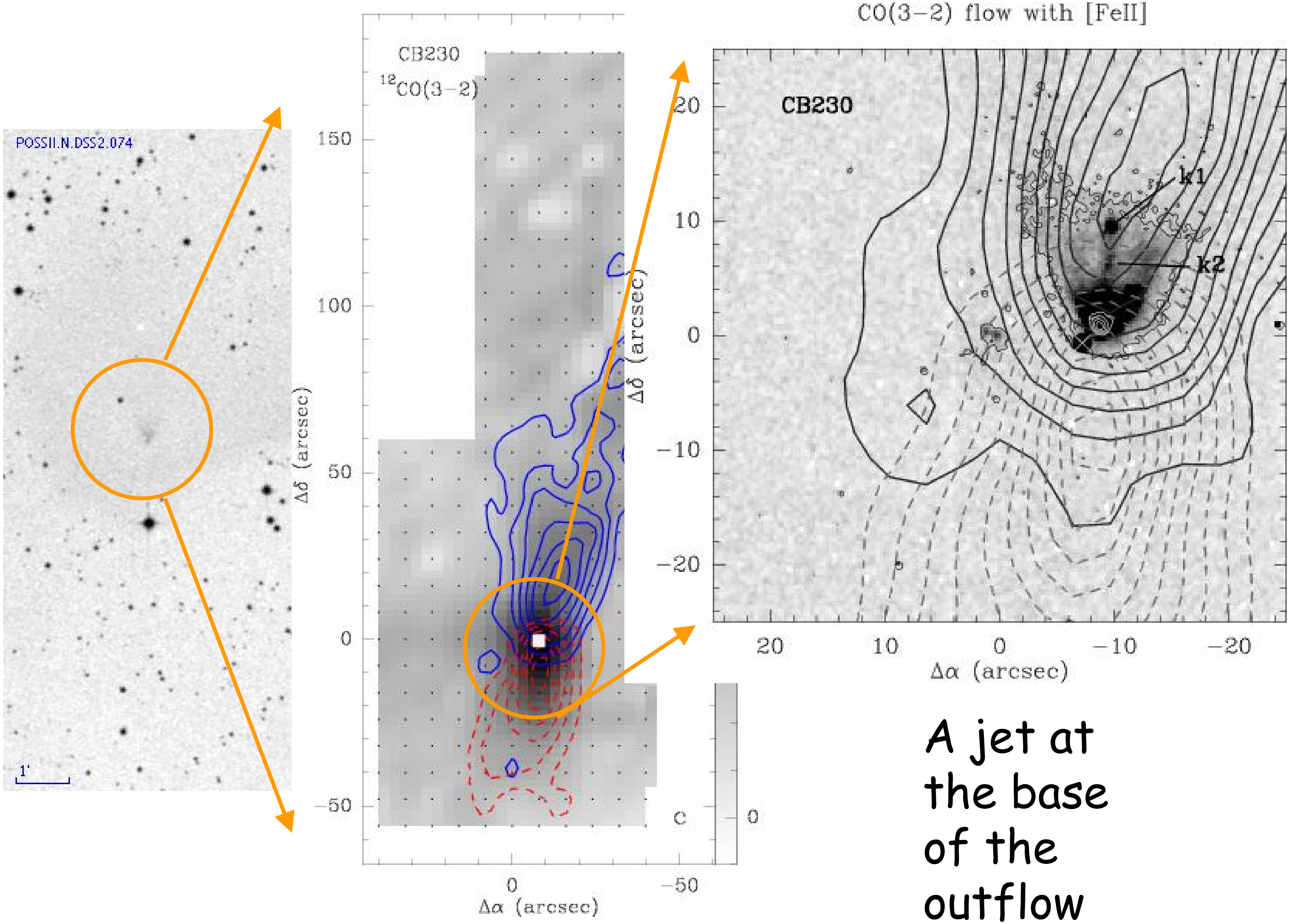

A jet at the base of the outflow

Brand et al., A&A 2007 (in prep.)

Two-level system

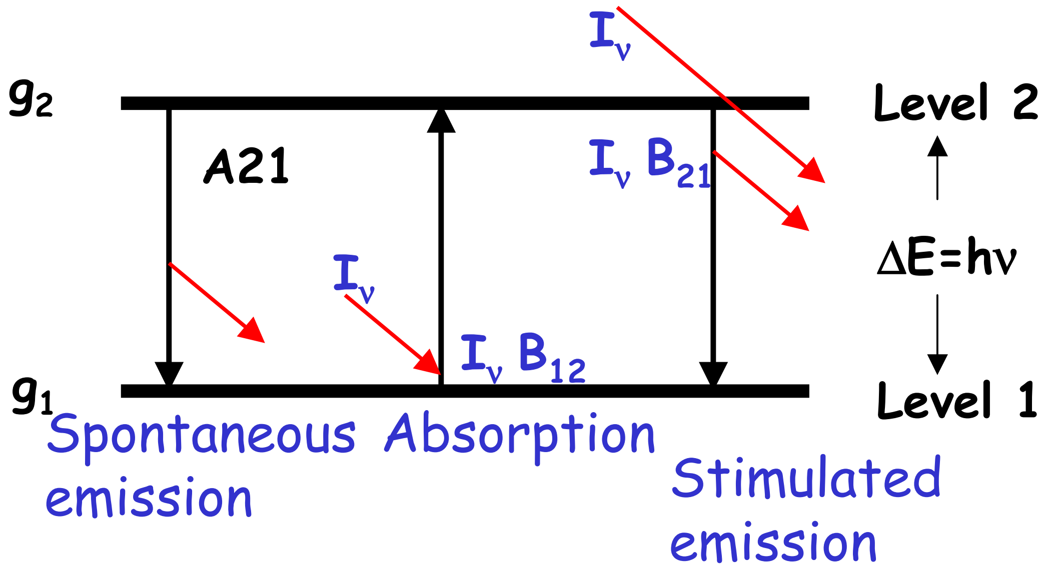

$$g_1 B_{12} = g_2 B_{21}\ ;\ A_{21} = (2h\nu^3/c^2)\ B_{21}$$

$$n_2/n_1 = (g_2/g_1)\exp(-\Delta E/kT_{ex})$$

$$n_2/n_1 < 1$$

Maser

$n_2 > n_1$: population inversion

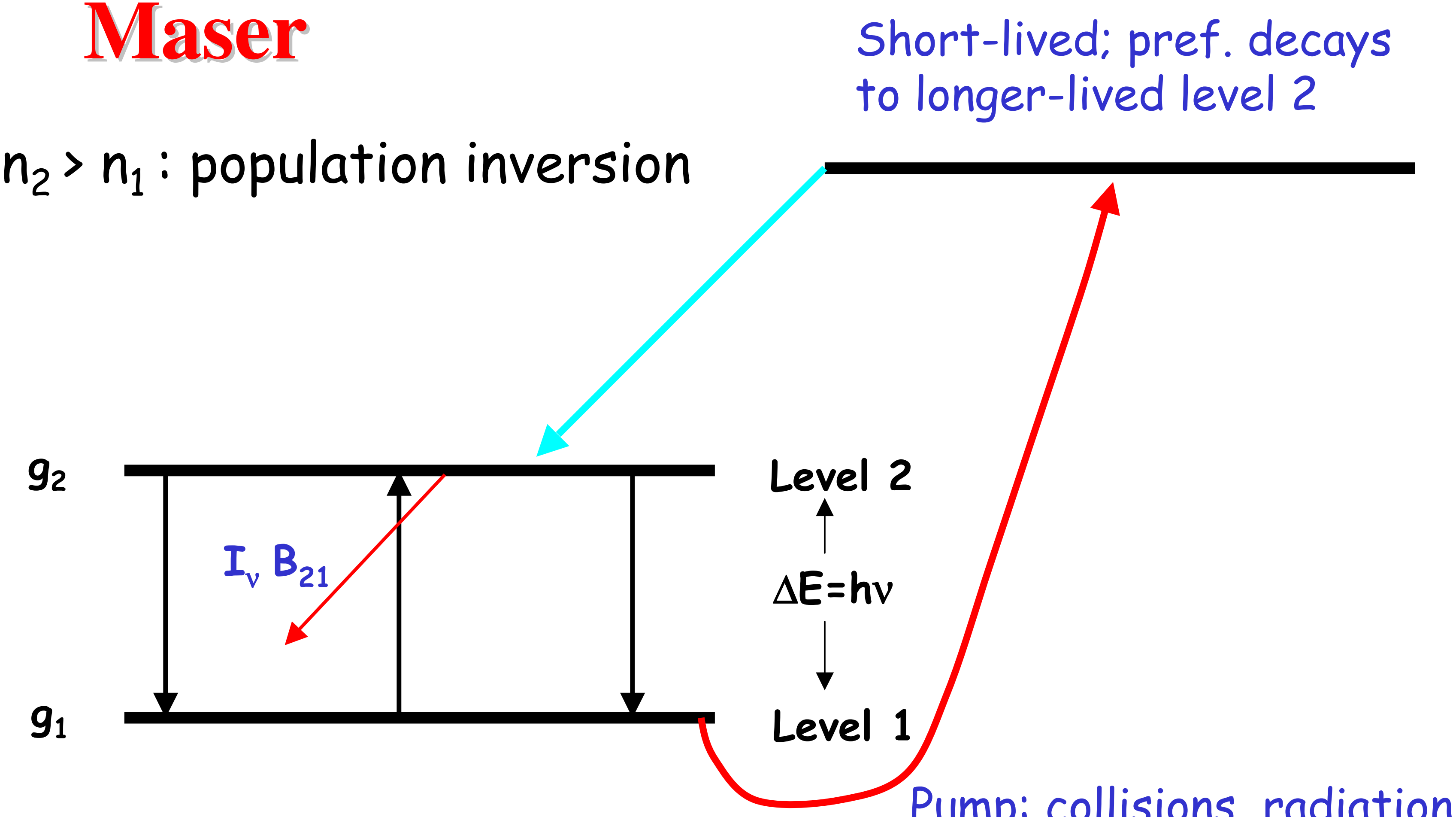

$$n_2 / n_1 = (g_2 / g_1) \exp(- \Delta E / kT_{ex})$$

$n_2 > n_1$: $T_{ex} < 0$

In region where mol's have same velo:
avalanche of induced emission

Energy levels H_2O

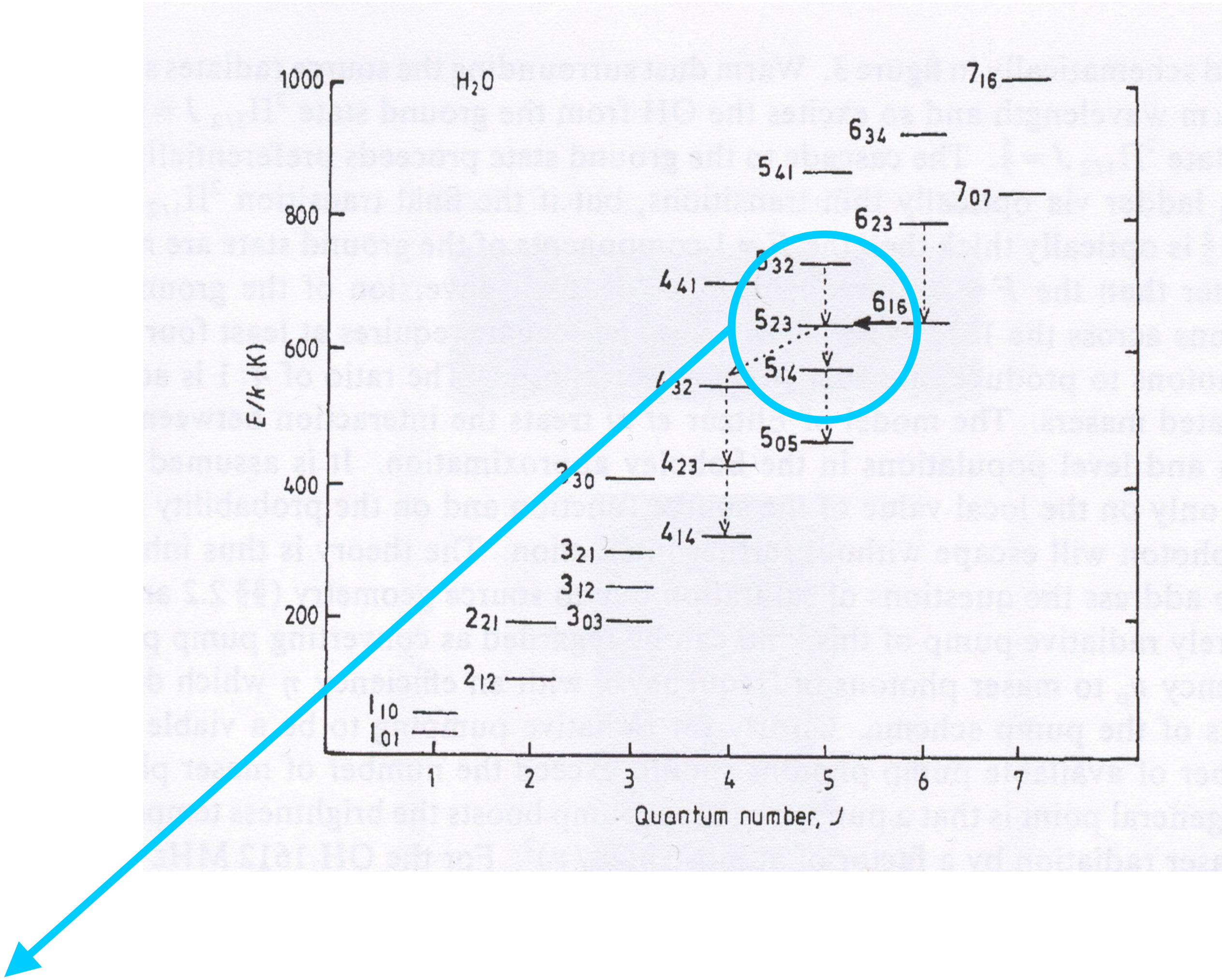

$6_{16} \rightarrow 5_{23}$ at 22 GHz (1.35 cm)

Kinematics of the masing gas

Star formation theory ∈ two main kinds of motions expected:

1) rotation and contraction (accretion disk); 2) expansion (jet/outflow system)

Kinematical Models

Conical Outflow

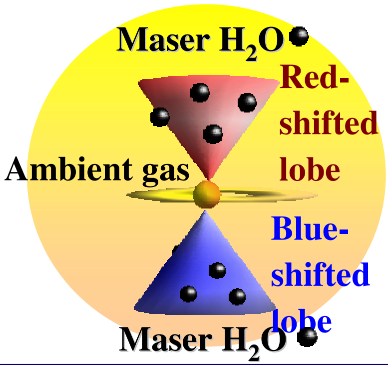

Hubble motion: v = a · r

Free parameters

α_c, δ_c : cone vertex coordinates

P_c , I_c : position and z-inclination angle of the cone axis

θ : (semi-)opening angle of the cone

a : "Hubble constant"

Keplerian Disk

Keplerian Motion: $V = (GM/R^2)^{1/2}$

Free parameters

α_D, δ_D : disk center coordinates

P_d , I_d : position and z-inclination angle of the disk axis

M_c : central mass

The best fit is obtained minimizing the (for the N detected features and the subset of N_p measured proper motions)

$$\chi^2 = \sum_{i=1}^{N} \left[\frac{(v_z^i - v_z^r) - (V_z^i - V_z^r)}{\sigma V_z^i} \right]^2 + \sum_{i=1}^{N_p} \sum_{j=1}^{2} \left[\frac{(v_j^i - v_j^r) - V_j^i}{\sigma V_j^i} \right]^2$$

IRAS 20126+4104

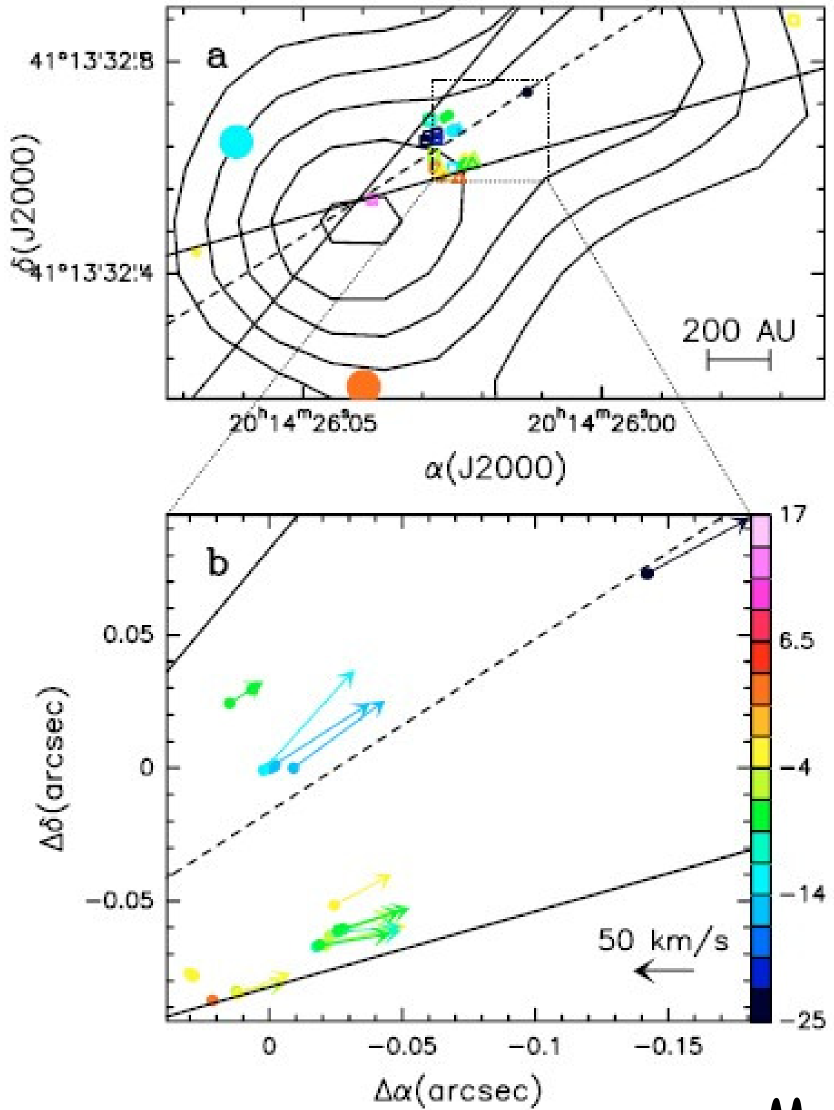

H_2O maser conical flow
at the base of the large-scale
molecular outflow

Moscadelli et al. 2005, A&A 438, 889

MASSIVE STAR FORMATION
in the Galaxy

The role of massive stars

* **Stir up the ISM: massive outflows, winds, champagne flows, supernovae**
  Thus can both destroy their natal molecular cloud AND trigger new star formation.
  Sculpt structure & energetics of ISM in galaxies

* **Energy and momentum input ISM (cosmic ray production)**

* **UV: ionization, HII regions (delineate spiral structure)**

* **Enrichment of the ISM (metals, dust)**

* **Source of neutron stars, BHs, high-energy phenomena such as XRBs, GRBs**

Galactic Ecology: Massive stars regulate ISM

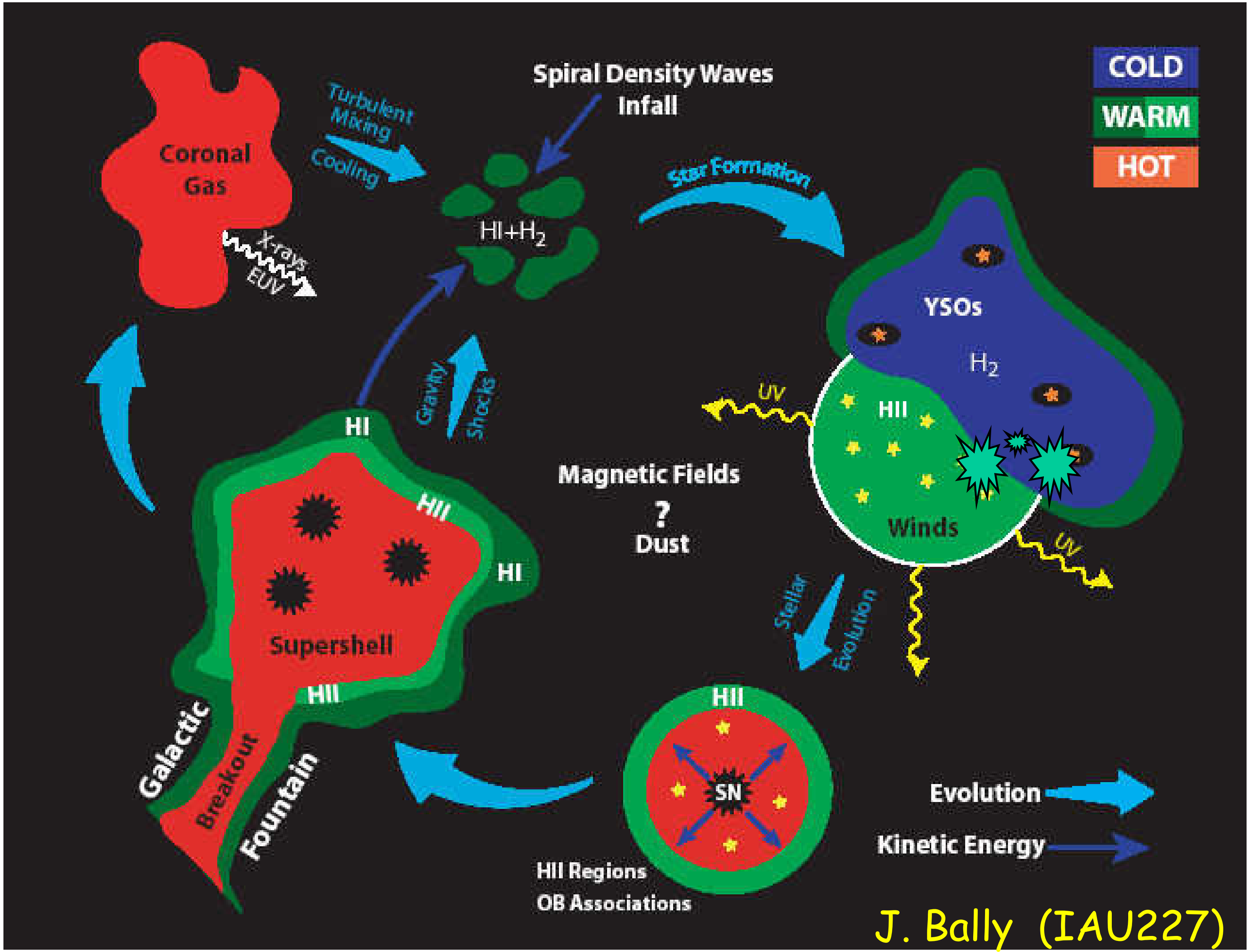

Massive stars interacting with their environment

Outflow

UV-radiation
(ionization)

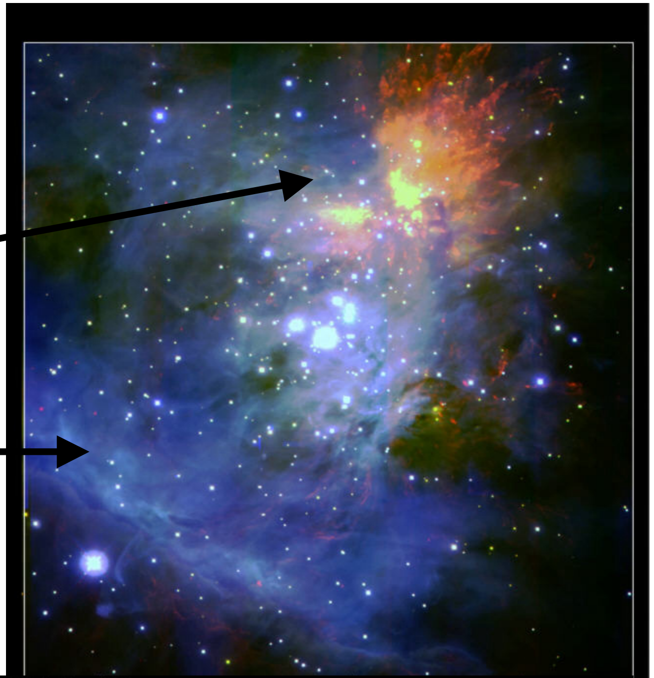

Stellar wind

Supernova explosion

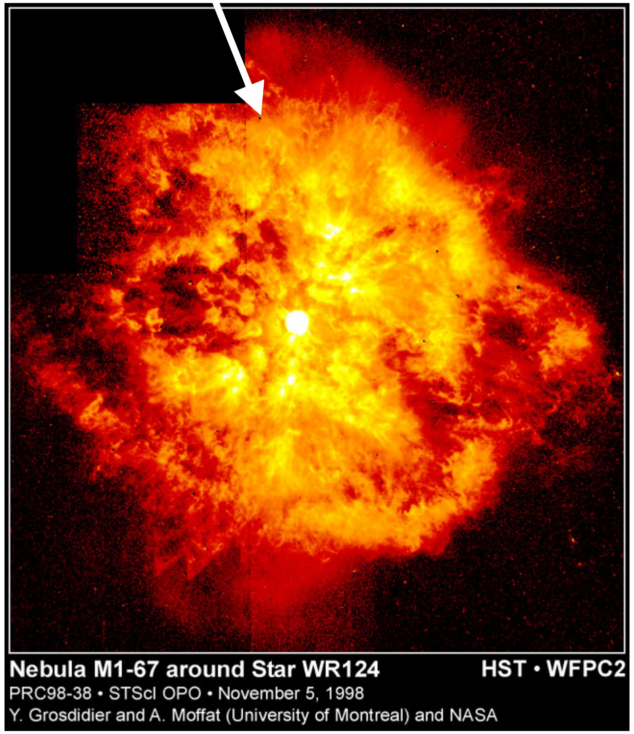

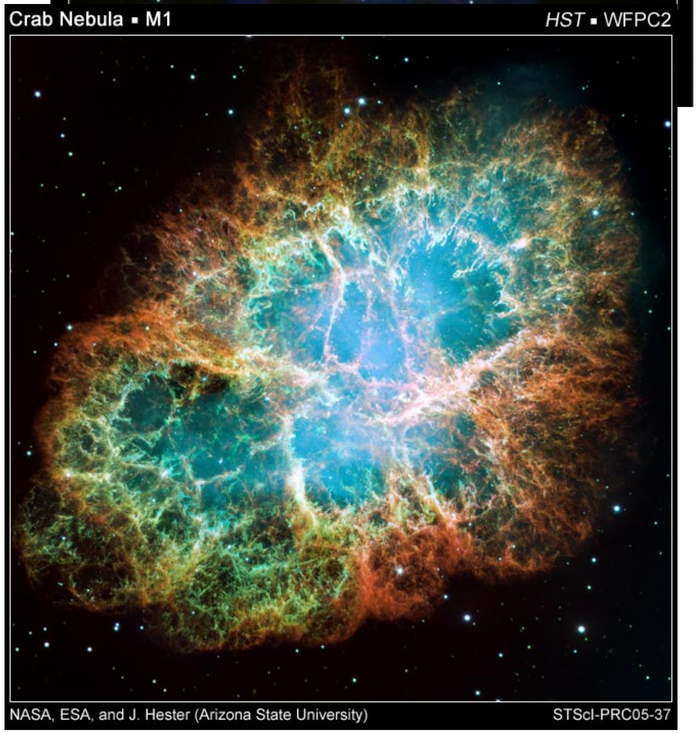

Massive stars: giant bubbles/gas shells

30 Doradus Nebula (LMC): superhells

ESO – VLT +FORS

(J. Bally - IAU227)

GS62.1+0.2. d=9.2 kpc, size = 340 pc x 160 pc.

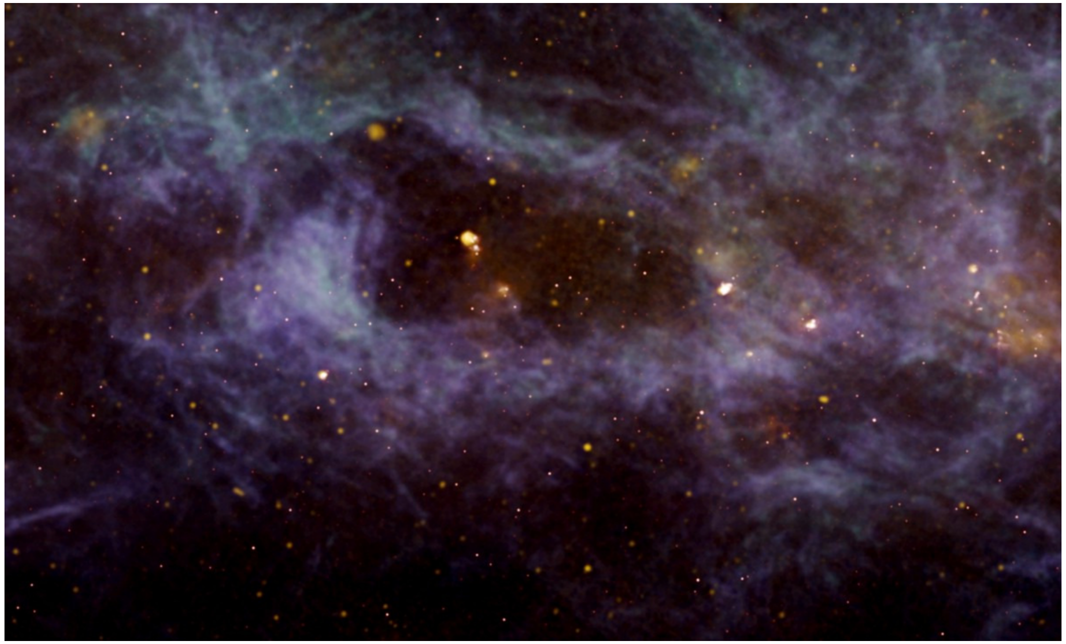

VLA, GBT HI

(NRAO /AUI / NSF)

Massive stars: triggers of star formation

Warm dust (orange) and ionized gas (blue)

Cold dust (contours)

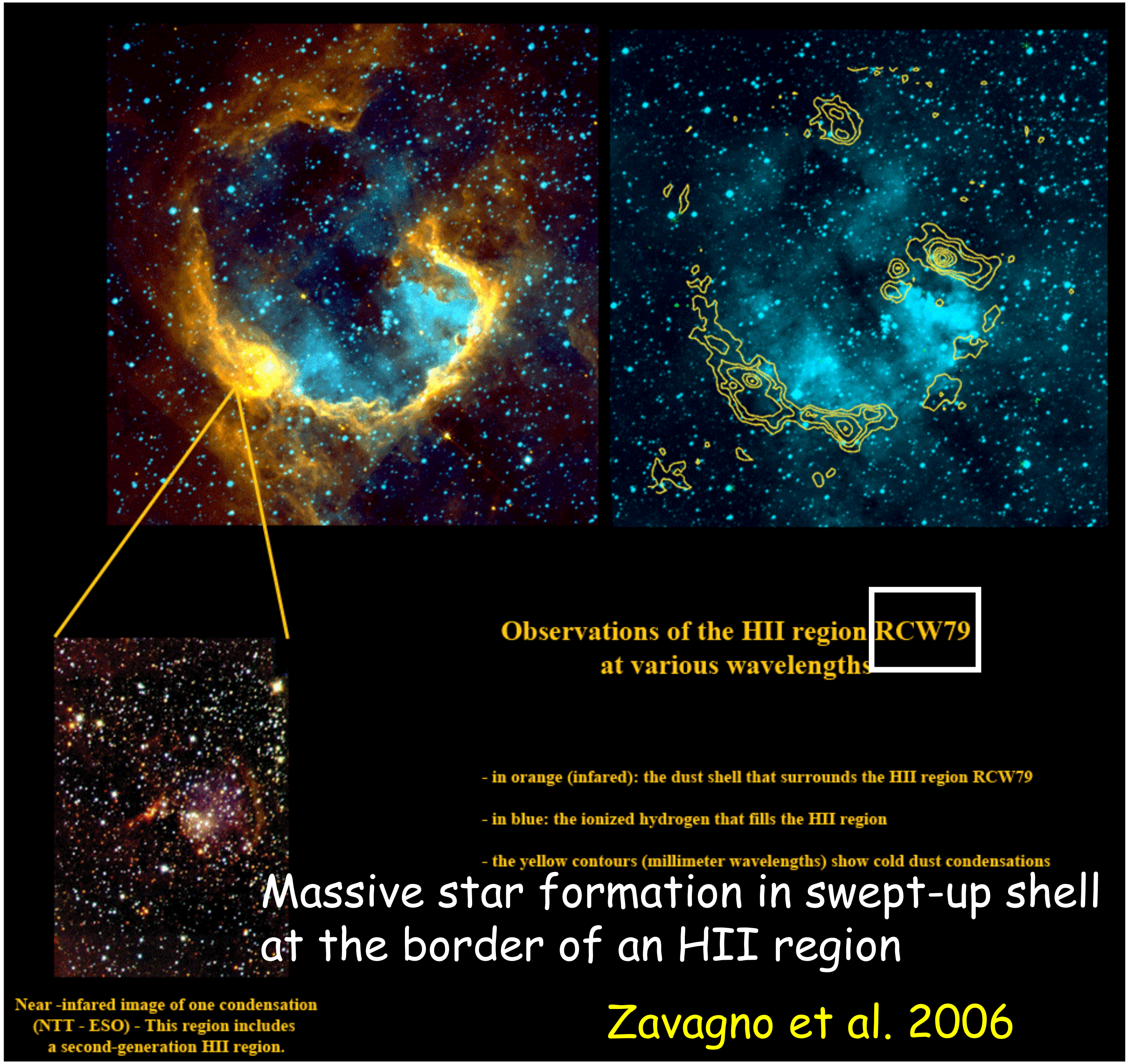

NIR cluster

Massive stars – HII regions: outline spiral structure

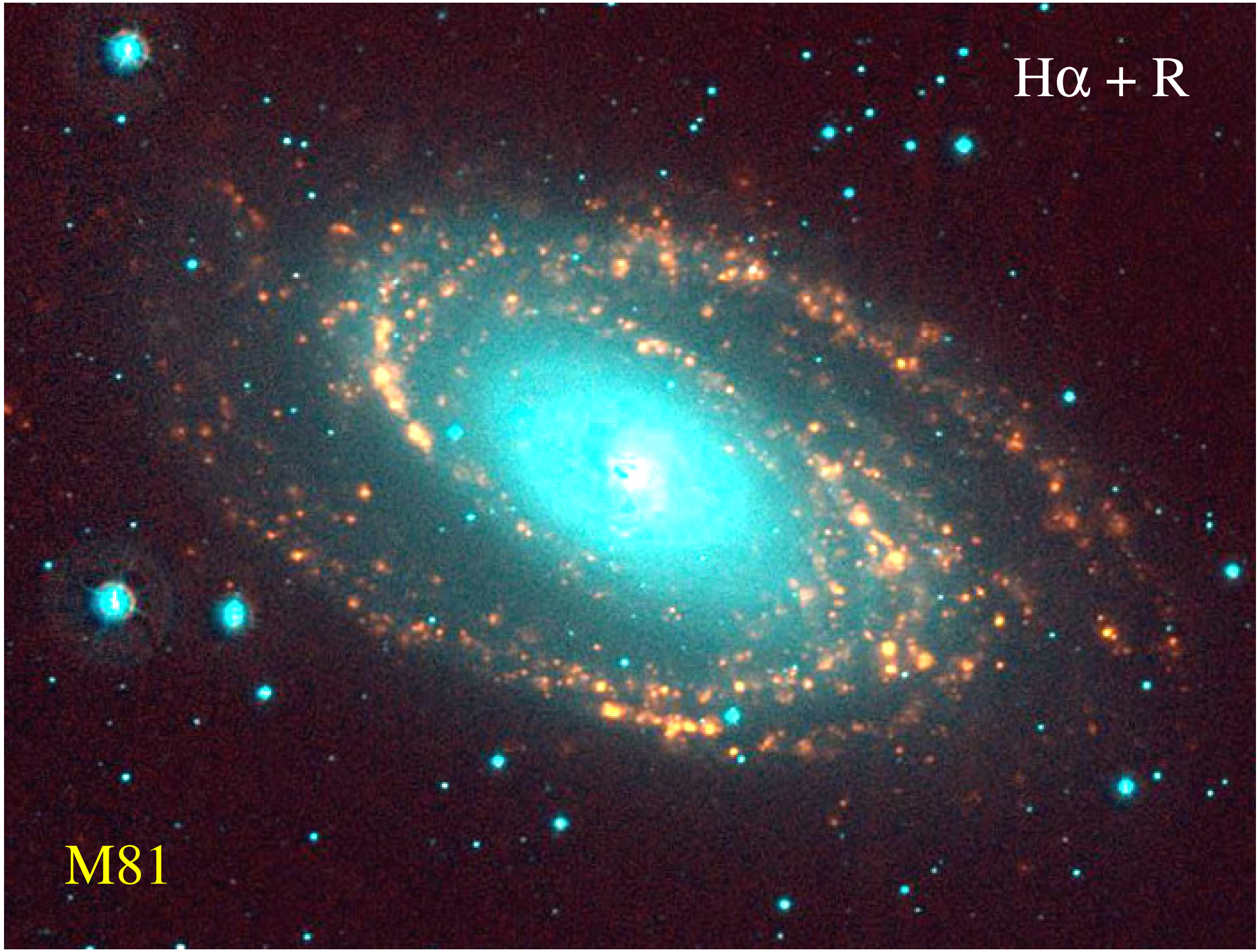

R. Kennicutt (IAU227)

The problem with massive stars

Massive stars important – but not well-understood

WHY?

They are rare and have a short lifetime

Difficult to observe during formation

Complex theoretical problem

The Initial Mass Function

Fundamental ingredient for study of star formation and galaxy evolution

IMF: Frequency distribution of stellar masses at birth

Number of stars per unit of (logarithmic) mass:

$\xi(\log m) \propto m^{\Gamma}$ or $\xi(m) \propto m^{\gamma}$

$\xi(\log m) = (\ln 10).m\ \xi(m)$

log[ξ(logm)] vs. logm

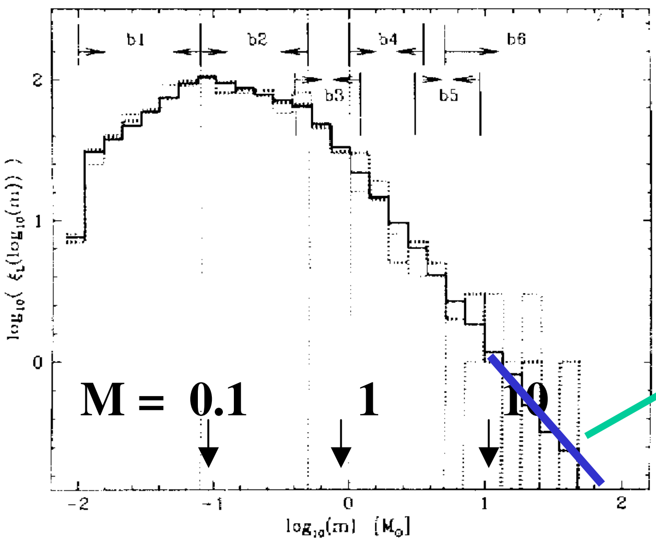

Scalo (1998): $\Gamma = -0.2 \pm 0.3$ for $0.1 < M < 1\ M_\odot$
$= -1.7 \pm 0.3$ for $1 < M < 10\ M_\odot$
$= -1.3 \pm 0.3$ for $10 < M < 100\ M_\odot$

i.e.: $\gamma = -1.2 \pm 0.3$ for $0.1 < M < 1\ M_\odot$
$= -2.7 \pm 0.3$ for $1 < M < 10\ M_\odot$
$= -2.3 \pm 0.3$ for $10 < M < 100\ M_\odot$

There are relatively few of them:

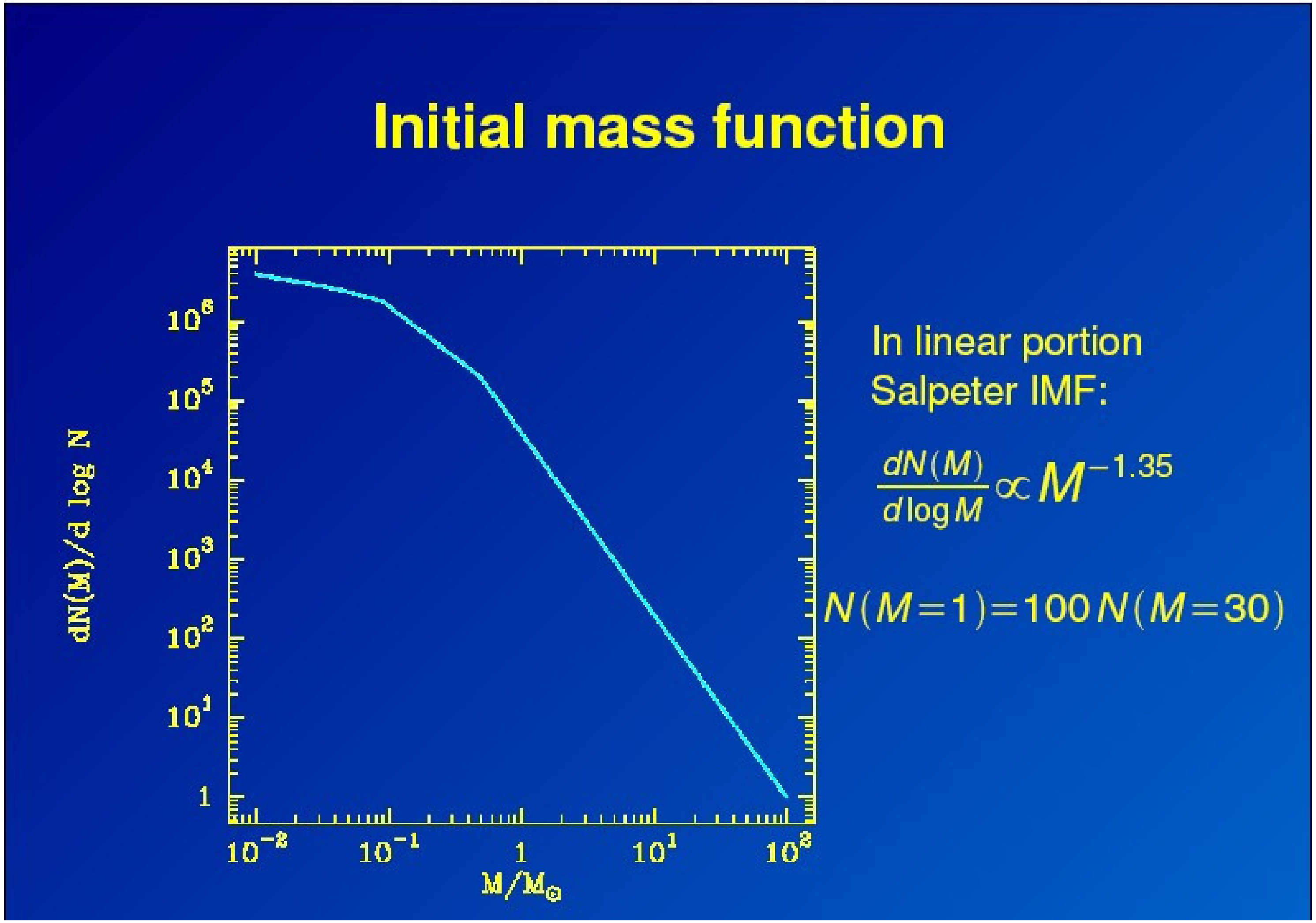

P. Schilke (2005)

They have very short lifes

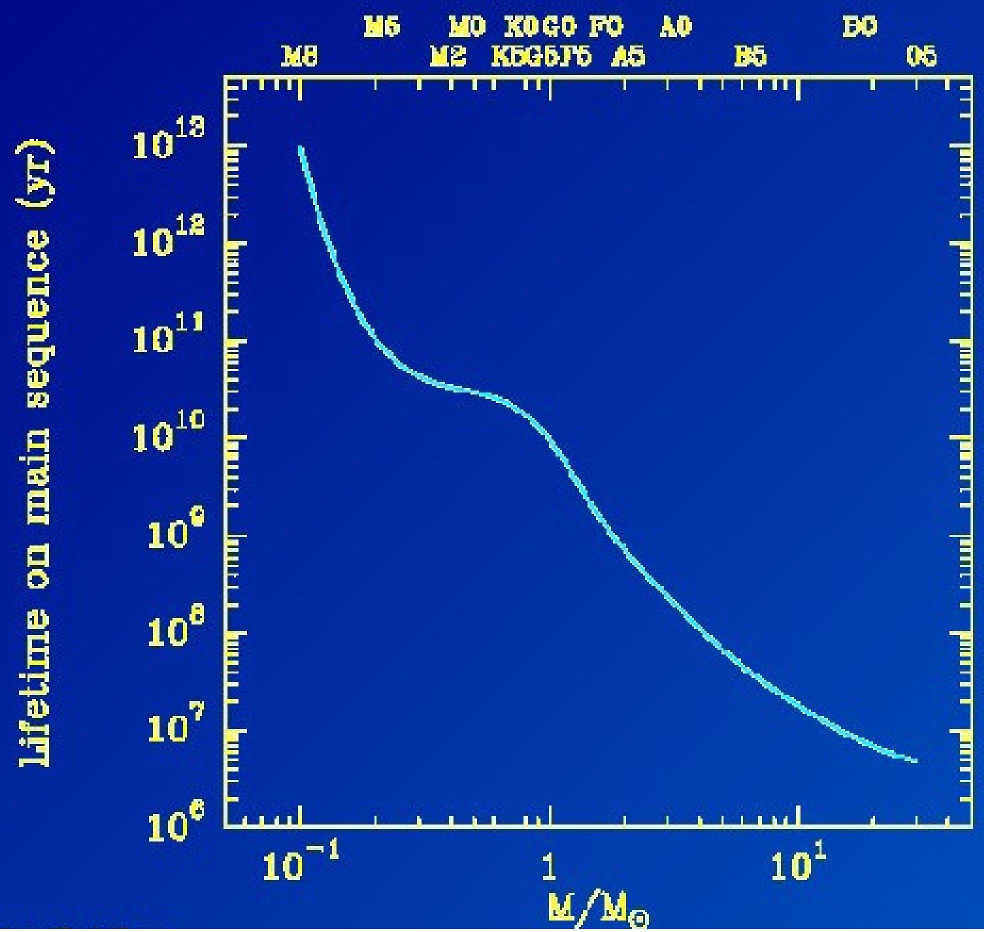

$t(M=1) = 2000\, t(M=30)$

P. Schilke (2005)

These two facts combined:

IMF => 1 star of $30M_\odot$ created for every 100 stars of $1M_\odot$
A $1M_\odot$ star lives 2000 times longer than a $30M_\odot$ star

hence

At any given time there are 2×10^5 more $1M_\odot$ stars than there are $30M_\odot$ stars!

and yet

$L(30M_\odot) = 10^5\ L(1M_\odot)$ => total luminosity is dominated by high-mass stars!

Formation of low- and high-mass stars

Infall of circumstellar material onto protostar

Two relevant timescales:

1) Kelvin-Helmholtz timescale

(timescale on which a star gets its luminosity from gravitational contraction)

$\tau_{KH} = E_{grav} / (dE_{grav} / dt)$

$E_{grav} = GM^2 / R, \quad dE_{grav} / dt = L$

$\Rightarrow \tau_{KH} = GM^2 / RL$

$L \propto M^{3.2}$; $R \propto M^{0.6}$ $\Rightarrow \tau_{KH} \propto M^{-1.8}$

10^7 yr/ $1M_\odot$ star; 10^5 yr/ $10M_\odot$ star

2) Accretion rate: $dM / dt \approx a^3 / G \approx 10^{-5}\ M_\odot$ /yr

10^5 yr/ $1M_\odot$ star; 10^6 yr/ $10M_\odot$ star

The problem of (OB) star formation:

accretion: $t_{acc} = M_{star}/(dM/dt)_{acc}$
contraction: $t_{KH} = GM_{star}/R_{star}L_{star}$

$M_{star} > 8\ M_{\odot}$ ➔ $t_{acc} > t_{KH}$ **(Palla & Stahler 1993)**

High-mass stars reach ZAMS still accreting!
Spherical symmetry ➔ $P_{radiation} > P_{ram}$ ➔

➔ **stars** $> 8\ M_{\odot}$ **should not form!??**

Proposed solutions

- **Accretion models:**

(non-spherical) inside-out collapse

(Wolfire & Cassinelli 1978, Yorke & Sonnhalter 2002, Tan & McKee 2003)

Rotation + ang. mom. conservation → Disk:
focuses accretion, boosts ram pressure
Outflow → channels stellar photons, lowers radiation pressure

- **Coalescence models:**

many low-mass stars merge into one massive star

(Bonnell et al. 1998)

Implications & (testable) predictions

- **Accretion models** :
  - presence of massive disks
    & massive collimated outflows: likely / yes
  - high accretion rates ($\geq 10^{-5}\ M_\odot$): evidence
  - isolated star formation: possible
  - formation at cluster center: with the other cluster members

- **Coalescence models** :
  - presence of massive disks
    & massive collimated outflows: unlikely
  - stellar collisions: not observed
  - isolated star formation: impossible
  - formation at cluster center: after the other cluster members
  - high stellar density required (> 10^7 pc^{-3})

➔ Detection of collimated massive outflows and accretion disks is crucial to understand O-B star formation

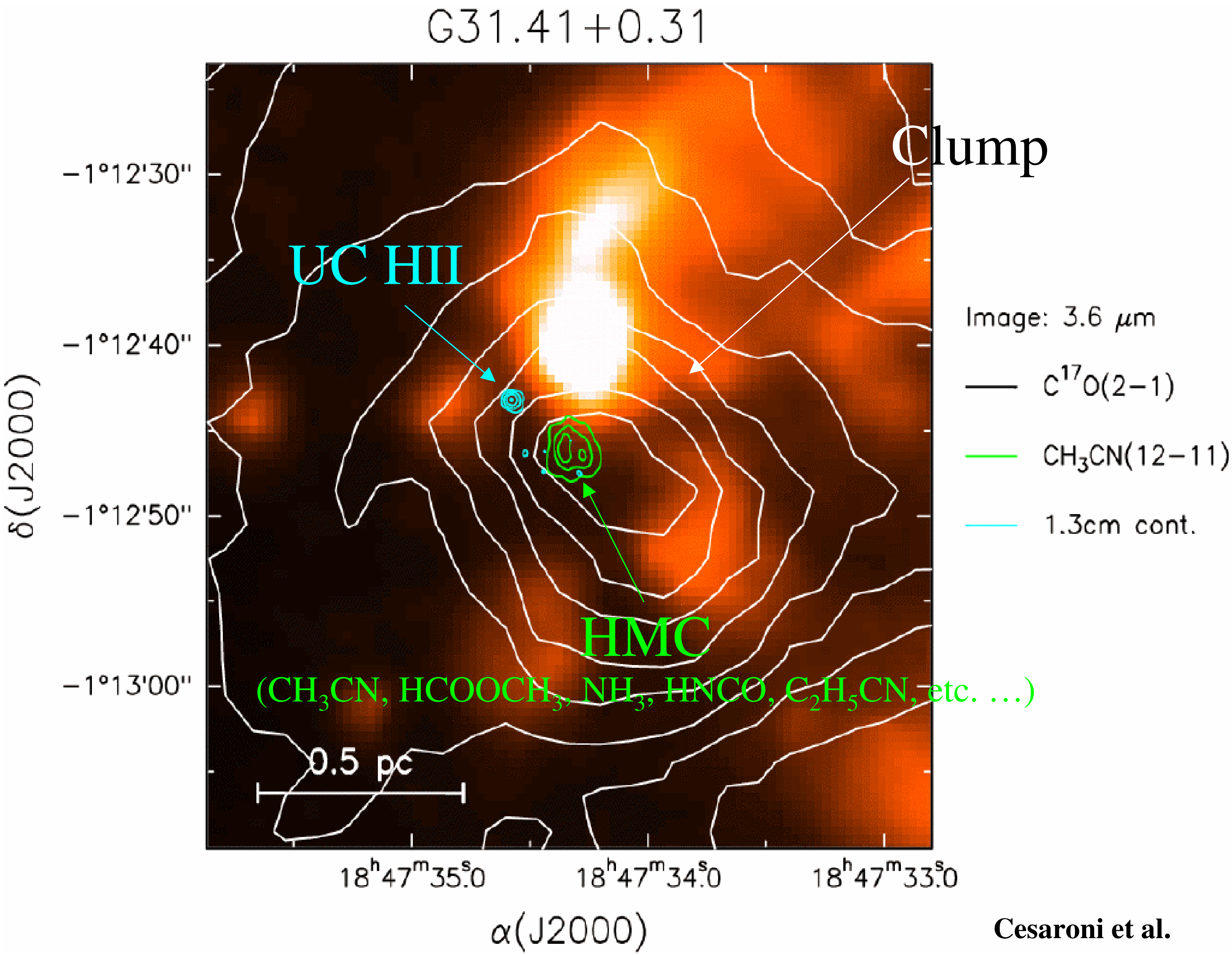

Cesaroni et al.

Hot molecular cores

- Typical values <0.1 pc, >100 K, 10^7 cm^{-3}, >10^4 L_O
- Many molecules: evaporation of grains
- Sometimes contain hypercompact HII regions

➔ Contain OB stars in formation

➔ Probable presence of **infall** (accretion) and **rotation** (disks)

<u>Hot molecular cores</u>

- Typical values <0.1 pc, >100 K, 10^7 cm^{-3}, $>10^4 L_o$
- Many molecules: evaporation of grains
- Sometimes contain hypercompact HII regions

➔ Contain OB stars being formed

➔ Probable presence of **<u>infall</u>** (accretion) and **<u>rotation</u>** (disks)

The search for disks: where

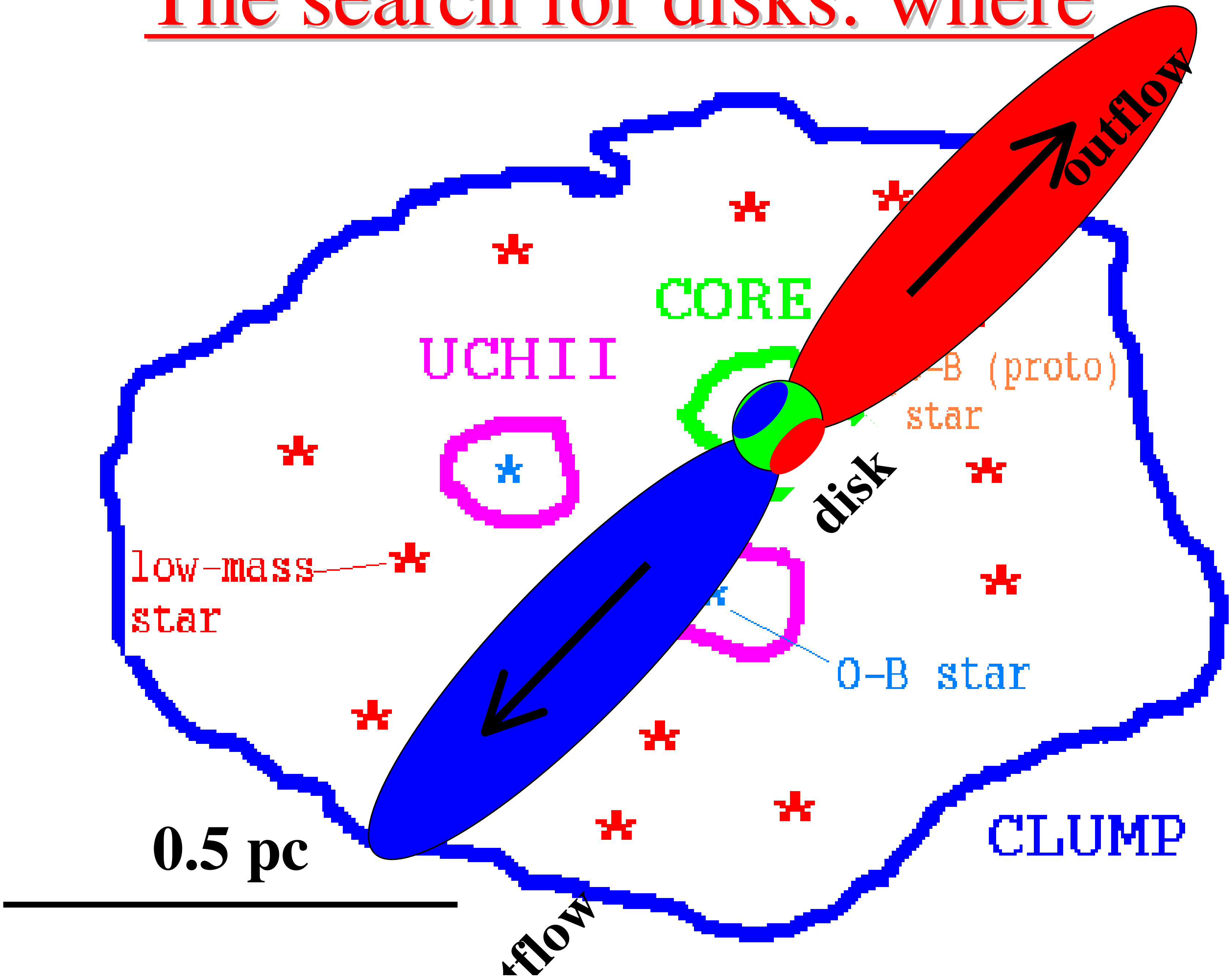

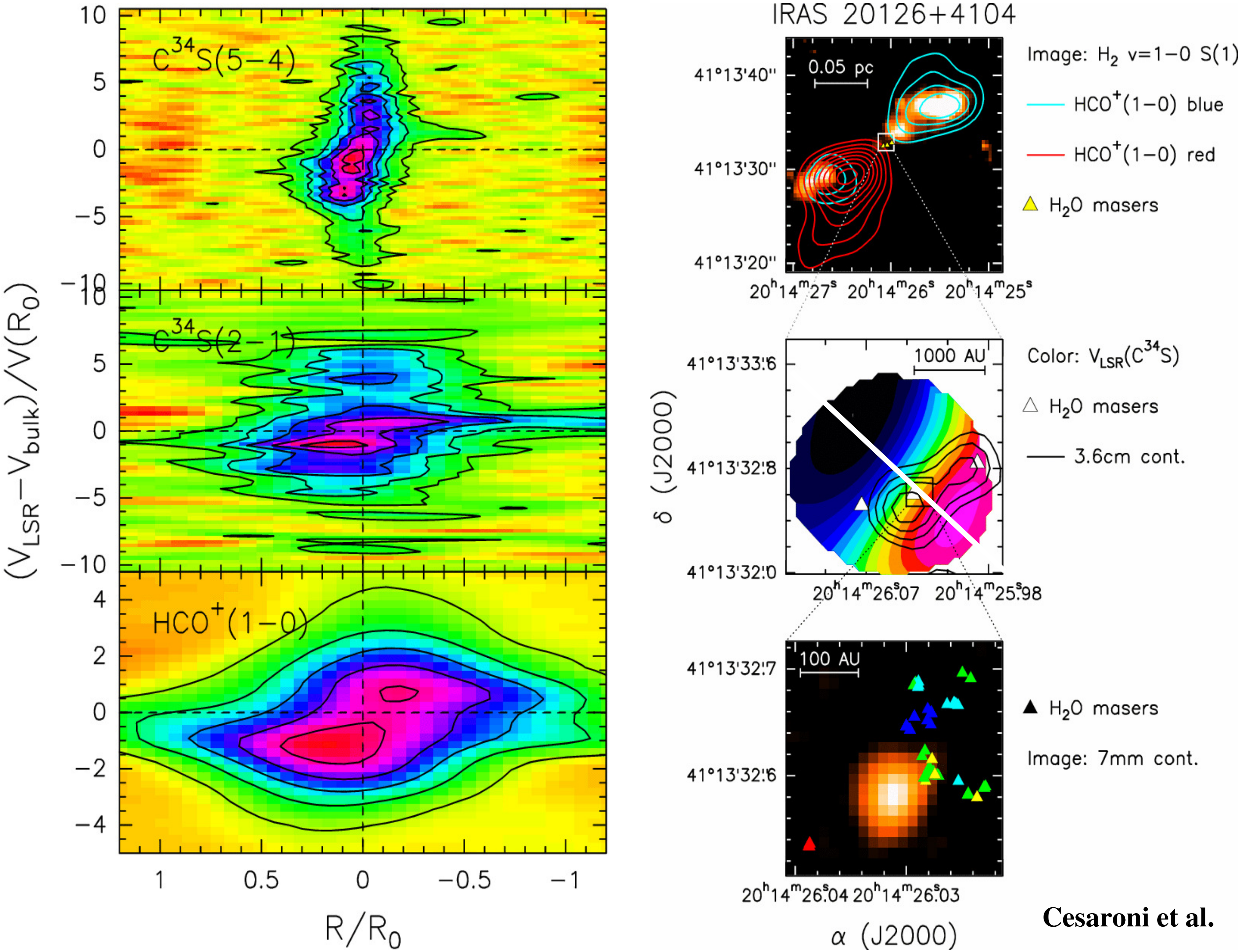

C34S(5−4)
C34S(2−1)
HCO+(1−0)
(VLSR−Vbulk)/V(R0)
R/R0
IRAS 20126+4104
0.05 pc
Image: H2 v=1−0 S(1)
HCO+(1−0) blue
HCO+(1−0) red
H2O masers
41°13'40''
41°13'30''
41°13'20''
20h14m27s 20h14m26s 20h14m25s
1000 AU
Color: VLSR(C34S)
H2O masers
3.6cm cont.
41°13'33.''6
41°13'32.''8
41°13'32.''0
20h14m26.s07 20h14m25.s98
δ (J2000)
100 AU
H2O masers
Image: 7mm cont.
41°13'32.''7
41°13'32.''6
20h14m26.s04 20h14m26.s03
α (J2000)
Cesaroni et al.

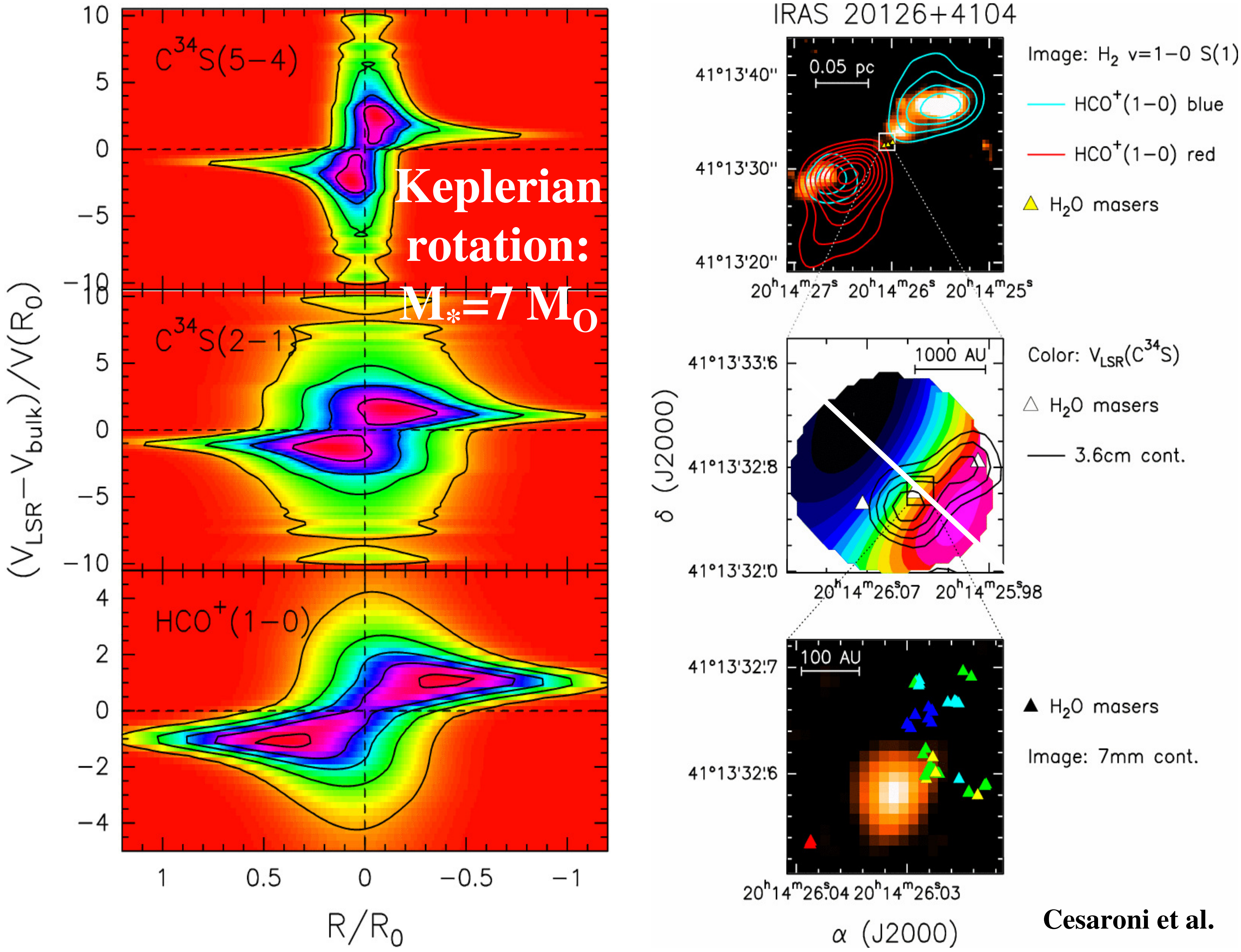
IRAS 20126+4104
$C^{34}S(5-4)$
$C^{34}S(2-1)$
$HCO^+(1-0)$
Keplerian rotation: $M_* = 7\ M_O$
$(V_{LSR}-V_{bulk})/V(R_0)$
R/R_0
Image: H_2 v=1−0 S(1)
$HCO^+(1-0)$ blue
$HCO^+(1-0)$ red
H_2O masers
0.05 pc
Color: $V_{LSR}(C^{34}S)$
H_2O masers
3.6cm cont.
1000 AU
100 AU
H_2O masers
Image: 7mm cont.
δ (J2000)
α (J2000)
Cesaroni et al.

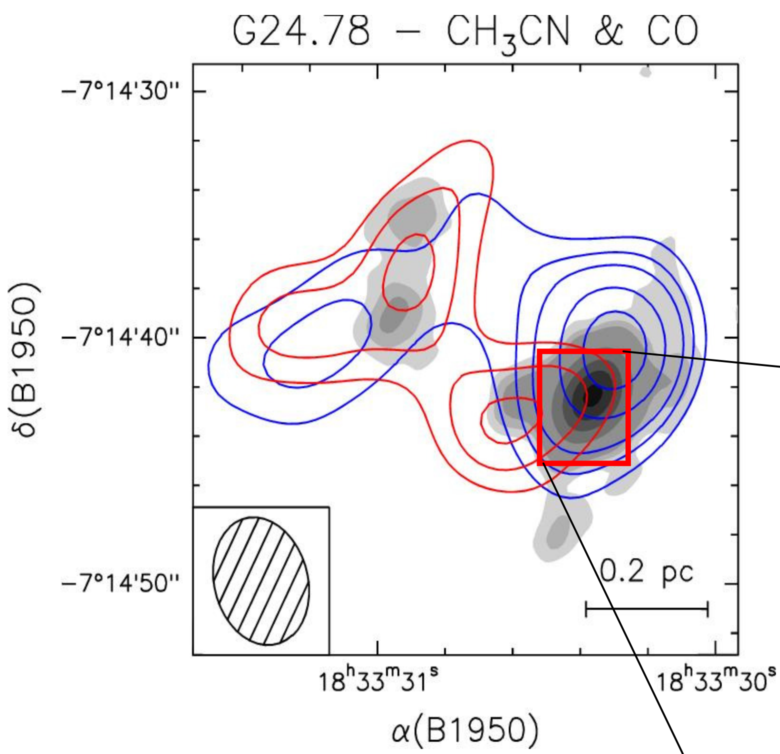

Furuya et al. (2002)

Beltran et al. (2004)

Beltran et al. (2005)

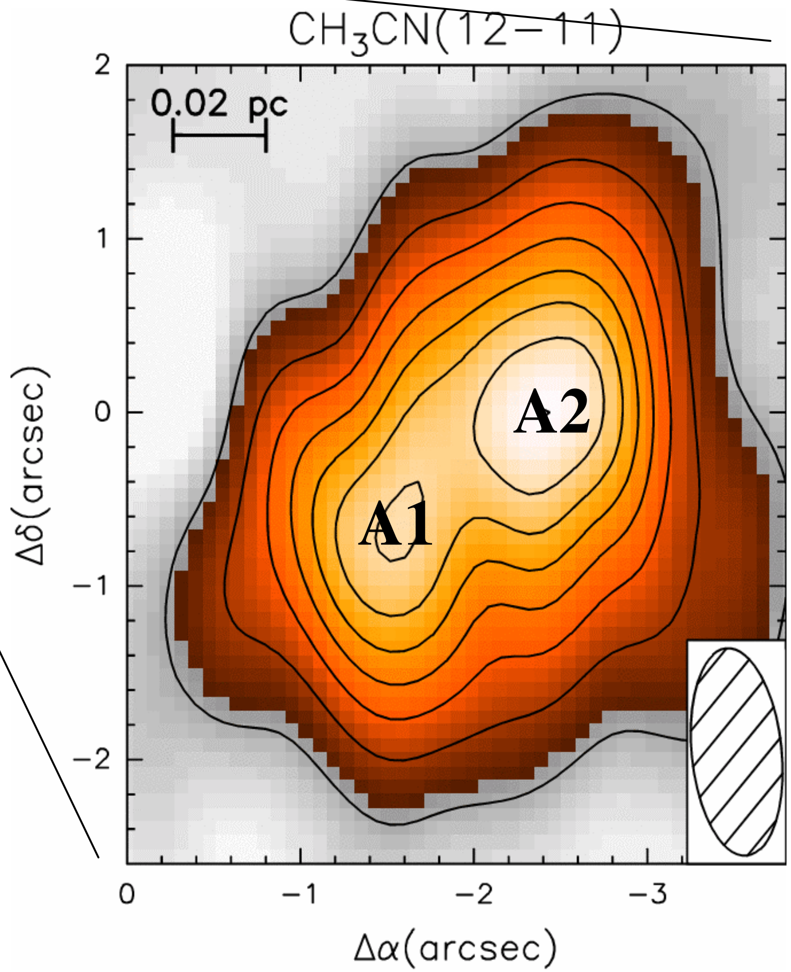

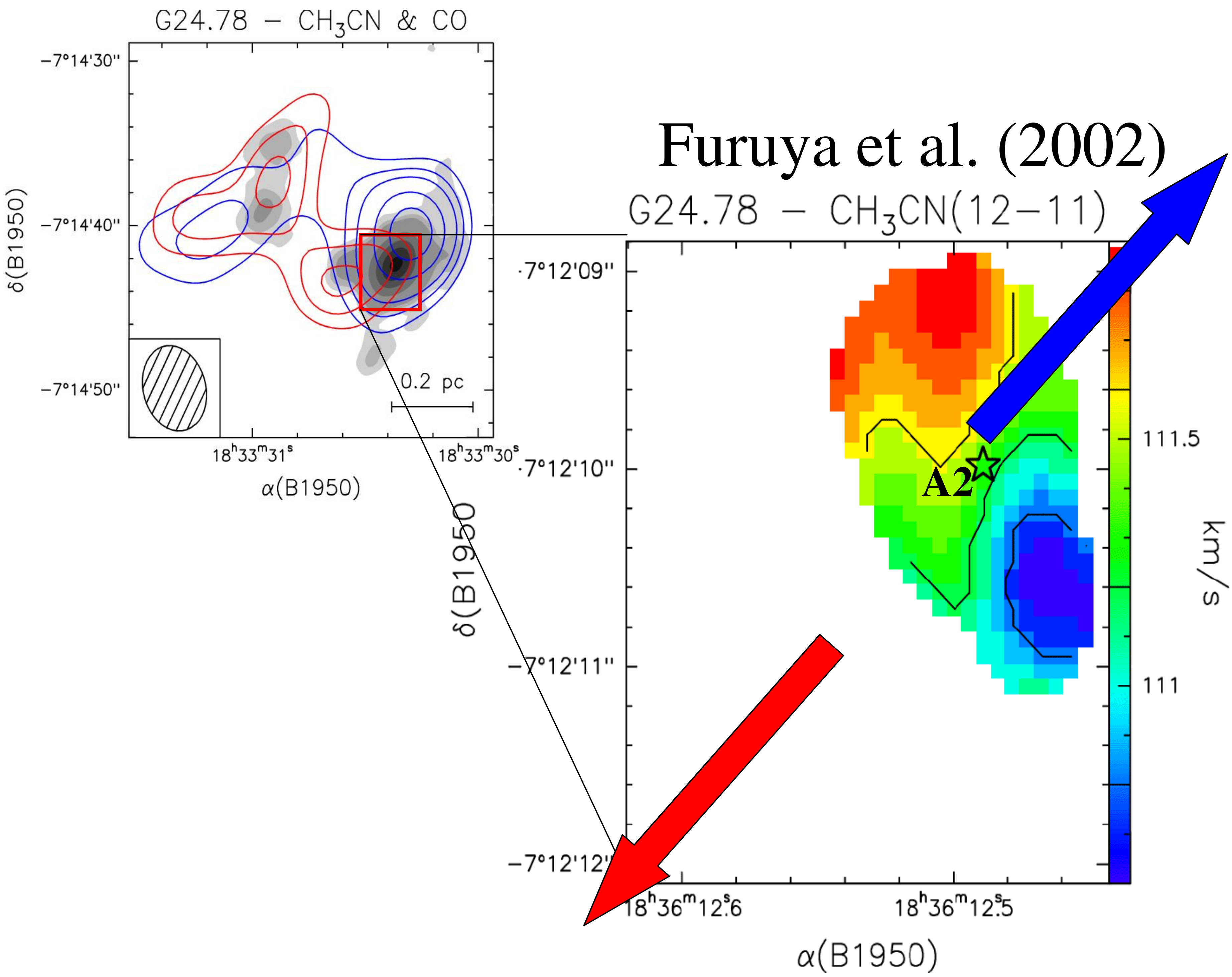
G24.78 – CH3CN & CO
−7°14'30''
−7°14'40''
−7°14'50''
δ(B1950)
0.2 pc
18h33m31s
18h33m30s
α(B1950)
Furuya et al. (2002)
G24.78 – CH3CN(12–11)
-7°12'09''
-7°12'10''
−7°12'11''
−7°12'12''
δ(B1950)
A2
111.5
111
km/s
18h36m12.6
18h36m12.5
α(B1950)

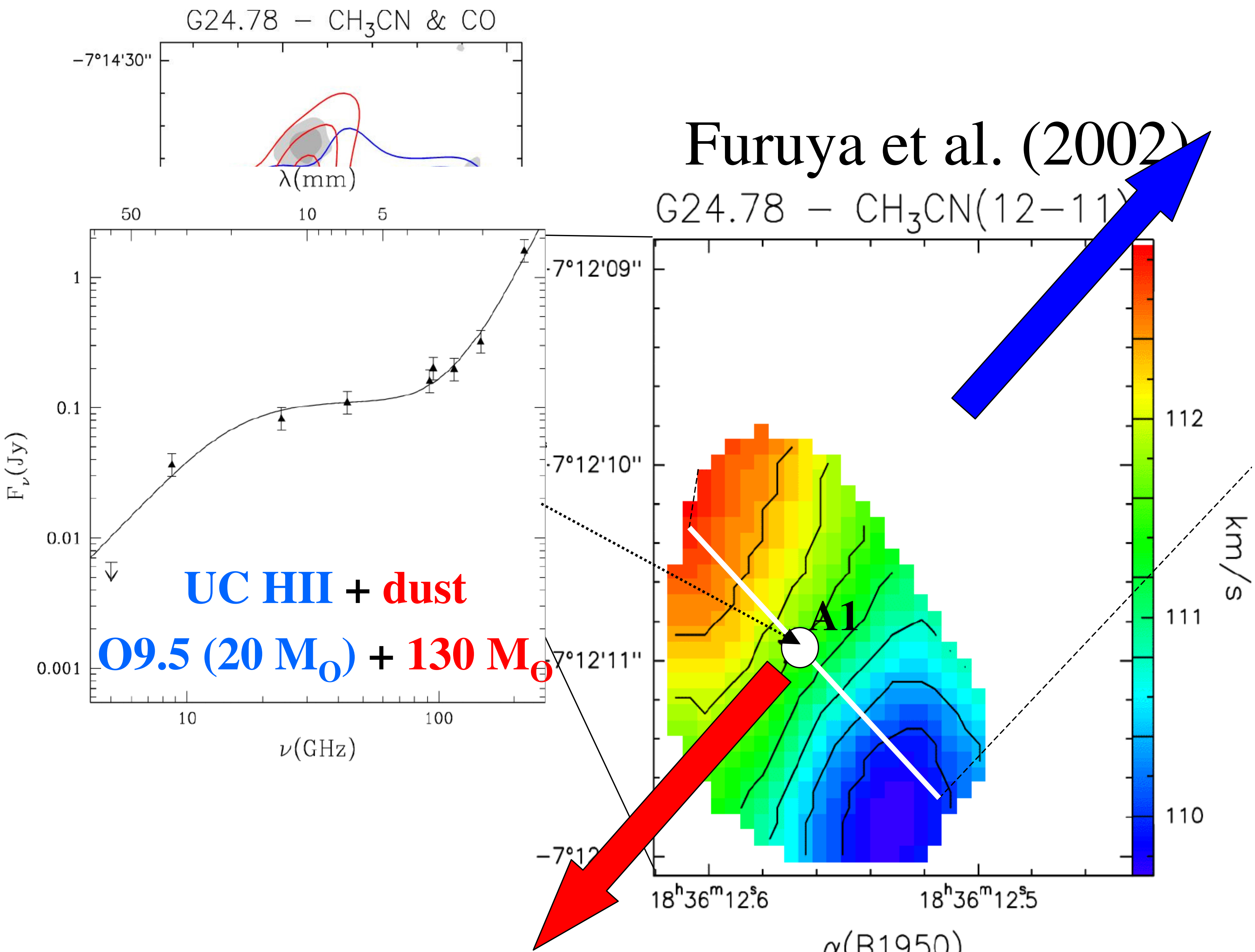

G24.78 – CH3CN & CO
−7°14'30"
λ(mm)
50
10
5
1
0.1
0.01
0.001
Fν(Jy)
10
100
ν(GHz)
UC HII + dust
O9.5 (20 MO) + 130 MO
Furuya et al. (2002)
G24.78 – CH3CN(12−11)
-7°12'09"
-7°12'10"
-7°12'11"
A1
18h36m12.6
18h36m12.5
α(B1950)
112
111
110
km/s

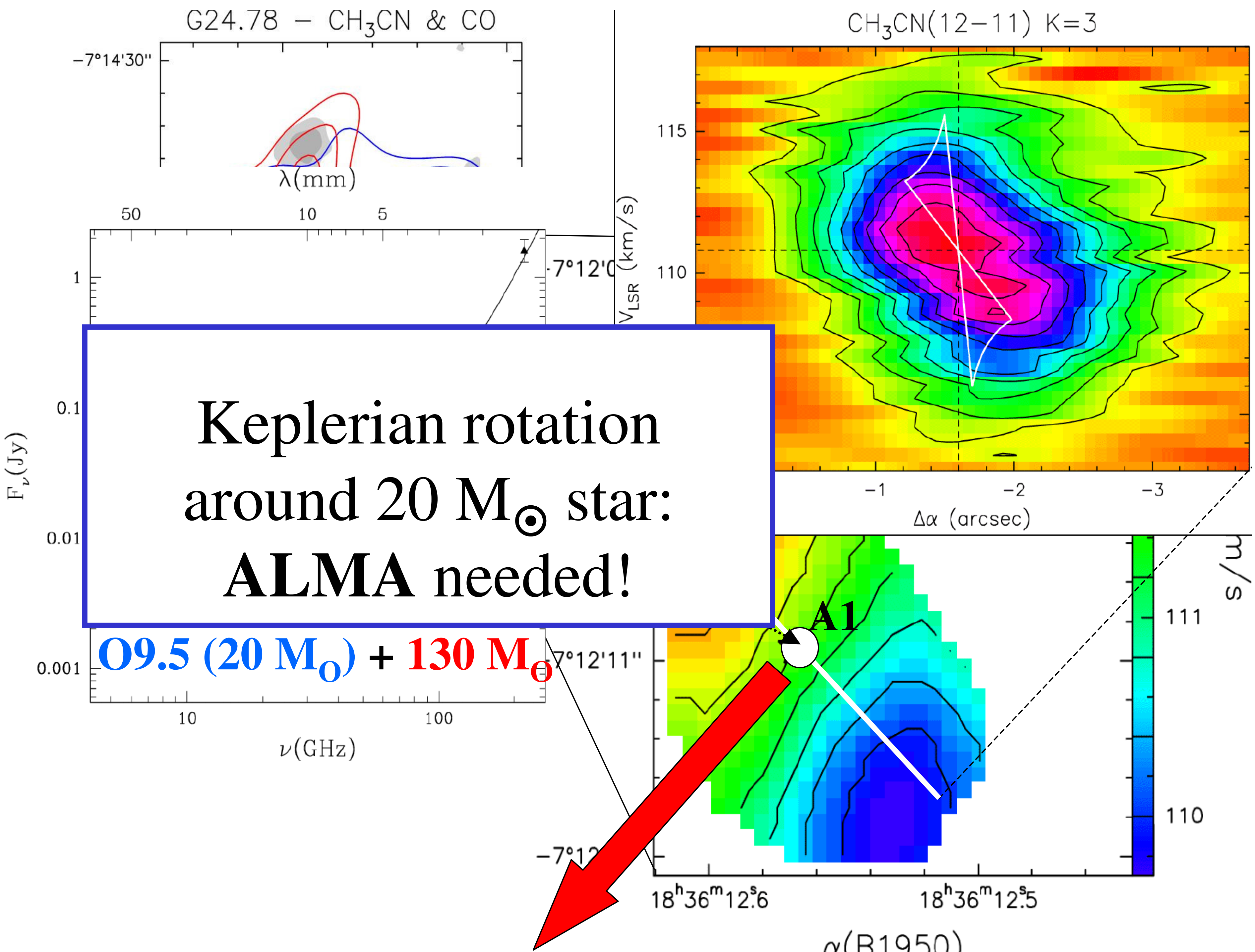

Keplerian rotation
around 20 $M_\odot$ star:
ALMA needed!

Results of disk search

Two types of objects found:

Disks in B stars

- $M < 10\ M_\odot$
- $R \sim 1000$ AU
- **$L \sim 10^4\ L_\odot$**
- $(dM/dt)_{star} \sim 10^{-4}\ M_\odot/yr$
- $t_{rot} \sim 10^4$ yr
- $t_{acc} \sim M/(dM/dt)_{star} \sim 10^5$ yr

→ **$t_{acc} >> t_{rot}$**

➔ equilibrium, circum*stellar* structures

Toroids in O stars

- $M > 100\ M_\odot$
- $R \sim 10000$ AU
- **$L >> 10^4\ L_\odot$**
- $(dM/dt)_{star} > 10^{-3}\ M_\odot/yr$
- $t_{rot} \sim 10^5$ yr
- $t_{acc} \sim M/(dM/dt)_{star} \sim 10^4$ yr

→ **$t_{acc} << t_{rot}$**

➔ non-equilibrium, circum-*cluster* structures

Is there a mass upper limit?

IMF => massive stars always form in clusters. So can only study upper limit in mass by observing cluster population.

Requirements:

*** cluster stellar mass > 10^4 $M_\odot$**
*** 1 Myr < cluster age < 3 Myr**
*** need to see individual stars**
*** need to be able to separate stars**

In the Galaxy: the Arches cluster (@ Galactic Centre)

Arches Cluster

160 O-stars

Brightest members have L = $10^{6.3}$ $L_\odot$

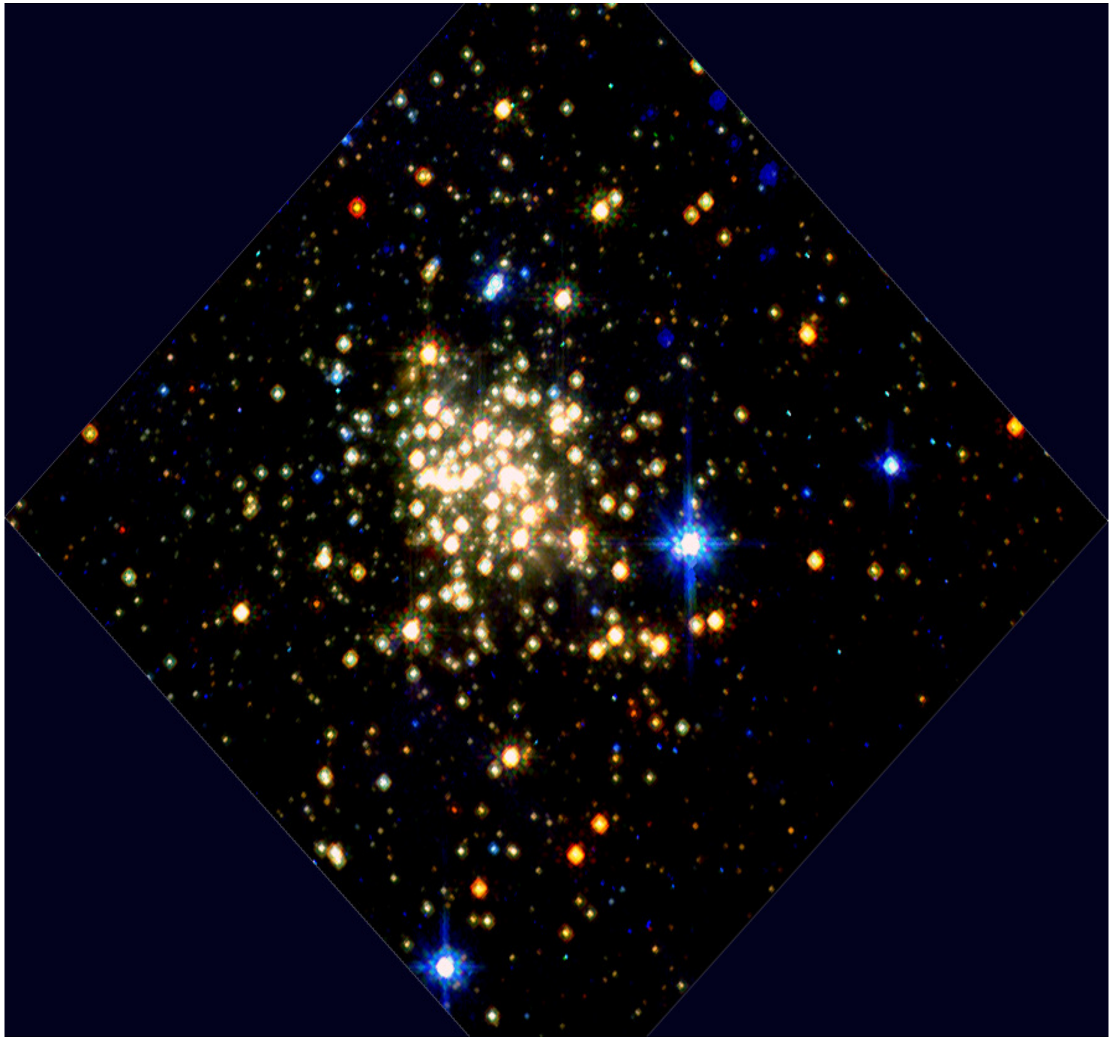

HST (1999)

Figer, Nature (2005)

Arches-cluster mass function

If there is no mass cut-off,
chances of not finding
such massive stars is:

10^{-8} if 18 are expected
(slope –1.35)

10^{-14} if 33 are expected
(slope –0.90)

Mass cut-off at 150 $M_{\odot}$

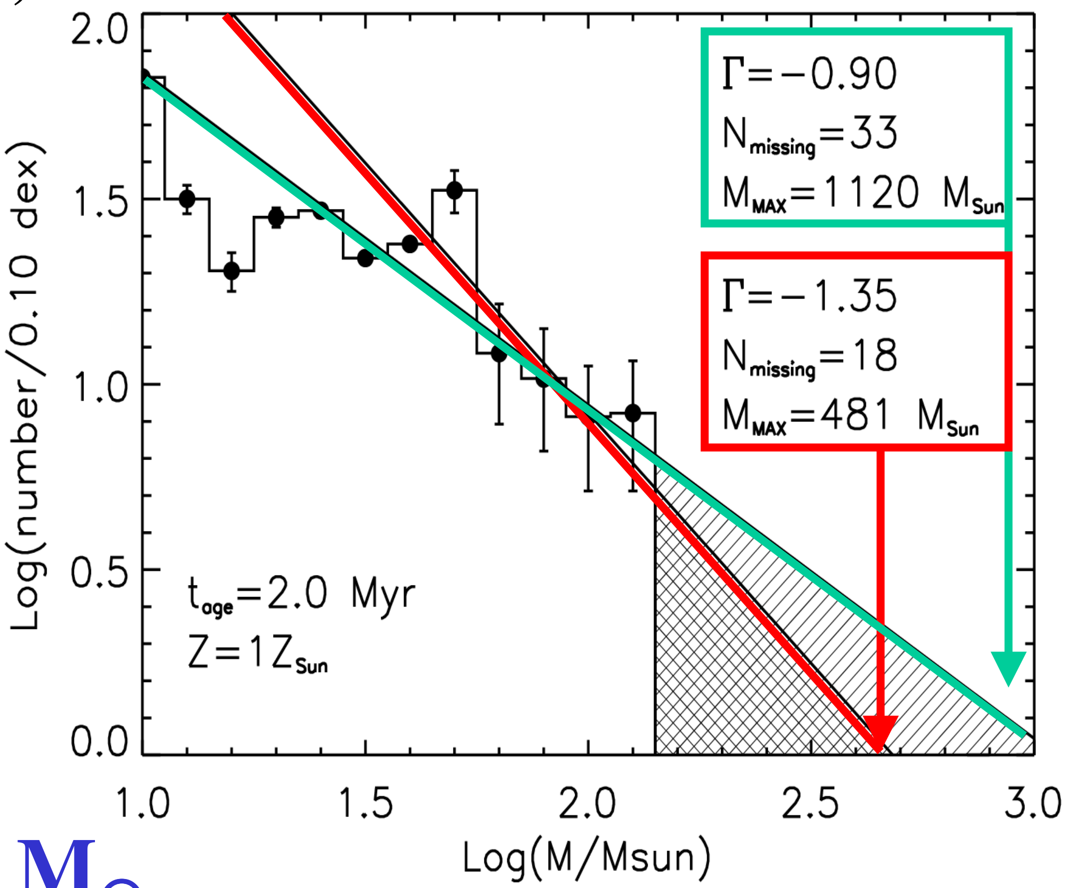

Figer, Nature (2005)

Are there stars more massive than 150 $M_\odot$?

Pistol star: 150-250 $M_\odot$?

But: not single?

G0.15-0.05

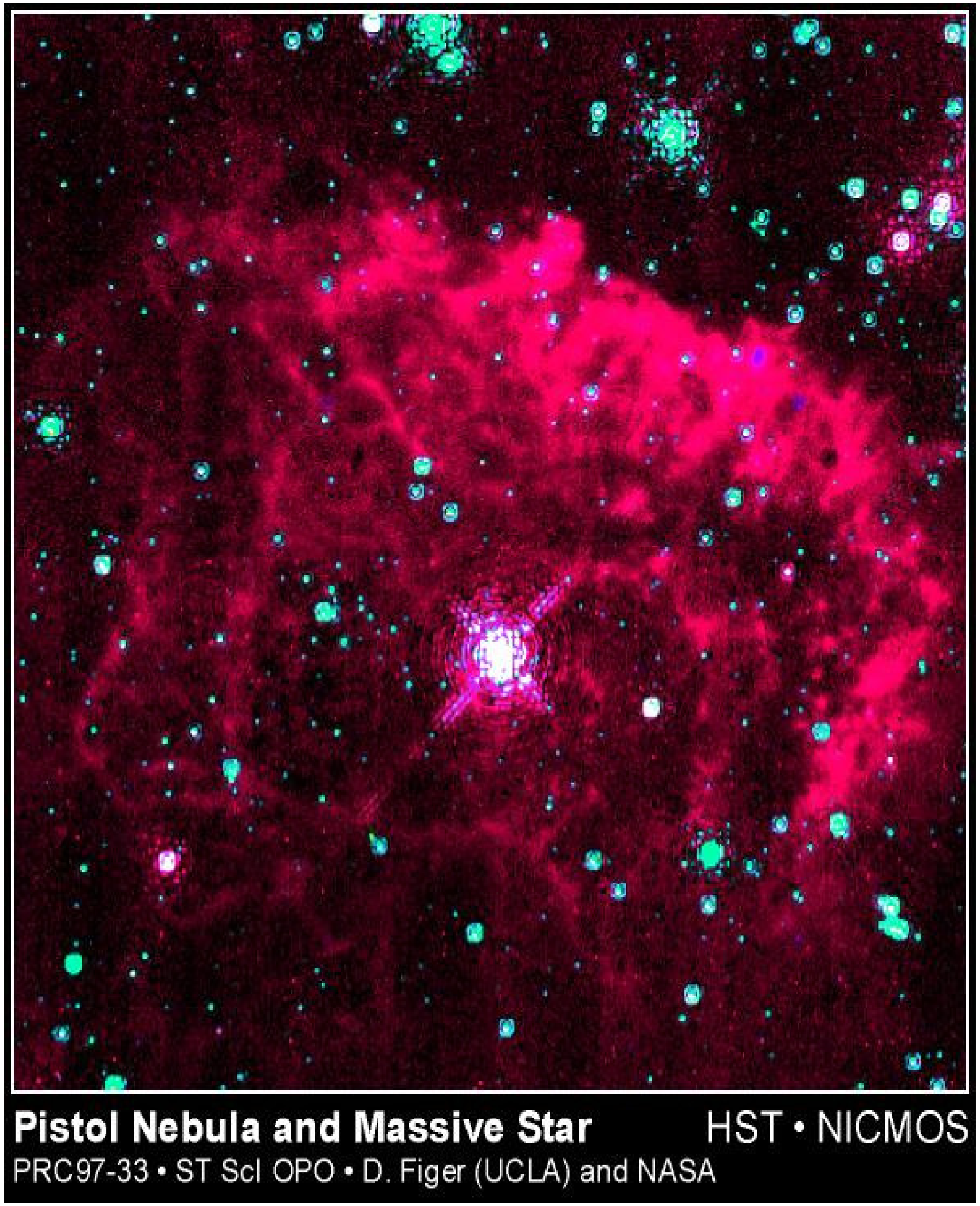

Figer et al. 1999, ApJ, 525, 759

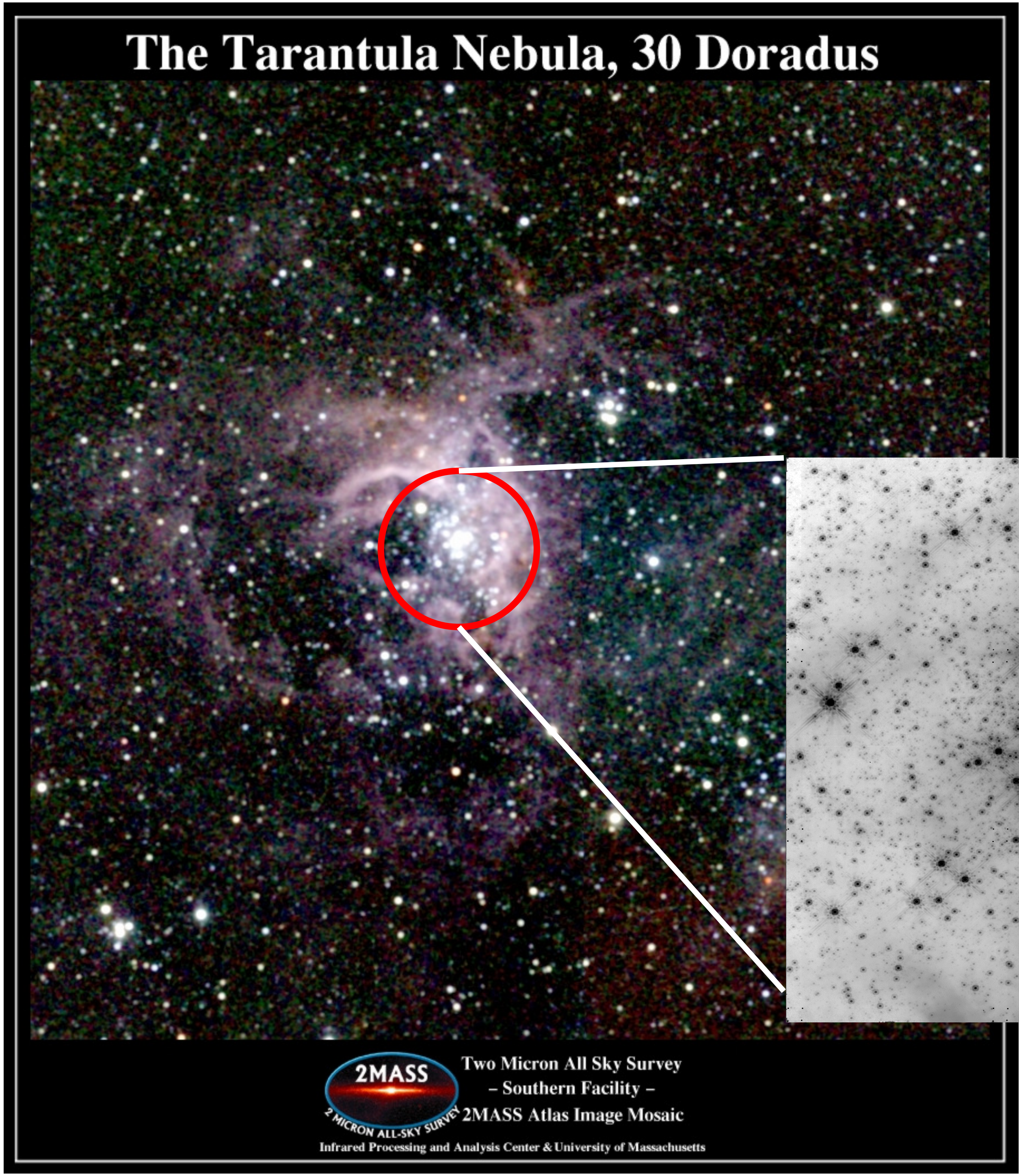

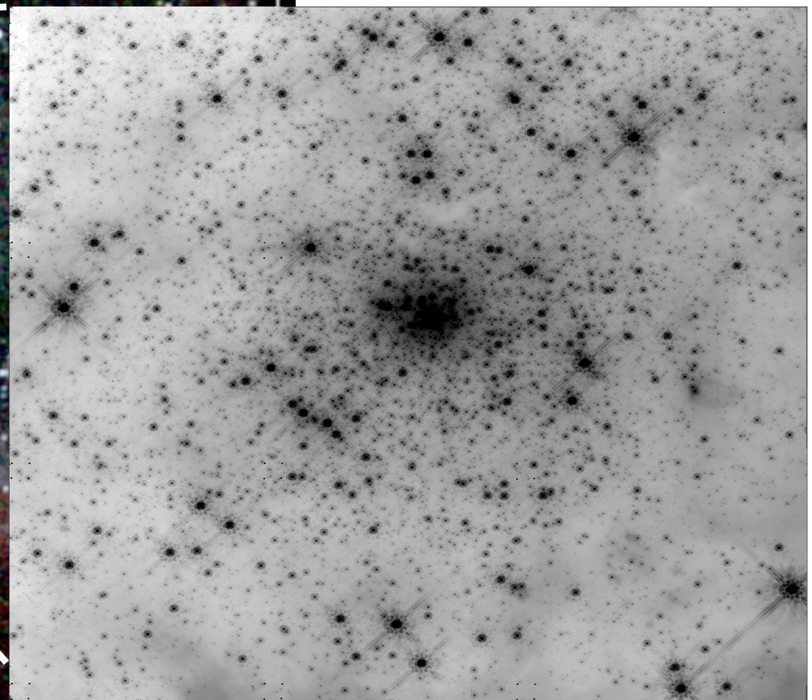

R136:
$M_{max} = 150\ M_\odot$

SUMMARY

Possibile evolutionary sequence for OB-stars

IR-dark cloud
↓ fragmentation
(hot) molecular core
↓ infall+rotation
(proto)star+disk+outflow
↓ accretion
hypercompact HII region
↓ expansion
extended HII region

Massive stars are rare, but very influential for Galactic "ecology";

HMPO difficult to find, and hard to study;

Outflows & disks & high accretion rates found, hence probably form by accretion (early B-stars; also O-stars?);

High-mass cut-off exists (150 $M_\odot$).